

# MONA OFFSHORE WIND PROJECT

## Preliminary Environmental Information Report

Volume 6, annex 6.1: Physical processes technical report



April 2023  
FINAL

Document status					
Version	Purpose of document	Authored by	Reviewed by	Approved by	Review date
Rev01	Draft for Client review	RPS	bpEnBW		12/09/2022
Rev02	Addressing client comments	RPS	bpEnBW		17/10/2022
Rev03	Final	RPS	bpEnBW	bpEnBW	01/12/2022

The report has been prepared for the exclusive use and benefit of our client and solely for the purpose for which it is provided. Unless otherwise agreed in writing by RPS Group Plc, any of its subsidiaries, or a related entity (collectively 'RPS') no part of this report should be reproduced, distributed or communicated to any third party. RPS does not accept any liability if this report is used for an alternative purpose from which it is intended, nor to any third party in respect of this report. The report does not account for any changes relating to the subject matter of the report, or any legislative or regulatory changes that have occurred since the report was produced and that may affect the report.

The report has been prepared using the information provided to RPS by its client, or others on behalf of its client. To the fullest extent permitted by law, RPS shall not be liable for any loss or damage suffered by the client arising from fraud, misrepresentation, withholding of information material relevant to the report or required by RPS, or other default relating to such information, whether on the client's part or that of the other information sources, unless such fraud, misrepresentation, withholding or such other default is evident to RPS without further enquiry. It is expressly stated that no independent verification of any documents or information supplied by the client or others on behalf of the client has been made. The report shall be used for general information only.

<b>Prepared by:</b>	<b>Prepared for:</b>
<b>RPS</b>	<b>Mona Offshore Wind Ltd</b>



## Contents

<b>1</b>	<b>PHYSICAL PROCESSES TECHNICAL REPORT</b>	<b>1</b>
1.1	Introduction	1
1.2	Study area	1
1.3	Methodology	3
1.4	Desktop study	6
1.5	Site-specific surveys	7
1.6	Baseline environment	7
1.6.1	Bathymetry	7
1.6.2	Hydrography	12
1.6.3	Wave climate	25
1.6.4	Littoral currents	40
1.6.5	Sedimentology and seabed substrate	43
1.6.6	Sediment transport	46
1.6.7	Suspended sediments	52
1.7	Potential environmental changes	54
1.7.1	Overview	54
1.7.2	Post-construction hydrography	55
1.7.3	Post-construction sedimentology	80
1.8	Potential changes during construction	89
1.8.2	Seabed preparation	89
1.8.3	Foundation installation	105
1.8.4	Cable installation	130
1.9	Summary	156
1.10	References	156

## Tables

Table 1.1:	MIKE suite of models	3
Table 1.2:	Summary of Modelled Environmental Variation Scenarios	4
Table 1.3:	Summary of Key Resources	6
Table 1.4:	Summary of survey undertaken to inform physical processes	7
Table 1.5:	Tidal Levels at Standard Ports	12

## Figures

Figure 1.1:	Physical processes study area	2
Figure 1.2:	Model domain (blue outline)	5
Figure 1.3:	Marine Environmental Data Information Network (MEDIN) bathymetric data coverage	8
Figure 1.4:	Morgan and Mona Scoping Array bathymetric survey data coverage – Source: Gardline (2022) and XOcean (2022)	9
Figure 1.5:	Model bathymetry within the east Irish Sea	10
Figure 1.6:	Model mesh with section of Mona Offshore Wind Project array area inset	11
Figure 1.7:	Extent and bathymetry of Irish Seas tidal and storm surge model	12
Figure 1.8:	Availability of metocean datasets across the eastern Irish Sea	13
Figure 1.9:	Location of calibration data presented	14
Figure 1.10:	Comparison of model and admiralty harmonic tide data for Llandudno	16
Figure 1.11:	Comparison of model and recorded Mona FLidar – current speed and direction spring	16
Figure 1.12:	Comparison of model and recorded Mona FLidar – current speed and direction neap	16
Figure 1.13:	Comparison of model and recorded Morgan FLidar – current speed and direction spring	16

Figure 1.14:	Comparison of model and recorded Morgan FLidar – current speed and direction neap	17
Figure 1.15:	Comparison of modelled metocean and recorded depth averaged (DA) ASG and SIG – current speed and direction spring	17
Figure 1.16:	Comparison of modelled Morgan metocean and recorded ASG – spring surface elevation	17
Figure 1.17:	Comparison of modelled metocean and recorded DA ASG and SIG depth averaged– current speed and direction neap	17
Figure 1.18:	Comparison of modelled Morgan metocean and recorded ASG – neap surface elevation	18
Figure 1.19:	Comparison of model and recorded data BODC Location A – current speed and direction spring	18
Figure 1.20:	Comparison of model and recorded data BODC Location A – current speed and direction neap	18
Figure 1.21:	Comparison of model and recorded data BODC Location B – current speed and direction spring	18
Figure 1.22:	Comparison of model and recorded data BODC Location B – current speed and direction neap	19
Figure 1.23:	Comparison of model and recorded data BODC Location C – current speed and direction spring	19
Figure 1.24:	Comparison of model and recorded data BODC Location C – current speed and direction neap	19
Figure 1.25:	Comparison of model and recorded data BODC Location D – current speed and direction spring	19
Figure 1.26:	Comparison of model and recorded data BODC Location D – current speed and direction neap	20
Figure 1.27:	Comparison of model and recorded data BODC Location E – current speed and direction spring	20
Figure 1.28:	Comparison of model and recorded data BODC Location E – current speed and direction neap	20
Figure 1.29:	Tidal flow patterns – neap tide flood	21
Figure 1.30:	Tidal flow patterns – neap tide ebb	22
Figure 1.31:	Tidal flow patterns – spring tide flood	23
Figure 1.32:	Tidal flow patterns – spring tide ebb	24
Figure 1.33:	Wave rose for Mona Offshore Wind Project Array Area	25
Figure 1.34:	Wind rose for Mona Offshore Wind Project Array Area	26
Figure 1.35:	Location of wave calibration data presented	27
Figure 1.36:	Validation of modelled mean wave direction with measured data at CIV	28
Figure 1.37:	Validation of modelled significant wave height with measured data at CIV	28
Figure 1.38:	Validation of Modelled Peak Wave Period with Measured Data at CIV	28
Figure 1.39:	Validation of modelled mean wave direction with measured data at GyM	28
Figure 1.40:	Validation of modelled significant wave height with measured data at GyM	28
Figure 1.41:	Validation of modelled peak wave period with measured data at GyM	29
Figure 1.42:	Validation of modelled mean wave direction with measured data at RhF	29
Figure 1.43:	Validation of modelled significant wave height with measured data at RhF	29
Figure 1.44:	Validation of modelled peak wave period with measured data at RhF	29
Figure 1.45:	Wave roses for model boundaries - 22 year ECMWF Dataset and wind rose for 40 year NOAA dataset	31
Figure 1.46:	Wave climate 1:1 year storm from 000° MHW	32
Figure 1.47:	Wave climate 1:1 year storm from 090° MHW	33
Figure 1.48:	Wave climate 1:1 year storm from 240° MHW	34
Figure 1.49:	Wave climate 1:1 year storm from 270° MHW	35
Figure 1.50:	Wave climate 1:20 year storm from 000° MHW	36
Figure 1.51:	Wave climate 1:20 year storm from 090° MHW	37
Figure 1.52:	Wave climate 1:20 year storm from 240° MHW	38
Figure 1.53:	Wave climate 1:20 year storm from 270° MHW	39
Figure 1.54:	Littoral current 1:1 year storm from 270° - Flood Tide	41
Figure 1.55:	Littoral current 1:1 year storm from 270° - Ebb Tide	42
Figure 1.56:	Seabed classification British Geological Survey	44
Figure 1.57:	Seabed substrate geology EMODnet	45
Figure 1.58:	Residual current spring tide	47

Figure 1.59: Potential sediment transport over the course of 1 day (two tide cycles). ....	48	Figure 1.100: Suspended sediment concentration with sediment re-mobilisation – offshore export cable path. ....	94
Figure 1.60: Sediment transport – flood tide. ....	49	Figure 1.101: Average suspended sediment concentration during operation – offshore export cable path. ....	95
Figure 1.61: Sediment transport – ebb tide. ....	50	Figure 1.102: Average sedimentation during operation – offshore export cable path. ....	96
Figure 1.62: Residual current spring tide with 1:1 year storm from 270°. ....	51	Figure 1.103: Average sedimentation during operation – offshore export cable path detailed view. ...	96
Figure 1.63: Turbidity levels from the Morgan metocean site. ....	52	Figure 1.104: Sedimentation 1day following cessation of operation – offshore export cable path. ....	97
Figure 1.64: Distribution of average non-algal suspended particulate matter – CEFAS. ....	53	Figure 1.105: Sedimentation 1day following cessation of operation – offshore export cable path detailed view. ....	97
Figure 1.65: Modelled array and trenching route indicative layout. ....	54	Figure 1.106: Suspended sediment concentration during dredging phase– inter-array cable path. ...	99
Figure 1.66: Post-construction tidal flow pattern – flood tide. ....	56	Figure 1.107: Suspended sediment concentration during dumping phase– inter-array cable path...	100
Figure 1.67: Change in tidal flow (post-construction minus baseline) – flood tide. ....	57	Figure 1.108: Suspended sediment concentration with sediment re-mobilisation – inter-array cable path. ....	101
Figure 1.68: Change in tidal flow (post-construction minus baseline) Mona Offshore Wind Project array area – flood tide detail view. ....	58	Figure 1.109: Average suspended sediment concentration during operation – inter-array cable path.102	
Figure 1.69: Post-construction tidal flow pattern – ebb tide. ....	59	Figure 1.110: Average sedimentation during operation – inter-array cable path. ....	103
Figure 1.70: Change in tidal flow (post-construction minus baseline) – ebb tide. ....	60	Figure 1.111: Average sedimentation during operation – inter-array cable path detailed view. ....	103
Figure 1.71: Change in tidal flow (post-construction minus baseline) Mona Offshore Wind Project array area – ebb tide detailed view. ....	61	Figure 1.112: Sedimentation 1day following cessation of operation – inter-array cable path. ....	104
Figure 1.72: Post-construction wave climate 1in1 year storm 000° MHW. ....	63	Figure 1.113: Sedimentation 1day following cessation of operation – inter-array cable path detail view. ....	104
Figure 1.73: Change in wave climate 1in1 year storm 000° MHW (post-construction minus baseline). ....	64	Figure 1.114: Location of modelled piled installation for piling - Scenario A. ....	106
Figure 1.74: Post-construction wave climate 1in20 year storm 000° MHW. ....	65	Figure 1.115: Average suspended sediment concentration – pile installation Scenario A. ....	107
Figure 1.75: Change in wave climate 1in20 year storm 000° MHW (post-construction minus baseline). ....	66	Figure 1.116: Suspended sediment concentration day 1 flood - pile installation Scenario A. ....	108
Figure 1.76: Post-construction wave climate 1in20 year storm 090° MHW. ....	67	Figure 1.117: Suspended sediment concentration day 1 ebb - pile installation Scenario A. ....	109
Figure 1.77: Change in wave climate 1in20 year storm 090° MHW (post-construction minus baseline). ....	68	Figure 1.118: Suspended sediment concentration day 3 flood - pile installation Scenario A. ....	110
Figure 1.78: Post-construction wave climate 1in20 year storm 240° MHW. ....	69	Figure 1.119: Suspended sediment concentration day 3 ebb- pile installation Scenario A. ....	111
Figure 1.79: Change in wave climate 1in20 year storm 240° MHW (post-construction minus baseline). ....	70	Figure 1.120: Average sedimentation during pile installation – Scenario A. ....	112
Figure 1.80: Post-construction wave climate 1in20 year storm 270° MHW. ....	71	Figure 1.121: Average sedimentation during pile installation – Scenario A detail view. ....	112
Figure 1.81: Change in wave climate 1in20 year storm 270° MHW (post-construction minus baseline). ....	72	Figure 1.122: Sedimentation 1day following cessation of pile installation – Pile Scenario A. ....	113
Figure 1.82: Post-construction littoral current 1in1 year storm from 270° - Flood Tide. ....	74	Figure 1.123: Sedimentation 1day following cessation of pile installation – Pile Scenario A detail view. ....	113
Figure 1.83: Change in littoral current 1in1 year storm from 270° - flood tide (post-construction minus baseline). ....	75	Figure 1.124: Location of modelled piled installation for piling Scenario B. ....	114
Figure 1.84: Change in littoral current 1in1 year storm from 270° - flood tide (post-construction minus baseline) detailed view. ....	76	Figure 1.125: Average suspended sediment concentration – pile installation Scenario B. ....	115
Figure 1.85: Post-construction littoral current 1in1 year storm from 270° - ebb tide. ....	77	Figure 1.126: Suspended sediment concentration day 1 flood- pile installation Scenario B. ....	116
Figure 1.86: Change in littoral current 1in1 year storm from 270° - ebb tide (post-construction minus baseline). ....	78	Figure 1.127: Suspended sediment concentration day 1 ebb- pile installation Scenario B. ....	117
Figure 1.87: Change in littoral current 1in1 year storm from 270° - ebb tide (post-construction minus baseline) detailed view. ....	79	Figure 1.128: Suspended sediment concentration day 3 flood- pile installation Scenario B. ....	118
Figure 1.88: Post-construction residual current spring tide. ....	81	Figure 1.129: Suspended sediment concentration day 3 ebb- pile installation Scenario B. ....	119
Figure 1.89: Change in residual current spring tide (post-construction minus baseline). ....	82	Figure 1.130: Average sedimentation during pile installation – Scenario B. ....	120
Figure 1.90: Change in residual current spring tide (post-construction minus baseline) Mona Offshore Wind Project detailed view. ....	83	Figure 1.131: Average sedimentation during pile installation – Scenario B detail view. ....	120
Figure 1.91: Post-construction potential sediment over the course of 1day (two tide cycles). ....	84	Figure 1.132: Sedimentation 1day following cessation of pile installation – Pile Scenario B. ....	121
Figure 1.92: Difference in potential sediment transport over the course of 1day (post-construction minus baseline). ....	85	Figure 1.133: Sedimentation 1day following cessation of pile Installation – Pile Scenario B detail view. ....	121
Figure 1.93: Post-construction residual current 1in1 year storm from 270° spring tide. ....	86	Figure 1.134: Location of modelled piled installation for Piling Scenario C. ....	122
Figure 1.94: Change in residual current 1in1 year storm from 270° spring tide (post-construction minus baseline). ....	87	Figure 1.135: Average suspended sediment concentration – pile installation Scenario C. ....	123
Figure 1.95: Change in residual current 1in1 year storm from 270° spring tide (post-construction minus baseline) detailed view. ....	88	Figure 1.136: Suspended sediment concentration day 1 flood- Pile Installation Scenario C. ....	124
Figure 1.96: Sand wave clearance paths modelled. ....	89	Figure 1.137: Suspended sediment concentration day 1 ebb- pile installation Scenario C. ....	125
Figure 1.97: Location of Constable Bank in relation to the cable corridor. ....	91	Figure 1.138: Suspended sediment concentration day 3 flood- pile installation Scenario C. ....	126
Figure 1.98: Suspended sediment concentration during dredging phase– offshore export cable path. ....	92	Figure 1.139: Suspended sediment concentration day 3 ebb- pile installation Scenario C. ....	127
Figure 1.99: Suspended sediment concentration during dumping phase– offshore export cable path. ....	93	Figure 1.140: Average sedimentation during pile installation – Scenario C. ....	128
		Figure 1.141: Average sedimentation during pile installation – Scenario C detail view. ....	128
		Figure 1.142: Sedimentation 1day following cessation of pile installation – Pile Scenario C. ....	129
		Figure 1.143: Sedimentation 1day following cessation of pile installation – Pile Scenario C detail view. ....	129
		Figure 1.144: Modelled inter-array cable route. ....	130

**MONA OFFSHORE WIND PROJECT**

Figure 1.145: Average suspended sediment concentration during inter-array cable trenching. ....131

Figure 1.146: Suspended sediment concentration day 2 flood – inter-array cable installation. ....132

Figure 1.147: Suspended sediment concentration day 2 ebb – inter-array cable installation. ....133

Figure 1.148: Suspended sediment concentration day 3 flood – inter-array cable installation. ....134

Figure 1.149: Suspended sediment concentration day 3 ebb – inter-array cable installation. ....135

Figure 1.150: Suspended sediment concentration day 4 flood – inter-array cable installation. ....136

Figure 1.151: Suspended sediment concentration day 4 ebb – inter-array cable installation. ....137

Figure 1.152: Average sedimentation during inter-array cable installation.....138

Figure 1.153: Sedimentation 1day following cessation of inter-array cable installation. ....139

Figure 1.154: Modelled export cable route. ....140

Figure 1.155: Average suspended sediment concentration during offshore export cable trenching..141

Figure 1.156: Suspended sediment concentration day 2 peak flood – offshore export cable installation. 142

Figure 1.157: Suspended sediment concentration day 2 peak ebb – offshore export cable installation. ....143

Figure 1.158: Suspended sediment concentration day 3 peak flood – offshore export cable installation. ....144

Figure 1.159: Suspended sediment concentration day 3 peak ebb – offshore export cable installation. ....145

Figure 1.160: Suspended sediment concentration day 4 peak flood – offshore export cable installation. ....146

Figure 1.161: Suspended sediment concentration day 4 peak ebb – offshore export cable installation. ....147

Figure 1.162: Average sedimentation during offshore export cable installation. ....148

Figure 1.163: Sedimentation 1day following cessation of offshore export cable installation.....149

Figure 1.164: Modelled offshore export cables in the intertidal area. ....150

Figure 1.165: Average suspended sediment concentration during offshore export cables in the intertidal area trenching. ....151

Figure 1.166: Average suspended sediment concentration during offshore export cables in the intertidal area trenching detailed view. ....151

Figure 1.167: Suspended sediment concentration flood – offshore export cables in the intertidal area installation. ....152

Figure 1.168: Suspended sediment concentration ebb – offshore export cables in the intertidal area installation. ....153

Figure 1.169: Average sedimentation during offshore export cables in the intertidal area installation.154

Figure 1.170: Average sedimentation during offshore export cables in the intertidal area installation detail view. ....154

Figure 1.171: Sedimentation 1day following cessation of offshore export cables in the intertidal area installation. ....155

Figure 1.172: Sedimentation 1day following cessation of offshore export cables in the intertidal area installation detail view. ....155



## Glossary

Term	Meaning
Bathymetry	The measurement of depth of water in oceans, seas, or lakes.
Bed resistance coefficient	Represents the roughness or friction applied to the flow by the seabed.
Ebb tide	The tidal phase during which the water level is falling.
Erosion	Depletion of sediment in the intertidal region.
Fetch	Length in the wind direction of the marine area where water waves are generated by wind.
Flood tide	The tidal phase during which the water level is rising.
High Water Mark	The level reached by the sea at high tide.
Highest Astronomical Tide	The highest tidal height predicted to occur under average meteorological conditions and any combination of astronomical conditions.
Hydrodynamic boundary conditions	The conditions used in a model boundary which can include surface elevation and velocity which will affect the rest of the model domain. The boundary condition can vary with time and along the boundary.
Intertidal region	An area of a shoreline that is covered at high tide and uncovered at low tide.
Lee	Shelter from wind or weather given by an object.
Littoral currents	Flow derived from tide and wave climate.
Low Water Mark	The level reached by the sea at low tide.
Lowest Astronomical Tide	The lowest tidal height predicted to occur under average meteorological conditions and any combination of astronomical conditions.
Mean High Water	The highest water level reached during and average tide.
Mean High Water Spring	The most inshore level location reached by the sea at high tide during mean high water spring tide. This is defined as the average throughout the year, of two successive high waters, during a 24-hour period in each month when the range of the tide is at its greatest.
Mean Low Water Spring	The most offshore location reached by the sea at low tide during low water spring tide. This is defined as the average throughout the year, of two successive low waters, during a 24-hour period in each month when the range of the tide is at its greatest.
Mean Sea Level	The average tidal height over a long period of time.
Metocean	Refers to the syllabic abbreviation of meteorology and (physical) oceanography.
Neap tide	Tide that occurs when the sun and moon are at right angles to each other and the gravitational pull of the sun partially cancels out the pull of the moon on the ocean.
Refraction	The change in direction of a wave passing from one medium to another caused by its change in speed.
Residual current	The net flow over the course of the tidal cycle. This is effectively the driving force of the sediment transport.
Sandwave	A lower regime sedimentary structure that forms across from tidal currents.

Term	Meaning
Scour protection	Measures to prevent loss of seabed sediment around any structure placed in or on the seabed (e.g. by use of protective aprons, mattresses, rock and gravel placement).
Sedimentation	The process of settling or being deposited as a sediment.
Significant wave height	Mean wave height (trough to crest) of the highest third of the waves.
Slack tide	Tidal phase at which the current turns from flood to ebb (high-water slack tide) or from ebb to flood (low-water slack tide).
Spectral waves	Describes the distribution of wave energy with frequency (1/ period) and direction.
Spring tide	Tide that occurs when the sun and moon are directly in line with the Earth and their gravitational pulls on the ocean reinforce each other.
Suspended Particulate Matter	Particles that are suspended in the water column.
Turbidity	The quality of being cloudy, opaque, or thick with suspended matter.
Wave height	The distance from trough to crest of a wave.
Wave period	The time it takes for two successive crests (one wavelength) to pass a specified point.

## Acronyms

Acronym	Description
2D UHRS	2D Ultra High Resolution Seismic
ASG	Aanderaa Seaguard
BERR	Department for Business Enterprise and Regulatory Reform
BODC	British Oceanographic Data Centre
CCO	Coastal Channel Observatory
CD	Chart Datum (generally defined as LAT)
CEFAS	Centre for Environment, Fisheries and Aquaculture Science
CIV	Cleveleys
CPT	Core Penetration Test
DA	Depth Averaged
DHI	Danish Hydraulic Institute
DSV	Digital Sound Velocity
ECMWF	European Centre for Medium Range Forecasts
EMODnet	European Marine Observation and Data Network
ES	Environmental Statement
GyM	Gwynt y Môr
HAT	Highest Astronomical Tide

**MONA OFFSHORE WIND PROJECT**

Acronym	Description
HWM	High Water Mark
LAT	Lowest Astronomical Tide
LWM	Low Water Mark
MBES	Multi-Beam Echo Sounder
MDS	Maximum Design Scenario
MEDIN	Marine Environmental Data and Information Network
MHW	Mean High Water
MHWN	Mean High Water Neaps
MHWS	Mean High Water Springs
MLWN	Mean Low Water Neaps
MLWS	Mean Low Water Springs
NOAA	National Oceanic and Atmospheric Administration
OSP	Offshore Service Platform
PEIR	Preliminary Environmental Report
RhF	Rhyl Flats
SBM	Sub-Bottom Profiler
SIG	Nortek Signature
SPM	Suspended Particulate Matter
SSS	Side Scan Sonar
ST	Sediment Transport
UKCS	United Kingdom Continental Shelf
UKHO	United Kingdom Hydrographic Office

Unit	Description
m/s	Metres per second (speed)
mg/l	Milligrams per litre (suspended sediment concentration)

**Units**

Unit	Description
°	Degrees (angle from True north)
cm/s	Centimetre per second (speed)
mm	Millimetre (distance)
m	Metre (distance)
m <sup>3</sup>	Cubic metres (volume)
m <sup>3</sup> /h	Cubic metres per hour (rate of change)
km	Kilometre (distance)
m <sup>3</sup> /d/m	Cubic metres transported per day per metre width of transport path (i.e. perpendicular to direction of transport)

# 1 PHYSICAL PROCESSES TECHNICAL REPORT

## 1.1 Introduction

1.1.1.1 This physical processes technical report provides information relating to the physical environment and processes for the Mona Offshore Wind Project. The purpose of the technical report is to provide details of the supporting study undertaken by means of numerical modelling. It describes the current baseline conditions and quantifies the potential changes due to the installation and presence of the Mona Offshore Wind Project.

1.1.1.2 The preparation of a Preliminary Environmental Information Report (PEIR) and subsequent application is a live process with refinements being made to the project description throughout this period, as information is acquired from the range studies and assessments undertaken. For this reason, the modelled scenarios presented in this technical report will, inevitably, vary by a small degree from those ultimately assessed. However, due to the limited nature of these refinements, the technical report would remain a legitimate resource for supporting information. When disparities occur, they will be cited within the assessment with reference to the applicability of the modelled data presented in this report and used to support the assessment.

1.1.1.3 This report is divided into three main sections:

- Baseline conditions – describing current hydrography and sedimentology
- Environmental variations – describing changes to baseline arising from the installation and presence of the Mona Offshore Wind Project
- Construction phase changes – describing the dispersion and fate of sediment mobilised during construction phase activities.

1.1.1.4 For the purposes of this physical processes technical report, physical processes are defined as encompassing the following elements:

- Tidal elevations and currents
- Waves
- Bathymetry
- Seabed sediments
- Suspended sediments
- Sediment transport.

## 1.2 Study area

1.2.1.1 The Mona physical processes study area is illustrated in Figure 1.1 and defined as the:

- Mona Array Area (the area within which the wind turbines, foundations, inter-array cables, interconnector cables, offshore export cables and Offshore Substation Platforms (OSPs) forming part of the Mona Offshore Wind Project will be located)

- Mona Offshore Cable Corridor (the corridor located between the Mona Array Area and the landfall up to Mean High Water Springs (MHWS), in which the offshore export cables will be located)
- Landfall area
- Seabed and coastal areas that may be influenced by changes to physical processes due to the Mona Offshore Wind Project defined as one spring tidal excursion which is the distance suspended sediment is transported prior to being carried back on the returning tide.

1.2.1.2 It is however noted that the physical processes study area forms the focus for the assessment and that the numerical model extent is not limited to this region. The modelling study therefore also identifies any potential impacts beyond the physical processes study area.



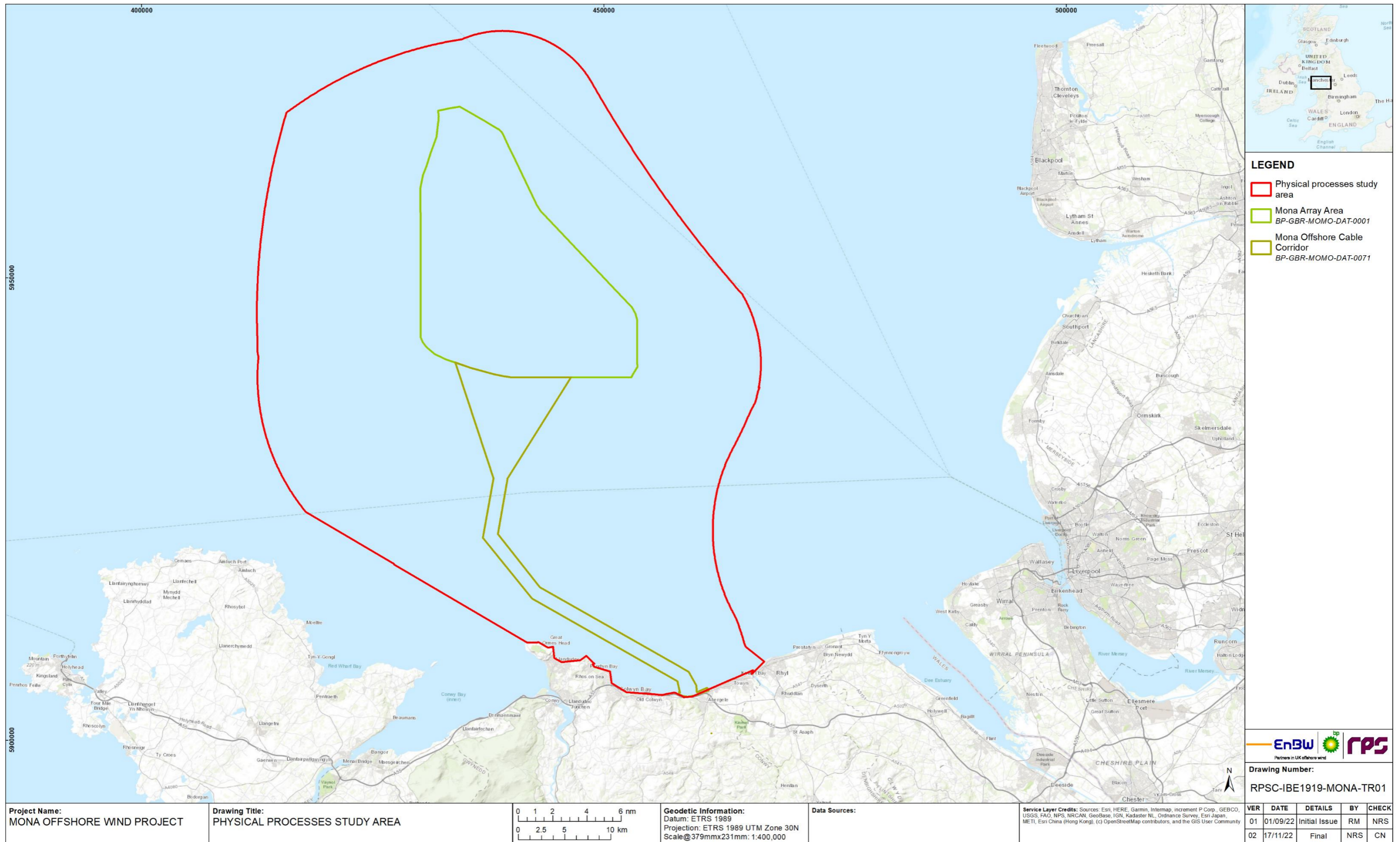


Figure 1.1: Physical processes study area.

### 1.3 Methodology

- 1.3.1.1 The physical processes study was undertaken to provide information of potential changes to physical processes and the fate of mobilised sediment during the construction phase by means of numerical modelling. Numerical models were developed and calibrated using a combination of publicly available datasets and those collected specifically for the Mona Offshore Wind Project.
- 1.3.1.2 These models were then implemented in comparative studies to determine the potential impact of the infrastructure on tidal flow, wave climate and sediment transport patterns for a representative project design scenario. It is noted that this method investigates the influence on the drivers of physical processes rather than instigating detailed morphological studies. In the event that significant potential impacts were identified more detailed studies may be required, such as three-dimensional modelling where density stratified regions may be impacted.
- 1.3.1.3 The models were also used to undertake simulations of site preparation, cable trenching and pile installation activities to quantify potential increases in suspended sediment concentration and subsequent deposition. This information was then applied in the context of the physical processes environmental impact assessment and those of related disciplines.

#### Numerical modelling

- 1.3.1.4 Numerical modelling techniques were used to describe tide, wave and sediment transport regimes. The MIKE suite of software was employed, as a single model mesh could be used to simulate these processes both individually and in combination. The model domain is shown in Figure 1.2. The MIKE suite of models is a widely used industry standard modelling suite developed by the Danish Hydraulic Institute (DHI). It has been approved for use by industry and government bodies including Natural Resources Wales. The MIKE suite is a modular system that contains a number of different but complementary modules encompassing different physical processes: these are summarised in Table 1.1 and described in further detail within the relevant sections. A summary of the modelled environmental scenarios is provided in Table 1.2.

**Table 1.1: MIKE suite of models.**

Simulation	Model	Description
Baseline and post-construction tidal flow	MIKE21 Flexible Mesh (FM) modelling system	The FM Module is a 2-dimensional, depth averaged hydrodynamic model which simulates the water level variations and flows in response to a variety of forcing functions in lakes, estuaries and coastal areas. The water levels and flows are resolved on a mesh covering the area of interest when provided with bathymetry, bed resistance coefficient, wind field, hydrodynamic boundary conditions, etc.
Baseline and post-construction wave climate	MIKE21 Spectral Wave (SW)	The wave modelling was undertaken using the spectral wave model, MIKE21 SW. The waves were computed on the same grid as the tidal flows. The model resolves the wave field by simulating wind generation of waves within the model domain and the propagation of externally generated swell waves through the domain. The model setup ensured that the detail of both locally generated wind waves and swell conditions from further afield were captured.

Simulation	Model	Description
Baseline and post-construction littoral currents	MIKE21 FM and SW	The MIKE suite facilitates the coupling of models. The depth averaged hydrodynamic model, used for the tidal modelling, coupled with a spectral wave model, provides a full wave climate incorporating the impact of water levels and currents on waves and wave breaking. Using this, the littoral currents (i.e. those currents driven by tidal, wave and meteorological forces) were examined.
Baseline and post-construction sediment transport	MIKE21 Sand Transport (ST)	This module enables assessment of bed sediment transport rates and initial rates of bed level change for non-cohesive sediment resulting from currents or combined wave-current flows. The model combines inputs from both the hydrodynamic model and, if required, the wave propagation model. It uses sediment size and gradation to determine the bed level changes and sediment transport rates.
Foundation installation	MIKE21 Mud Transport (MT)	A sample of four representative pile installation scenarios were simulated to cover the range of conditions across the Mona Offshore Wind Project array area both in terms of tidal currents and sediment type. The MIKE Mud Transport (MT) module allows the modelling of erosion, transport and deposition of cohesive and cohesive/granular sediments. This model is suited to sediment releases in the water column and allows sediment sources which may vary spatially and temporally.
Cable installation	MIKE21 Particle Tracking (PT)	The Particle Tracking module was implemented for cable installation as it has the advantage that it could be used to describe the transport of material released in a specific part of the water column. In this way, the dispersion would not be over-estimated, or the corresponding sedimentation underestimated.



**Table 1.2: Summary of Modelled Environmental Variation Scenarios.**

Variation/operation	Description	Parameter modelled
Hydrography Section 1.7.2	Models updated to take account of the installation of the Mona Offshore Wind Project and associated features to quantify: <ul style="list-style-type: none"> <li>Changes to tidal currents;</li> <li>Changes to wave climate; and</li> <li>Changes to littoral currents.</li> </ul>	<ul style="list-style-type: none"> <li>Wind turbines: 68 installations with four-legged suction bucket foundations, each jacket leg with a diameter of 5m, spaced 48m apart, and each bucket with a diameter of 16m. Scour protection to a height of 2.5m. Total footprint of 10,816m<sup>2</sup> per wind turbine</li> <li>OSPs: four installations with three-legged suction bucket foundations, each jacket leg with a diameter of 3m, spaced 30m apart, and each bucket with a diameter of 14m. Scour protection to a height of 2.5m. Total footprint of 3,277m<sup>2</sup> footprint per OSP</li> <li>Inter-array cables: cable protection with a height of 3m and 5m width. Cable crossings, each crossing with a height of 4m, a width of 32m and a length of 60m</li> <li>Interconnector cables: cable protection with a height of 3m and 10m width. Cable crossings, each crossing with a height of 3m, a width of 20m and a length of 50m</li> <li>Export cables: cable protection with a height of 3m and 10m width. Cable crossings, each crossing with a height of 3m, a width of 30m and a length of 50m</li> </ul>
Sedimentology Section 1.7.3	Models updated to take account of the installation of the Mona Offshore Wind Project and associated features to quantify: <ul style="list-style-type: none"> <li>Changes to sediment transport characteristics.</li> </ul>	As above with the addition of: <ul style="list-style-type: none"> <li>Scour protection simulated using an area of fixed bed around each structure.</li> </ul>
Seabed features clearance Section 1.8.2	Dispersion modelling relating to sandwave clearance. Dredging of sandwave crest and disposal at troughs is undertaken in a cycle along cable routes.	<ul style="list-style-type: none"> <li>Clearance is undertaken at 100m/h along 5km sample cable routes of a width of 104m with dredging undertaken at 10,000m<sup>3</sup>/h with a spill rate of 3%.</li> <li>Mona Offshore Cable Corridor clearance is undertaken to an average depth of 5.1m;</li> <li>Inter-array cable clearance is undertaken to an average depth of 5.1m;</li> <li>With sediment released through water column.</li> </ul>

Variation/operation	Description	Parameter modelled
Augured pile installation Section 1.8.3	Dispersion modelling of suspended sediment arising from augured pile installation. Under a range of tidal conditions.	Four sample scenarios are presented, in each case: <ul style="list-style-type: none"> <li>Piles are 16m in diameter and 60m deep;</li> <li>Two adjacent operations occur simultaneously.</li> <li>Drilling undertaken at 0.89m/h;</li> <li>13,460m<sup>3</sup> of material mobilised per pile;</li> <li>Released throughout water column.</li> </ul>
Cable installation Section 1.8.4	Dispersion modelling of suspended sediment arising from cable installation via trenching. Relating to <ul style="list-style-type: none"> <li>Offshore export cable</li> <li>Inter-array cable</li> <li>Intertidal cable</li> </ul>	For offshore and inter-array cables sample trenching operations are presented. <ul style="list-style-type: none"> <li>Trench 3m wide at seabed and 3m deep with triangular cross section;</li> <li>Trenching is undertaken at 450m/h;</li> </ul> Intertidal trenching is undertaken for an 800m route over an eight hour period for a trench 1m wide and 3m deep.



MONA OFFSHORE WIND PROJECT

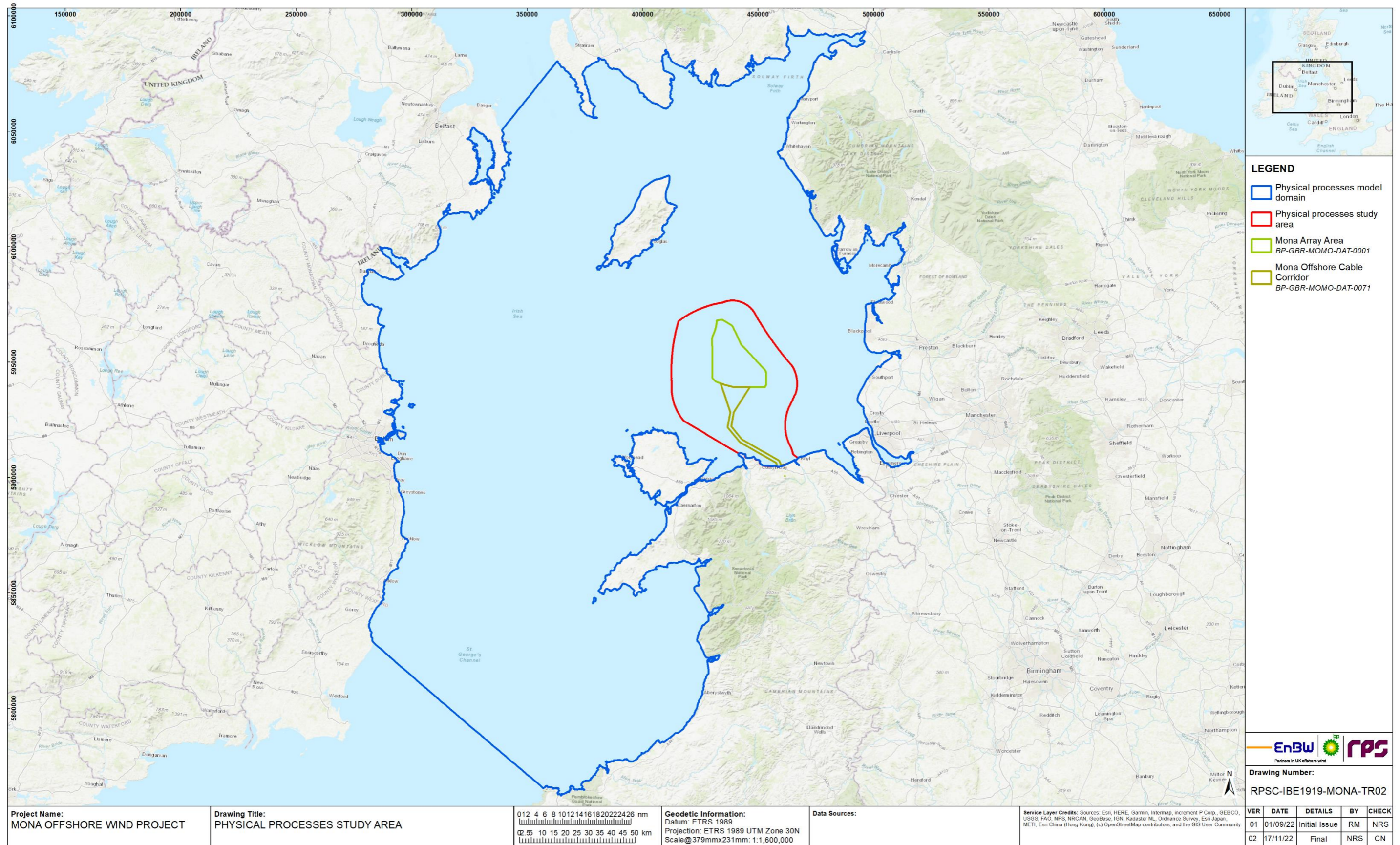


Figure 1.2: Model domain (blue outline).



## 1.4 Desktop study

1.4.1.1 Information on the physical environment within the physical processes study area and beyond to the model domain was collected through a detailed desktop review of existing studies and datasets. These are summarised in Table 1.3.

**Table 1.3: Summary of Key Resources.**

Title	Source	Year	Author
European Marine Observation and Data Network (EMODnet) – Seabed classification	<a href="https://www.emodnet-geology.eu/">https://www.emodnet-geology.eu/</a>	2022	EMODnet
European Marine Observation and Data Network (EMODnet) – Bathymetry data	<a href="https://www.emodnet-bathymetry.eu/">https://www.emodnet-bathymetry.eu/</a>	2022	EMODnet
European Marine Observation and Data Network (EMODnet) – Metocean data	<a href="https://map.emodnet-physics.eu/">https://map.emodnet-physics.eu/</a>	2022	EMODnet
Department for Environment Food and Rural Affairs – Bathymetry data	<a href="https://environment.data.gov.uk/DefraDataDownload">https://environment.data.gov.uk/DefraDataDownload</a>	2022	DEFRA
National Oceanic and Atmospheric Administration (NOAA) – Atmospheric data	DHI Metocean Data Portal	2022	NOAA
National Network of Regional Coastal Monitoring Programmes	<a href="https://coastalmonitoring.org/cc/o/">https://coastalmonitoring.org/cc/o/</a>	2022	Coastal Channel Observatory
Centre for Environment, Fisheries and Aquaculture Science (CEFAS) – wave data	<a href="https://wavenet.cefas.co.uk/map">https://wavenet.cefas.co.uk/map</a>	2022	CEFAS
ABPmer Data explorer	<a href="https://www.seastates.net/explore-data/">https://www.seastates.net/explore-data/</a>	2022	ABPmer
Hydrography of the Irish Sea, SEA6 Technical Report	UK Government	2005	Howarth M.J.
Atlas of UK Marine Renewable Energy Resources	<a href="https://www.renewables-atlas.info/">https://www.renewables-atlas.info/</a>	2022	ABPmer
Geology of the seabed and shallow subsurface: The Irish Sea.	British Geological Survey	2015	Mellett <i>et al.</i>
British Geological Survey – sediment sample data	<a href="https://mapapps2.bgs.ac.uk/geoindex_offshore">https://mapapps2.bgs.ac.uk/geoindex_offshore</a>	2022	BGS
Suspended Sediment Climatologies around the UK.	Department for Business, Energy & Industrial Strategy (BEIS)	2016	Cefas
Metocean Data collection for the Ormonde offshore wind project.	Marine Data Exchange	2011	Geotechnical Engineering and Marine Surveys (GEMS)
Irish Sea Zone Hydrodynamic measurement campaign	Marine Data Exchange	2010-2013	EMU Ltd (now Fugro Ltd)

Title	Source	Year	Author
Admiralty Tide Tables	United Kingdom Hydrographic Office (UKHO)	2022	UKHO
Marine Environmental Data Information Network (MEDIN) Seabed Mapping Programme	Admiralty Marine Data Portal	2022	MEDIN
Integrated Mapping for the Sustainable Developments of Ireland’s Marine Resource (INFOMAR) Seabed Mapping Programme	Geological Survey Ireland (GSI) and Marine Institute	2022	INFOMAR
Long term wind and wave datasets	European Centre for Medium-range Weather Forecast (ECMWF)	2022	ECMWF
UK tide gauge network and database of current observation	British Oceanographic Data Centre (BODC)	2021	BODC
UK Climate Projections (UKCP)	Met Office	2018	Met Office
A user-friendly database of coastal flooding in the UK from 1915-2014	Scientific Data (journal)	2015	Haigh <i>et al.</i>
British Oceanographic Data Centre	National Oceanography Centre	various	National Oceanography Centre
Review of aggregate dredging off the Welsh coast	HR Wallingford	2016	HR Wallingford

## 1.5 Site-specific surveys

1.5.1.1 A summary of the surveys undertaken of relevance to physical processes and utilised within the physical processes modelling study is outlined in Table 1.4. Results from recent geophysical and benthic surveys of the cable corridor route available after the model study completion will be used to verify the data used within the physical processes modelling and to inform the Environmental Statement (ES).

**Table 1.4: Summary of survey undertaken to inform physical processes.**

Title	Extent of survey	Overview of survey	Survey contractor	Date	Reference to further information
Environmental Baseline Surveys and Habitat Assessments	Mona Array Area	Geophysical survey to determine characteristics of seabed sediment, characterise benthic communities (infauna and epifauna) and identification of any environmentally significant habitats (e.g., potential Habitats Directive Annex I and priority marine features).  Deployment included multi-beam echo sounder (MBES), digital sound velocity (DSV) sensor, side scan sonar system (SSS), Sub-Bottom Profiler (SBP) & 2D Ultra High Resolution Seismic (2D UHRS) sensor. Additionally, seabed imagery was collected along with grab samples and core penetration testing (CPT).	Gardline Ltd	June to September 2021	Gardline (2022)
Geophysical survey	Mona Array Area	Geophysical survey to establish bathymetry, seabed sediment and identify seabed features.  Deployment included MBES with multibeam backscatter.	XOCEAN Ltd	June 2021 to March 2022	XOCEAN (2022)
Metocean survey	Morgan and Mona Array Area	Metocean and FLidar deployments to ascertain wind, wave, and tidal currents.	Fugro	November 2021 to November 2022	Fugro (2022)

## 1.6 Baseline environment

### 1.6.1 Bathymetry

1.6.1.1 The model domain had full bathymetry data coverage and was populated using a combination of data sources. The site-specific geophysical survey undertaken for both the Morgan and Mona Array Areas and the resulting bathymetry data, as detailed in Table 1.4, was used to populate the model. The extent of this survey data is shown in Figure 1.4, Gardline (2022) and XOcean (2022).. The survey data provided to Lowest Astronomical Tide (LAT) vertical datum was converted to model mean sea level datum using reference values published by Admiralty.

1.6.1.2 Where additional data was required for the model extent beyond the survey area, bathymetry data was sourced from the Marine Environmental Data Information Network (MEDIN) Seabed Mapping Programme via the Admiralty Marine Data Portal as shown in Figure 1.3. Each of the datasets for the east Irish Sea area was combined into a single set giving priority to the most recent survey data. For areas within region which did not have coverage from the MEDIN dataset further data was sourced from the DEFRA Survey Data Download site. This was undertaken for specific bays such as Conwy Bay and the Dee Estuary.

1.6.1.3 For the remaining model domain, the European Marine Observation and Data Network (EMODnet) 100m resolution tiled data was utilised. This database is available under the European Inspire Directive and provides access to data in a variety of formats, datums and resolutions based on a combination of survey datasets. All data was converted, where necessary, to mean sea level datum generally with a resolution of at least three times the mesh resolution to ensure that coastal features were represented within the numerical modelling, as illustrated in Figure 1.5.

1.6.1.4 The resolution of the model bathymetry was designed to reflect variations in water depth and bed forms for the accurate simulation of tidal currents. Additional model resolution was also included to incorporate the installation of the Mona Offshore Wind Project. This enabled the same cell arrangement to be used for the baseline and post-construction assessment, thereby avoiding the introduction of any numerical mesh effects into the assessment. Across the Mona Offshore Wind Project the resolution varied between circa 50m down to 10m in order that the influence of scour protection on the tidal flow and sediment transport for the Mona Offshore Wind Project could be quantified. With increasing distance from the physical processes study area, the cell size was increased but maintained at a level which retained model accuracy. Figure 1.6 illustrates the mesh resolution with an inset of the mesh within the Mona Array Area.

1.6.1.5 The extent of the domain, Figure 1.2, was designed to provide the basis for a model which could be utilised for tide, wave and sediment transport modelling. The focus of the study is a tidal excursion from the Mona Offshore Wind Project to quantify any changes due to the installation however a larger domain is required to develop wave fields and ensure that tidal currents are simulated and had the benefit of identifying any potential effects beyond the physical processes study area.



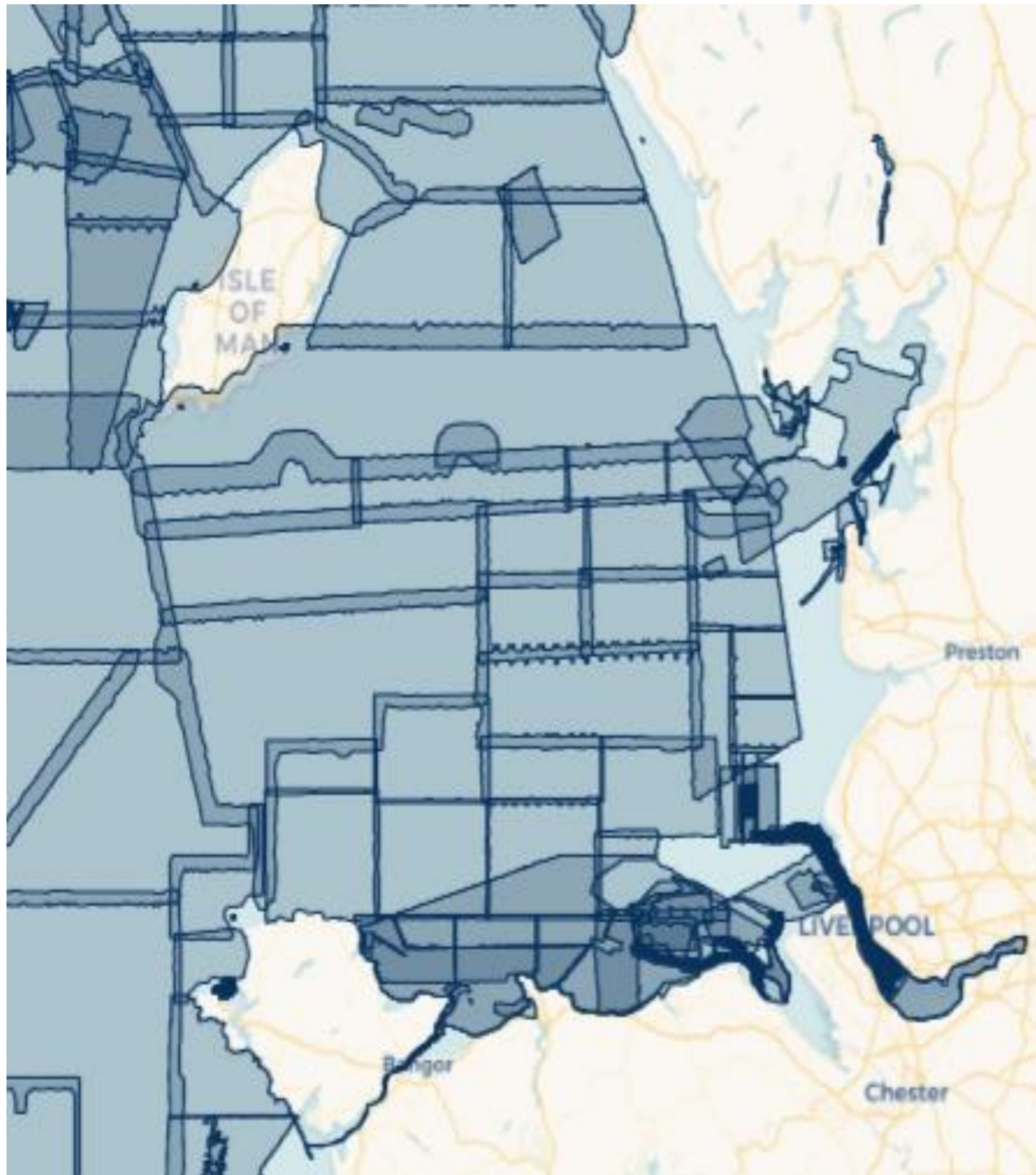


Figure 1.3: Marine Environmental Data Information Network (MEDIN) bathymetric data coverage.

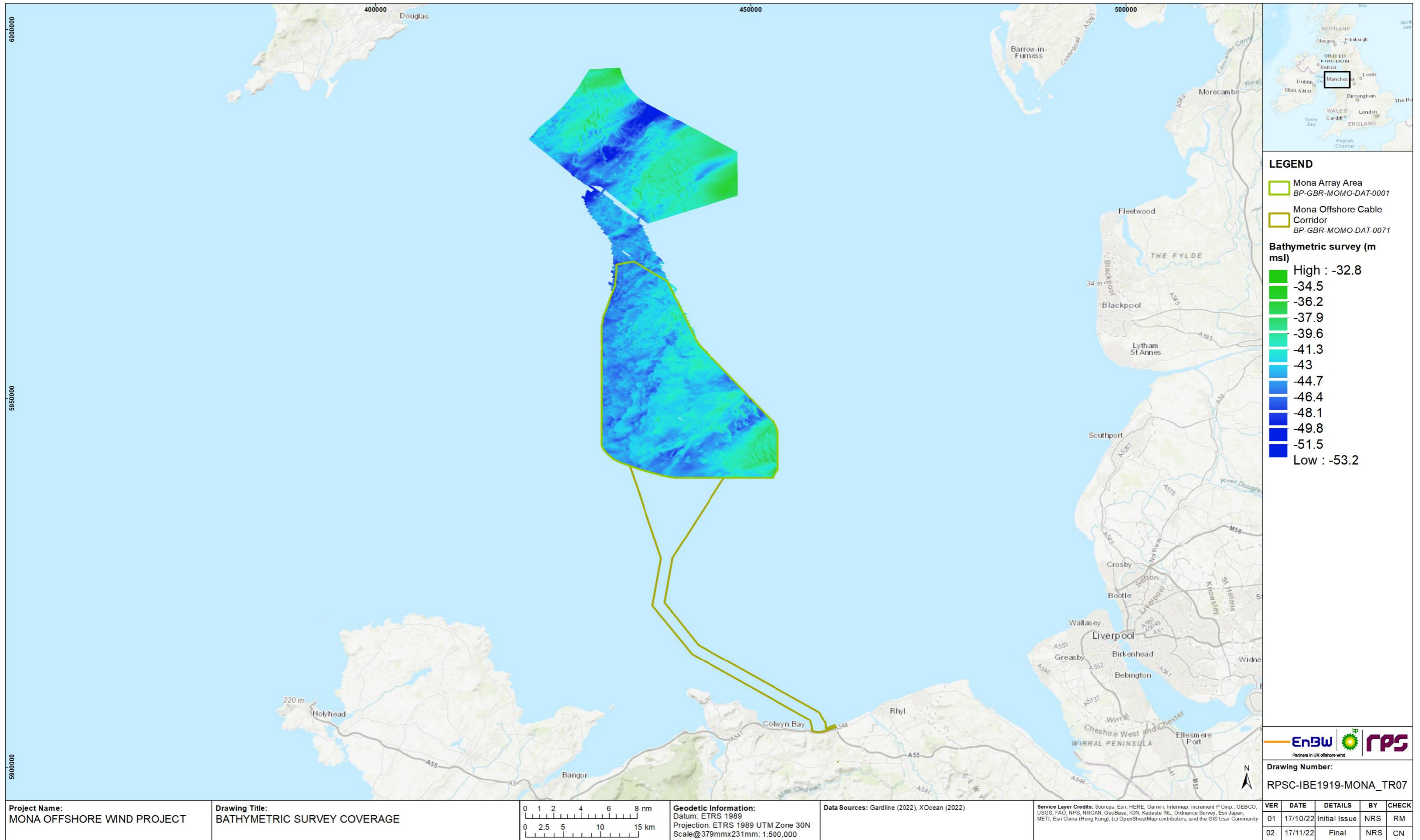


Figure 1.4: Morgan and Mona Scoping Array bathymetric survey data coverage – Source: Gardline (2022) and XOcean (2022).



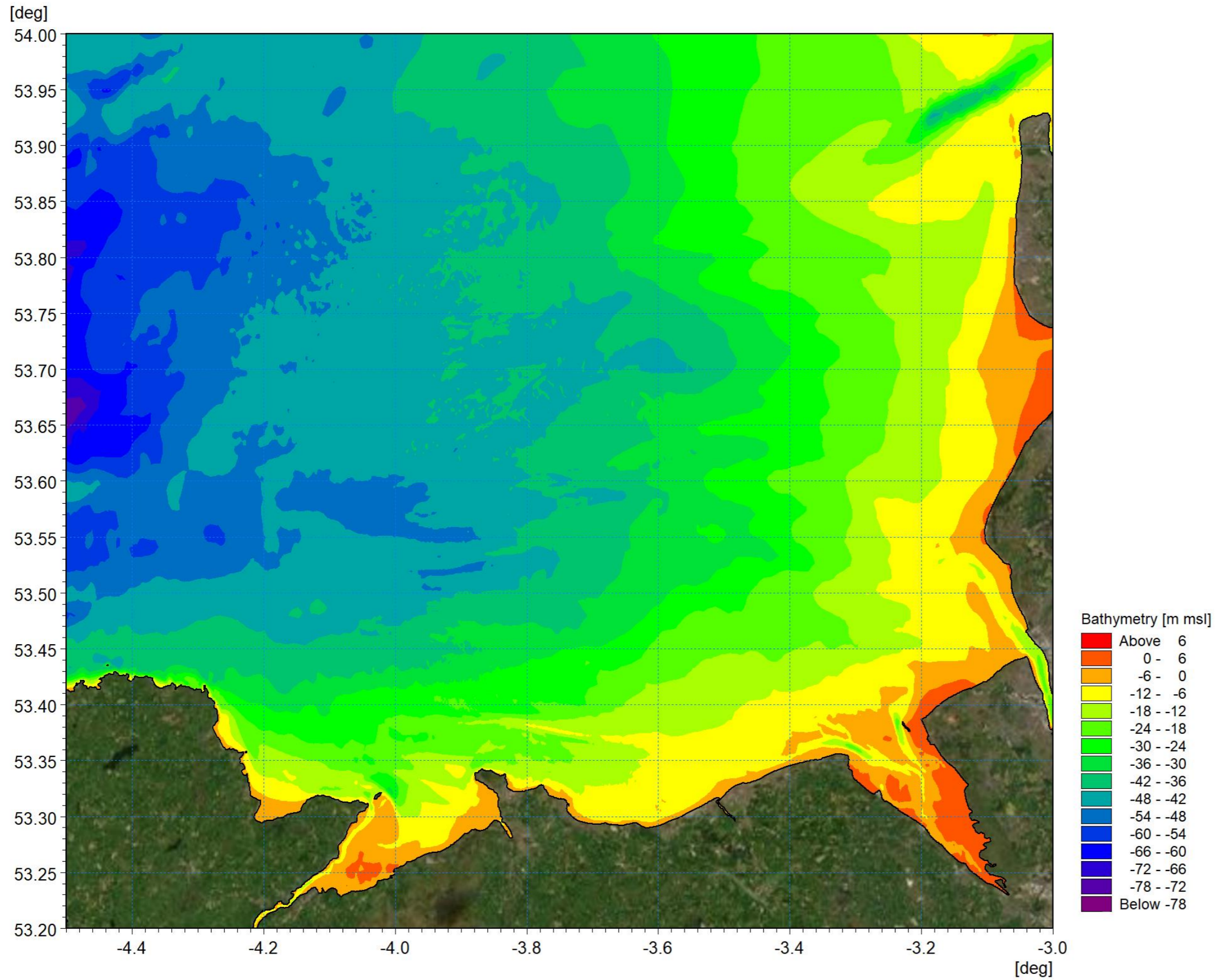


Figure 1.5: Model bathymetry within the east Irish Sea.



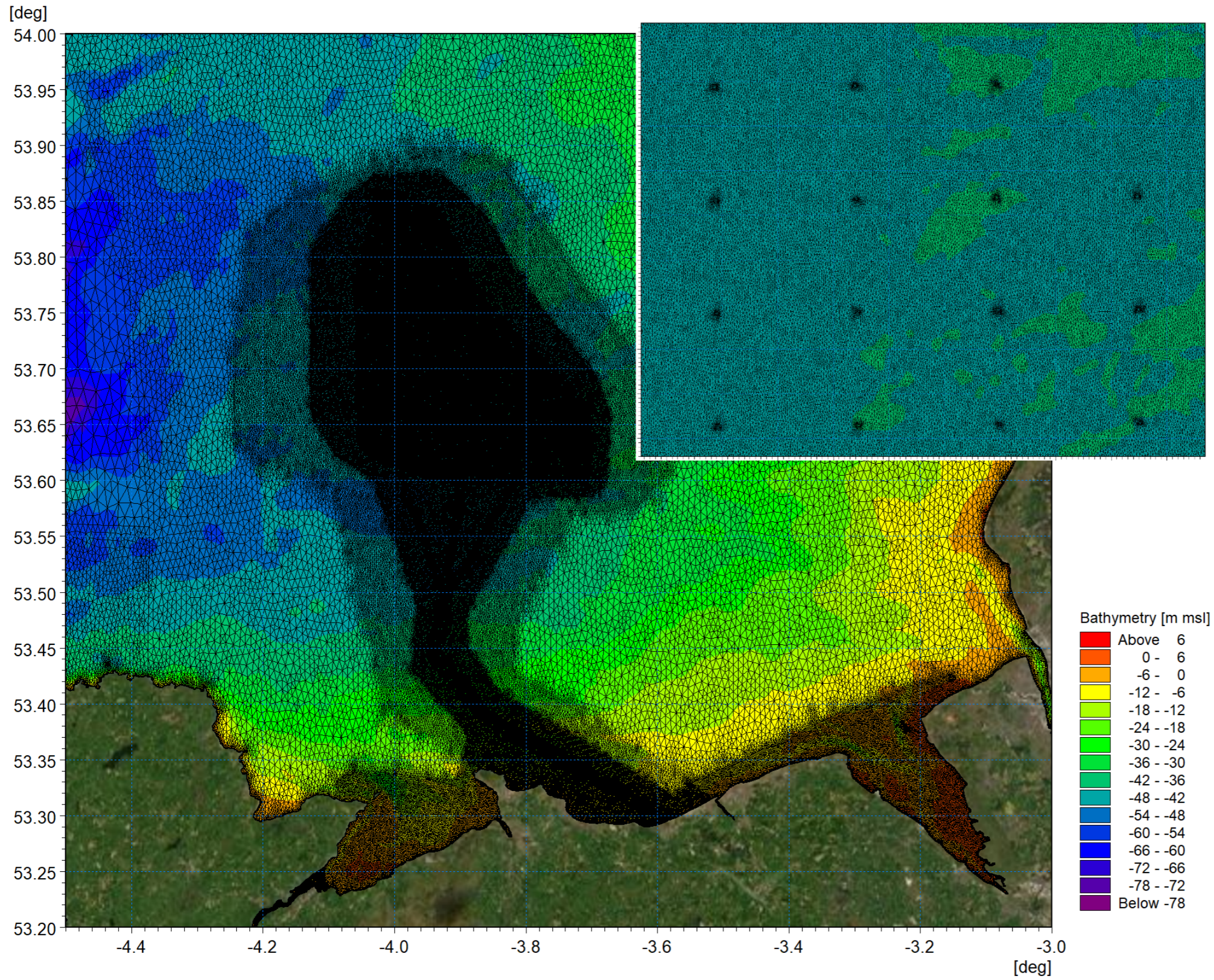


Figure 1.6: Model mesh with section of Mona Offshore Wind Project array area inset.



## 1.6.2 Hydrography

1.6.2.1 The UKHO states that the mean tidal range at the Standard Port of Holyhead is approximately 3.65m whilst at Douglas it is 4.55m. The tidal characteristics shown in Table 1.5 in metres referenced to Chart Datum (CD):

**Table 1.5: Tidal Levels at Standard Ports.**

Tidal level (m CD)	Holyhead	Douglas
Lowest Astronomical Tide (LAT)	0.0	-0.3
Mean Low Water Springs (MLWS)	0.7	0.8
Mean Low Water Neaps (MLWN)	2.0	2.4
Mean Sea Level (MSL)	3.3	3.8
Mean High Water Neaps (MHWN)	4.4	5.4
Mean High Water Springs (MHWS)	5.6	6.9
Highest Astronomical Tide (HAT):	6.3	7.9

1.6.2.2 The semi-diurnal tides are the dominant physical process in the Irish Sea moving into the Irish Sea from the Atlantic Ocean through both the North Channel and St. George’s Channel. The tidal range in the Irish Sea is highly variable with the range in Liverpool Bay exceeding 10m on the largest spring tides, the second largest in Britain.

1.6.2.3 The tidal flow simulations which form the basis of the study were undertaken using the MIKE21 FM flexible mesh modelling system. The FM Module is a two-dimensional, depth averaged hydrodynamic model which simulates the water level variations and flows in response to a variety of forcing functions in lakes, estuaries and coastal areas. The water levels and flows are resolved on a mesh covering the area of interest when provided with bathymetry, bed resistance coefficient, hydrodynamic boundary conditions, etc.

1.6.2.4 The tidal model was driven using boundary conditions extracted from RPS’ Tide and Storm Surge Forecast (TSSF) model of Irish coastal waters (RPS, 2018), the extent and bathymetry of which is illustrated in Figure 1.7. This model was also developed using flexible mesh technology with the mesh size (model resolution) varying from circa 24km along the offshore Atlantic boundary to circa 200m around the Irish coastline. These boundaries were fully defined ‘flather’ boundaries for which both surface elevation and current vectors are specified.

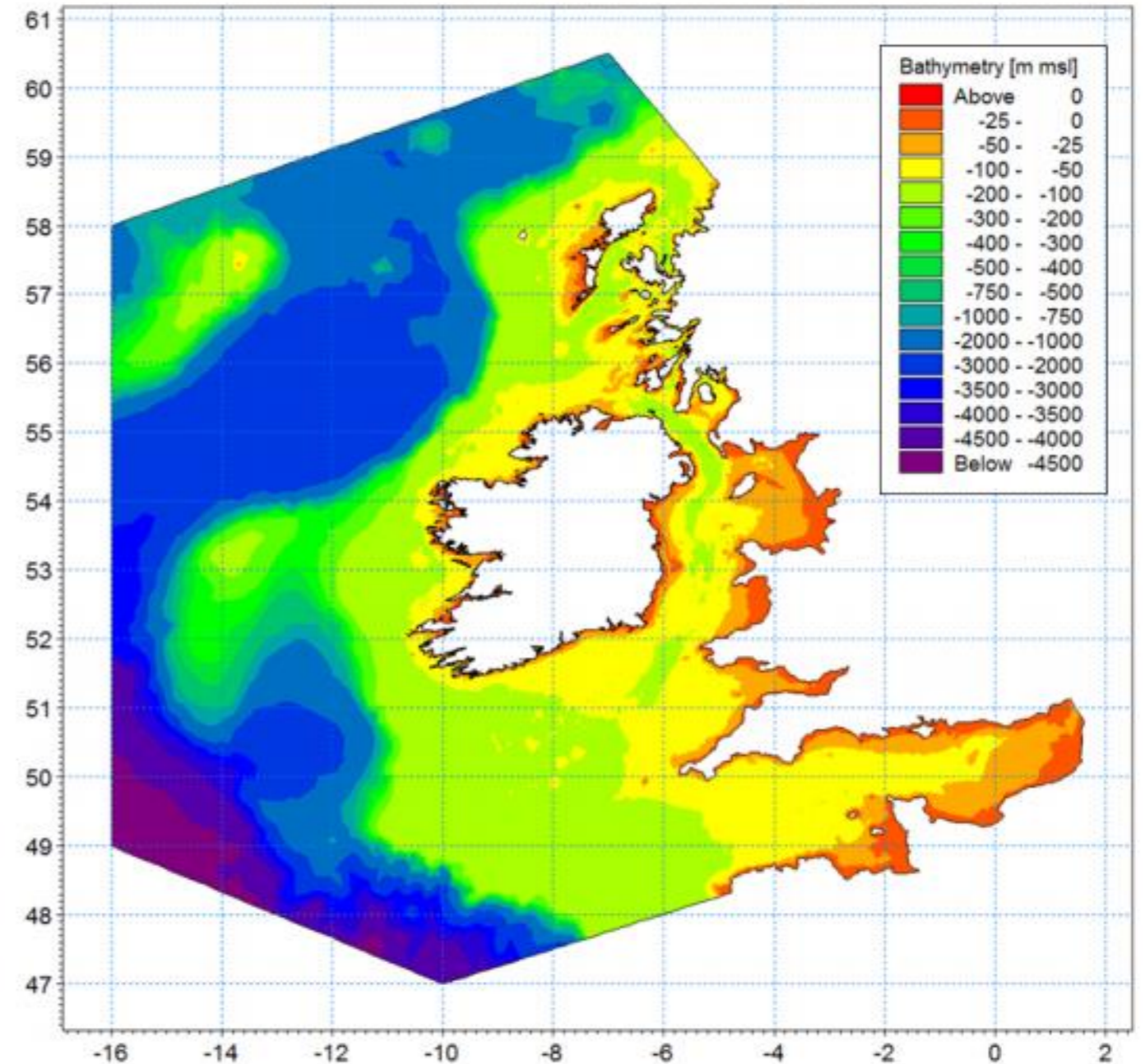


**Figure 1.7: Extent and bathymetry of Irish Seas tidal and storm surge model.**

1.6.2.5 A large amount of hydrometric data was available across the model domain as detailed in Table 1.3. The principal resources such as Admiralty tidal harmonics, British Oceanographic Data Centre (BODC) and Coastal Channel Observatory (CCO) are illustrated in Figure 1.8 with a range of these datasets being implemented during model calibration. The locations of the selection of calibration data presented in this document for tidal flow is shown in Figure 1.9.



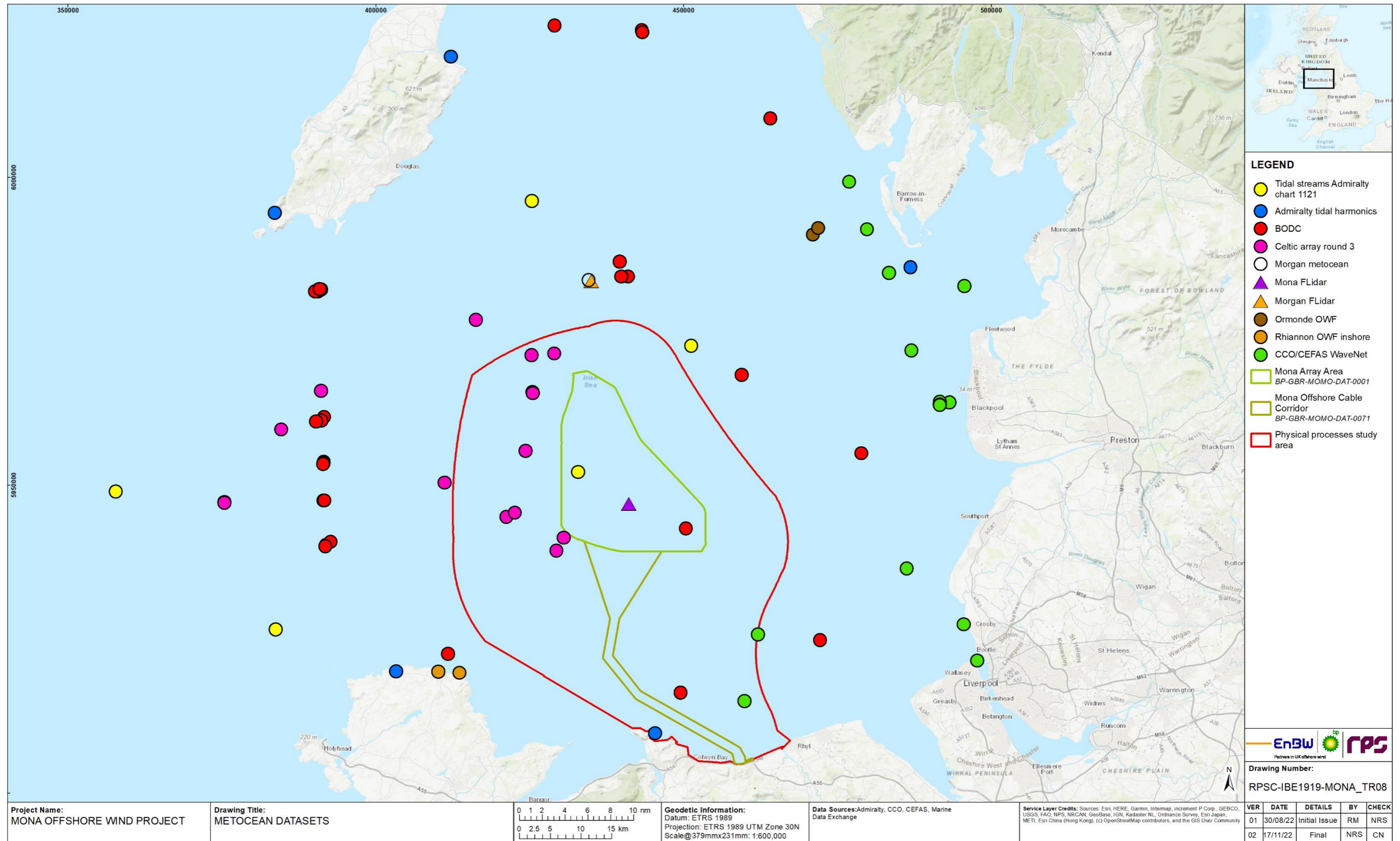


Figure 1.8: Availability of metocean datasets across the eastern Irish Sea.



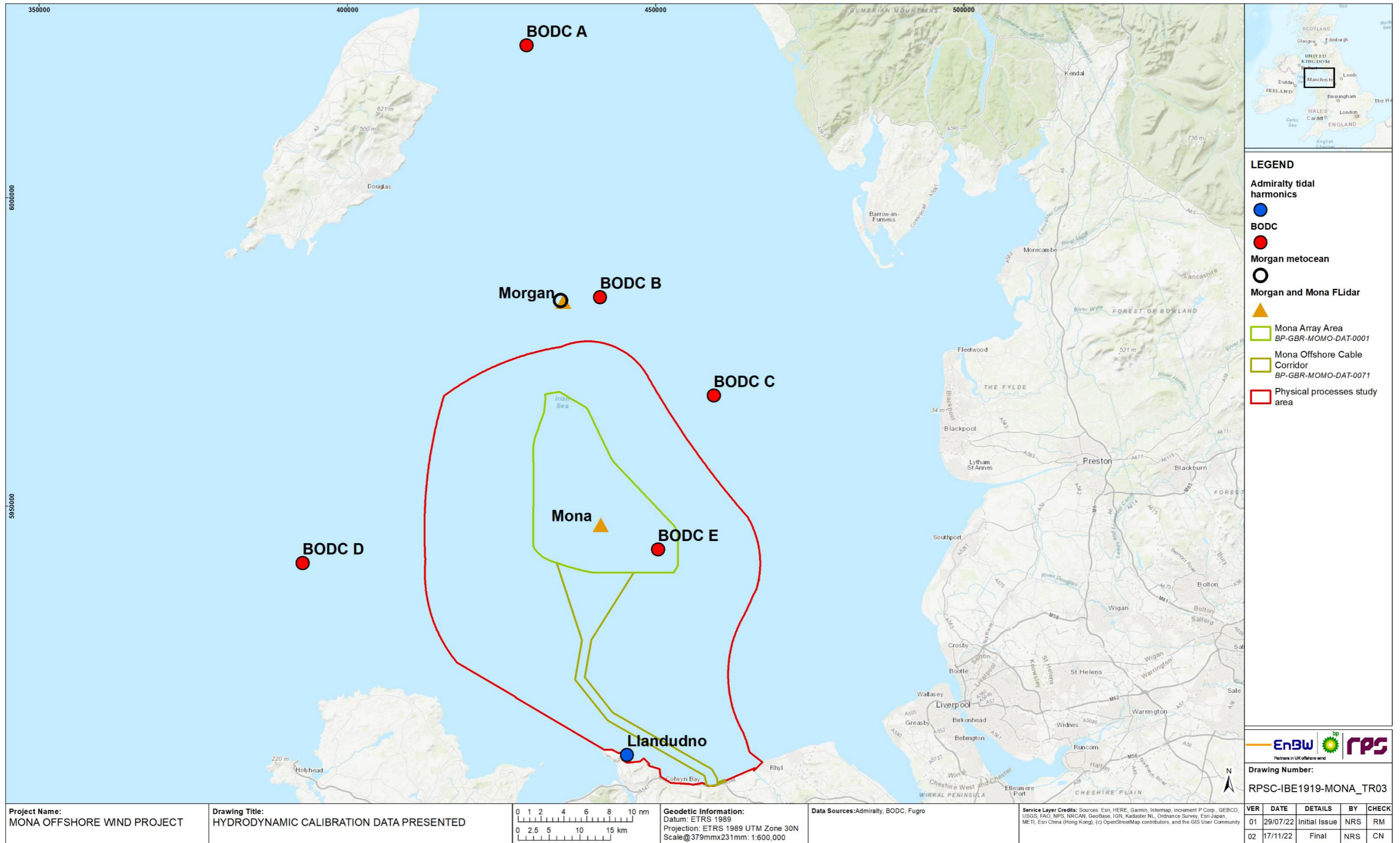


Figure 1.9: Location of calibration data presented.

- 1.6.2.6 Figure 1.10 shows the comparison of the modelled (red) and Admiralty tidal levels predicted from harmonic analysis (blue) at Llandudno. The model correlated well through both spring and neap tidal phases. The comparative study undertaken to quantify the potential changes in tidal currents was undertaken during both and neap spring tides to ensure a wide range of tidal conditions were applied in the modelling. The validation data presented therefore includes both tidal phases for each location.
- 1.6.2.7 For site specific calibration data, Mona floating lidar plots (FLidar) are presented first illustrating spring and neap tides within the Mona Array Area. Each plot displays the current speed data on the left axis and the current direction on the right axis. The modelled depth average current speed is shown by a red trace and current direction by an orange trace. The measured data was collected at various water depths noted within the legend.
- 1.6.2.8 The Mona FLidar and Morgan FLidar tidal current data are presented in Figure 1.11 to Figure 1.14 and show similar trends in that current speeds during neap tides are half of the speed during spring tides. As well as the flood tide approaching from an easterly direction with the ebb tide being slightly weaker. The modelled data fits within the range of the Mona and Morgan measured data following similar tidal flow patterns
- 1.6.2.9 Figure 1.15 to Figure 1.17 show the comparison between the Aanderaa Seaguard (ASG) and Nortek Signature (SIG) measuring devices against modelled metocean data during different tidal phases. The two devices were deployed at the Morgan site and the depth averaged (DA) current speed and direction are reported. The model current directionality correlates between both the ASG and SIG devices however current speeds between the model and ASG are more correlated than with the SIG device during the spring tide. In the neap tidal phase, the device speed and direction are within the range of the modelled data however the correlation is weaker than during the spring tidal phase. Comparisons of surface elevation between the ASG and modelled data are illustrated for both spring and neap tidal phases in Figure 1.16 and Figure 1.18.
- 1.6.2.10 For each location of BODC data, a pair of plots are presented firstly relating to spring tides and secondly neap tides. In each plot the current speed data is presented on the left axis whilst the current direction is presented to the right. The modelled depth average current speed is shown by a red trace and current direction by an orange trace. The measured data was collected at various water depths noted within the legend.
- 1.6.2.11 Sites A and B are presented in Figure 1.19 to Figure 1.22 and indicate that the flood tide which approaches the Mona Offshore Wind Project from an easterly direction is more dominant than the ebb tide. Peak neap tidal current speeds are typically half of those experienced during spring tide. The modelled data largely lie within the range of the measured data and replicates the asymmetric tidal flows patterns.
- 1.6.2.12 This is also the case for site C shown in Figure 1.23 and Figure 1.24 for spring and neap respectively. Current directions and the dominance of flood tides are replicated with the model domain. Tidal currents at site D are more strongly bi-directional as flow is accelerated around Anglesey as illustrated in Figure 1.25 and Figure 1.26. It is noted that there is a wide variation in the measured tidal currents with respect to depth and 70m at this location would represent near bed conditions. The model does however correlate in terms of current directionality and the dominance of flood tide currents.
- 1.6.2.13 Finally, at the Mona Array Area, site E, the tidal current speeds and directions are well represented by the model. This is the case for both spring, Figure 1.27, and neap, Figure 1.28, tidal flows. The calibration data demonstrates that the numerical model simulates the tidal currents in the region. This includes the representation of the dominant flood tide.
- 1.6.2.14 To provide a representation of tidal flows across the domain Figure 1.29 and Figure 1.30 illustrates tidal patterns during peak ebb and flood on a neap tide whilst Figure 1.31 and Figure 1.32 illustrates the spring tide. These points in the tidal cycle are used as reference for the assessment of potential impacts and changes to tidal flows due to the Mona Offshore Wind Project. The period selected for the comparative study represents a spring tide on the upper end of the range experienced in the region; this was to ensure the study included the greatest variation in tidal conditions, (i.e. water depth and current speed). Residual tidal flows and how they drive sediment transport regimes are examined in section 1.6.6.



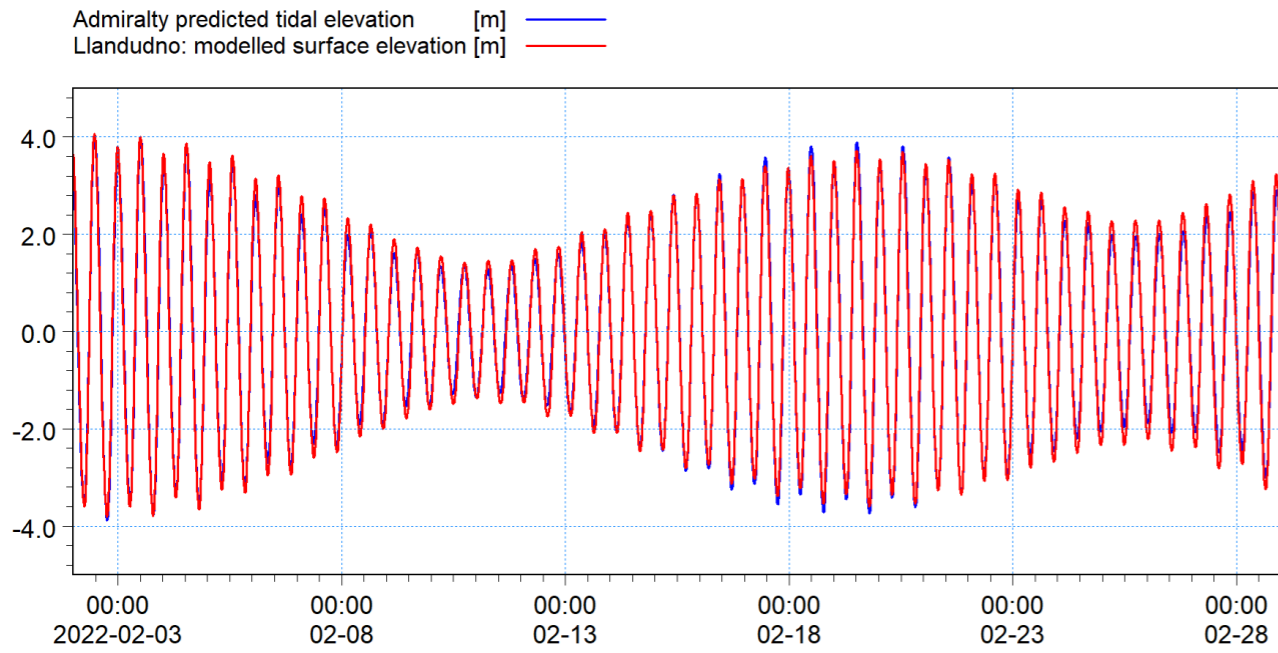


Figure 1.10: Comparison of model and admiralty harmonic tide data for Llandudno.

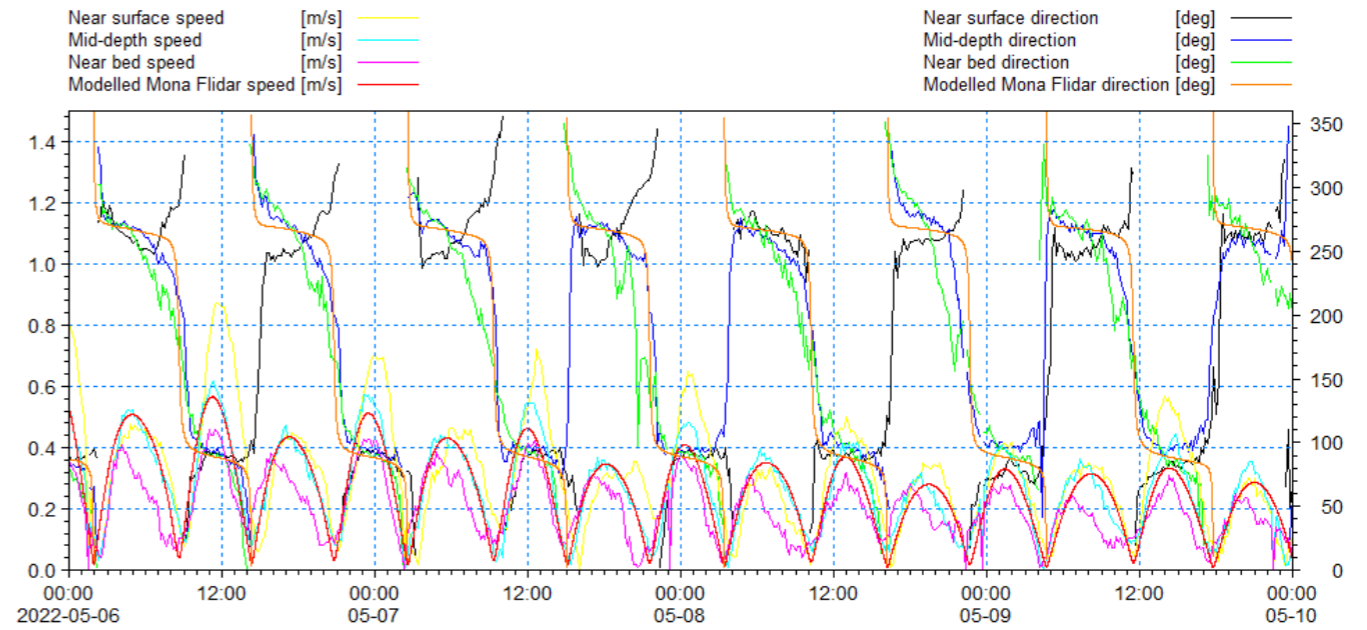


Figure 1.12: Comparison of model and recorded Mona FLidar – current speed and direction neap.

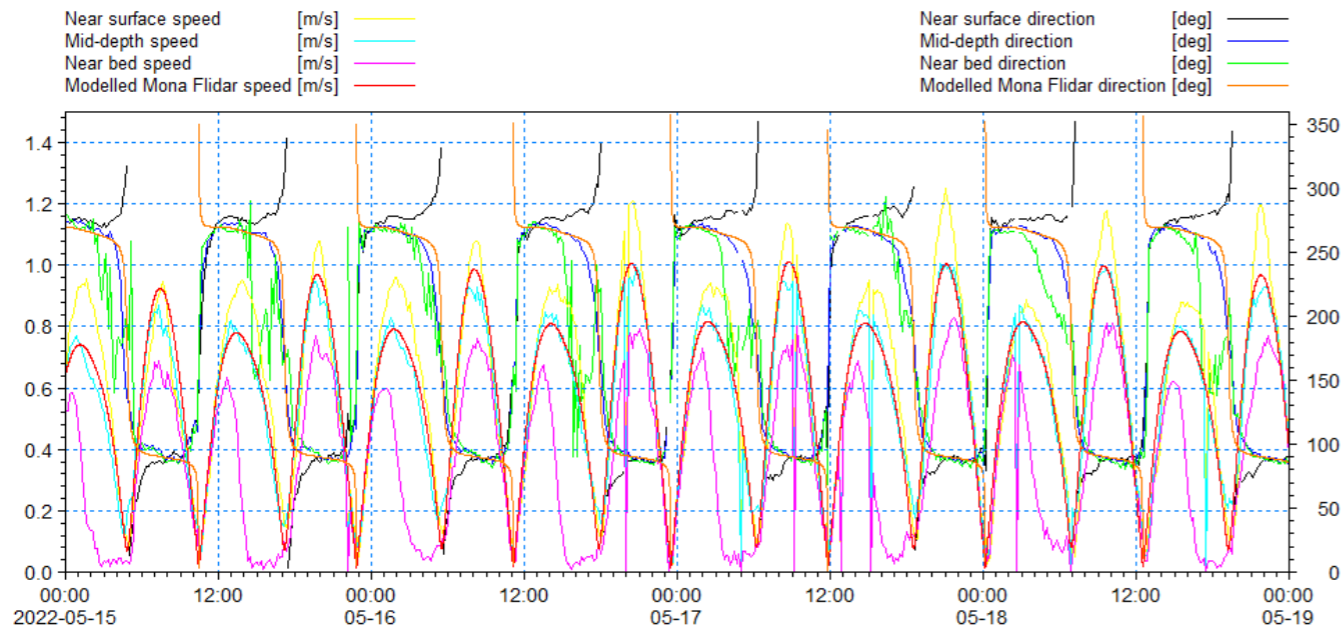


Figure 1.11: Comparison of model and recorded Mona FLidar – current speed and direction spring.

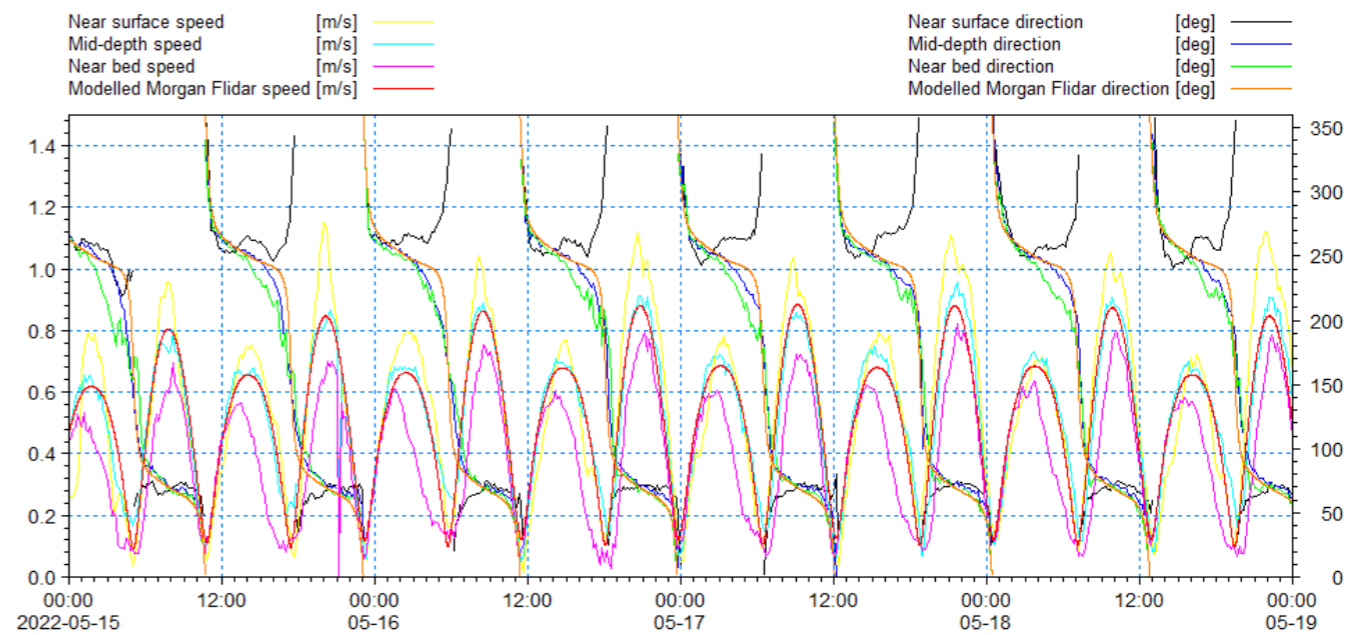


Figure 1.13: Comparison of model and recorded Morgan FLidar – current speed and direction spring.

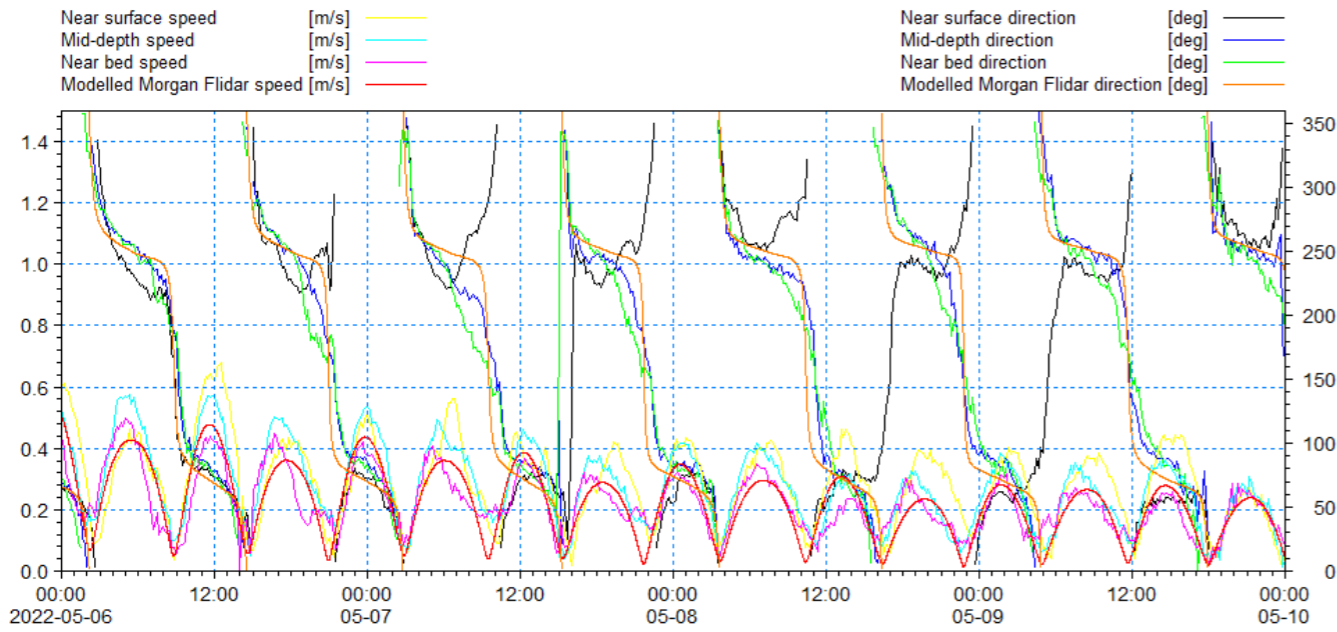


Figure 1.14: Comparison of model and recorded Morgan FLidar – current speed and direction neap.

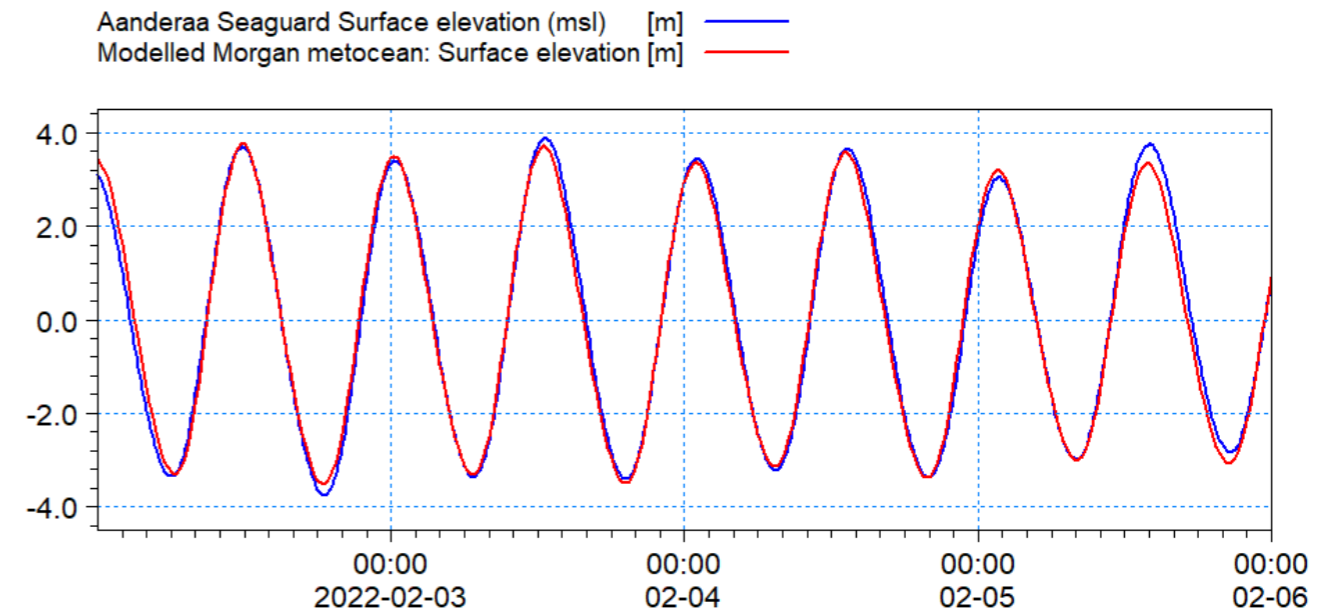


Figure 1.16: Comparison of modelled Morgan metocean and recorded ASG – spring surface elevation.

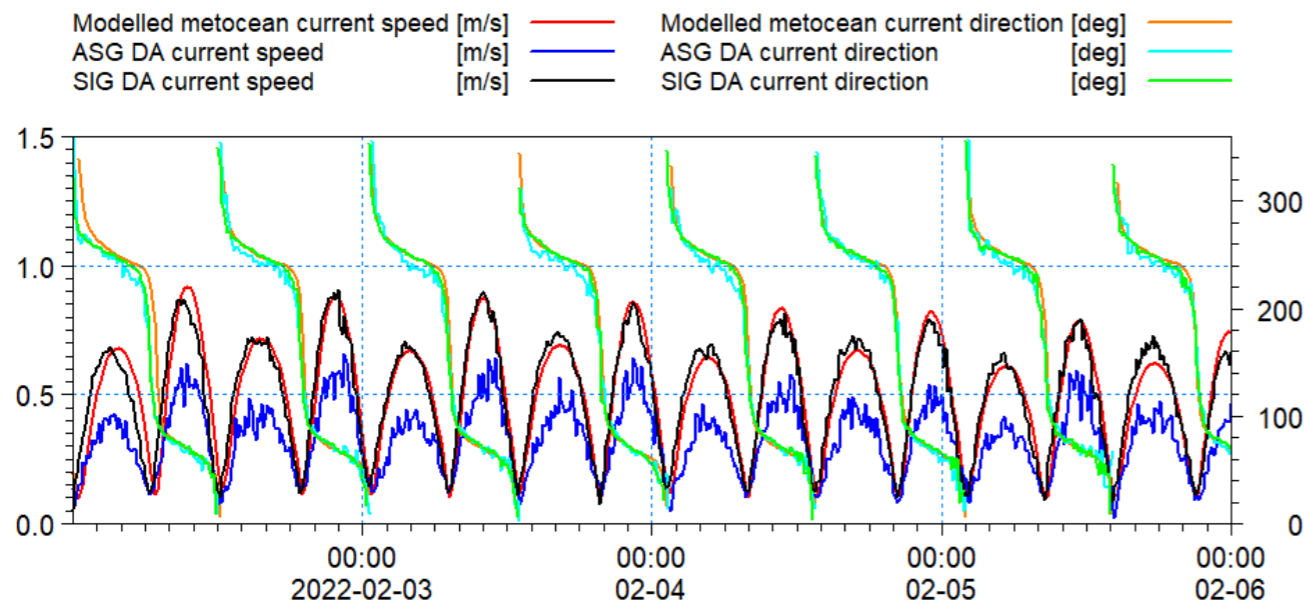


Figure 1.15: Comparison of modelled metocean and recorded depth averaged (DA) ASG and SIG – current speed and direction spring.

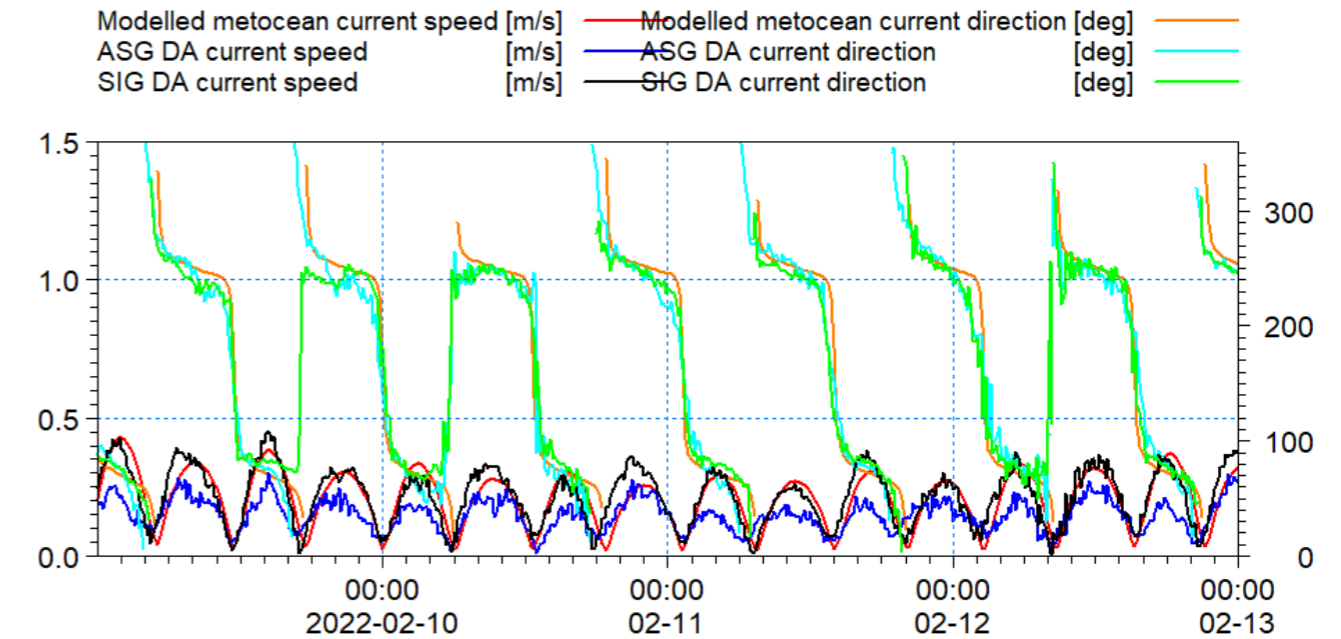


Figure 1.17: Comparison of modelled metocean and recorded DA ASG and SIG depth averaged– current speed and direction neap.



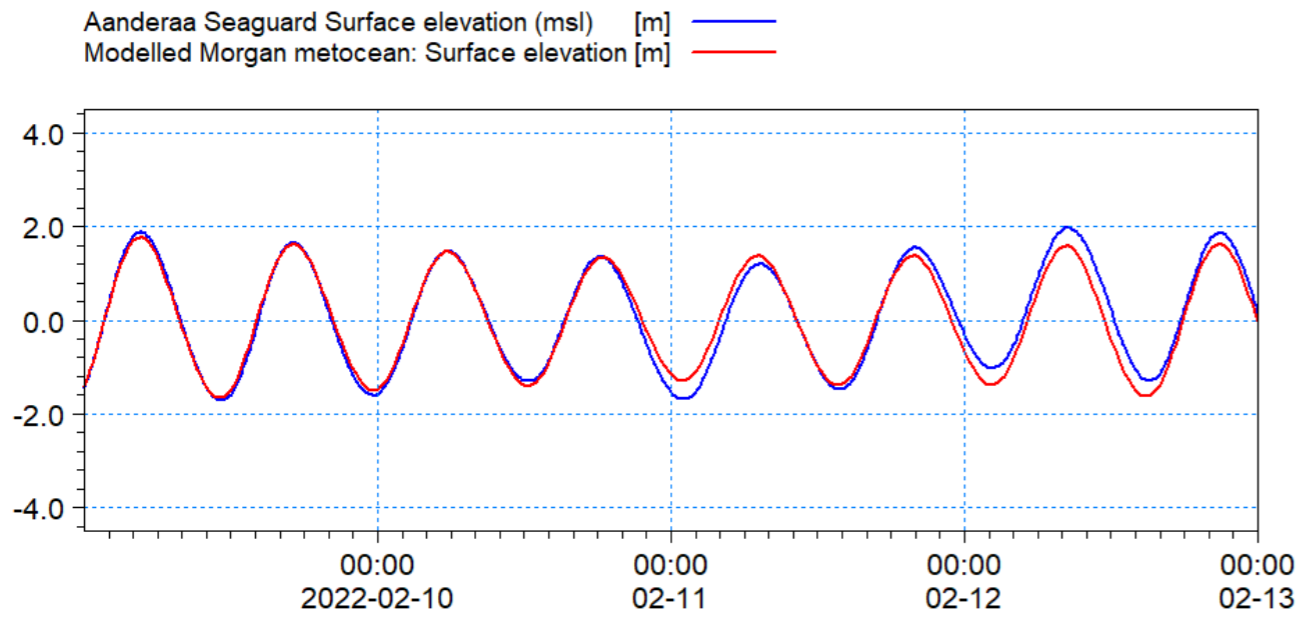


Figure 1.18: Comparison of modelled Morgan metocean and recorded ASG – neap surface elevation.

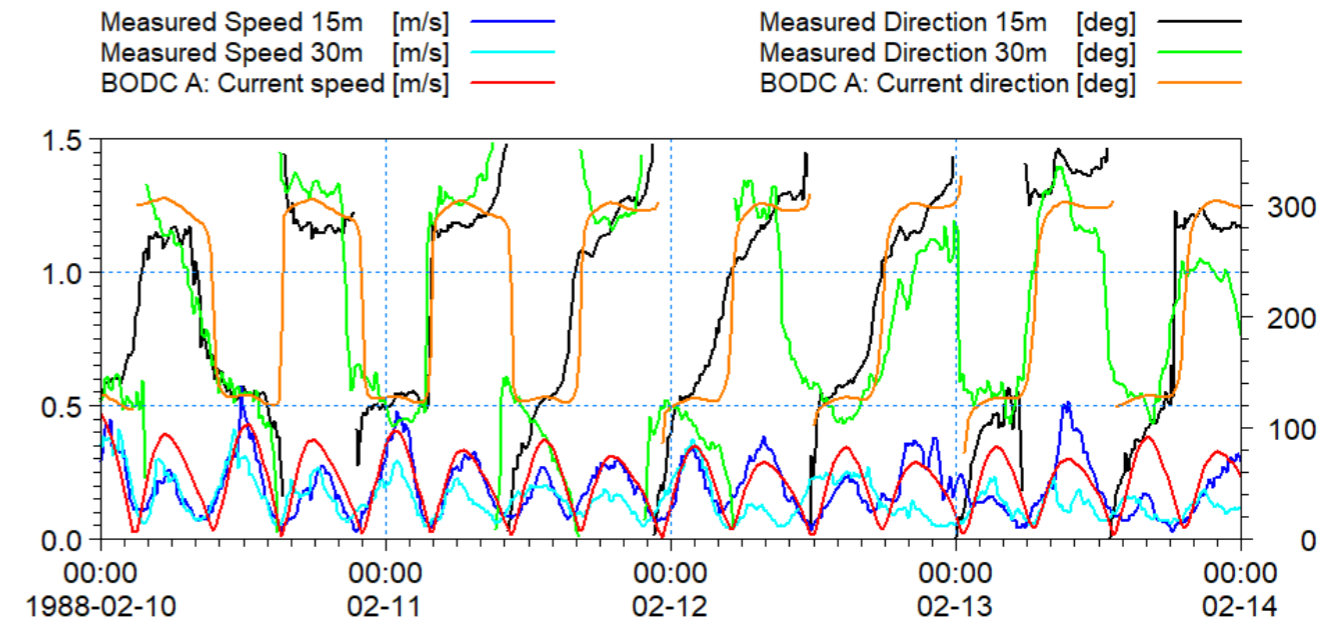


Figure 1.20: Comparison of model and recorded data BODC Location A – current speed and direction neap.

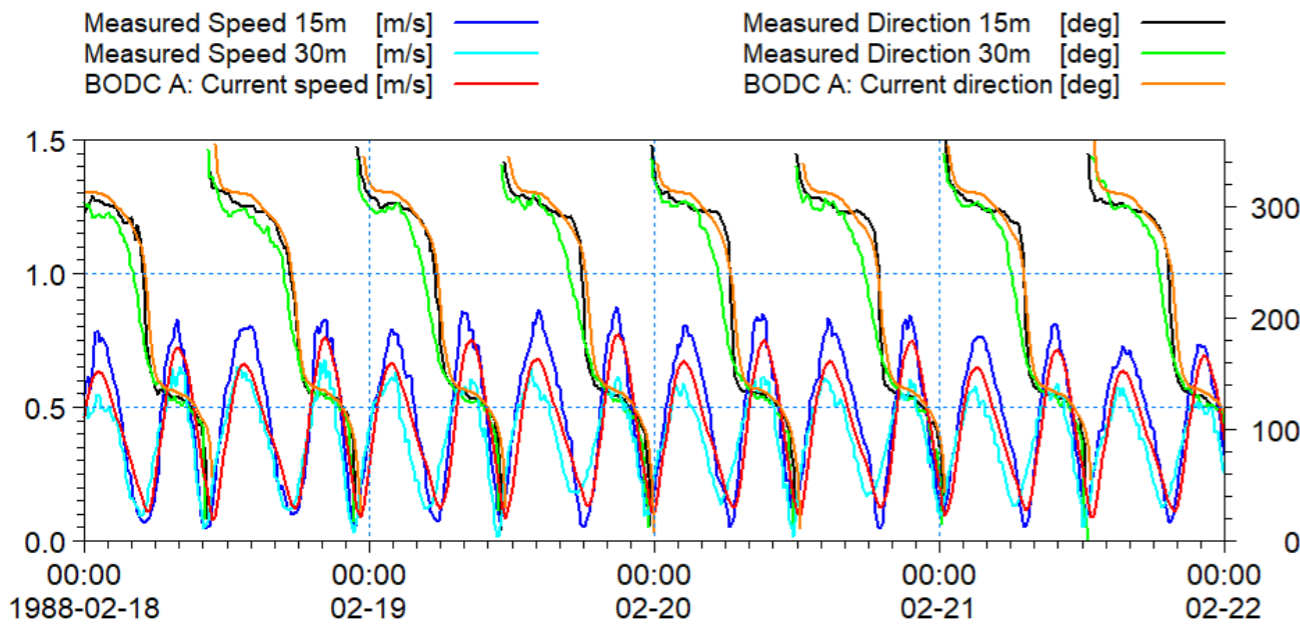


Figure 1.19: Comparison of model and recorded data BODC Location A – current speed and direction spring.

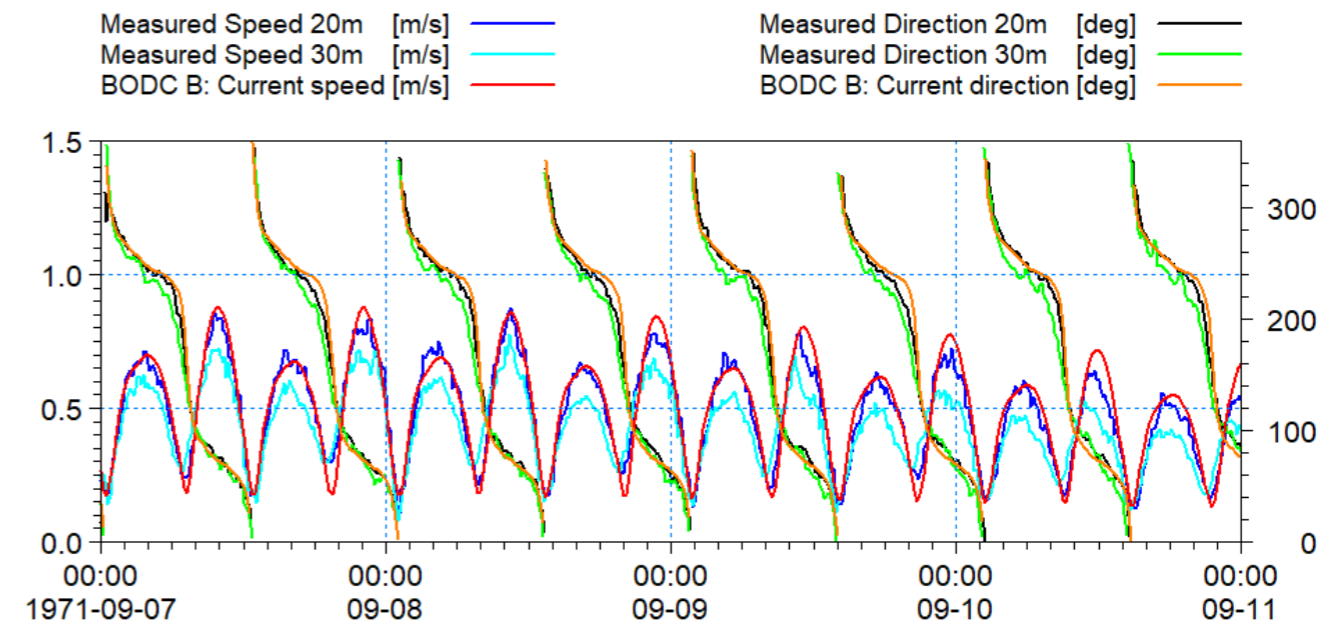


Figure 1.21: Comparison of model and recorded data BODC Location B – current speed and direction spring.

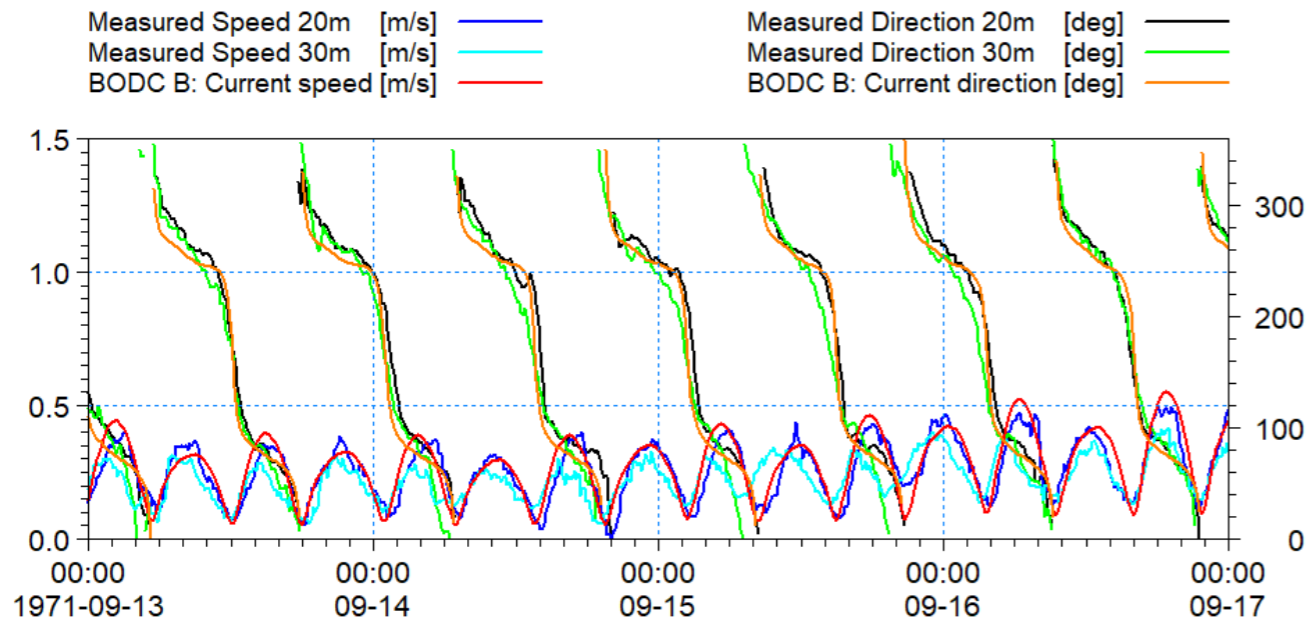


Figure 1.22: Comparison of model and recorded data BODC Location B – current speed and direction neap.

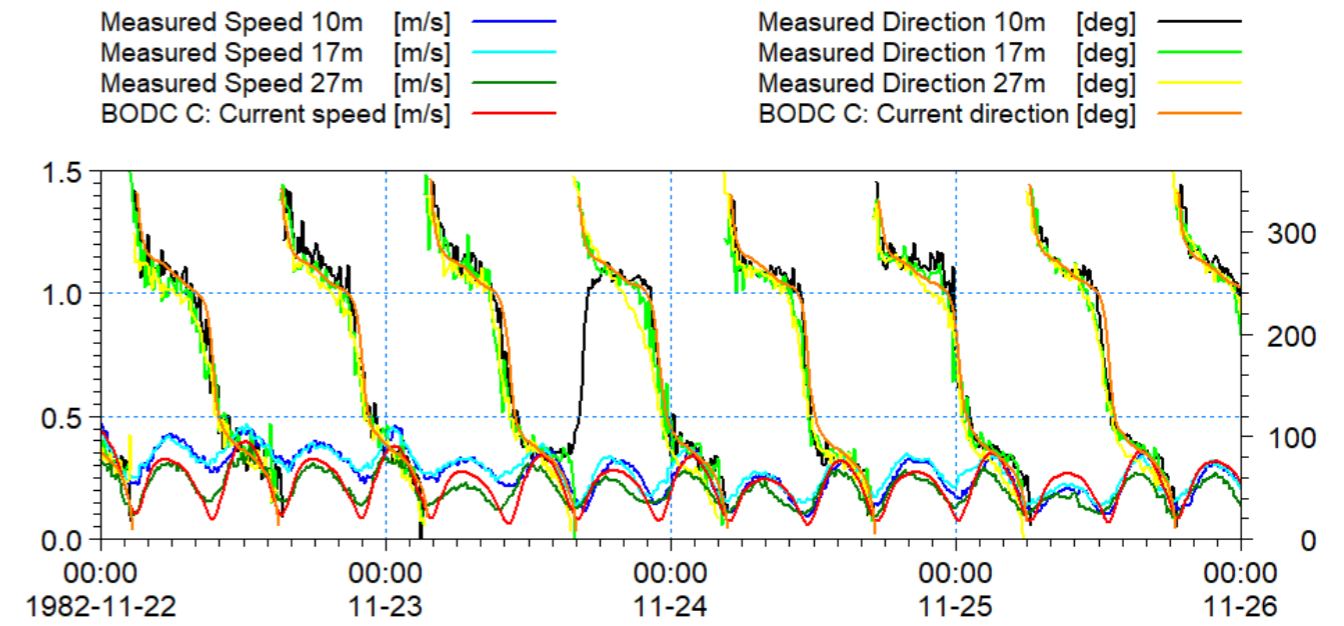


Figure 1.24: Comparison of model and recorded data BODC Location C – current speed and direction neap.

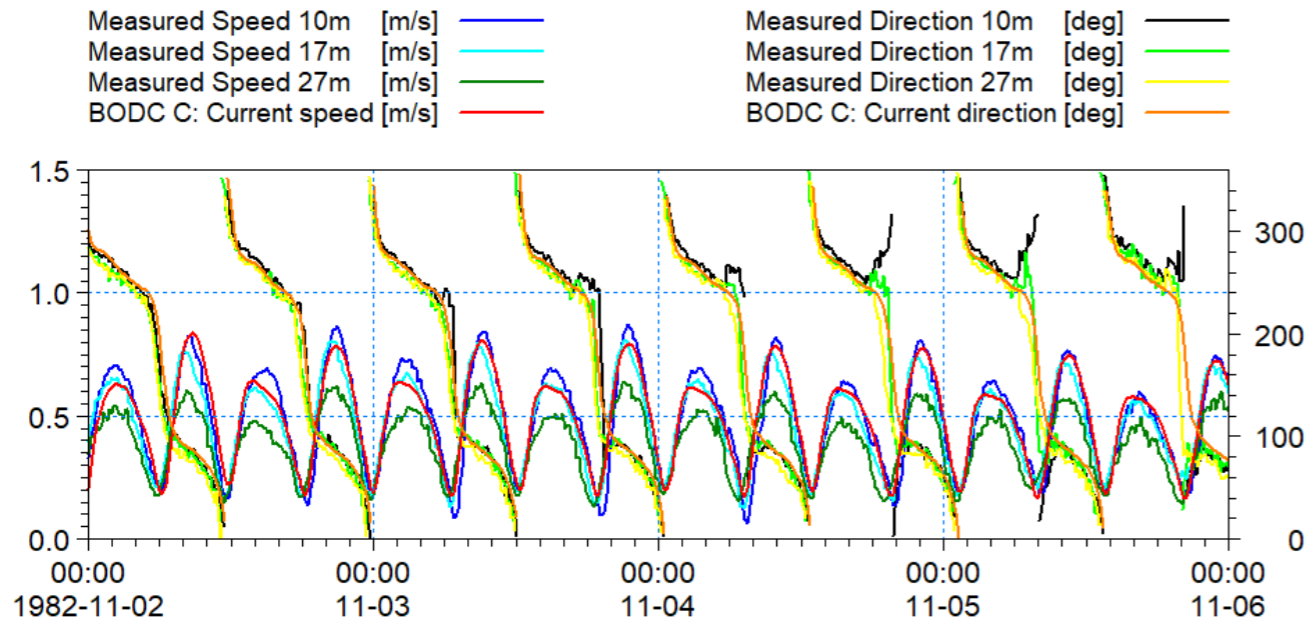


Figure 1.23: Comparison of model and recorded data BODC Location C – current speed and direction spring.

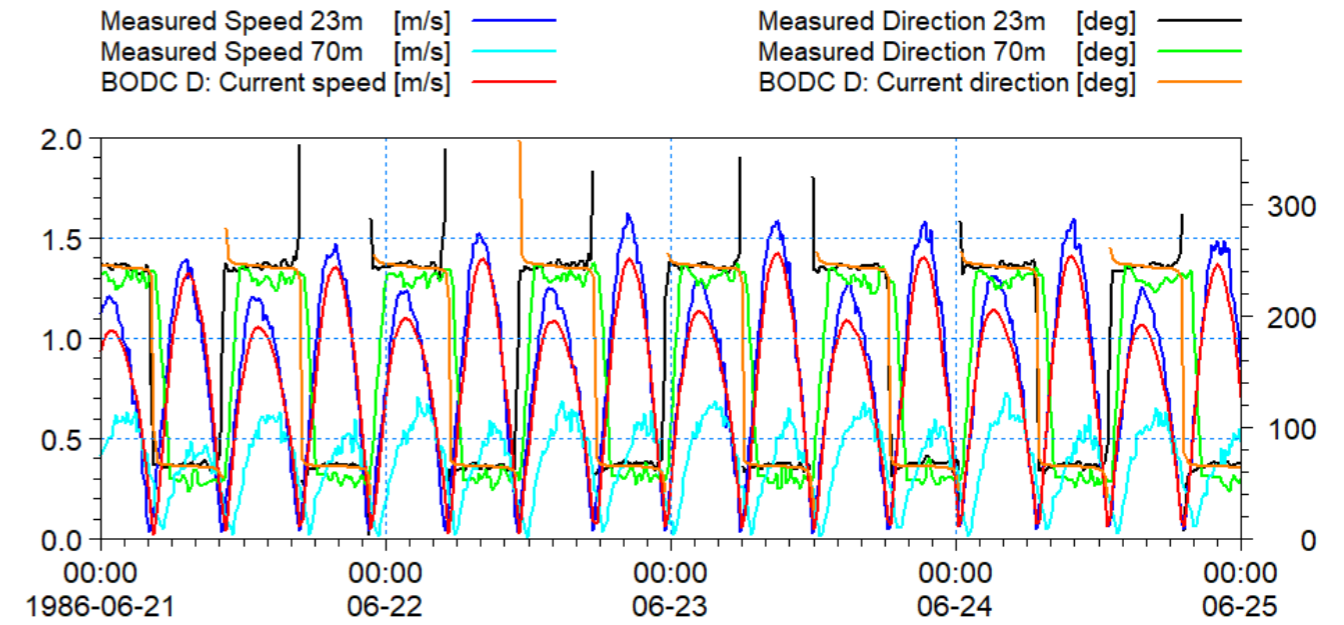


Figure 1.25: Comparison of model and recorded data BODC Location D – current speed and direction spring.



MONA OFFSHORE WIND PROJECT

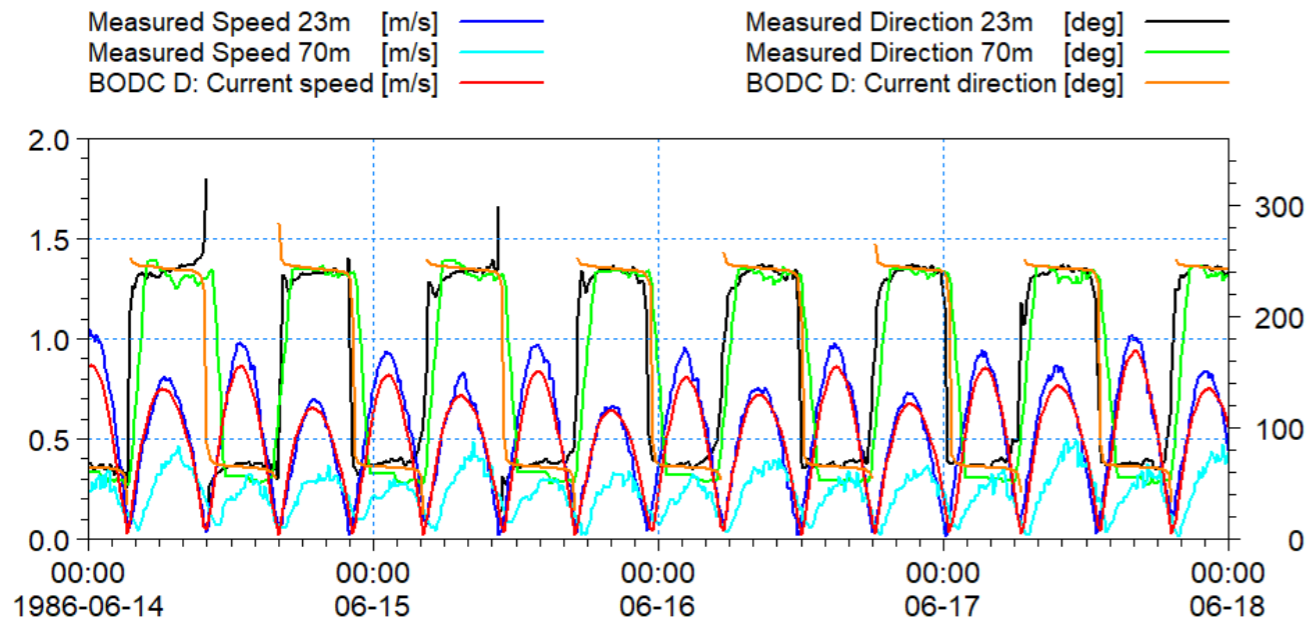


Figure 1.26: Comparison of model and recorded data BODC Location D – current speed and direction neap.

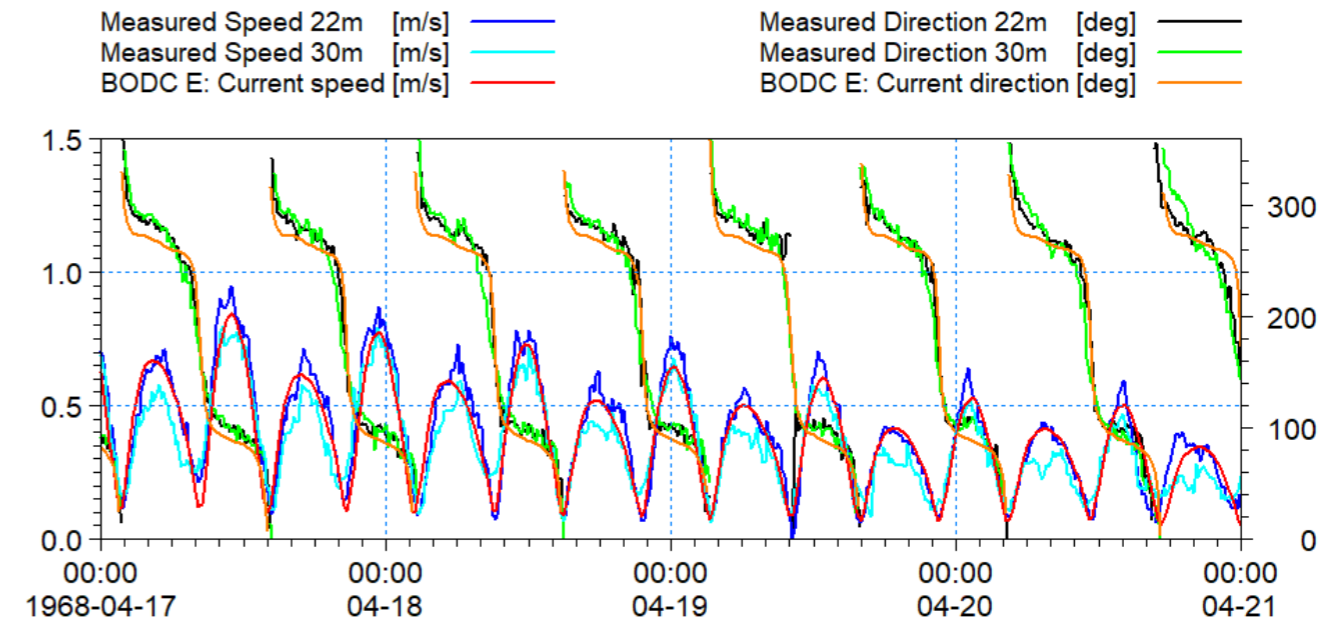


Figure 1.28: Comparison of model and recorded data BODC Location E – current speed and direction neap.

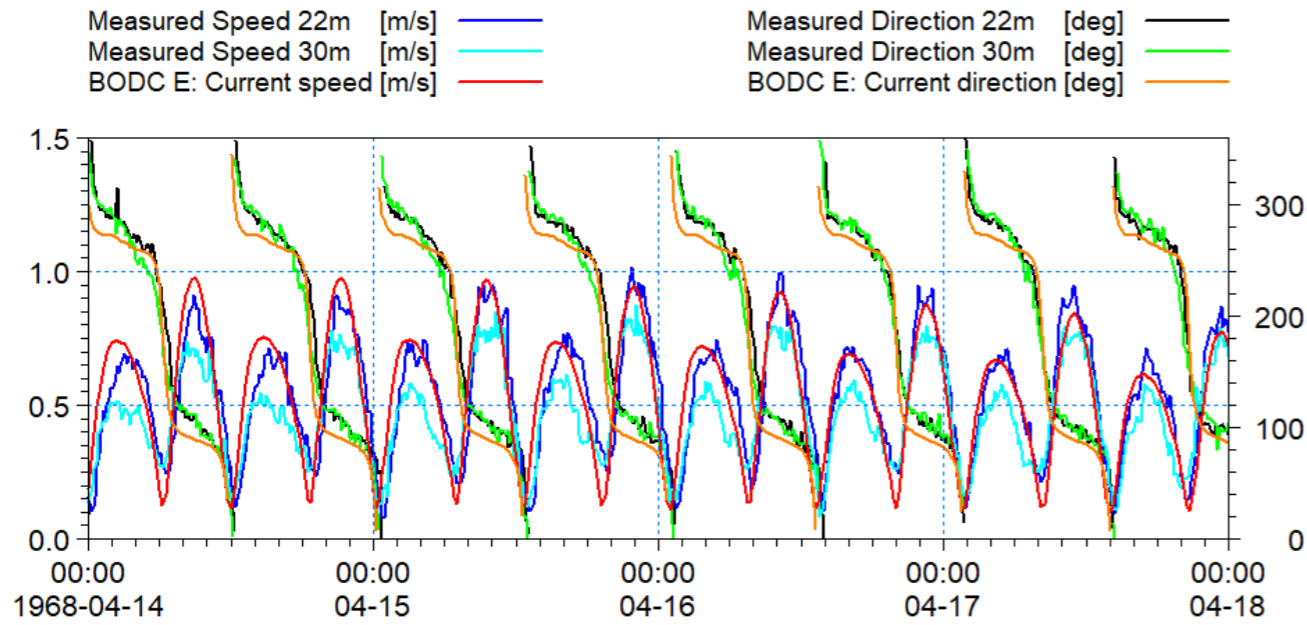


Figure 1.27: Comparison of model and recorded data BODC Location E – current speed and direction spring.

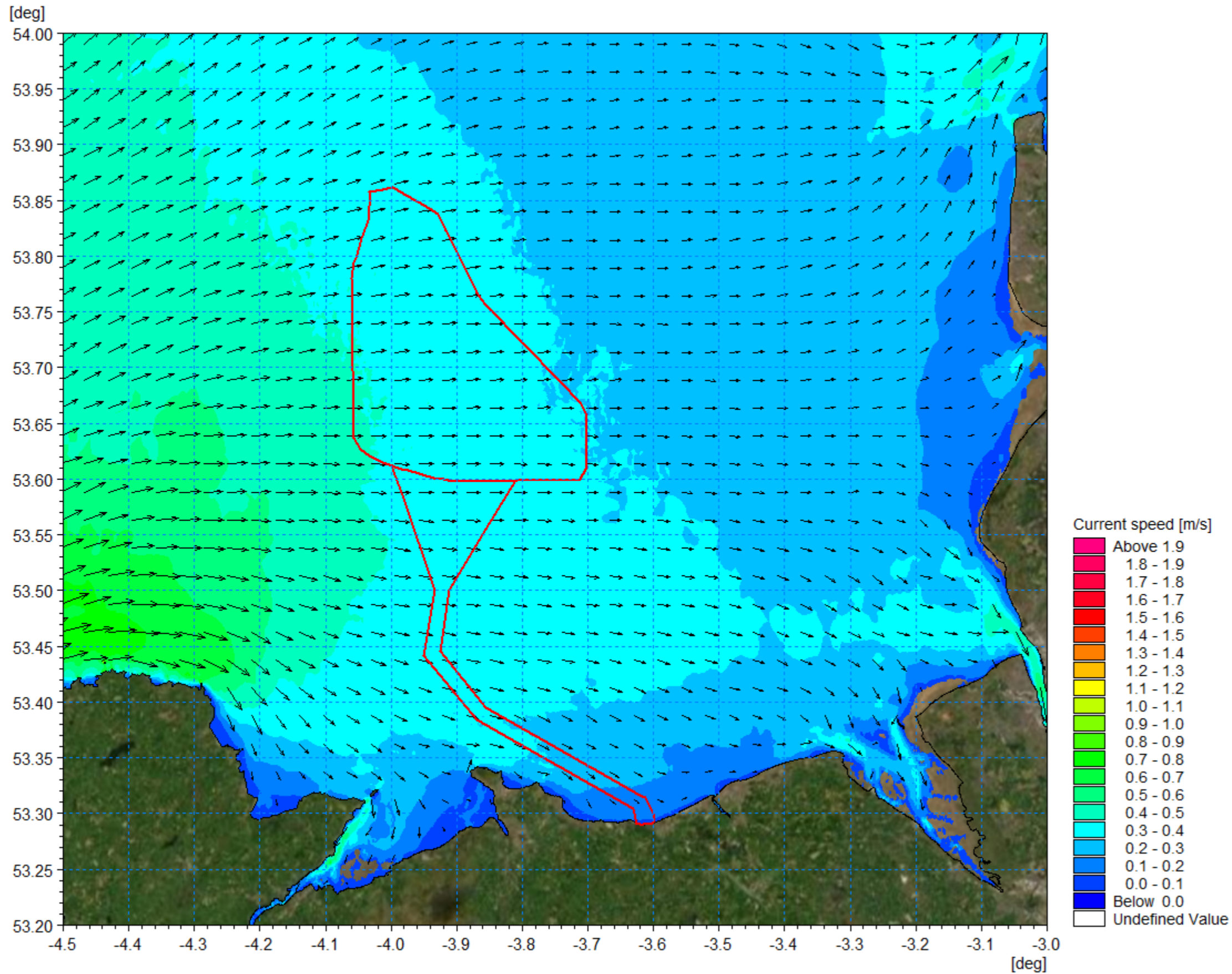


Figure 1.29: Tidal flow patterns – neap tide flood.



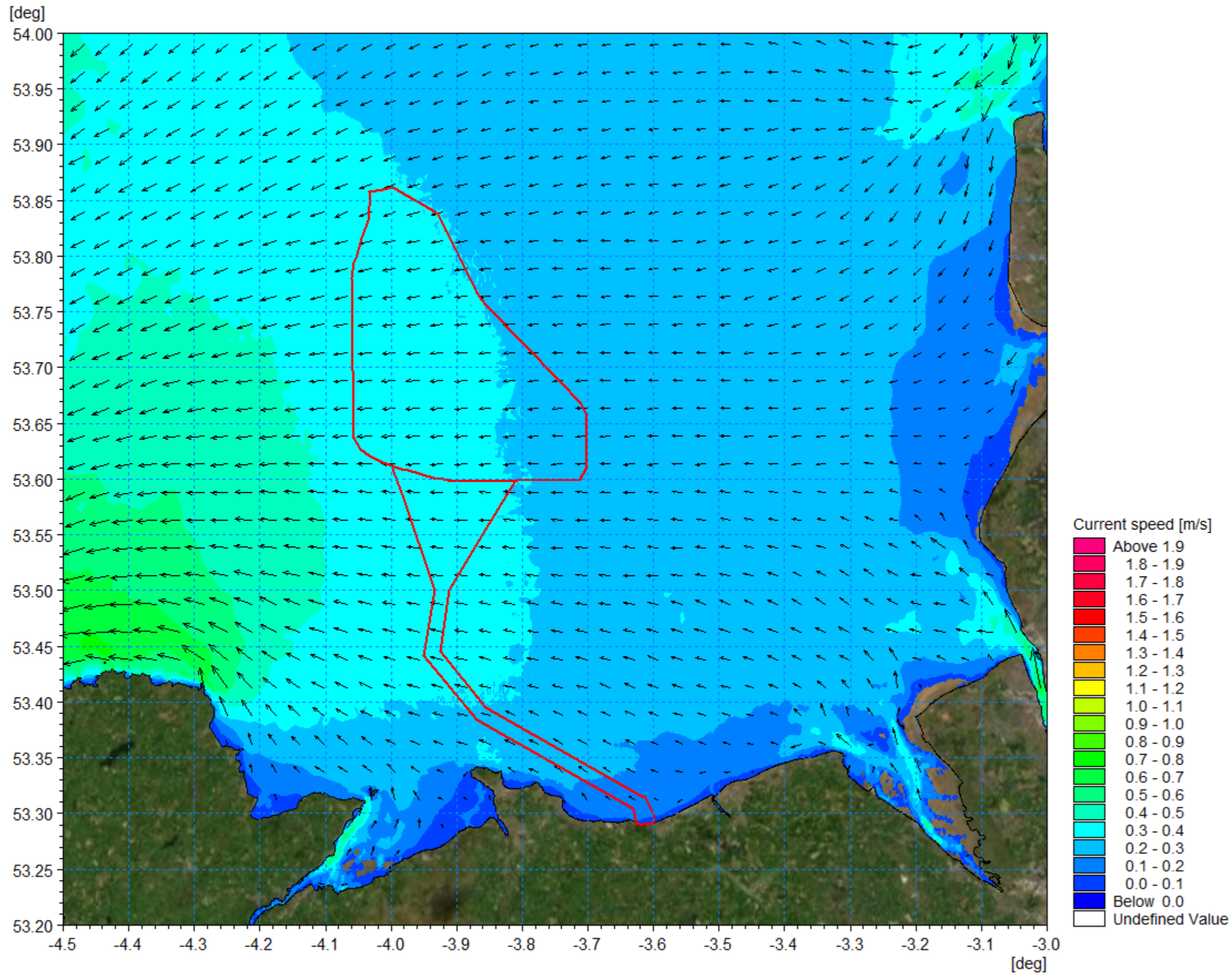


Figure 1.30: Tidal flow patterns – neap tide ebb.

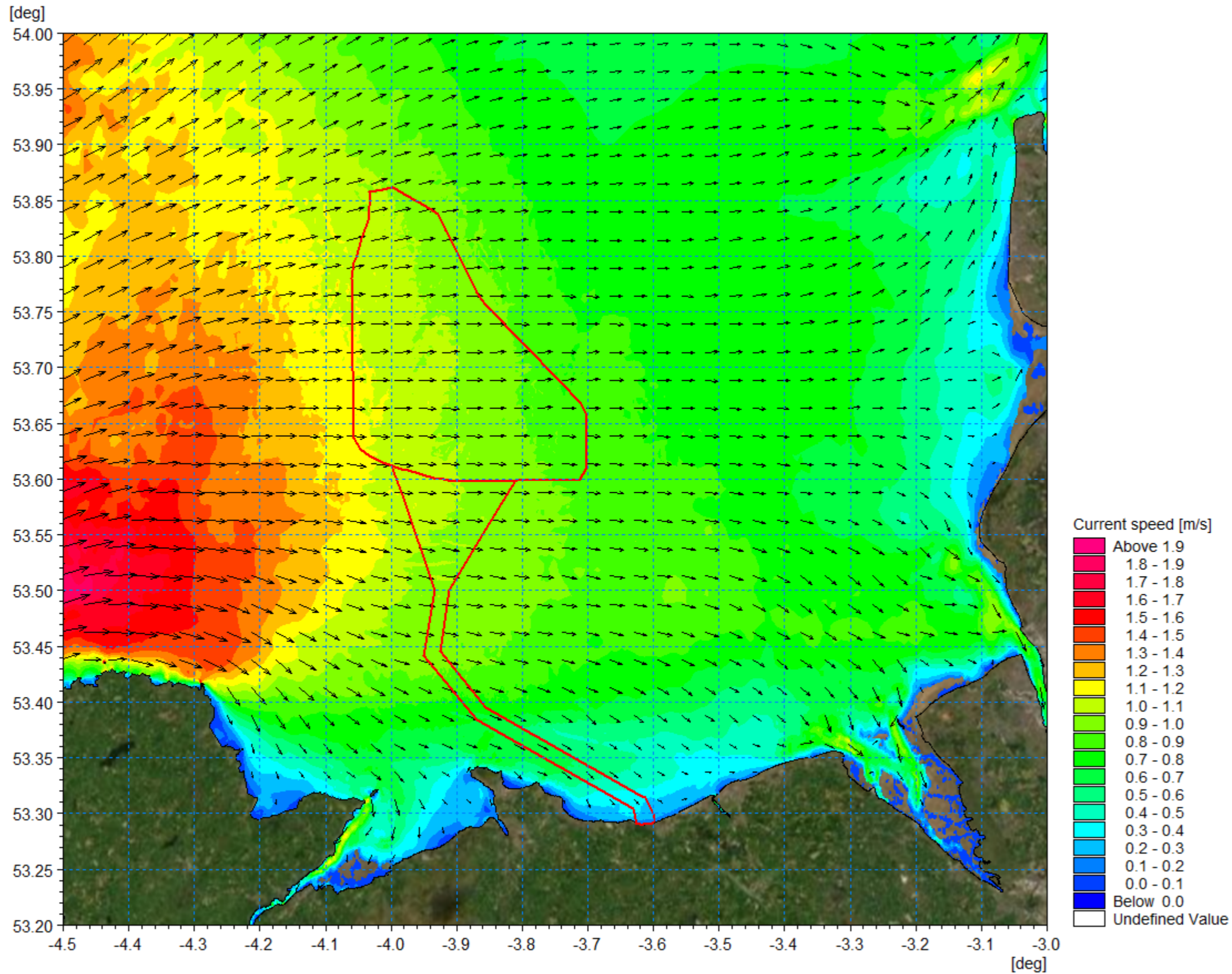


Figure 1.31: Tidal flow patterns – spring tide flood.



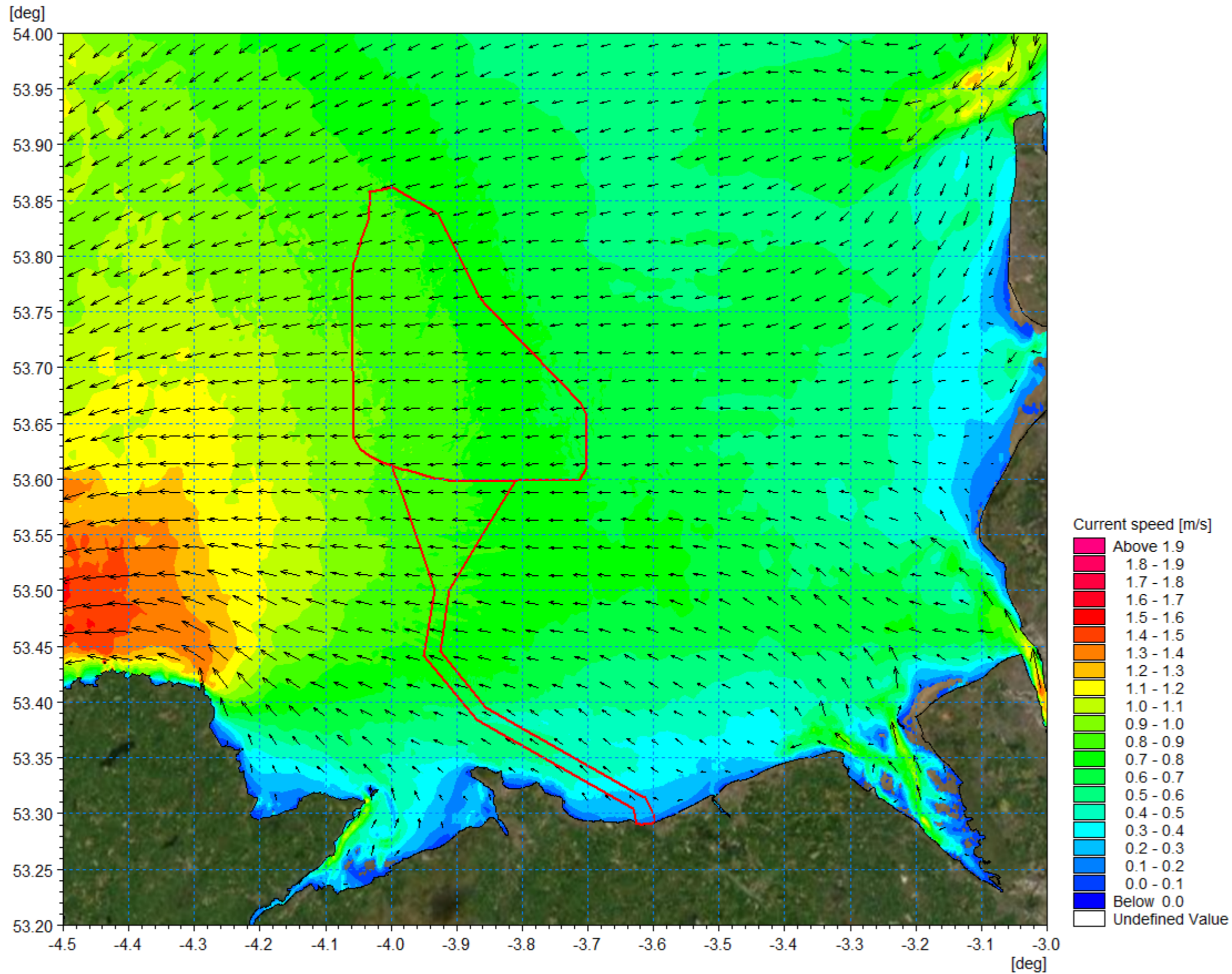


Figure 1.32: Tidal flow patterns – spring tide ebb.

**1.6.3 Wave climate**

1.6.3.1 Waves in the east Irish Sea are highest to the southwest of the Isle of Man with the highest mean annual significant wave height of 1.39m recorded between the Isle of Man and Anglesey. Significant wave height is reduced closer to the coast with the lowest significant wave height of 0.73m recorded to the west of the Dee Estuary (ABPmer, 2008). In the Mona physical processes study area mean annual wave height ranges from 1.1m to 1.3m. Over 40% of the waves arise from the southwest with all significant wave heights (>4m) arriving from the southwest or west (ABPmer, 2018). This is illustrated in Figure 1.33 which shows the wave rose for a point located within this area. Similarly, the corresponding wind rose presented in Figure 1.33 which illustrates the predominant winds are from the southwest with the site being located in the lee of the Isle of Man.

1.6.3.2 As offshore waves transfer from the deep offshore water to shallower coastal areas, a number of important modifications may result due to interactions of offshore deep-water waves with the seabed, with the resultant modifications producing shallow water waves. These physical ‘wave transformation’ interactions include:

- Shoaling and refraction (due to both depth and current interactions with the wave)
- Energy loss due to breaking
- Energy loss due to bottom friction
- Momentum and mass transport effect.

1.6.3.3 The wave model developed for the assessment was calibrated using data collected during storm Christoph which occurred during January 2021. The model simulated water levels using boundary data extracted from the RPS storm surge model and applied meteorological conditions from the European Centre for Medium-range Weather Forecasting (ECMWF) operational dataset. Wave conditions at the model boundary were also provided from the ECMWF operational dataset.

1.6.3.4 The model output data was then compared with measured data obtained from the National Network of Regional Coastal Monitoring Programmes held by the CCO at the locations shown in Figure 1.35. For each of the three location three parameters are presented relating to mean wave direction, significant wave height and peak wave period.

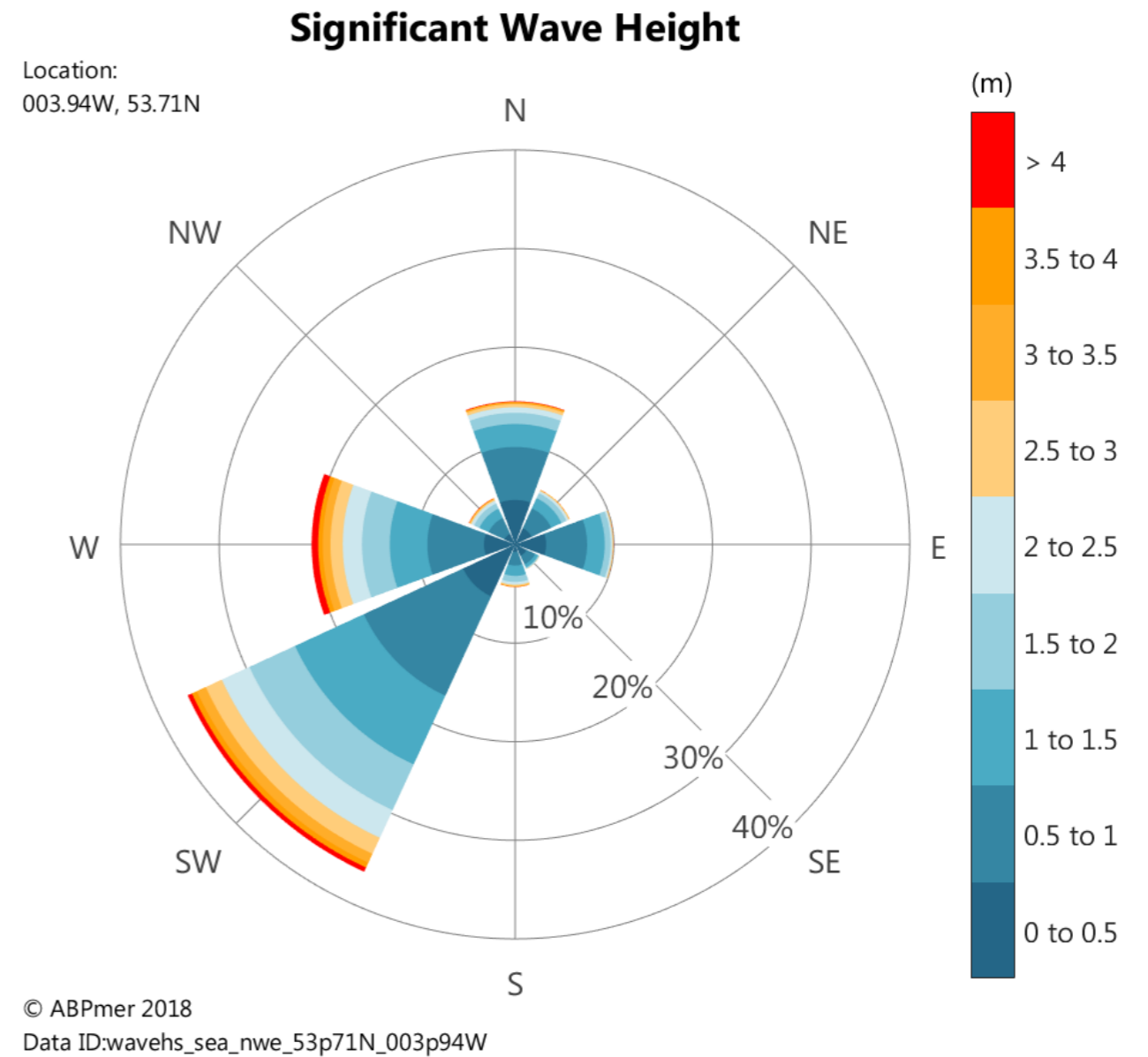


**Figure 1.33: Wave rose for Mona Offshore Wind Project Array Area.**



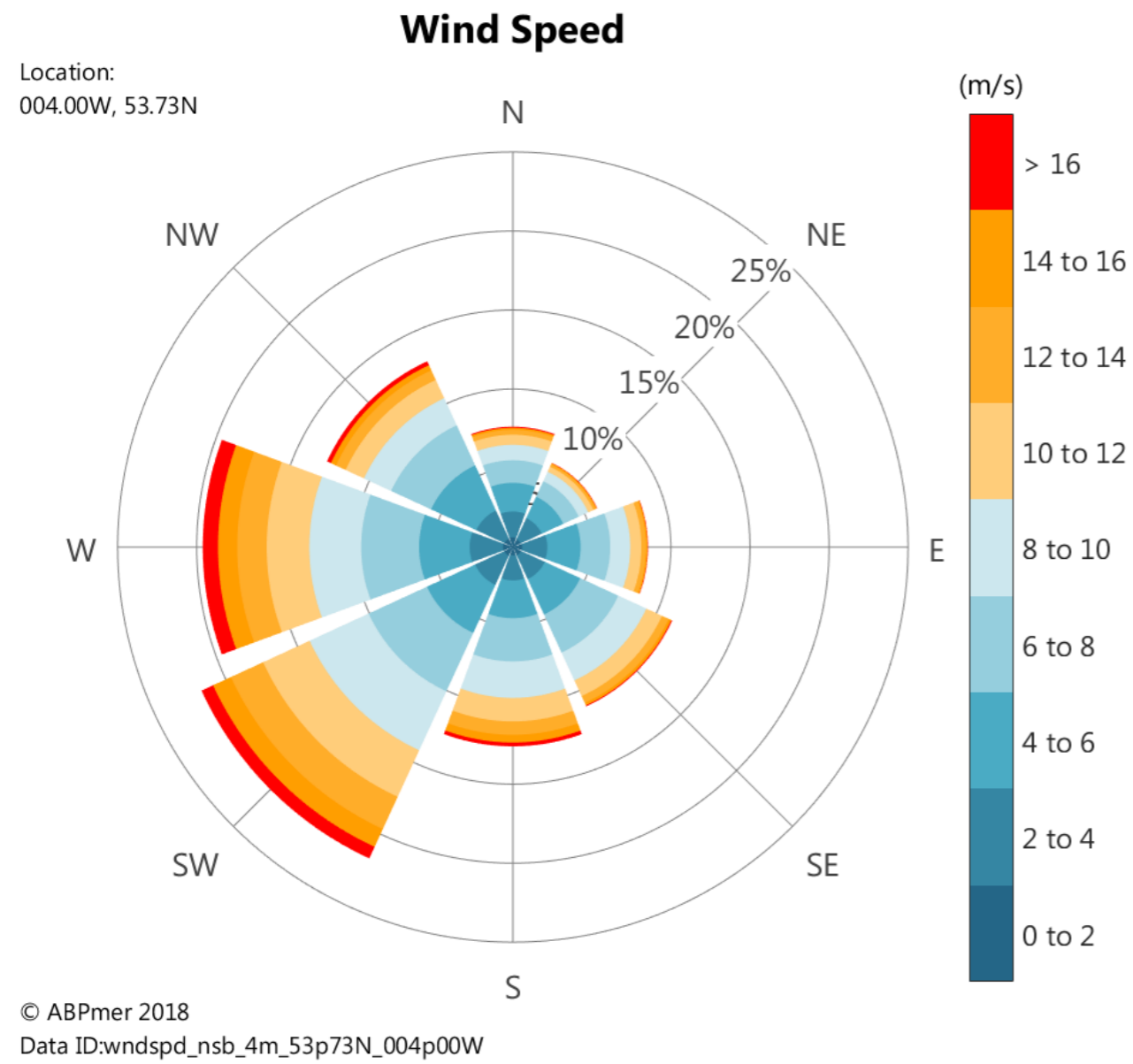


Figure 1.34: Wind rose for Mona Offshore Wind Project Array Area.

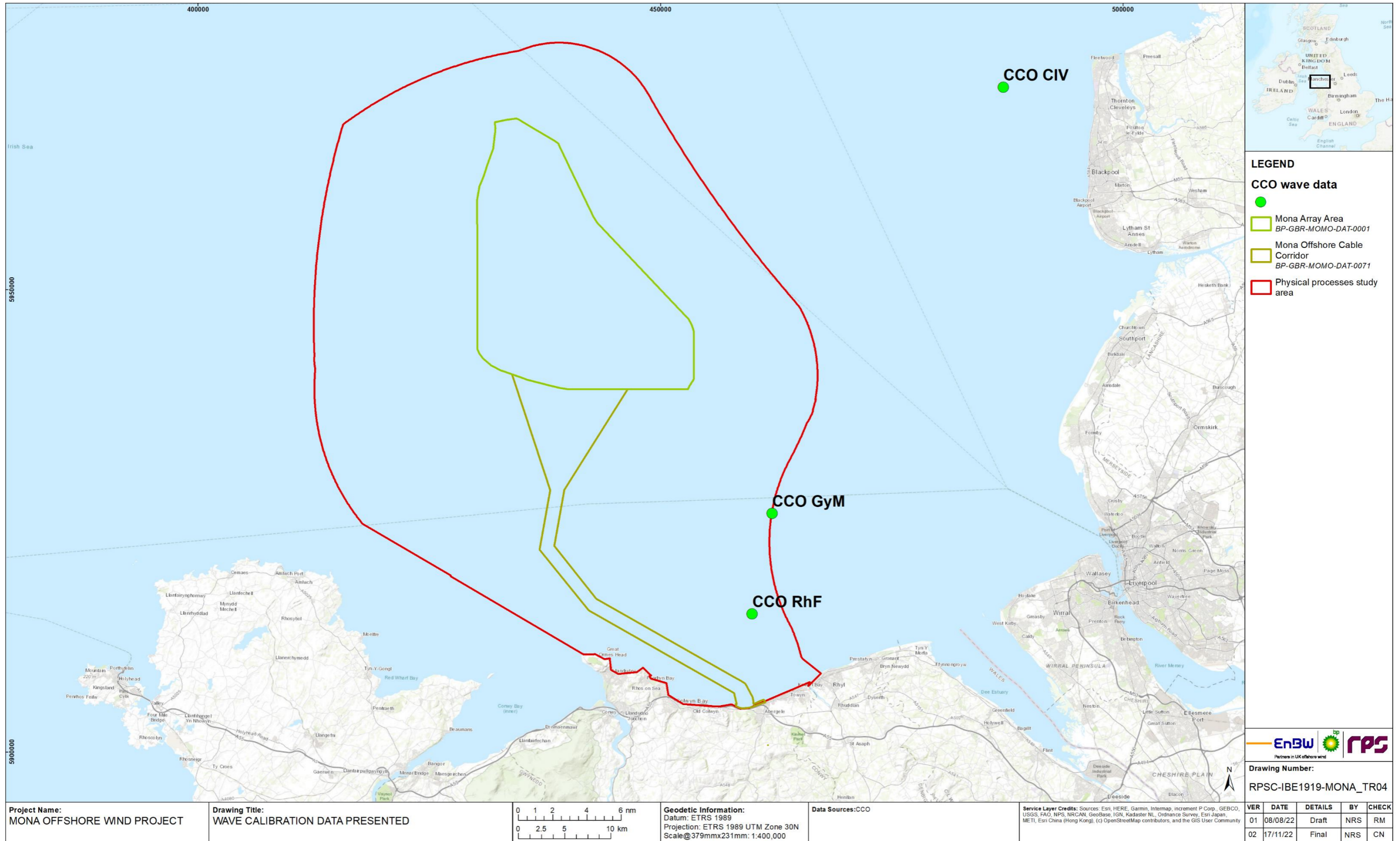


Figure 1.35: Location of wave calibration data presented.



MONA OFFSHORE WIND PROJECT

1.6.3.5 Storm Christoph approached the east Irish Sea from an easterly direction and therefore the calibration site located to the east of the physical processes study area provide a good indicator as to how well the wave model transforms wave through the physical processes study area. Model and measured data for site Cleveleys (CIV) located at the mouth of Morecambe Bay are presented in Figure 1.36 to Figure 1.38. In each case it can be seen that the hourly interval model data tracks the progress of the storm. It is noted that the model is less 'peaky', but this is to be expected given that the ECMWF data is at three hourly intervals and linear interpolation was applied.

1.6.3.6 For the two southerly sites Gwynt y Môr (GyM) (Figure 1.39 to Figure 1.41) and Rhyl Flats (RfH) (Figure 1.42 to Figure 1.44) located on the south east extent of the physical processes study area there is also a good correlation between modelled and monitored data. This indicated that the wave model was suitable for use in the comparative study of the potential impacts of the Mona Offshore Wind Project infrastructure on wave climate.

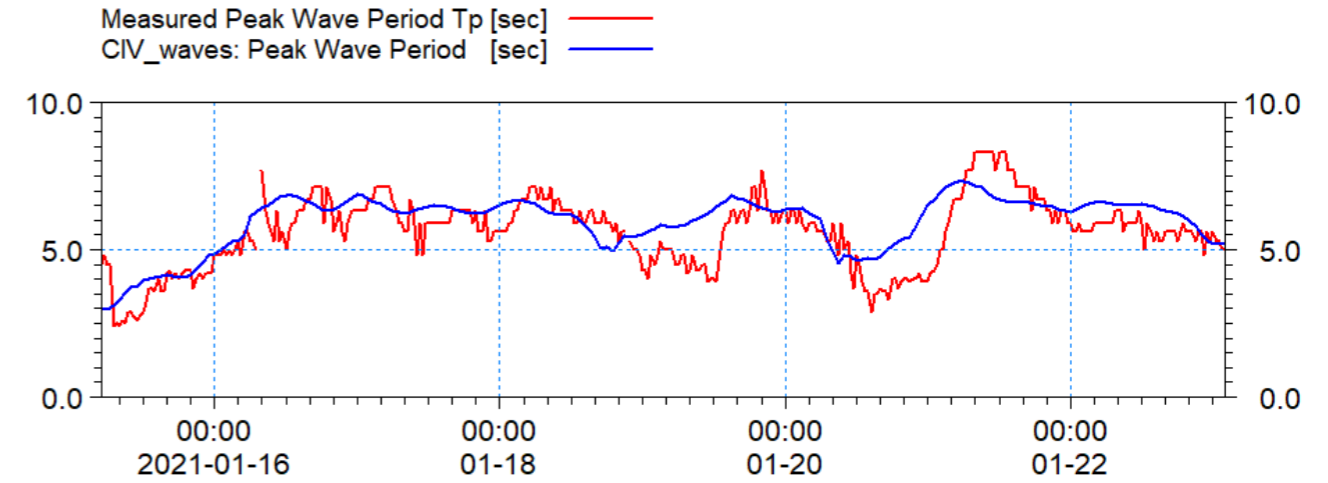


Figure 1.38: Validation of Modelled Peak Wave Period with Measured Data at CIV

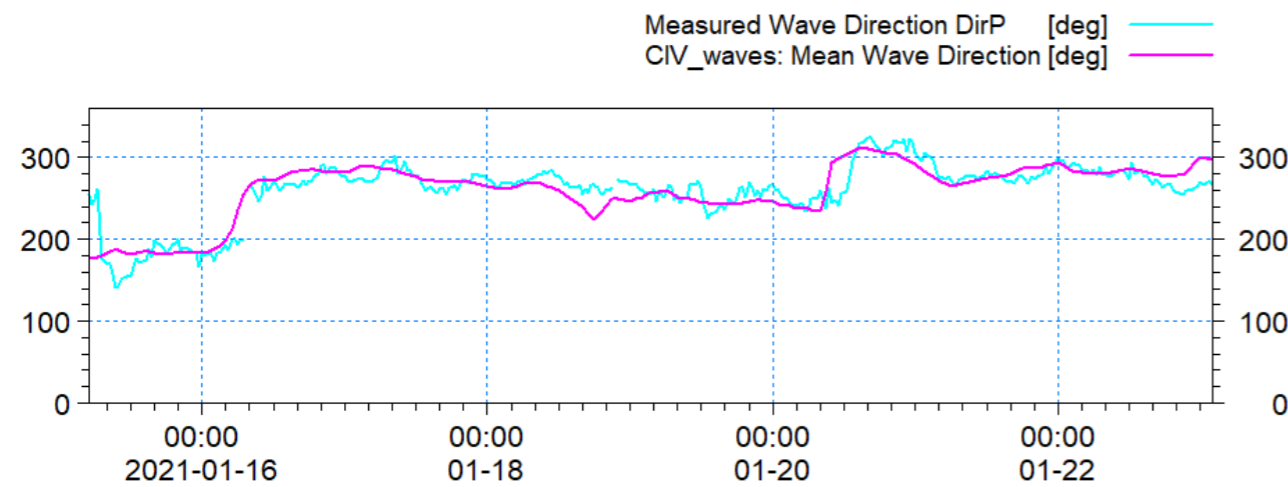


Figure 1.36: Validation of modelled mean wave direction with measured data at CIV.

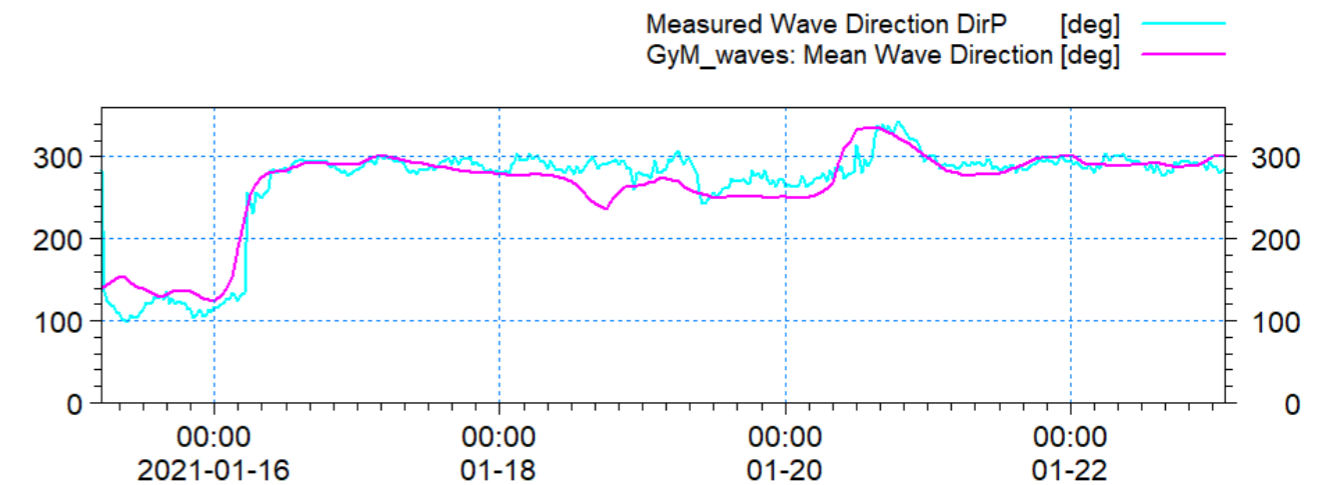


Figure 1.39: Validation of modelled mean wave direction with measured data at GyM.

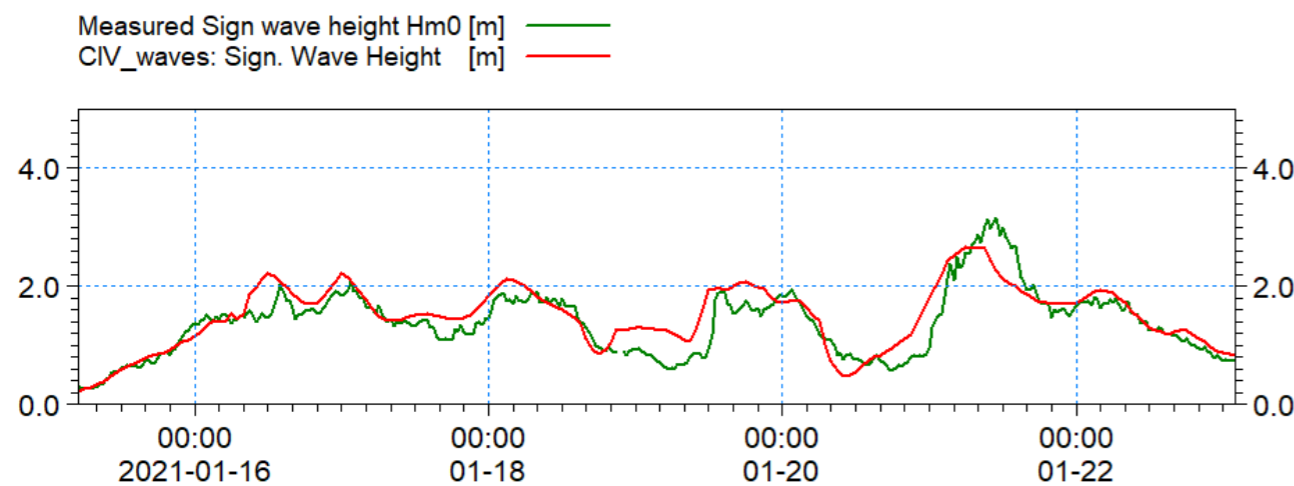


Figure 1.37: Validation of modelled significant wave height with measured data at CIV.

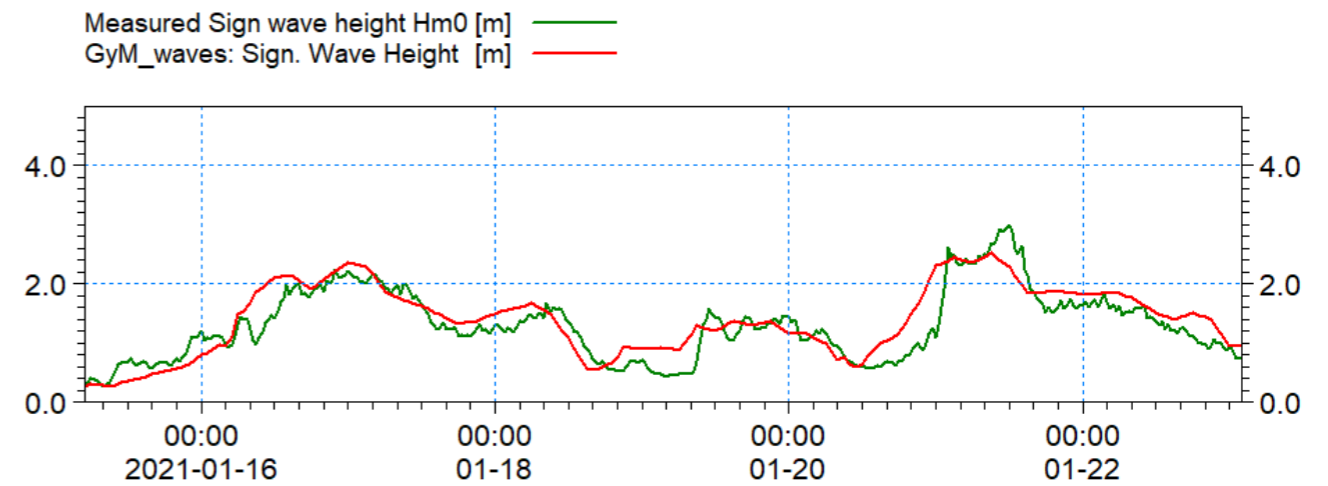


Figure 1.40: Validation of modelled significant wave height with measured data at GyM.

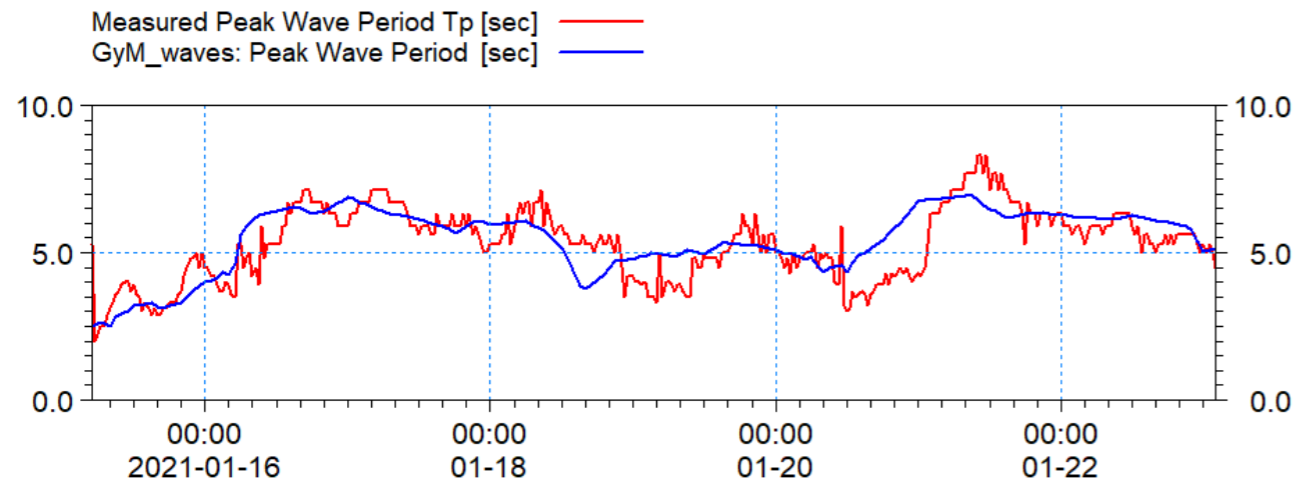


Figure 1.41: Validation of modelled peak wave period with measured data at GyM.

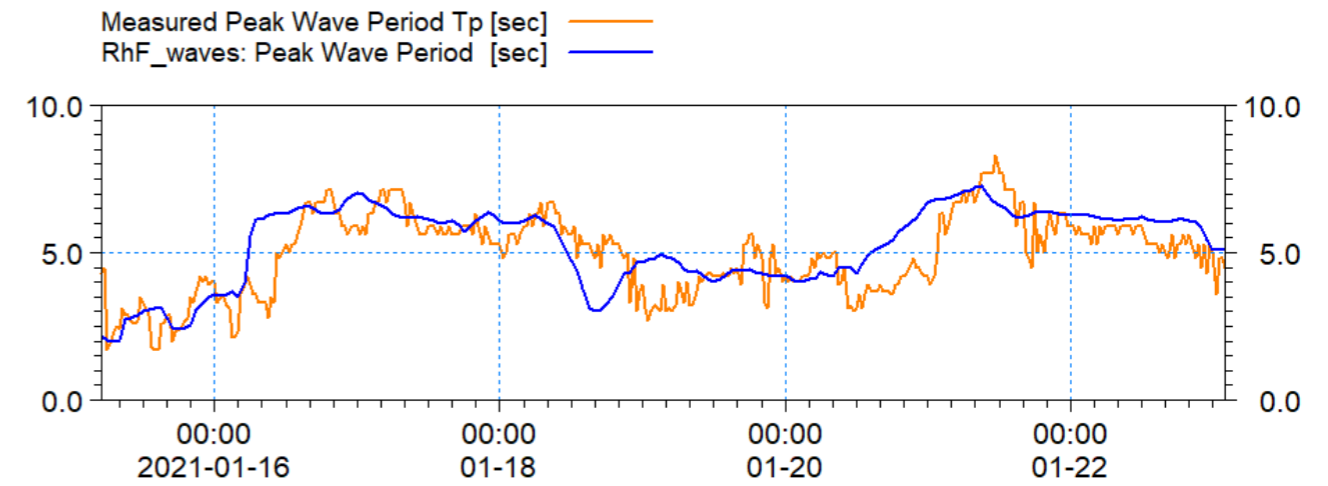


Figure 1.44: Validation of modelled peak wave period with measured data at RhF.

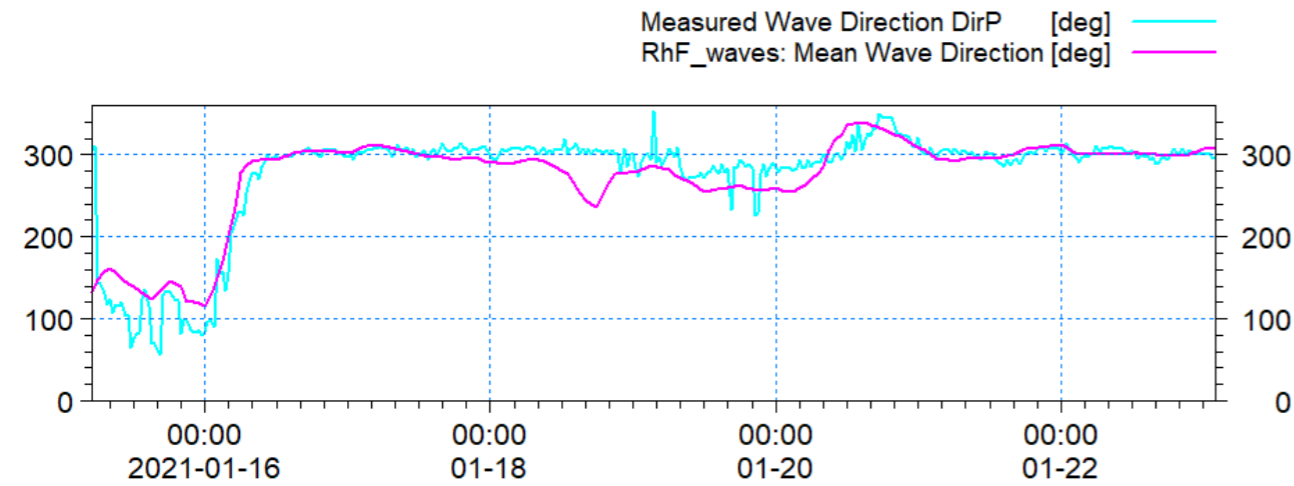


Figure 1.42: Validation of modelled mean wave direction with measured data at RhF.

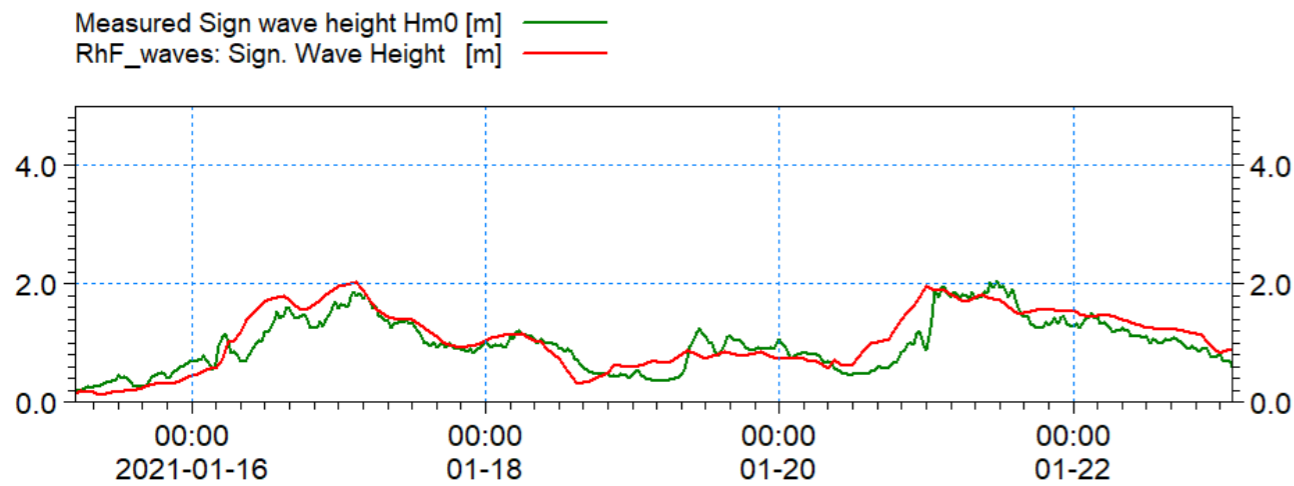


Figure 1.43: Validation of modelled significant wave height with measured data at RhF.

1.6.3.1 In order to evaluate the potential changes in wave climate due to the Mona Offshore Wind Project, a comparative study was carried out. This meant that baseline wave climate was required; due to the comparative nature of the assessment, a full metocean study was not essential however representative sea-states were required.

1.6.3.2 An analysis was undertaken to determine the offshore conditions for which waves reach the site from all directions. Twenty-two years of data were obtained from the ECMWF operational dataset for locations on the north and south boundaries of the model domain. Extreme value analysis using peak over threshold was undertaken for each 30° sector to determine the 1in1 and 1in20 year offshore wave climate. These were then used as boundary conditions within the wave modelling to determine the resultant wave climate at the site and across the physical processes study area.

1.6.3.3 In addition to boundary wave data, it was necessary to analyse the wind field to include the contribution of local wind seas. For this, for a representative point for each of the key directions, was identified and utilised from the National Oceanic and Atmospheric Administration (NOAA) 40year dataset. This was analysed on the same sectoral basis as the wave data to give an indication of the return period wind speed. Figure 1.45 shows the model domain with wind and wave roses relating to the forcing data.

1.6.3.4 The wave modelling was undertaken using the spectral wave model, MIKE21 SW, to provide a full wave climate and wave breaking across the physical processes study area. The model used a quasi stationary formulation which meant that for each event the wave field fully established over a number of numerical iterations until convergence was reached. The model resolves the wave field by simulating wind generation of waves within the model domain and the propagation of externally generated swell waves through the domain. The model setup ensured that the detail of both locally generated wind waves and swell conditions from further afield were captured.

1.6.3.5 The following set of figures (Figure 1.46 to Figure 1.49) show the wave climate for four 1in1 year return period events from the principal directions; north (000°), northeast (030°), southwest (240°) and west (270°) direction respectively. These sectors were selected to be representative of the characteristics of the wave climate and also for sectors for which the Mona Offshore Wind Project may potentially affect marine processes along the coastline. The wave modelling was undertaken at mean high



water (MHW) being the high water level on an average tide. Figure 1.49 shows the waves approaching from the west and demonstrates, as anticipated, the largest waves approach from this sector.

1.6.3.6 A second set of figures are presented relating to the 1in20 year return period; Figure 1.50 to Figure 1.53. These show data for the same sectors and tidal height as the 1in1 year return period. They have been introduced to ensure that the baseline for a more arduous conditions is established for assessment of the potential effect of the Mona Offshore Wind Project on wave climate.



MONA OFFSHORE WIND PROJECT

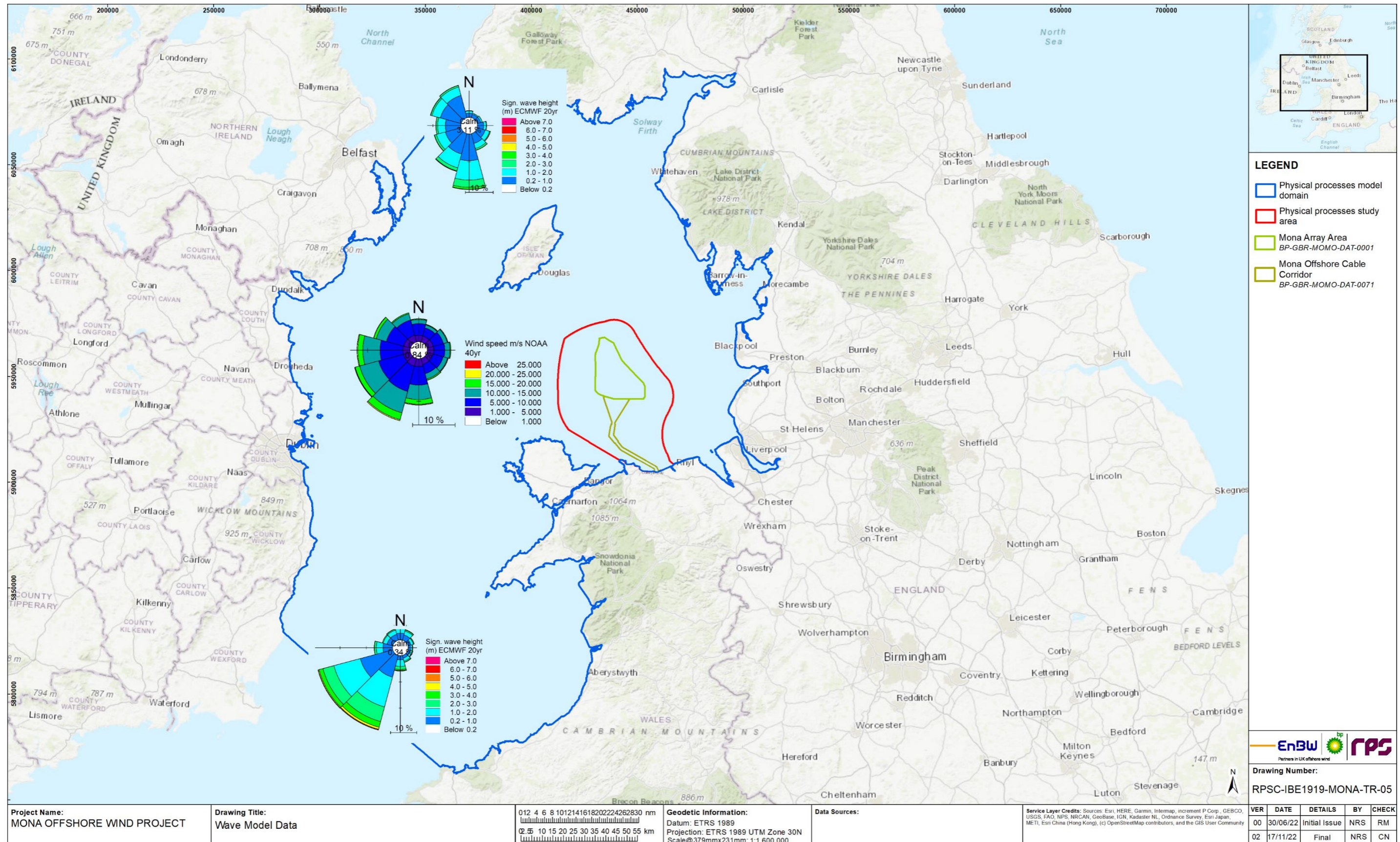


Figure 1.45: Wave roses for model boundaries - 22 year ECMWF Dataset and wind rose for 40 year NOAA dataset.



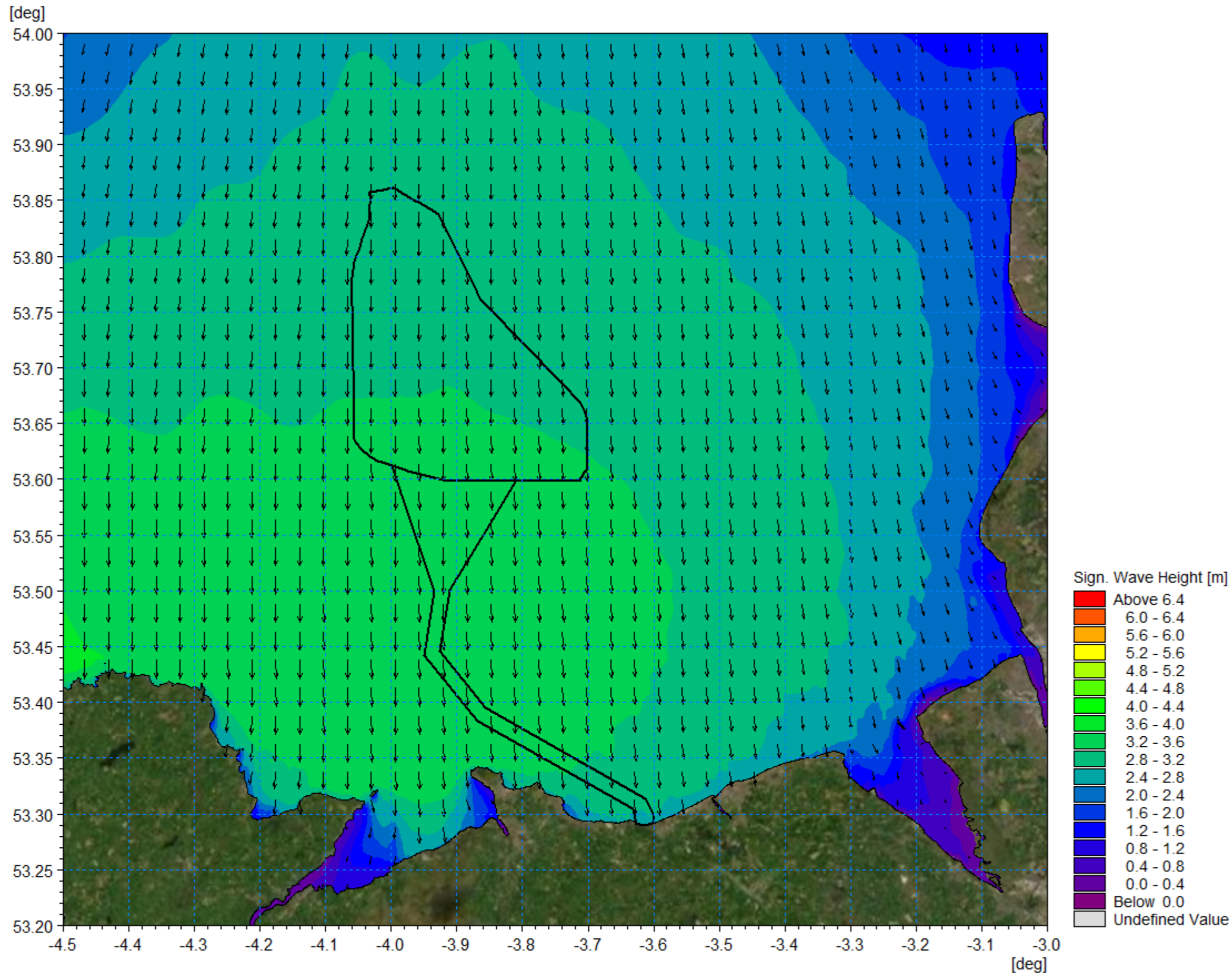


Figure 1.46: Wave climate 1:1 year storm from 000° MHW.



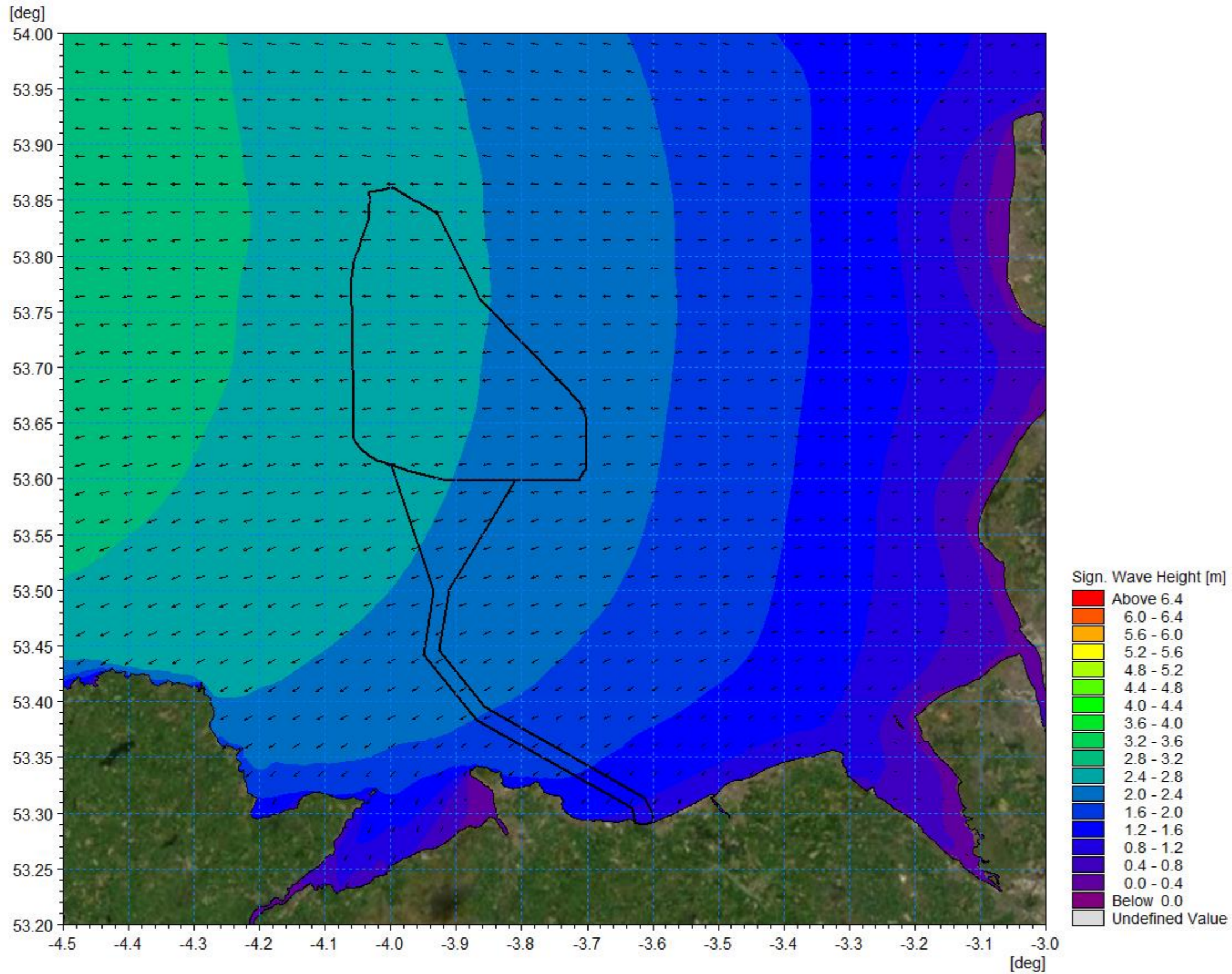


Figure 1.47: Wave climate 1:1 year storm from 090° MHW.



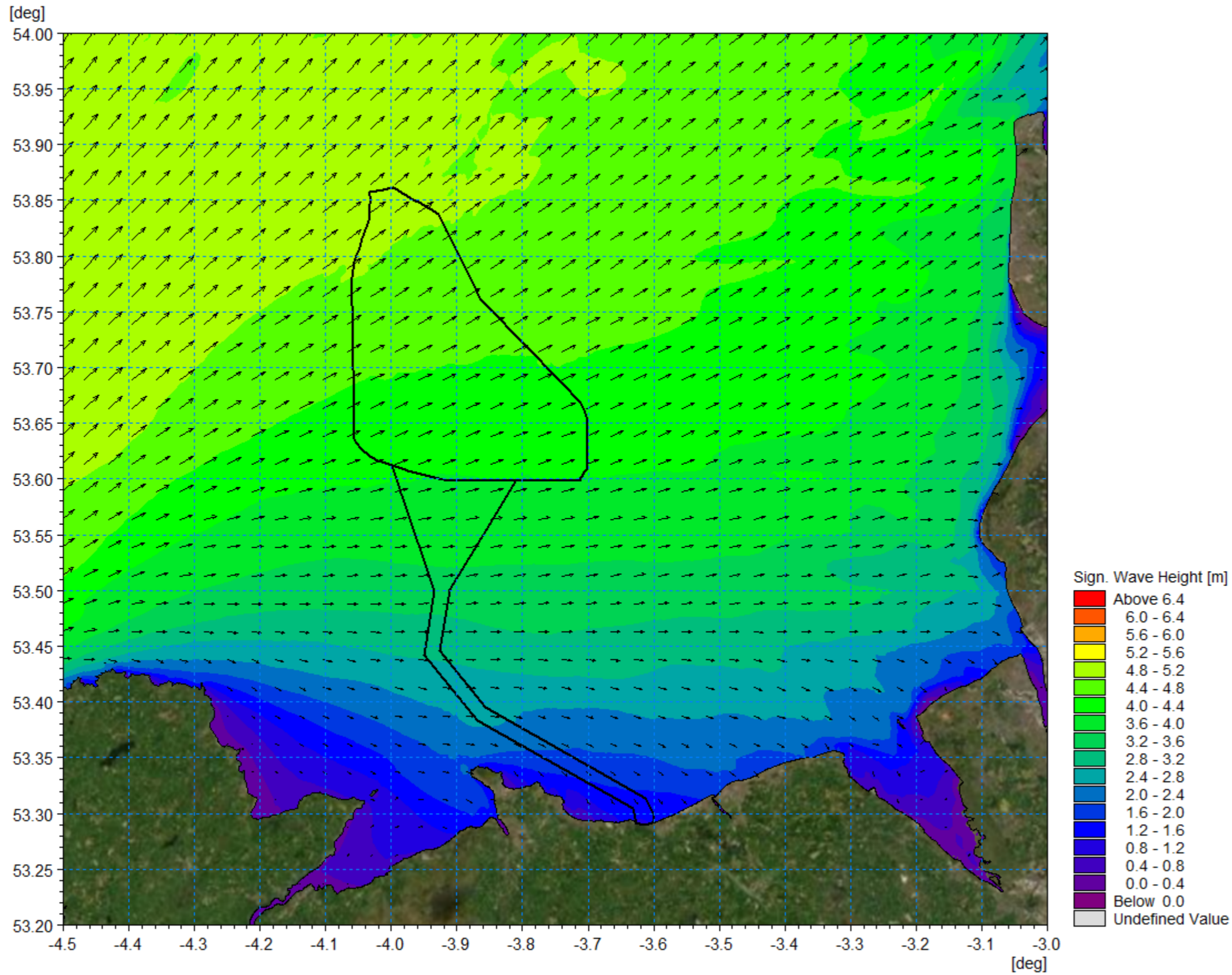


Figure 1.48: Wave climate 1:1 year storm from 240° MHW.

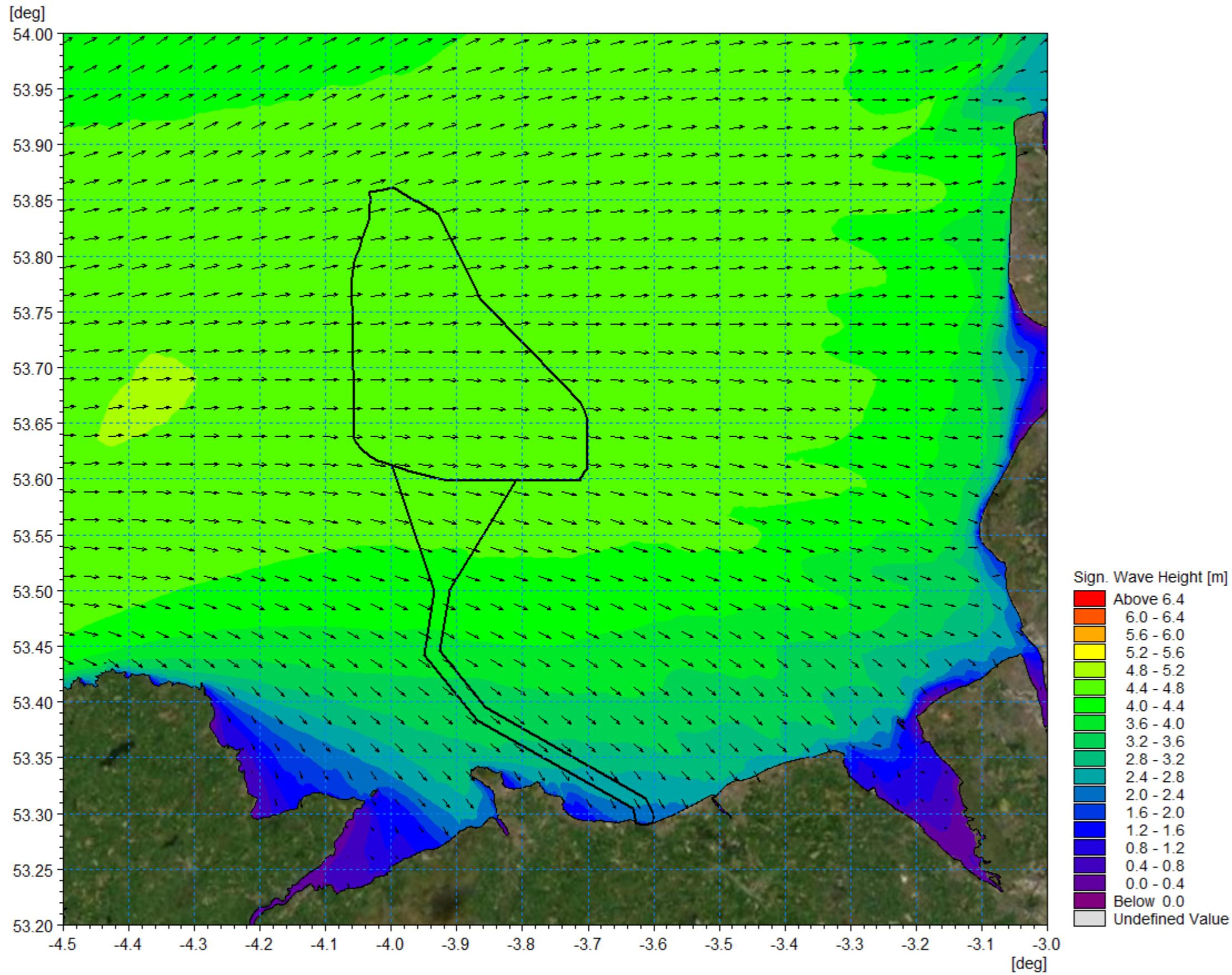


Figure 1.49: Wave climate 1:1 year storm from 270° MHW.



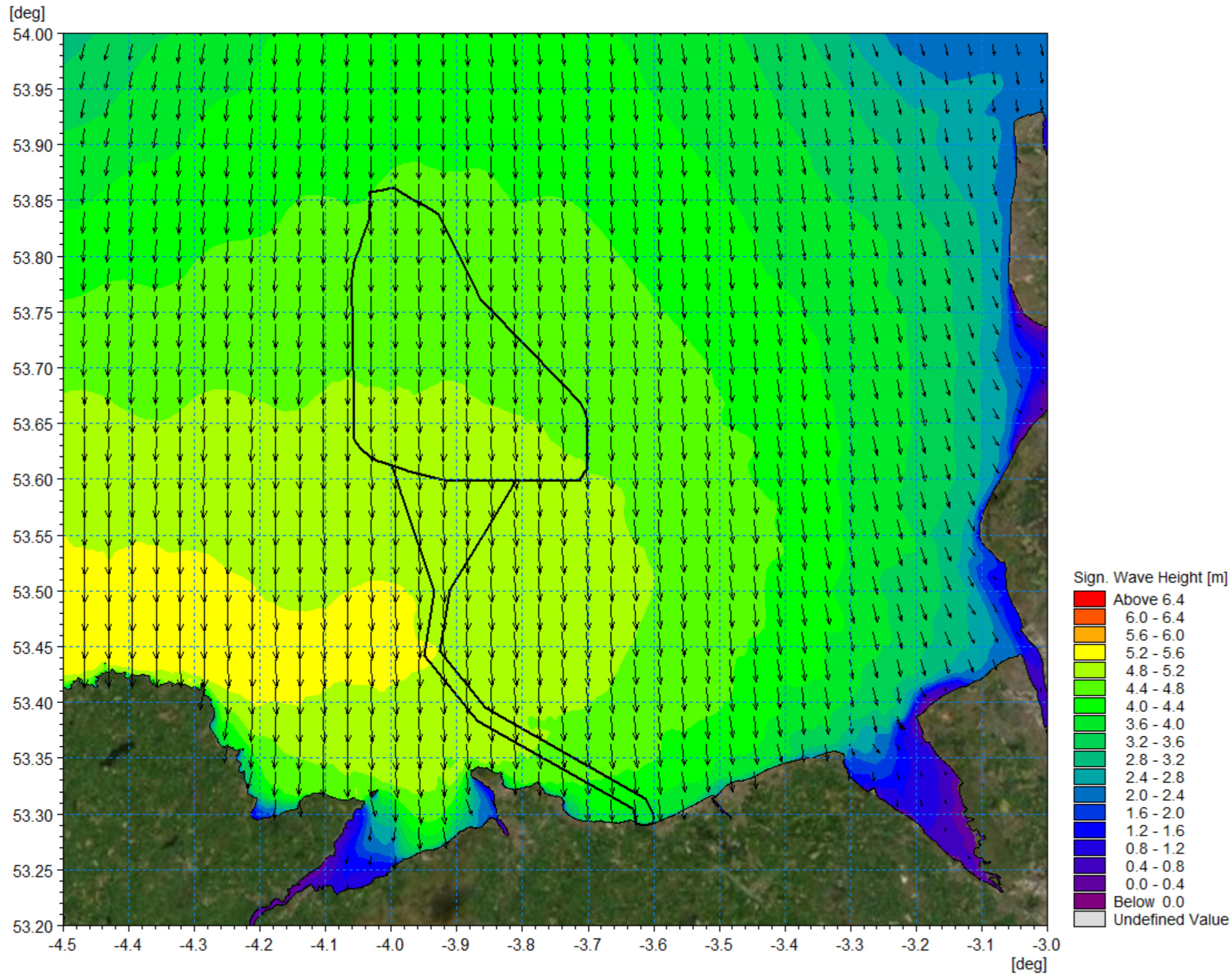


Figure 1.50: Wave climate 1:20 year storm from 000° MHW.

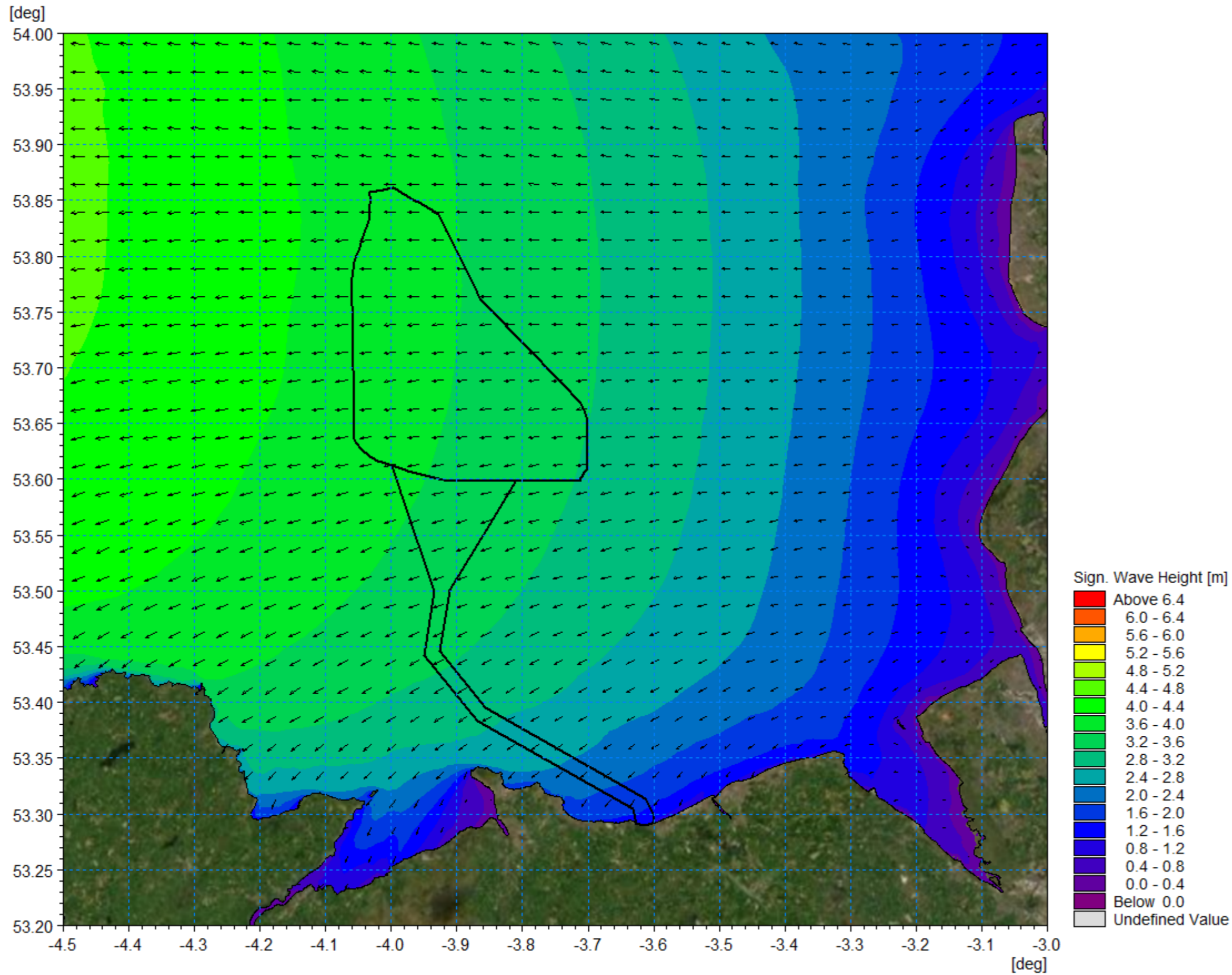


Figure 1.51: Wave climate 1:20 year storm from 090° MHW.



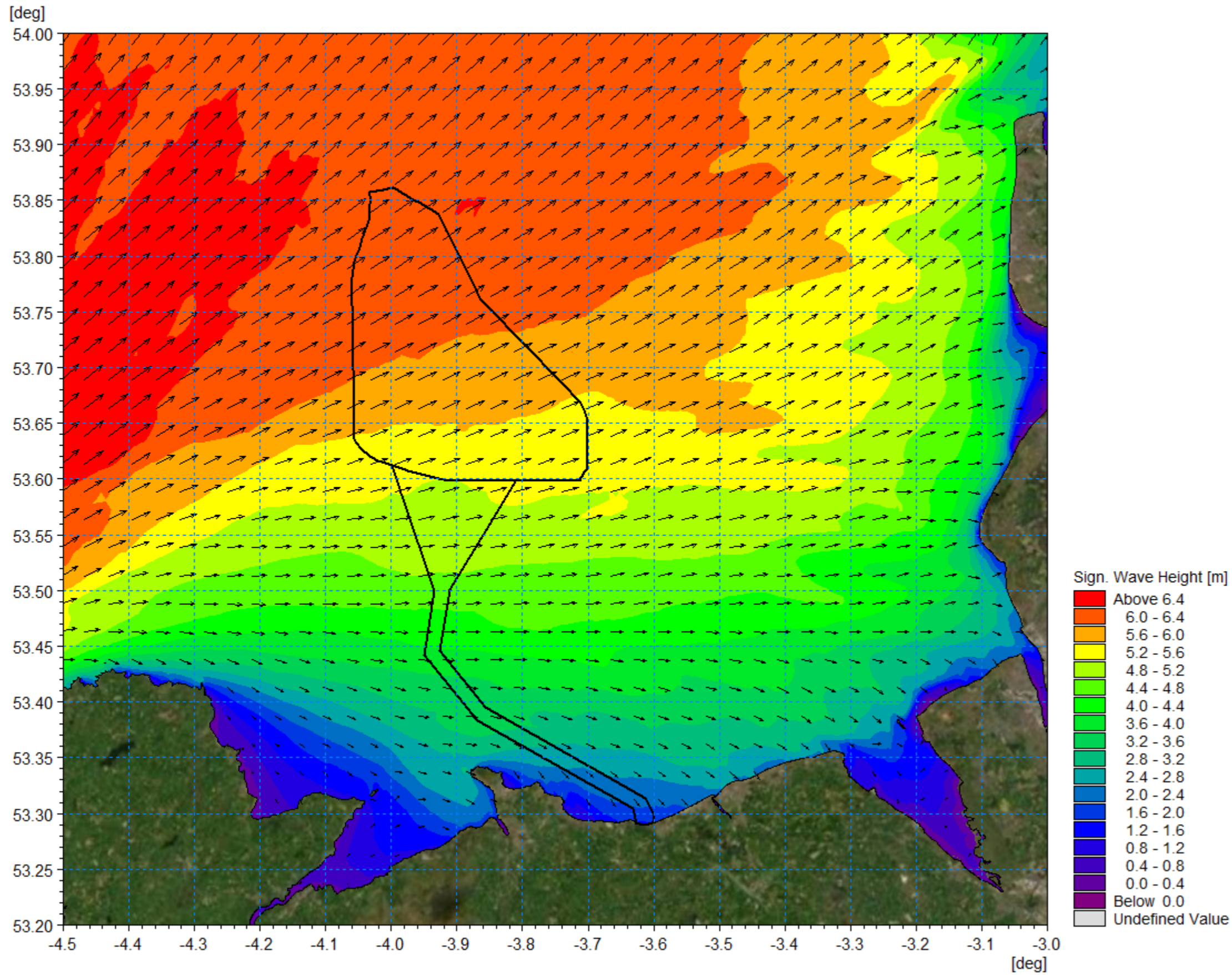


Figure 1.52: Wave climate 1:20 year storm from 240° MHW.

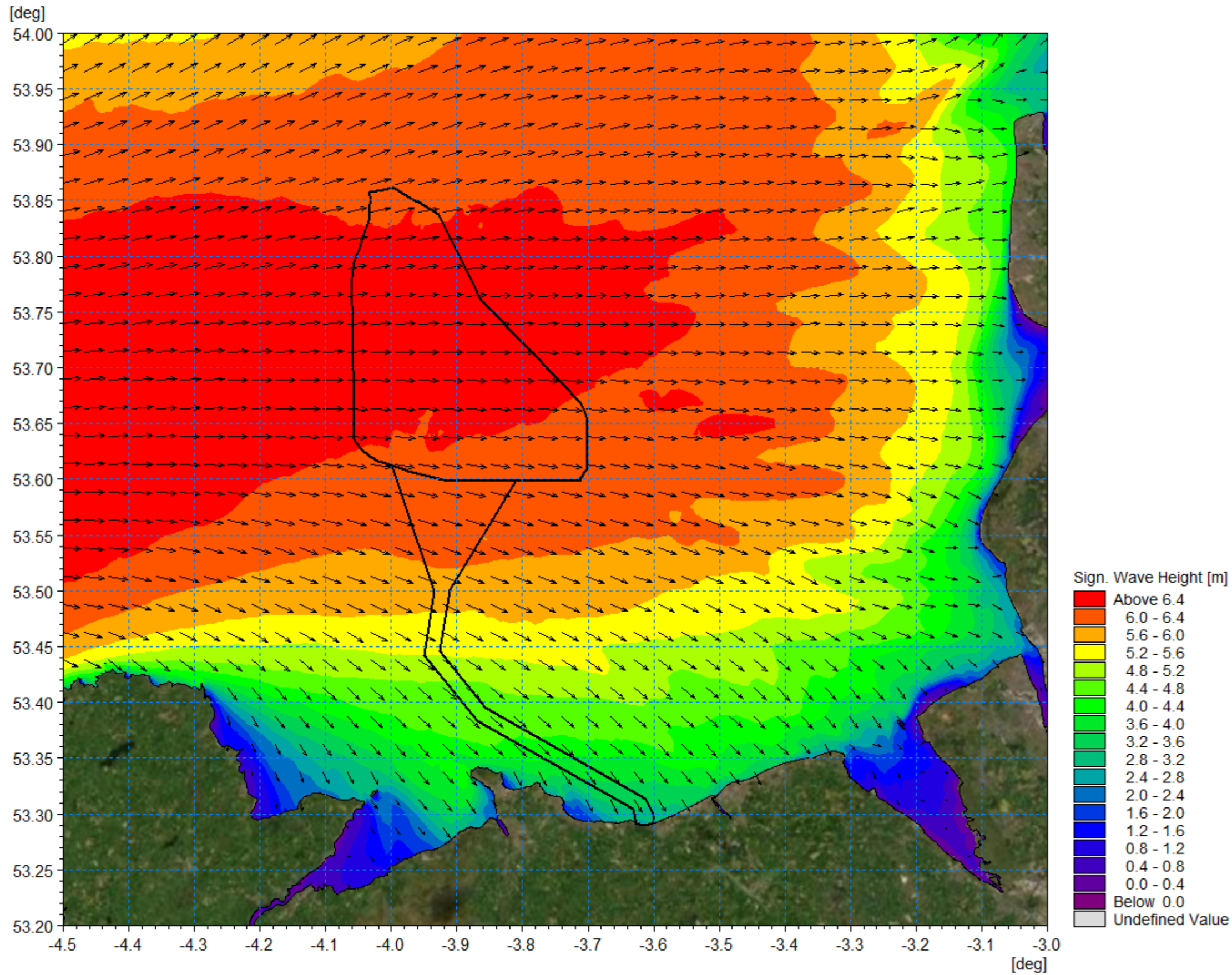


Figure 1.53: Wave climate 1:20 year storm from 270° MHW.



## 1.6.4 Littoral currents

- 1.6.4.1 The MIKE suite facilitates the coupling of models. The depth averaged hydrodynamic model, used for the tidal modelling, coupled with the spectral wave model, provides a full wave climate incorporating the impact of water levels and currents on waves and wave breaking. Using this, the littoral currents (i.e. those currents driven by tidal, wave and meteorological forces) were examined.
- 1.6.4.2 The 1in1 year storm from 270° sector was simulated with the inclusion of spring tides to encompass a wide range of tidal conditions and the resulting flood and ebb currents are presented in Figure 1.54 and Figure 1.55 respectively. These correspond with the (calm) tidal plots presented in Figure 1.31 and Figure 1.32. As expected, the presence of the southeast going waves increase the currents on the flood tide whilst reducing them on the ebb.

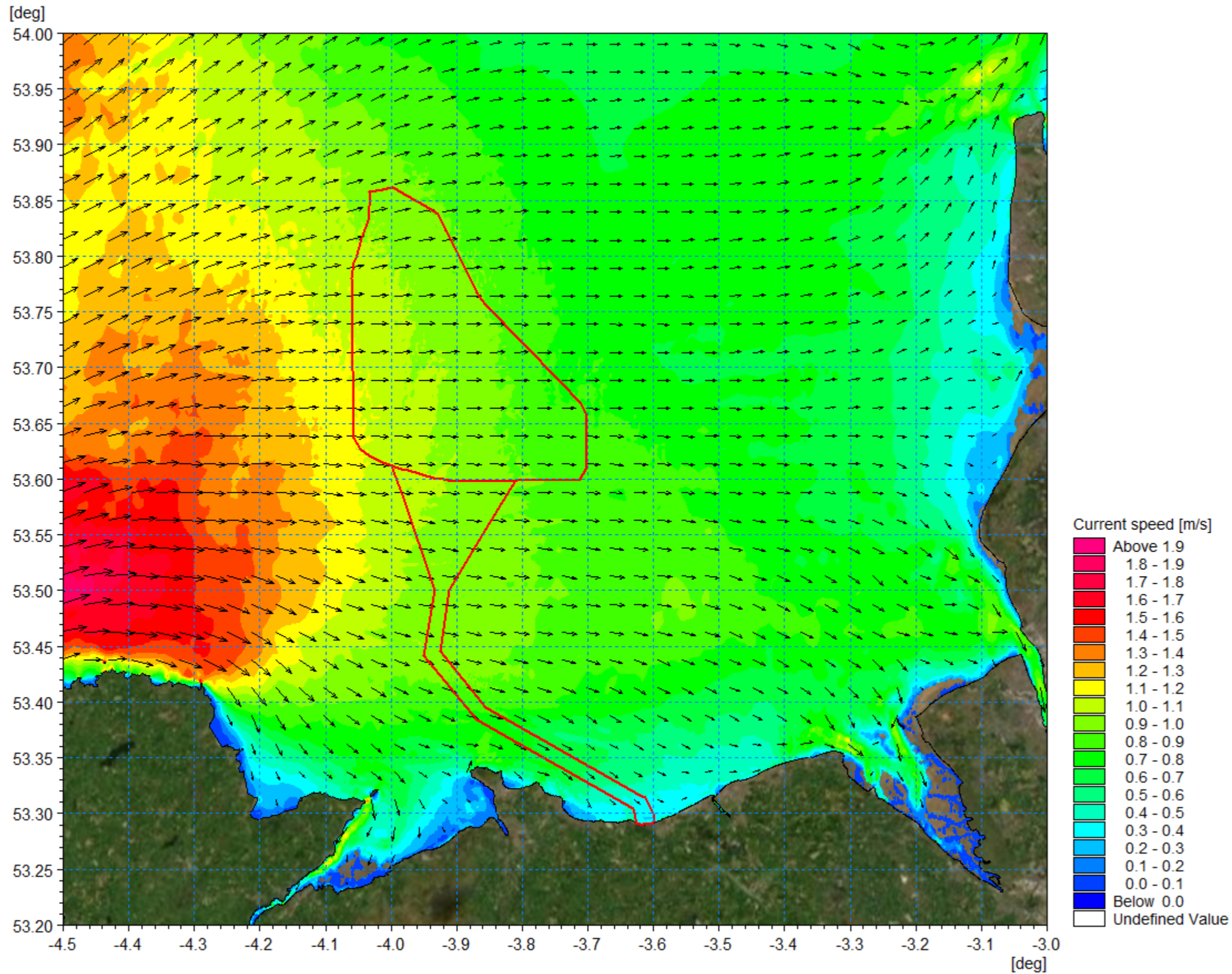


Figure 1.54: Littoral current 1:1 year storm from 270° - Flood Tide.



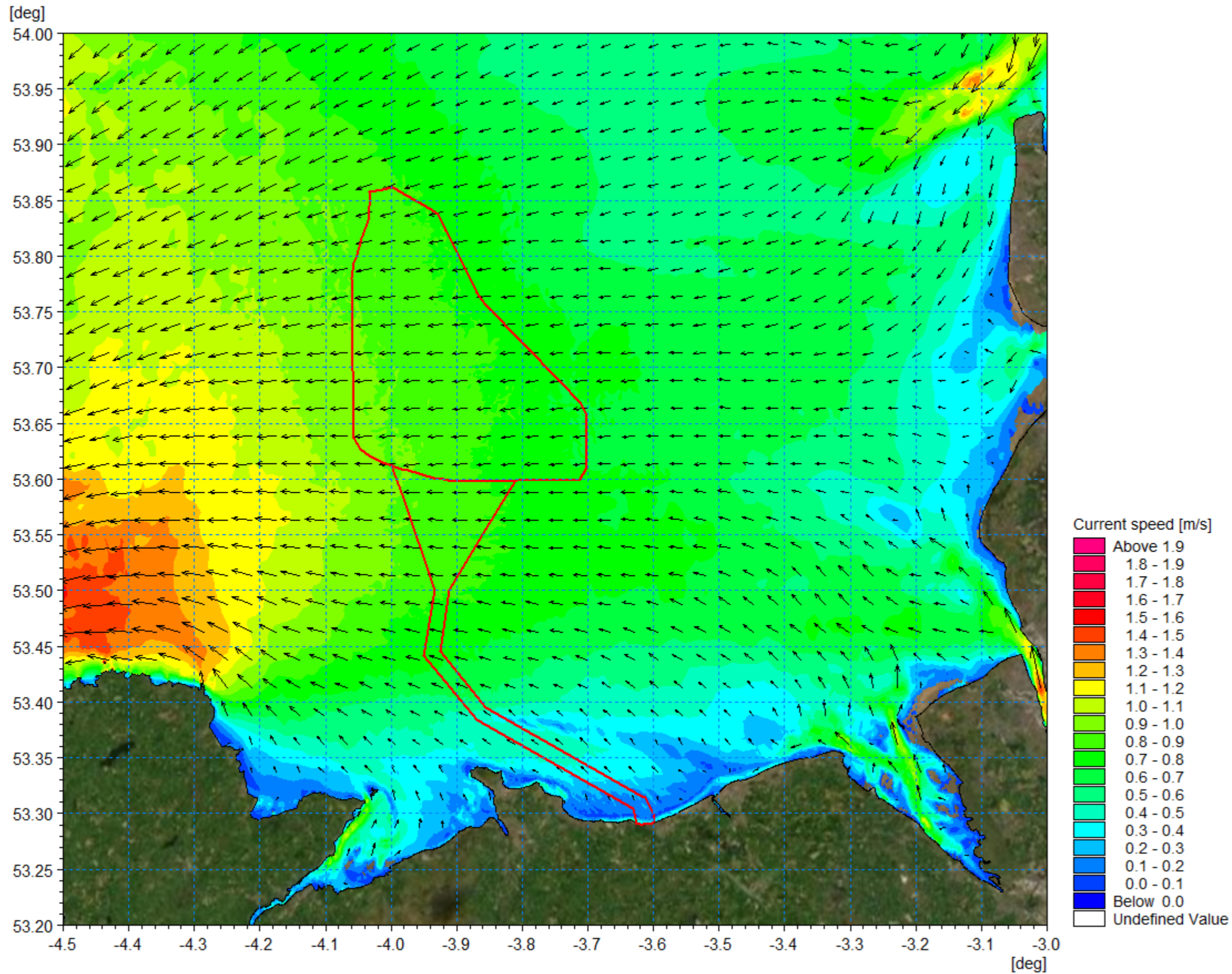


Figure 1.55: Littoral current 1:1 year storm from 270° - Ebb Tide.

## 1.6.5 Sedimentology and seabed substrate

- 1.6.5.1 An overview of surficial sediment geology and the seabed features data is presented in this section, based on a range of data sources including both publicly available datasets and interpretation undertaken of the SSS data collected during the recent geophysical surveys (Table 1.4). An understanding of seabed substrate types is required to assess the potential impacts which may arise due to the installation of wind turbines, offshore platform foundations, array cables and export cables.
- 1.6.5.2 The sediment grading properties applied within the modelling for both sediment transport assessment and characterisation of mobilised material during seabed preparation and installation operations was derived from British Geological Survey (BGS) datasets as illustrated in Figure 1.56. These datasets included both generalised Folk classification from borehole logs and detailed particle analysis data.
- 1.6.5.3 The SSS interpretation defined a range of sediment types within the Mona Array Area comprising sand, gravelly sand and sandy gravel. Sandwaves and megaripples are associated with these sediment types. To inform the modelling study seabed sediment information was required beyond the extent of the survey data and the EMODnet Geology database was utilised. The seabed classification shown in Figure 1.57 shows both the datasets.



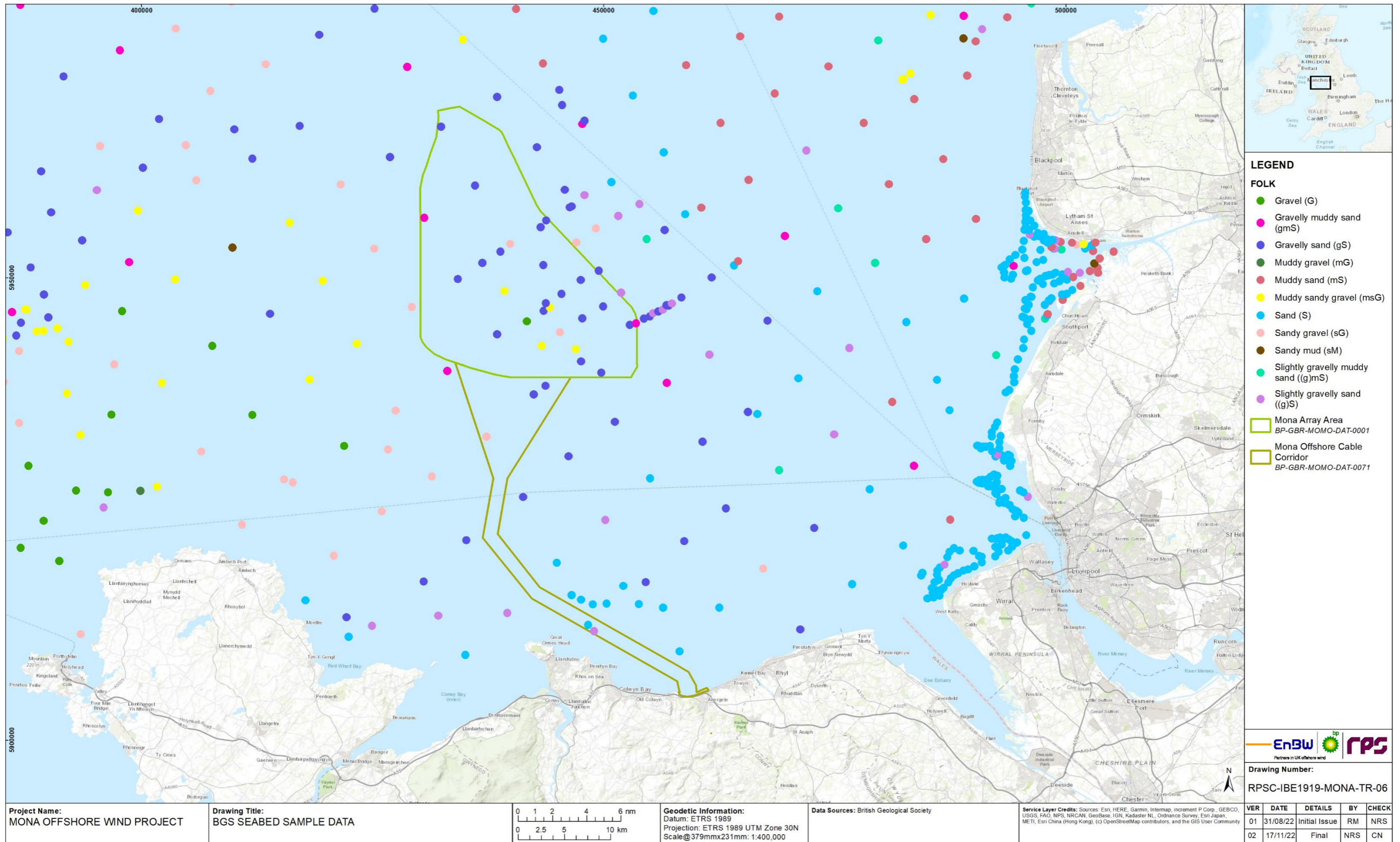


Figure 1.56: Seabed classification British Geological Survey.



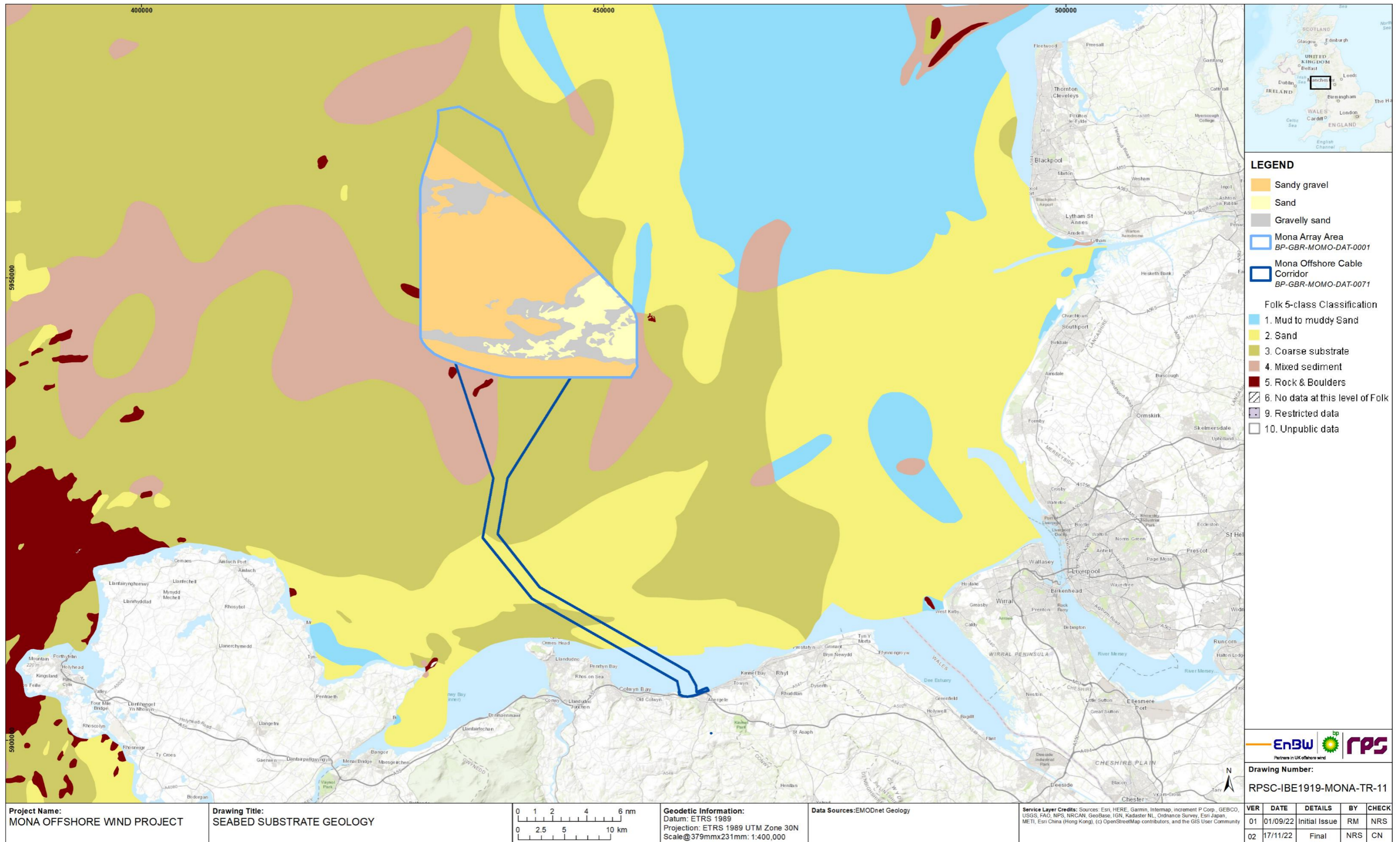


Figure 1.57: Seabed substrate geology EMODnet.



## 1.6.6 Sediment transport

- 1.6.6.1 The MIKE21 Sediment Transport module enables assessment of bed sediment transport rates for non-cohesive sediment resulting from currents or combined wave-current flows. It was used to determine the sediment transport pattern within the model domain. The model combines inputs from both the hydrodynamic model and, if required, the wave propagation model. It used sediment characterisation provided by the recent survey and EMODnet data as presented in the previous section to determine the sediment transport characteristics. For each region a representative sample from the BGS was used to define the bed sediment and grading.
- 1.6.6.2 It is noted that for a detailed sediment transport study greater detail of sediment characteristics across the model domain and along the coastline would be required. In the context of a comparative study to identify the impact of the Mona Offshore Wind Project infrastructure on sediment transport patterns the sediment characteristics identified within the survey and sampling were interpolated to those areas in the EMODnet data with similar sediment classifications.
- 1.6.6.3 The model domain was set up with a layer of mobile bed sediment. In areas where sediment is present an initial layer depth was set to 3m and tapered to zero in the areas of rocky outcrops to ensure that sediment was not exhausted during the simulated events. Sediment transport was examined relating to spring tidal conditions over the course of two tidal cycles (one day) to provide a 'snap-shot' for comparison. The simulation included a period for the hydrodynamics to stabilise and develop across the domain prior to sediment transport being enabled (i.e. a "warm-up" period).
- 1.6.6.4 Three aspects were examined:
- Residual current, which is the net flow over the course of the tidal cycle. This is effectively the driving force of the sediment transport
  - Potential sediment transport over this period
  - Potential sediment transport during flood and ebb tides. This provides information for a 'snap-shot' in time to enable the process to be illustrated.
- 1.6.6.5 The residual current is presented in Figure 1.58 and it should be noted that a log scale has been used to cover the range of residual current speeds encountered. The current vectors indicate residual flow into the east Irish Sea from the north and west which correlates with this region being a sediment sink. There are strong circulatory currents where tidal flows interact with headlands and embayments.
- 1.6.6.6 An indication of transport rate is shown in Figure 1.59, again using a log scale palette as the values within the offshore regions are several orders of magnitude smaller than those along the coastline. The greatest transport rates are seen in areas where finer sand fractions are present and in estuaries and at headland where tidal currents are strongest. The mechanism is more clearly illustrated in Figure 1.60 and Figure 1.61 for flood and ebb tides respectively. It is evident that transport rates are highest during the dominant flood tide and the region is a sediment sink.
- 1.6.6.7 By way of completeness, and for use in the comparative study, residual currents relating to the 1 in 1 year return period storm approaching from 270° are also presented, Figure 1.62. As anticipated, the littoral currents and dominant flood tide significantly increase easterly residual currents particularly along the Welsh coastline. This in turn would result in increased sediment transport rates during storm conditions.

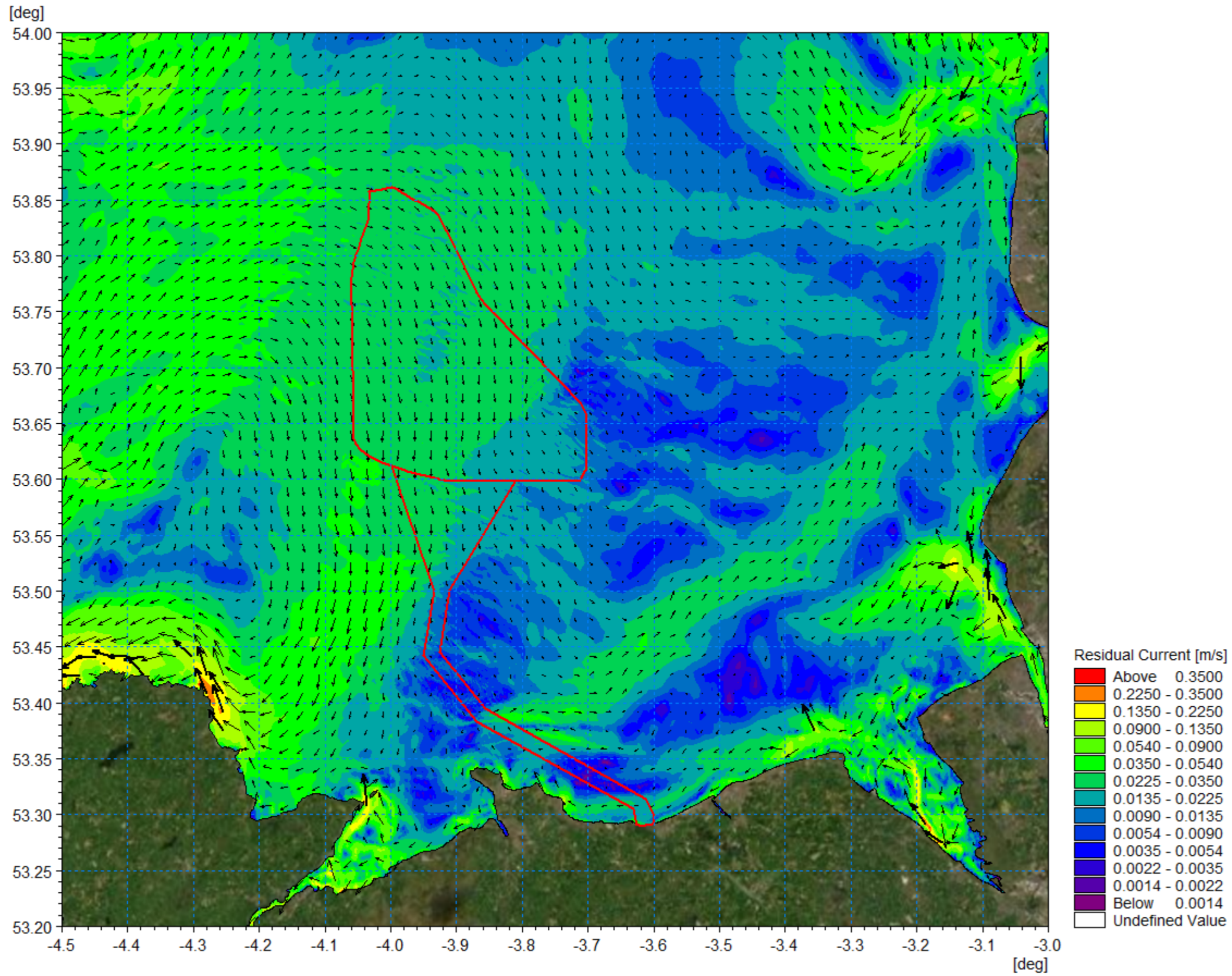


Figure 1.58: Residual current spring tide.



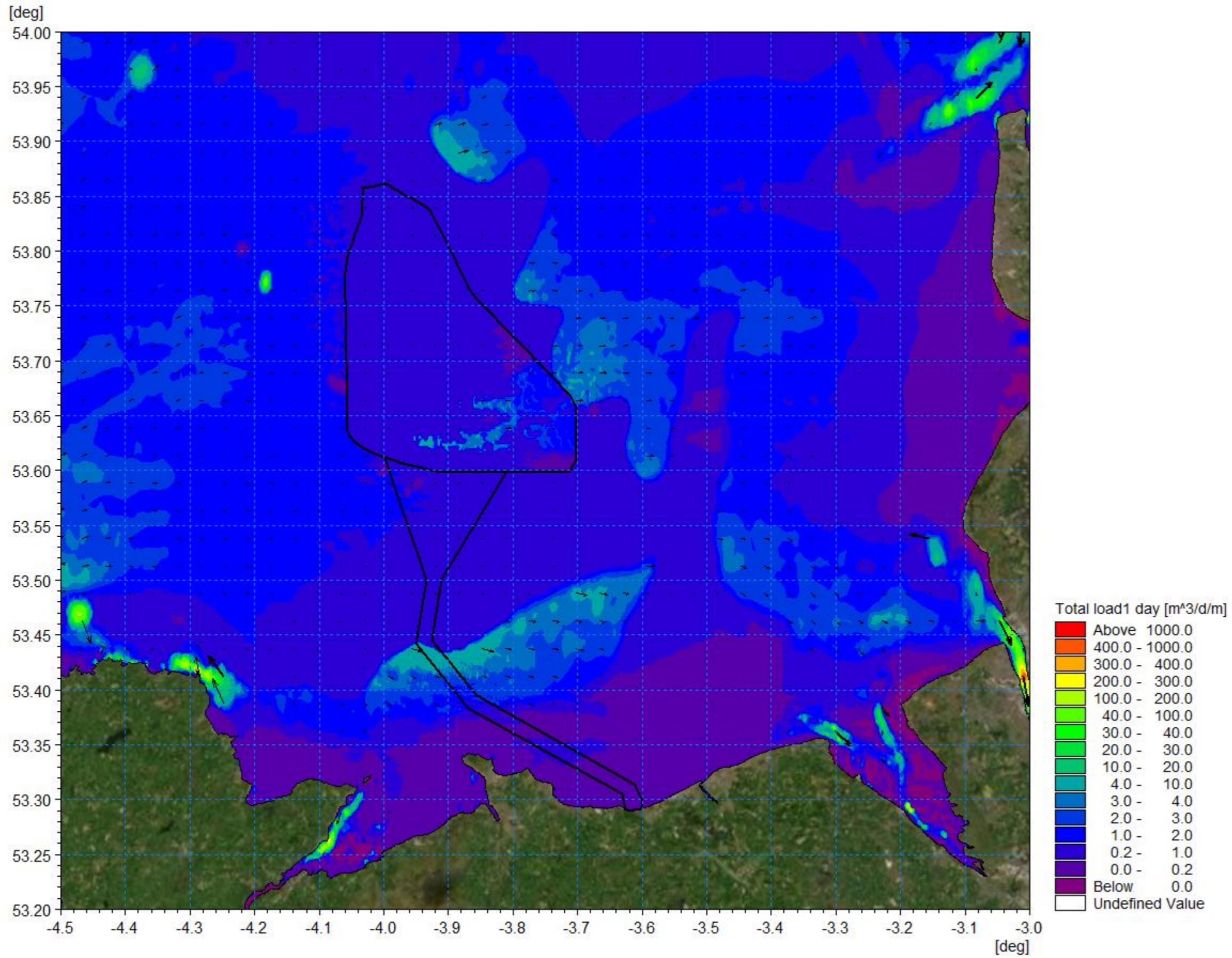


Figure 1.59: Potential sediment transport over the course of 1 day (two tide cycles).



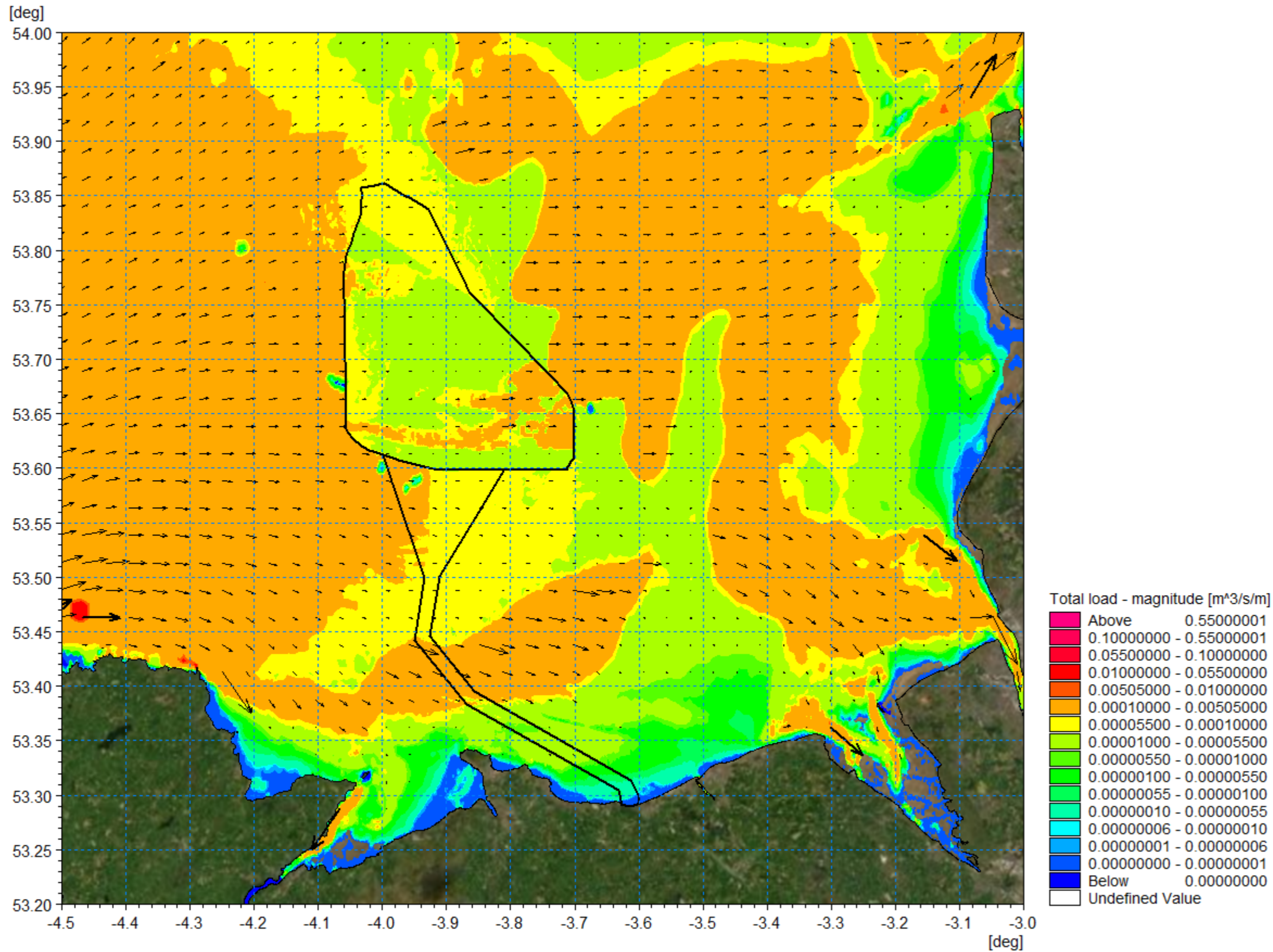


Figure 1.60: Sediment transport – flood tide.



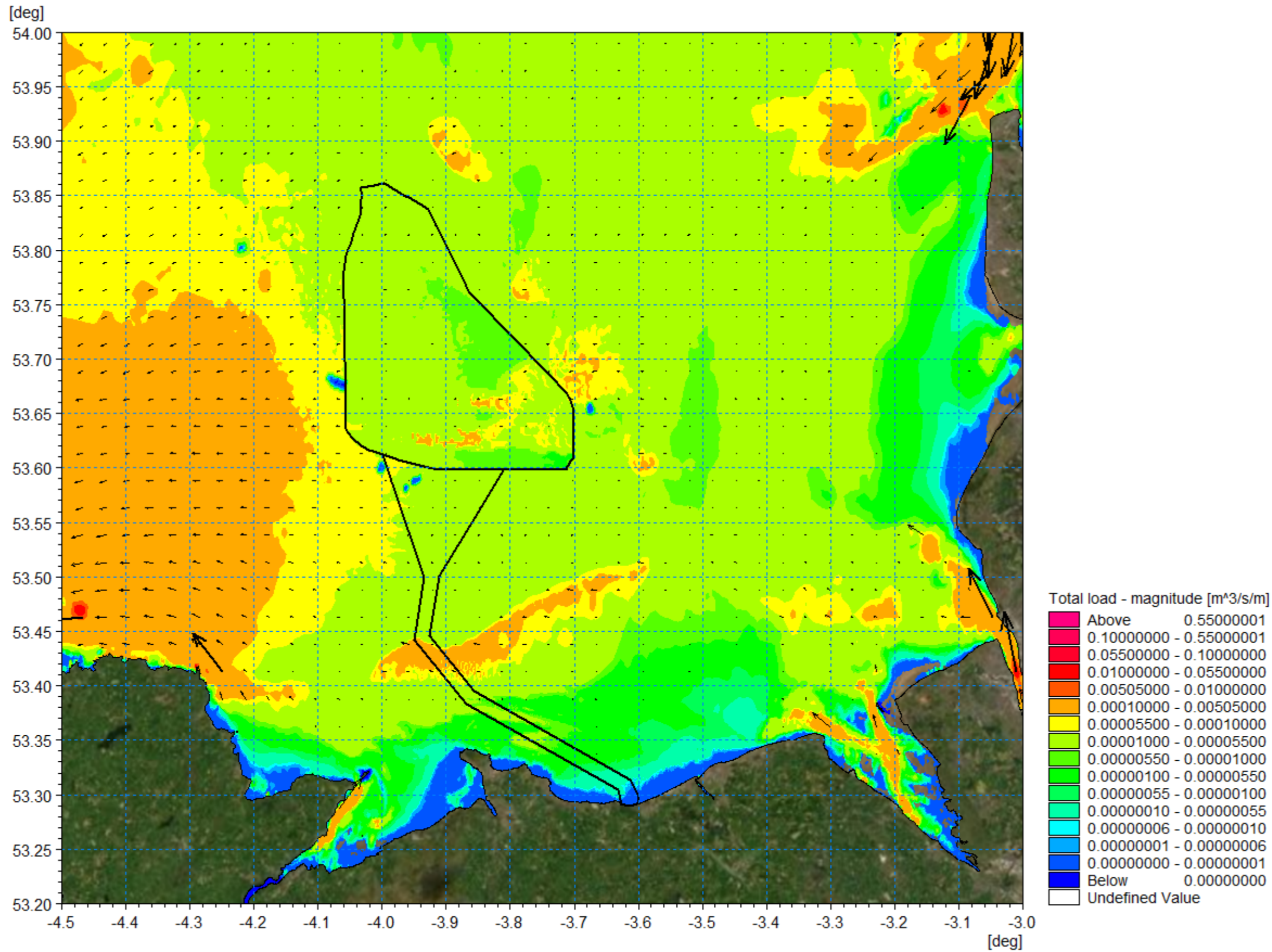


Figure 1.61: Sediment transport – ebb tide.

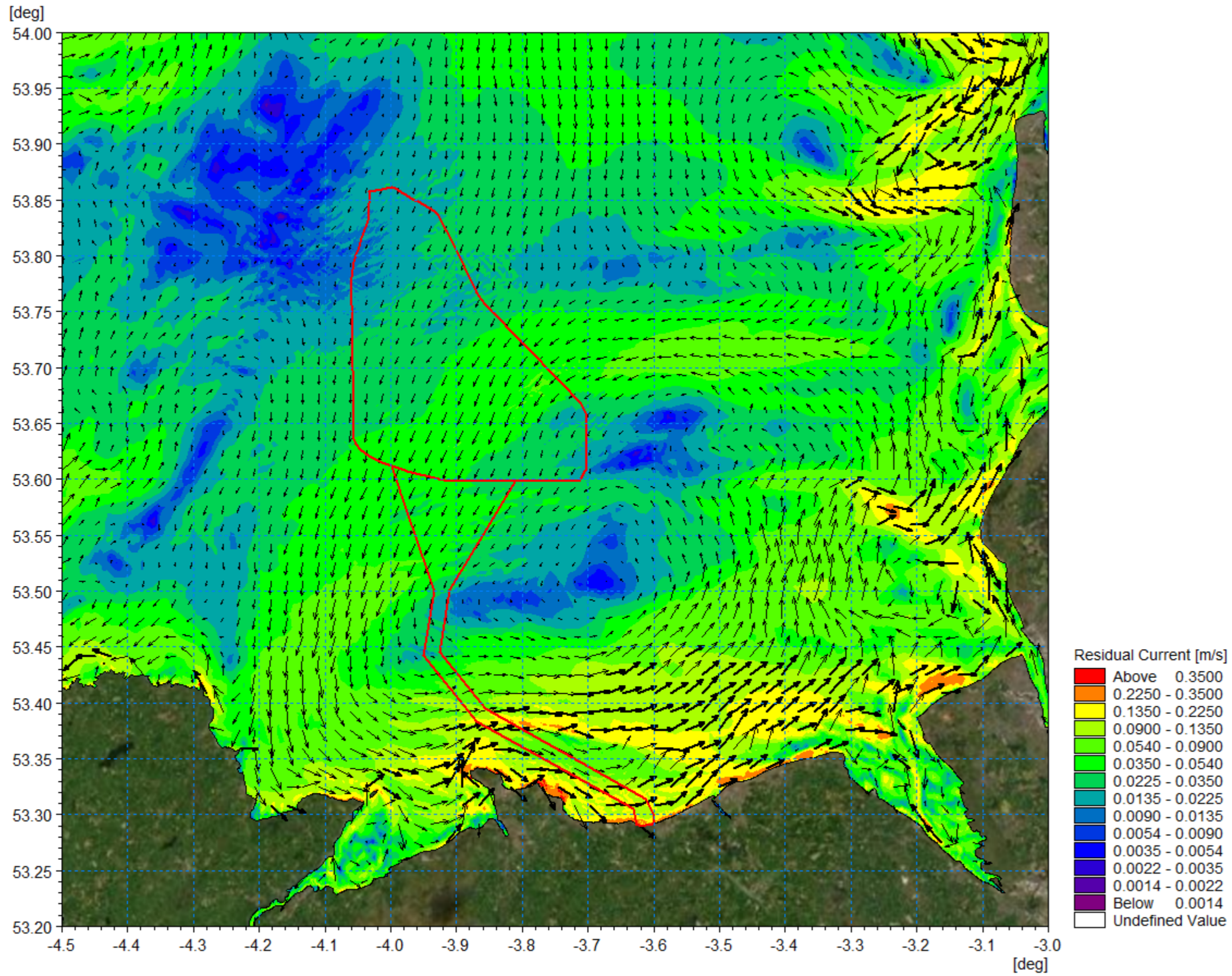


Figure 1.62: Residual current spring tide with 1:1 year storm from 270°.



**1.6.7 Suspended sediments**

1.6.7.1 The principal mechanisms governing Suspended Sediment Concentration (SSC) in the water column are tidal currents, with fluctuations observed across the spring-neap cycle and across the different tidal stages (high water, peak ebb, low water, peak flood) observed throughout both datasets. It is key to note that SSCs can also be temporarily elevated by wave-driven currents during storm events. During high-energy storm events, levels of SSC can rise significantly, both near bed and extending into the water column. Following storm events, SSC levels will gradually decrease to baseline conditions, regulated by the ambient regional tidal regimes. The seasonal nature and frequency of storm events supports a broadly seasonal pattern for SSC levels.

1.6.7.2 Based on the data recorded within the Morgan metocean study site, located in close proximity to the Mona Offshore Wind Project, the average near bed turbidity associated is circa 2mg/l. As shown in Figure 1.63, spikes in near surface turbidity correspond with increases in the significant wave height during storm conditions. The data is presented for the November 2021 to March 2022 period with peaks reaching circa 20mg/l.

1.6.7.3 For more generalised conditions the Cefas Climatology Report 2016 (Cefas, 2016) and associated dataset provides the spatial distribution of average non-algal Suspended Particulate Matter (SPM) for the majority of the UK Continental Shelf (UKCS). Between 1998 and 2005, the greatest plumes are associated with large rivers such as those that discharge into the Thames Estuary, The Wash and Liverpool Bay, which show mean values of SPM above 30mg/l. The levels of SPM reported by CEFAS between 1998 to 2005 of approximately 0.9mg/l to 3mg/l are similar to the values recorded at Morgan. Higher levels of SPM are experienced more commonly in the winter months; however, due to the tidal influence, even during summer months the levels may become elevated.

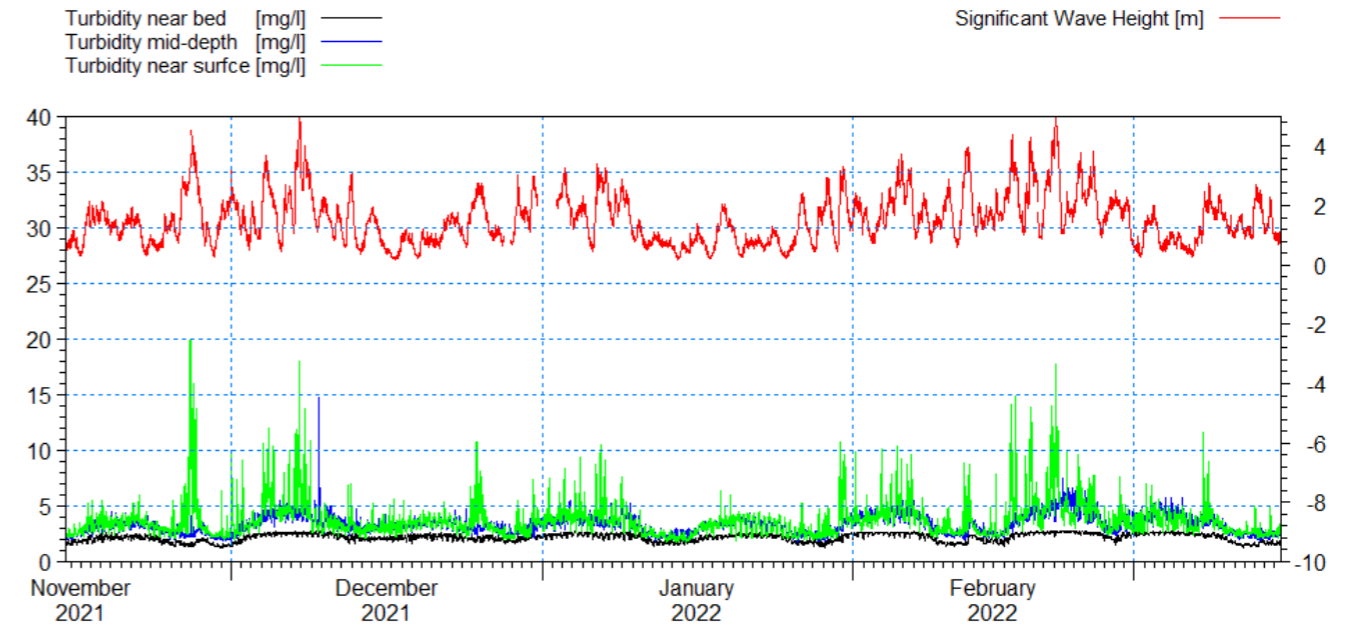


**Figure 1.63: Turbidity levels from the Morgan metocean site.**

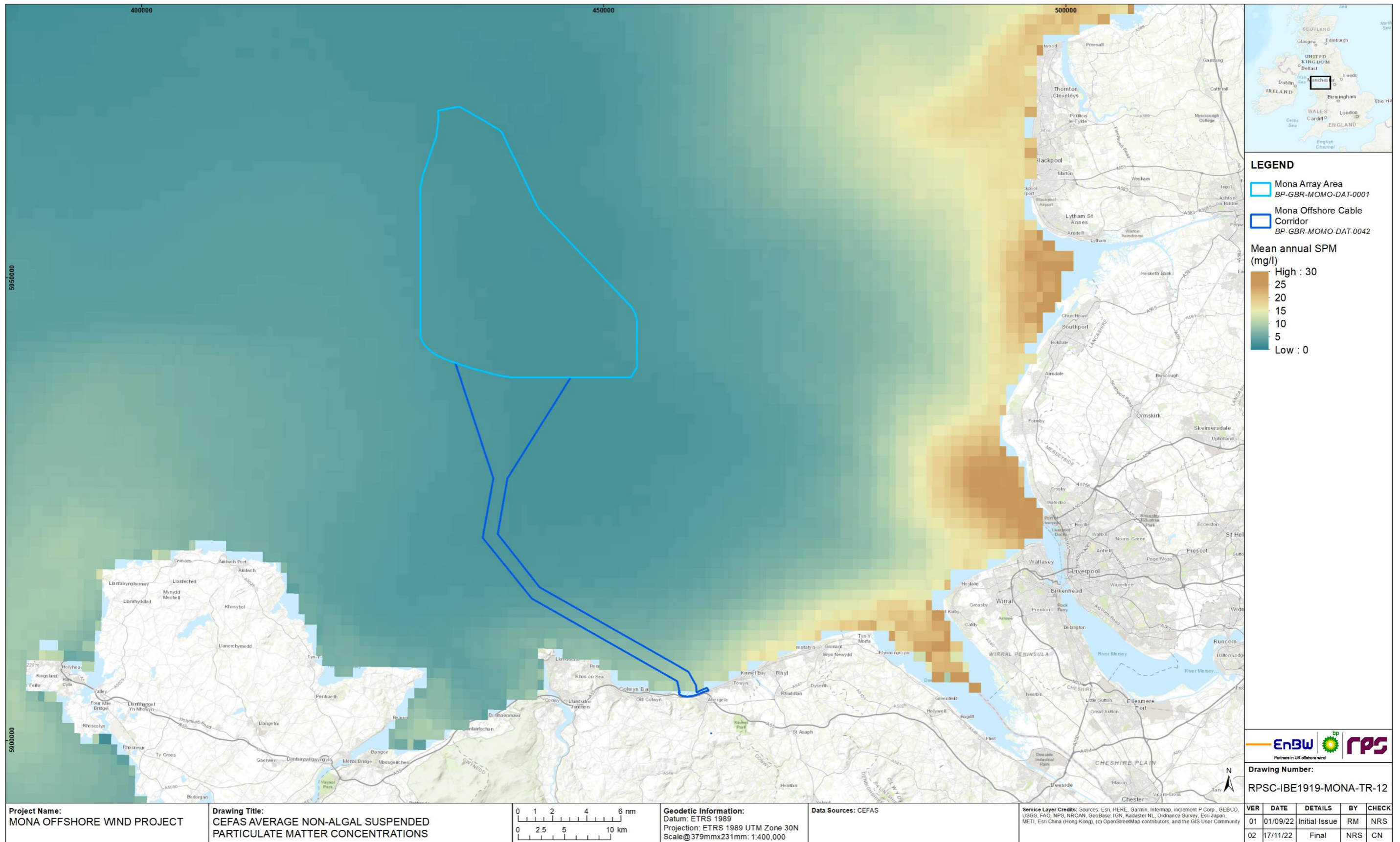


Figure 1.64: Distribution of average non-algal suspended particulate matter – CEFAS.



## 1.7 Potential environmental changes

### 1.7.1 Overview

1.7.1.1 The potential changes to the baseline hydrographic conditions as a result of the installation and presence of the Mona Offshore Wind Project are quantified in the following sections. These changes relate to the presence of the infrastructure within the water column and seabed and are therefore associated with turbine legs along with cable and scour protection. The potential changes to sea state and sediment transport regimes were established by repeating the modelling undertaken in the previous section with the inclusion of the Mona Offshore Wind Project. The modelling was undertaken using an indicative layout which included the following changes in line with the maximum design scenario for physical processes:

- Leg structures 5m in diameter relating to 68 wind turbines each comprising four legs
- Scour protection 56m diameter and 2.5m in height associated with 16m suction bucket foundations for each wind turbine leg
- Leg structures 3m in diameter relating to 4 OSPs each comprising three legs
- Scour protection 49m diameter and 2.5m in height associated with 14m suction bucket foundations for each OSP leg
- Inter-array cable protection to a height of 3m and 10m width with cable crossings 4m in height, 32m width and 60m length
- Interconnector cable protection to a height of 3m and 10m width with cable crossings 3m in height, 20m width and 50m length
- Offshore export cable protection to a height of 3m and 10m width with cable crossings 3m in height, 30m width and 50m length.

1.7.1.2 In addition to these structures the modelling also included provision of an Offshore Booster Substation located mid-distance along the offshore export cable. The need for this infrastructure has subsequently been removed from the Mona Offshore Wind Project therefore the modelling results of potential environmental changes presented here would be conservative.

1.7.1.3 It should be noted that the scale of the model mesh meant that the general flow and sediment patterns around the structures could be observed on the wider scale. The detailed impact of secondary scour is localised, site and design specific in nature. The modelling included the provision of scour protection as defined in the project description presented in volume 1, chapter 3: Project description of the PEIR and a detailed assessment of the effectiveness of the scour protection proposed at each foundation location was not undertaken as this was not the purpose of the computational modelling. The scour protection does not have implications on the global scale and is restricted to reducing sediment erosion in the vicinity of the foundations; there would be larger implications if scour protection were not provided (Whitehouse *et al.*, 2006).

1.7.1.4 The methodology implemented for the modelling used parameters selected from the project description outlined in volume 1, chapter 3: Project description of the PEIR, to ascertain the most influential and likely scenario for each physical process aspect

under examination. The indicative layout used within the modelling study is presented in Figure 1.65 it applied cable protection in regions where trenching to 3m depth was unlikely (i.e. in the vicinity of rocky outcrops) and where inter-array cable connect with generating assets.

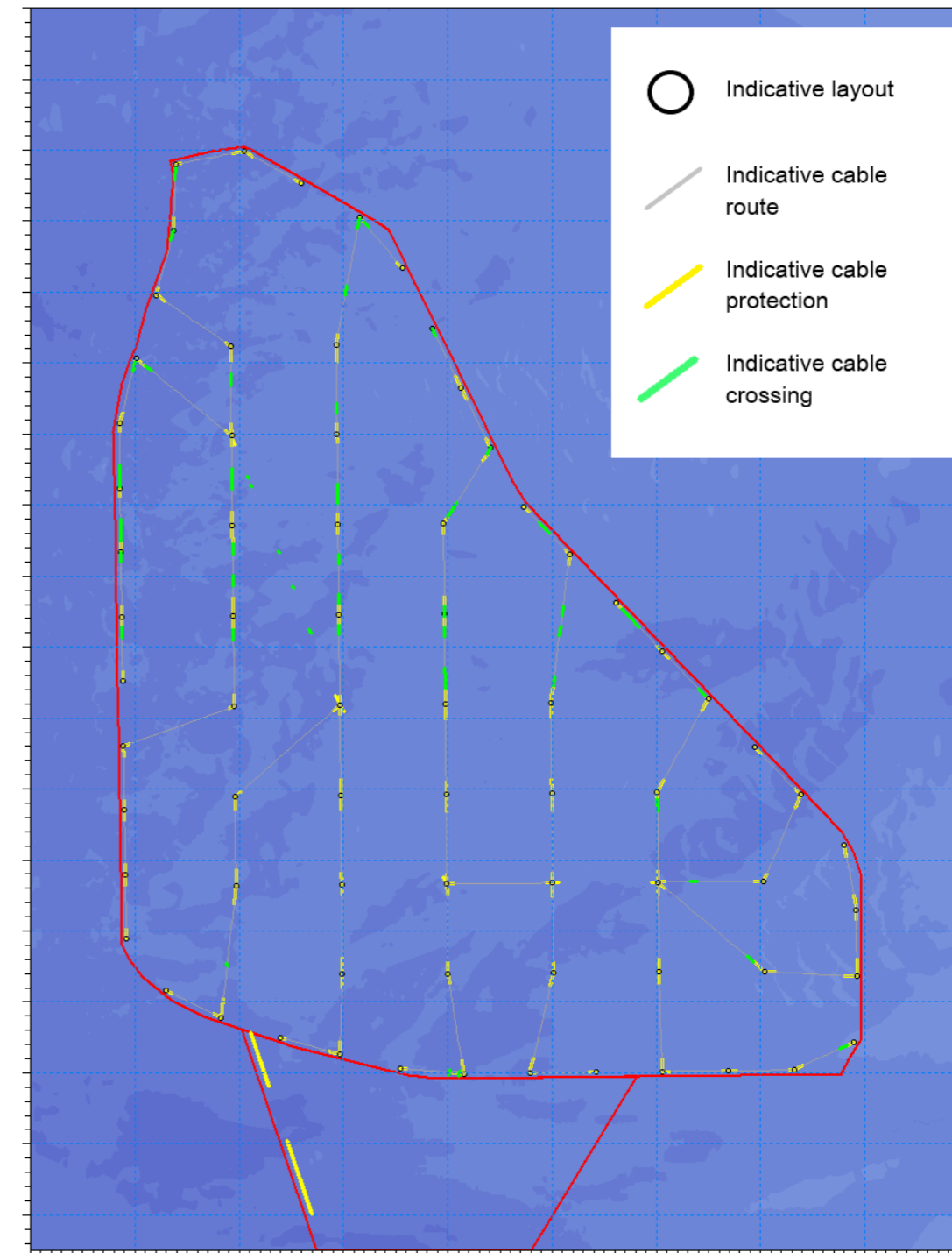


Figure 1.65: Modelled array and trenching route indicative layout.

## 1.7.2 Post-construction hydrography

### Tidal flow

- 1.7.2.1 The hydrodynamic simulations were repeated with the addition the infrastructure as outlined in the previous section. The bathymetry was also amended to take account of scour and cable protection. The following figures show the same mid flood and mid ebb steps from the simulation as were presented in Figure 1.31 and Figure 1.32 respectively, but with the Mona Offshore Wind Project foundation and structures in place. Where appropriate, the Mona Offshore Cable Corridor has been indicated on the figures along with the array area, to indicate the locality of the works without obscuring the model results. Due to the limited magnitude of the changes, difference plots have also been provided. These are the proposed minus the baseline condition, therefore increases in current speed will be positive. The same procedure for calculating differences and plotting figures has been implemented throughout this report.
- 1.7.2.2 Figure 1.66 shows the post-construction flood tide flow patterns with Figure 1.67 showing the changes and as the changes are limited to the vicinity of the development a more focused plot is provided in Figure 1.68. In the difference figures a log scale has been introduced to accentuate the values for clarity. Similarly, Figure 1.69, Figure 1.70 and Figure 1.71 show the same information for the ebb tide. During peak current speed the flow is redirected in the immediate vicinity of the structures and cable protection. The variation is a maximum of 5cm/s in the immediate vicinity of the structure which constitutes less than 5% of the peak flows. This reduces significantly with increased distance from each structure with changes being significantly smaller in the areas where cable protection is present within 200m of the installation changes are <2mm which would be indiscernible for baseline conditions.



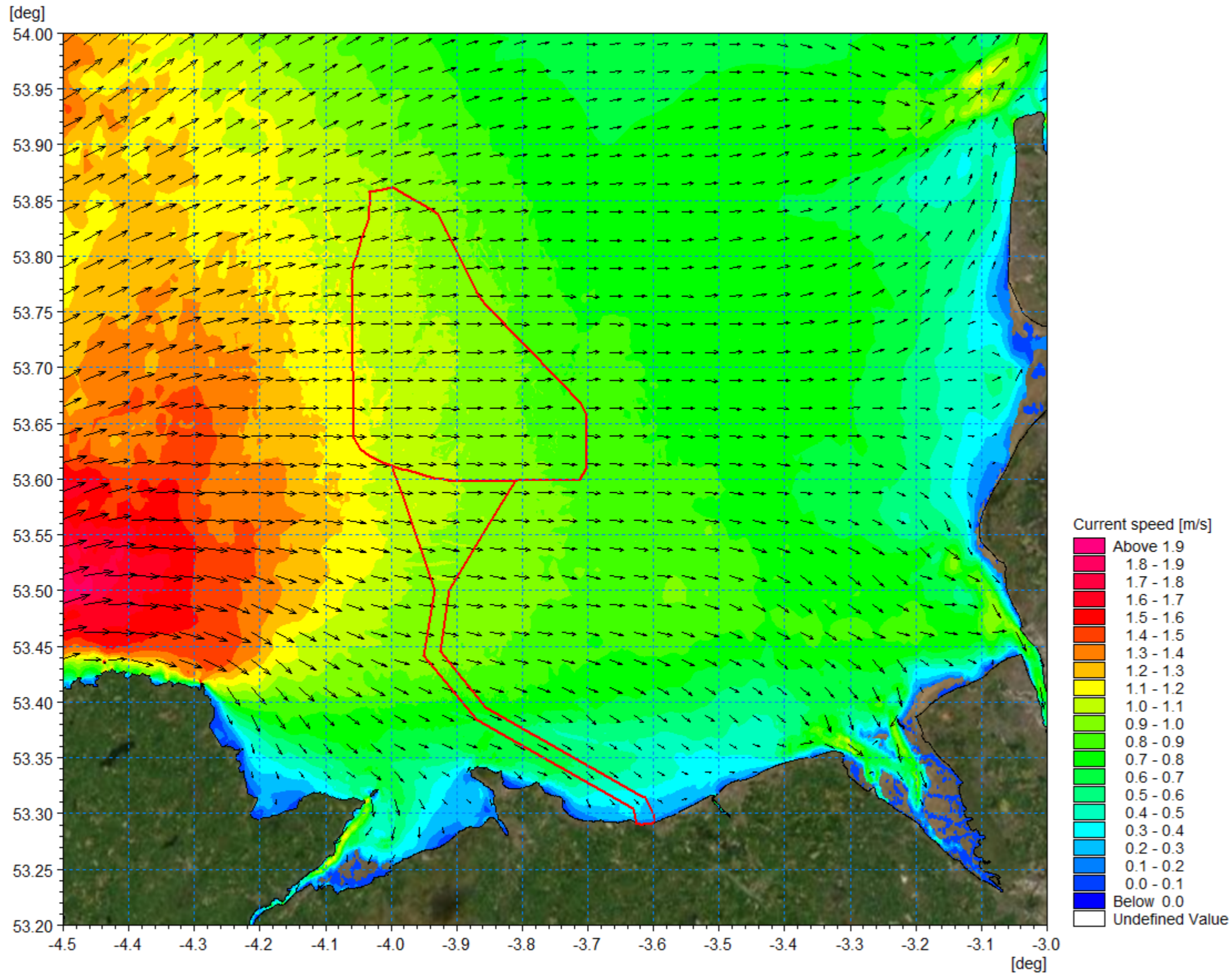


Figure 1.66: Post-construction tidal flow pattern – flood tide.

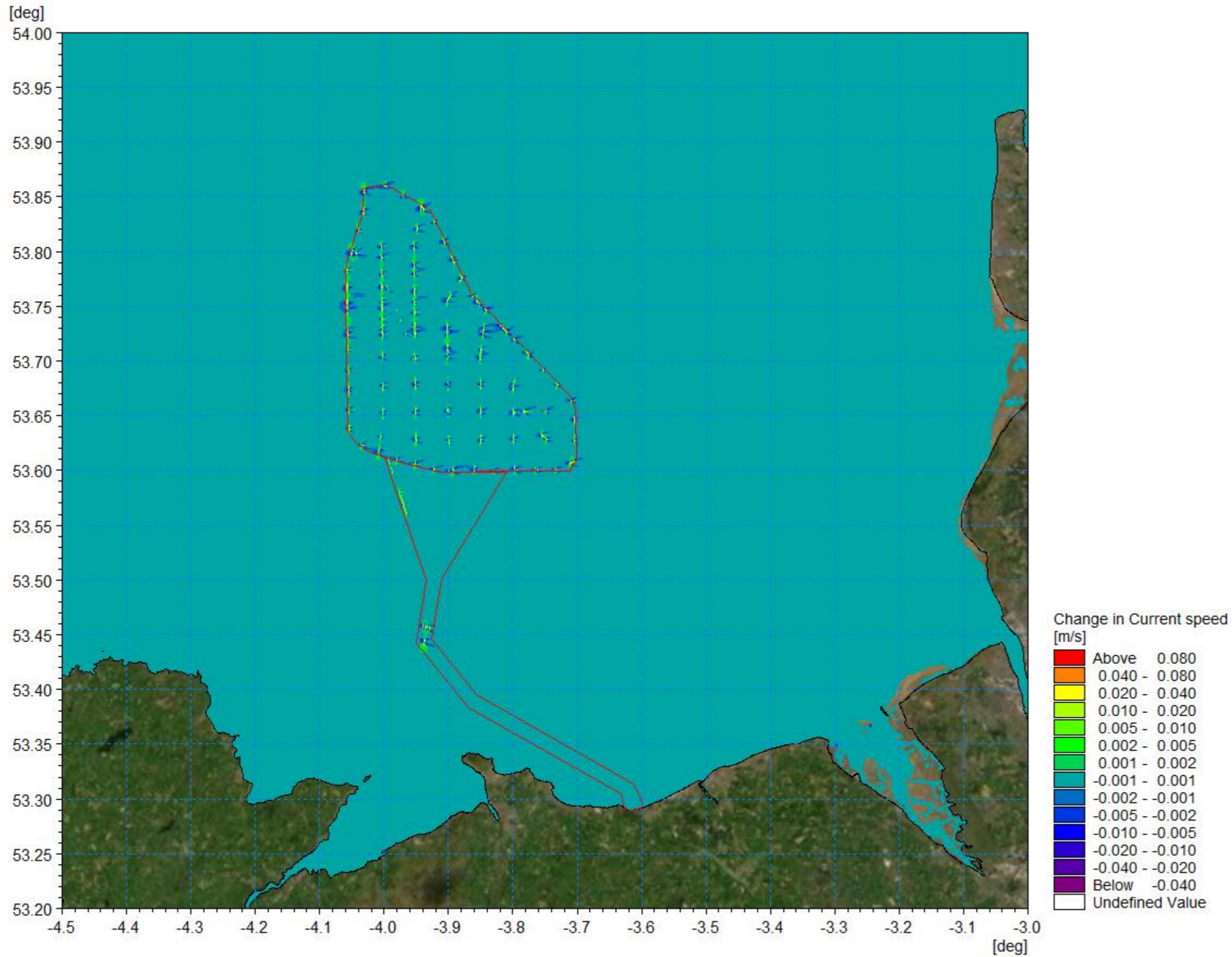


Figure 1.67: Change in tidal flow (post-construction minus baseline) – flood tide.



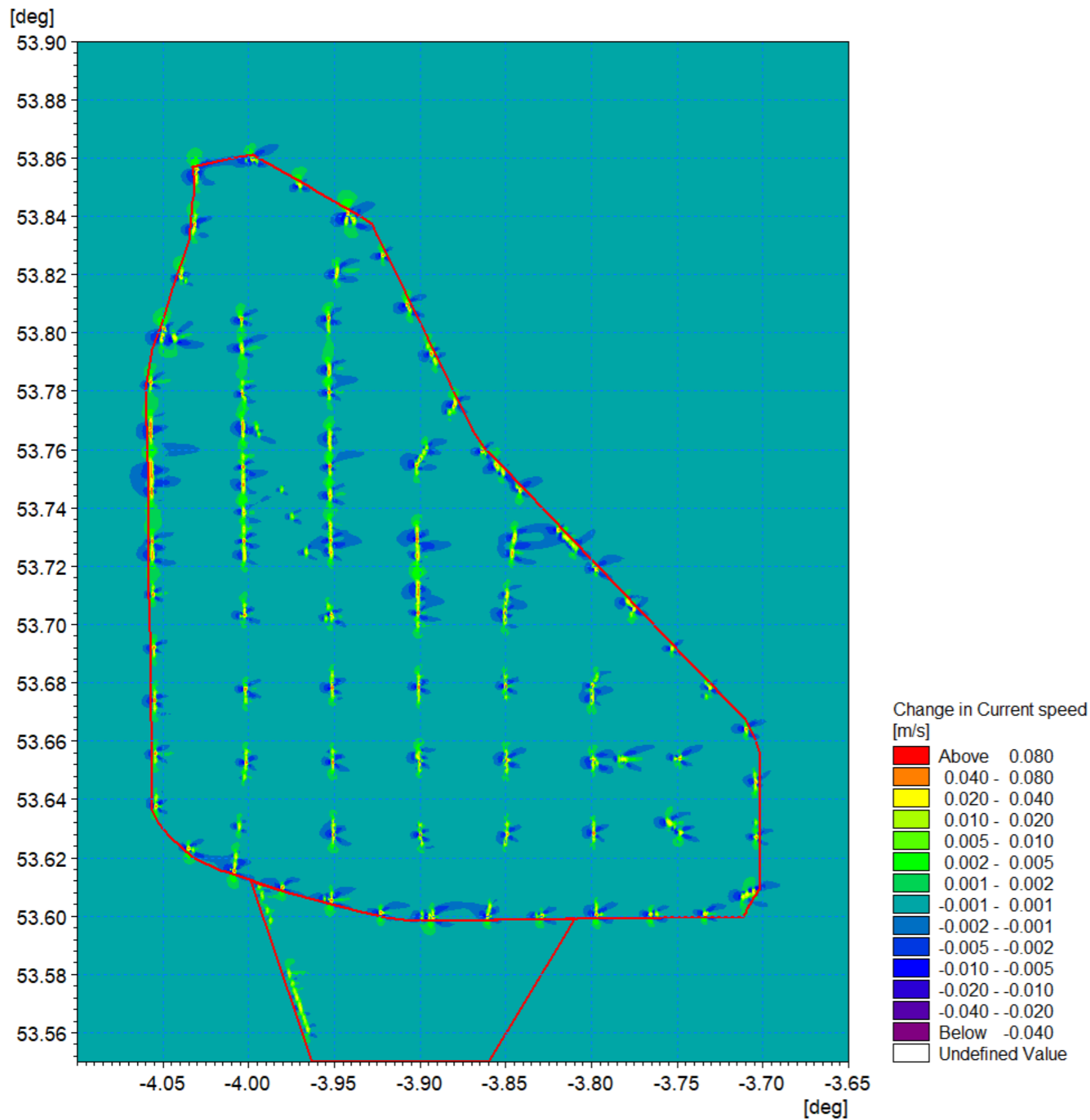


Figure 1.68: Change in tidal flow (post-construction minus baseline) Mona Offshore Wind Project array area – flood tide detail view.

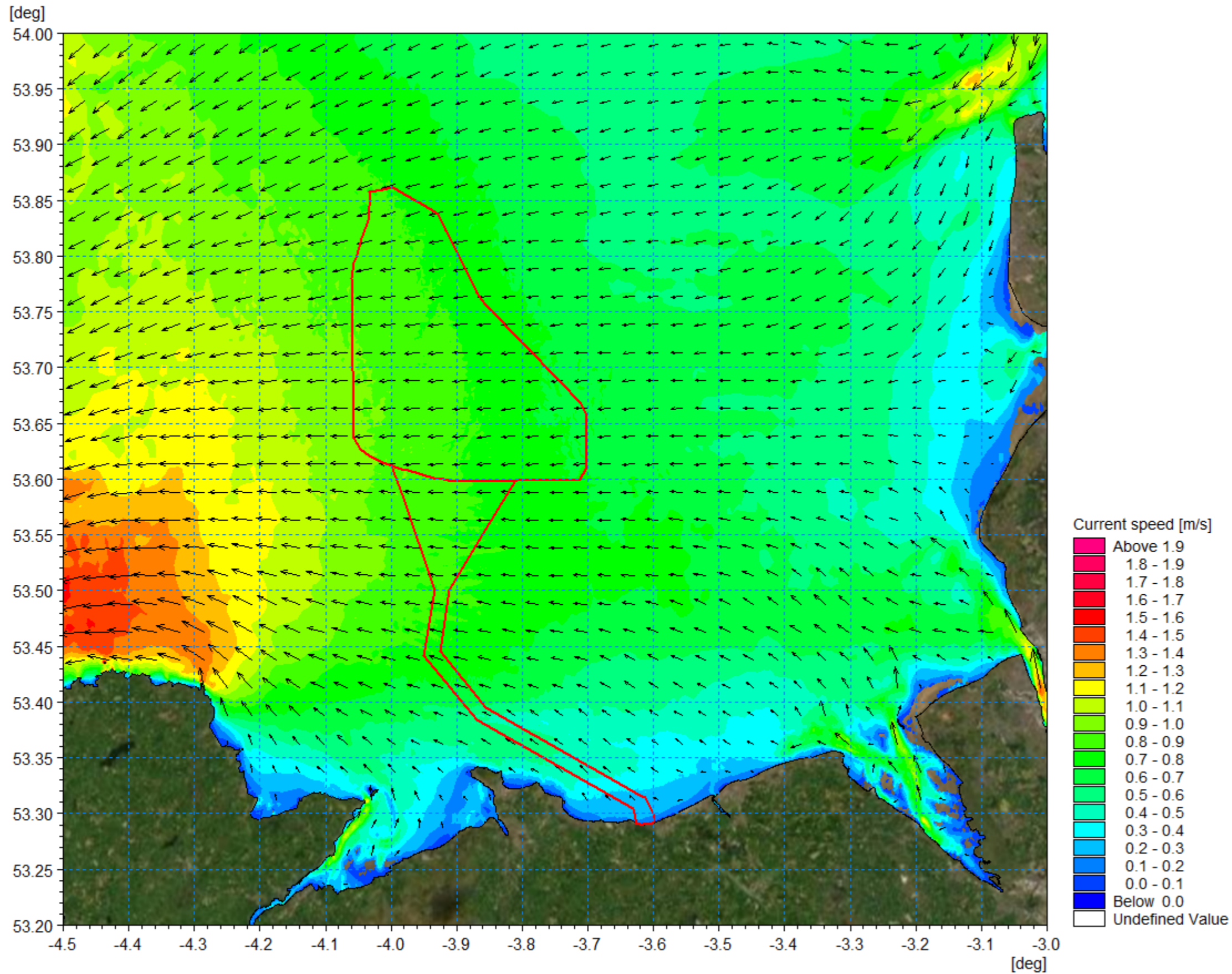


Figure 1.69: Post-construction tidal flow pattern – ebb tide.



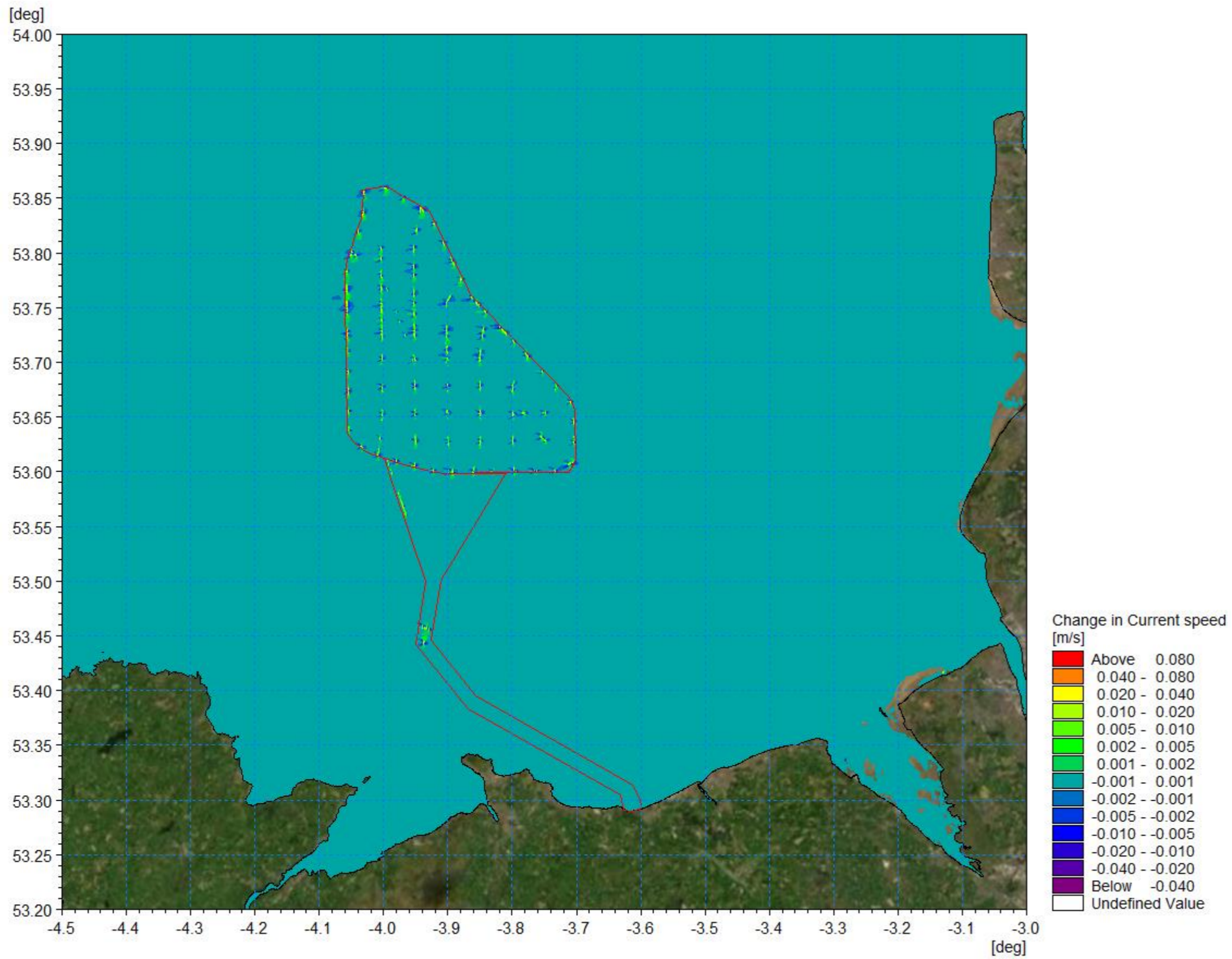


Figure 1.70: Change in tidal flow (post-construction minus baseline) – ebb tide.

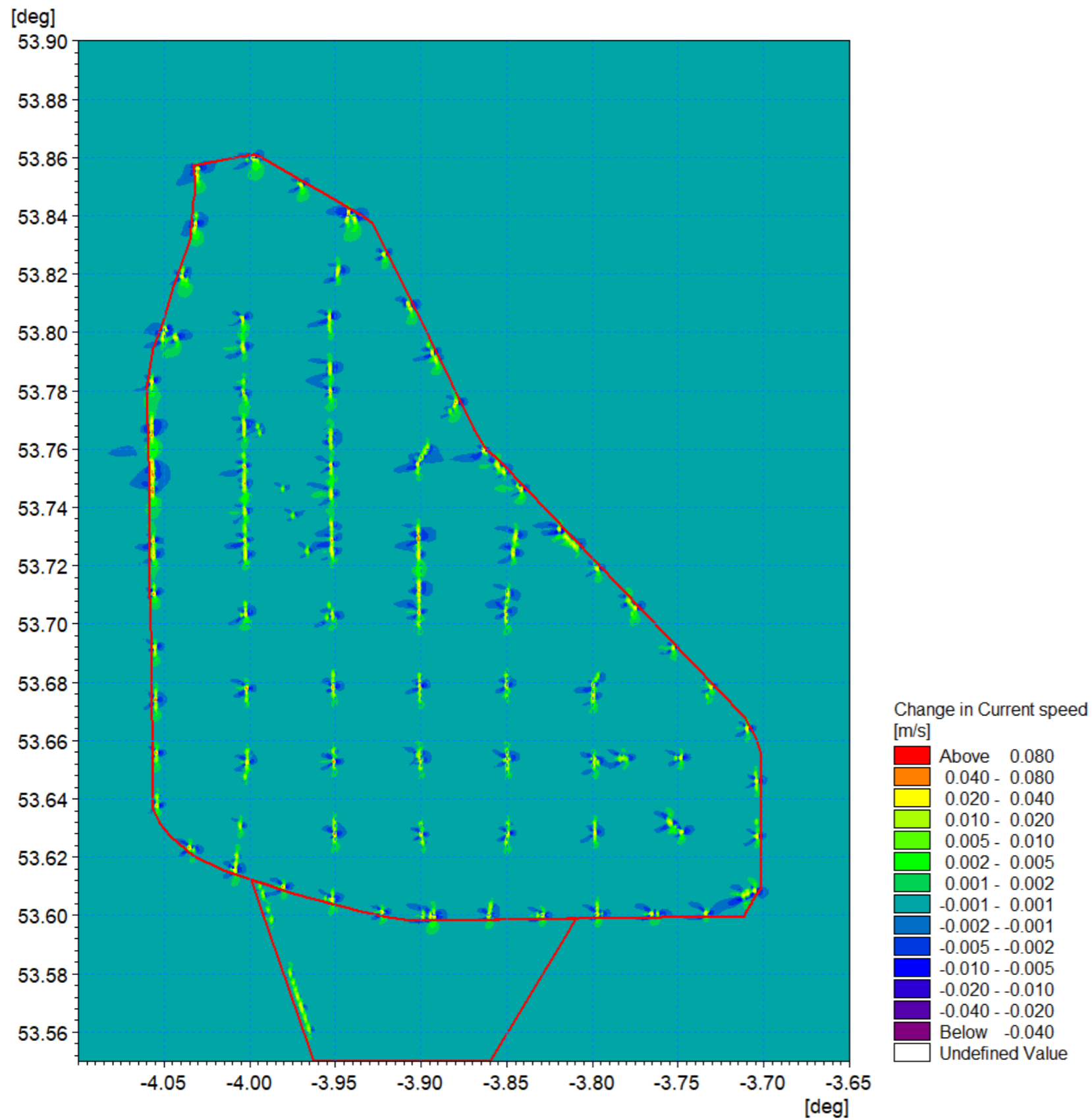


Figure 1.71: Change in tidal flow (post-construction minus baseline) Mona Offshore Wind Project array area – ebb tide detailed view.



### Wave climate

- 1.7.2.3 Using the same principle as for the tidal modelling, the wave climate modelling was repeated with the inclusion of the Mona Offshore Wind Project structures, foundations and cable protection. Again, changes were found to be indiscernible from the baseline scenario by visual inspection therefore difference plots have been provided and using the same scale for all scenarios. The same principal directions are presented for the 1in1 year storm and 1in20 year storm as presented for the baseline in section 1.6.3.
- 1.7.2.4 The post construction phase 000° storm is presented for the 1in1 year in Figure 1.72 with the difference shown in Figure 1.73. Similarly, the 1in20 year storm from this direction is presented in Figure 1.74 and Figure 1.75. The changes are seen as reductions in the lee of the structures. The maximum changes are in the order of 3cm for the annual event and 4.5cm for the more extreme storm event which represents less than 1% of the baseline significant wave height. The wave shadow is typically less than one half of this value. These changes would be indiscernible from the baseline wave climate and would not impact on the shoreline or nearshore banks.
- 1.7.2.5 The potential change in wave climate relative to baseline conditions for annual and more extreme storms are of similar proportions so, for brevity, only the 1in20 year results are presented for the remain directions. Figure 1.76 depicts the 030° post construction scenario with Figure 1.77 showing the change from baseline conditions. The magnitude of the changes at the location of the structures is a reduction in wave height of 3cm whilst, once again the shadow if typical less 2cm which is less than 1% of the baseline condition.
- 1.7.2.6 For the westerly storms from 240° and 270° the incident wave heights are typically twice that of the fetch limited directions. For these scenarios the effect of the presence of the infrastructure is much smaller with changes in wave height typically less than 0.25% as presented in Figure 1.78 to Figure 1.81.
- 1.7.2.7 In summary, the presence of the Mona Offshore Wind Project was seen to have the greatest influence when storms approached from the northerly sectors where baseline wave height were smallest. In all cases the changes in wave climate would be imperceptible and would not interact with the shoreline or nearshore banks and morphology.

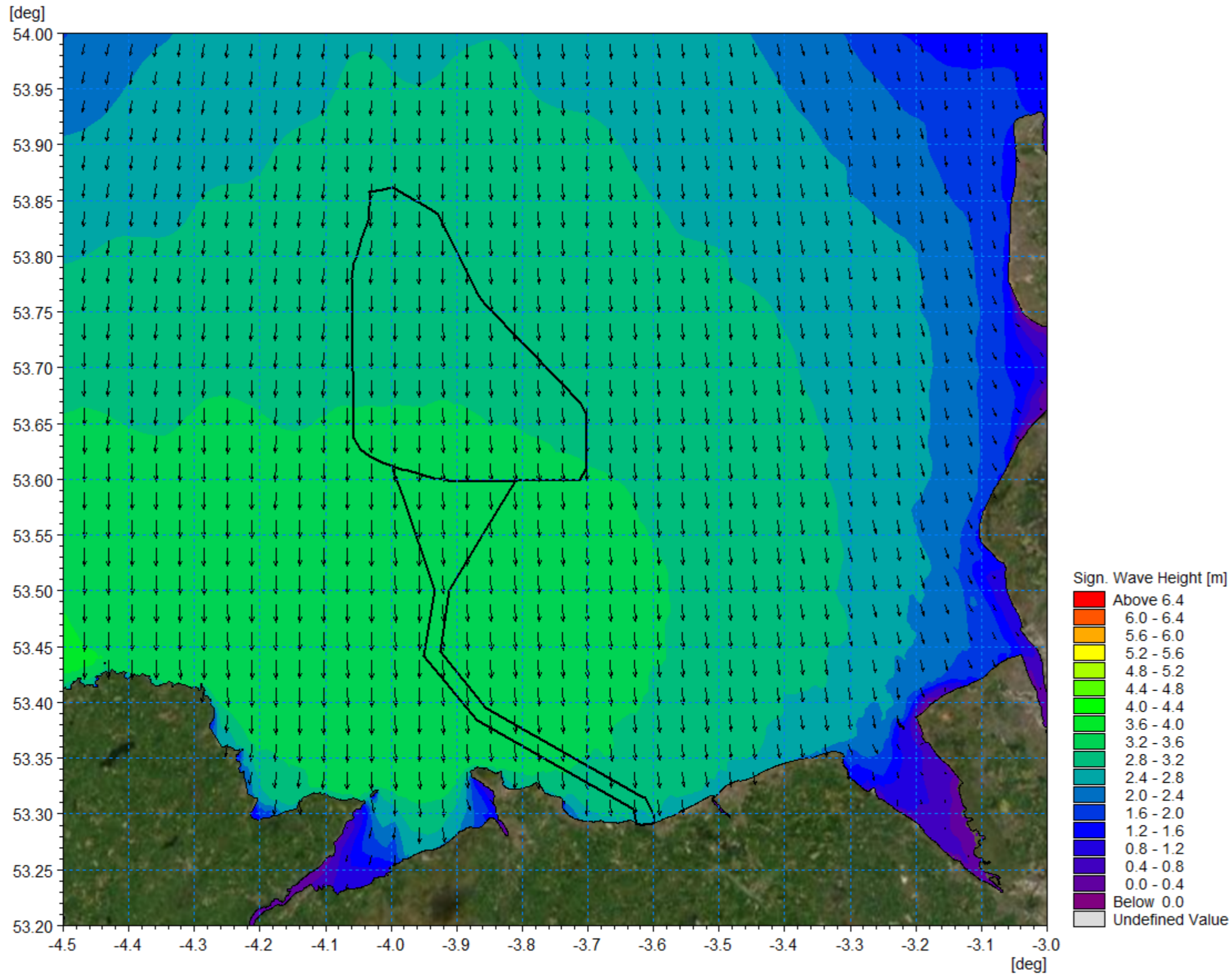


Figure 1.72: Post-construction wave climate 1in1 year storm 000° MHW.



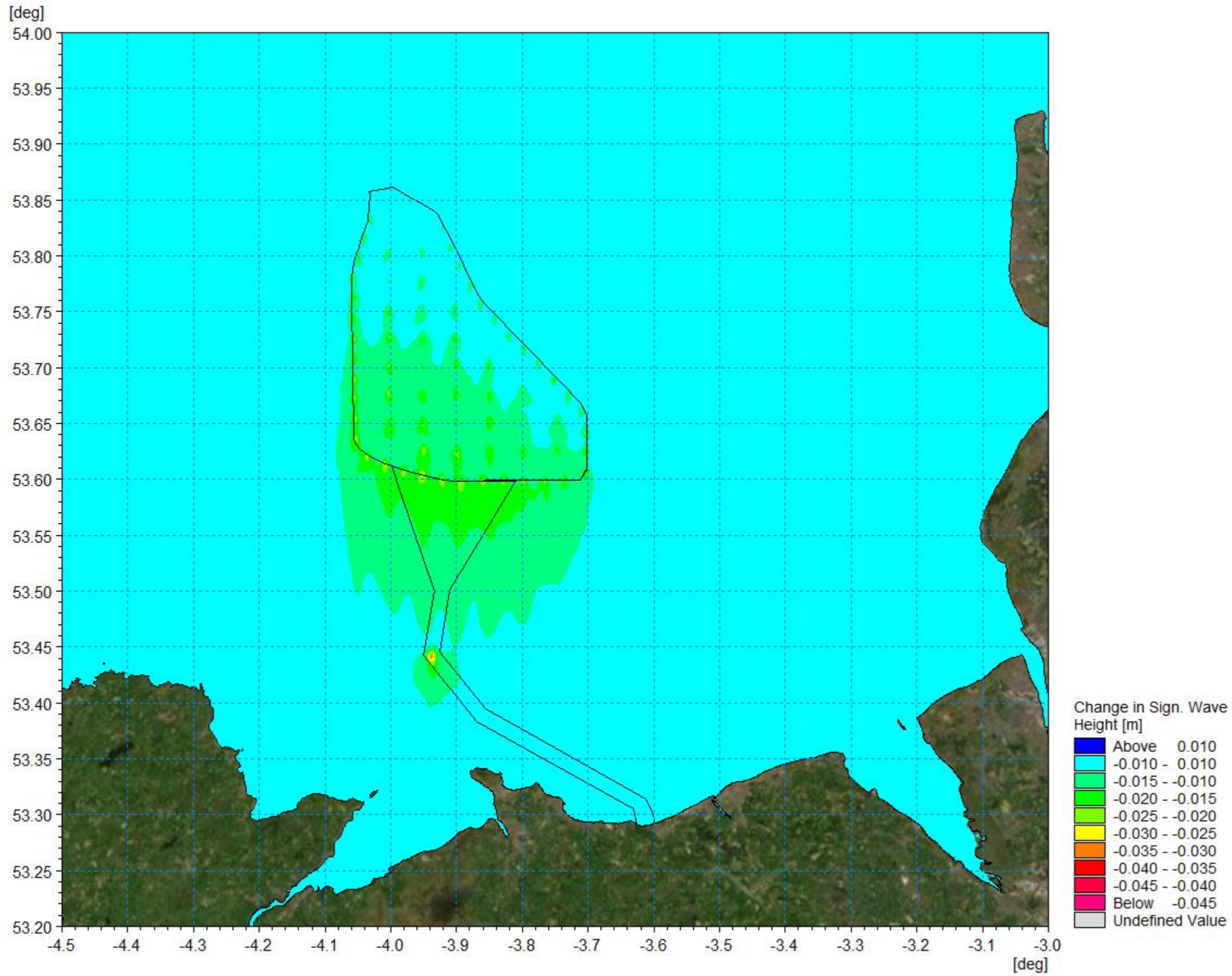


Figure 1.73: Change in wave climate 1in1 year storm 000° MHW (post-construction minus baseline).

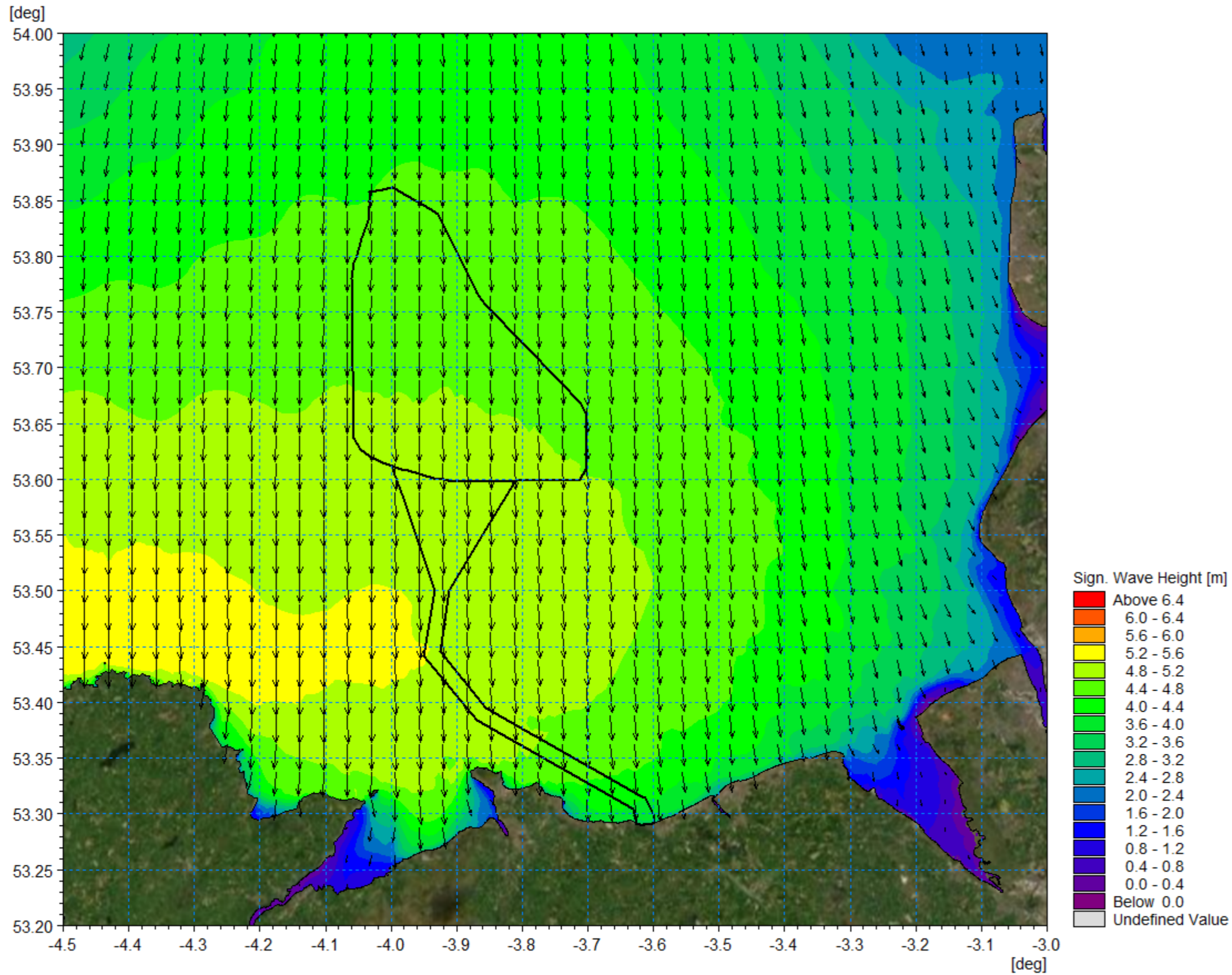


Figure 1.74: Post-construction wave climate 1in20 year storm 000° MHW.



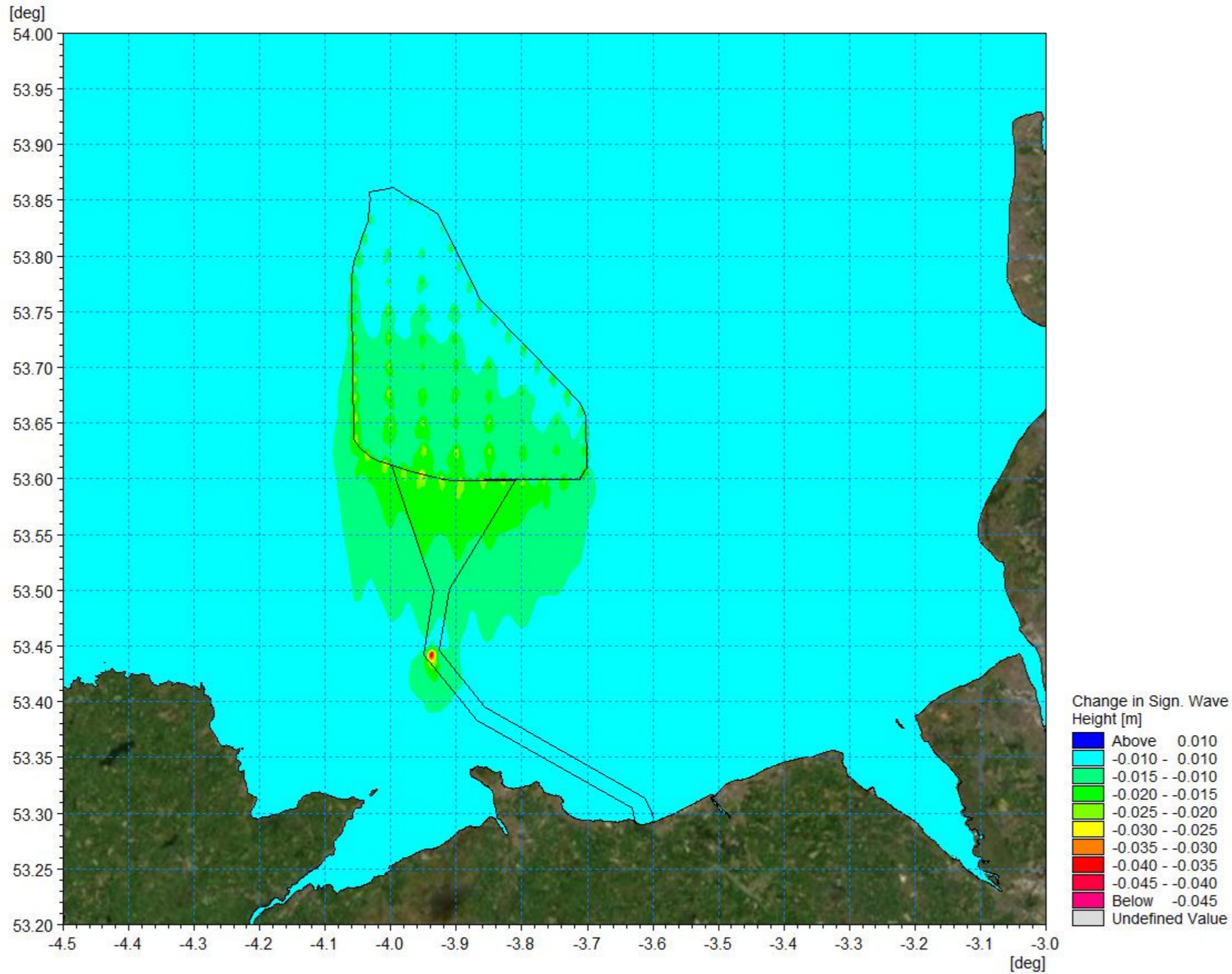


Figure 1.75: Change in wave climate 1in20 year storm 000° MHW (post-construction minus baseline).

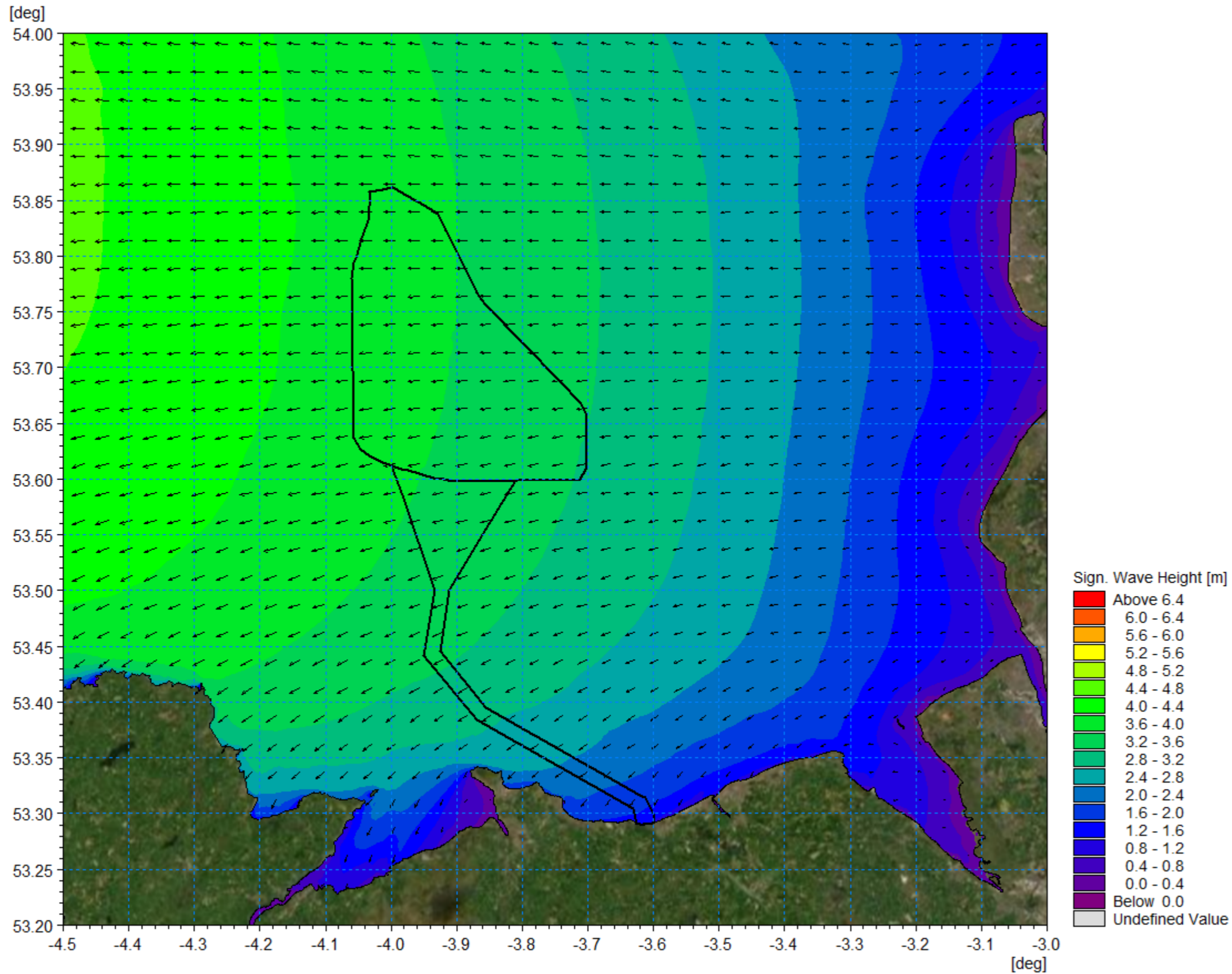


Figure 1.76: Post-construction wave climate 1in20 year storm 090° MHW.



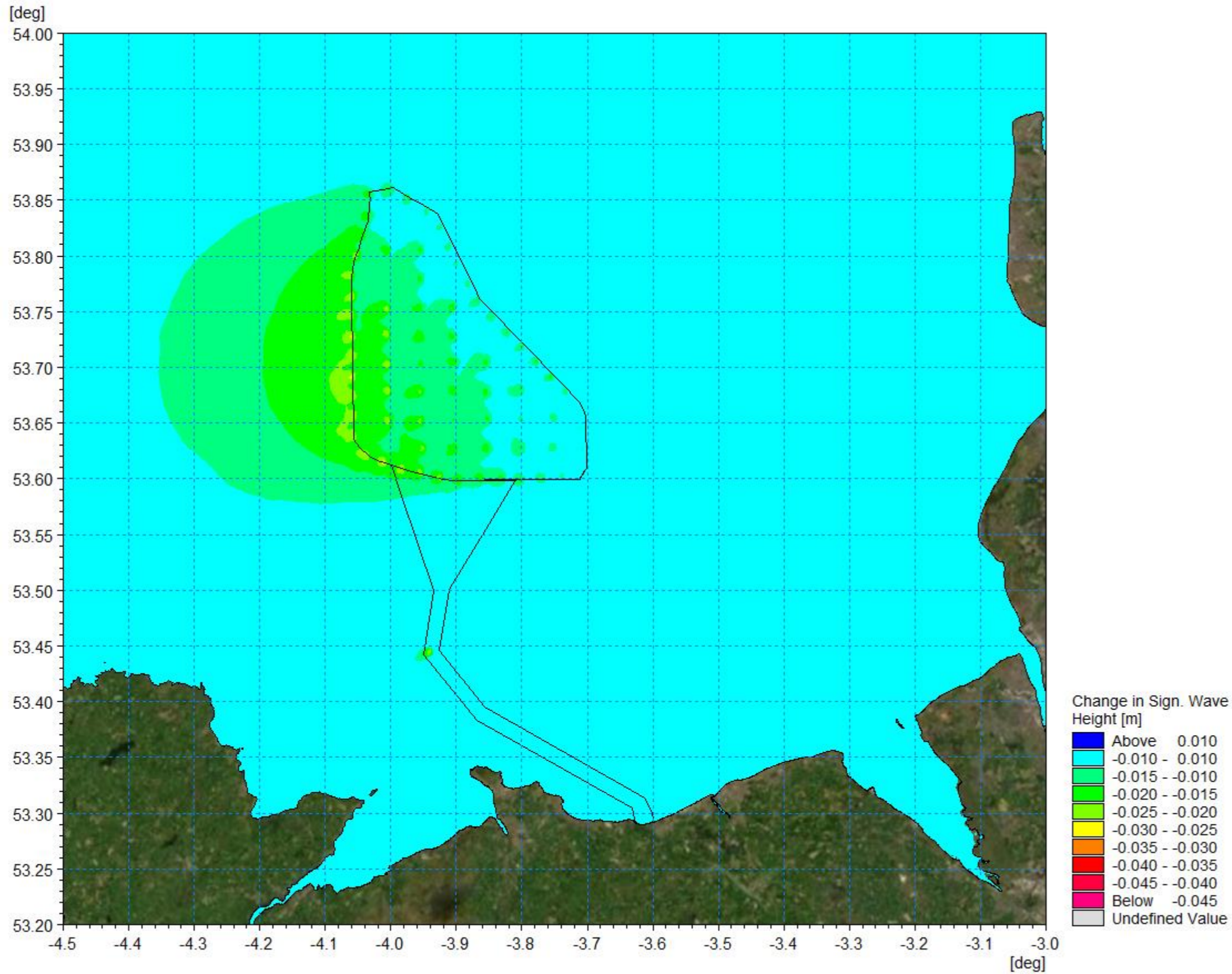


Figure 1.77: Change in wave climate 1in20 year storm 090° MHW (post-construction minus baseline).

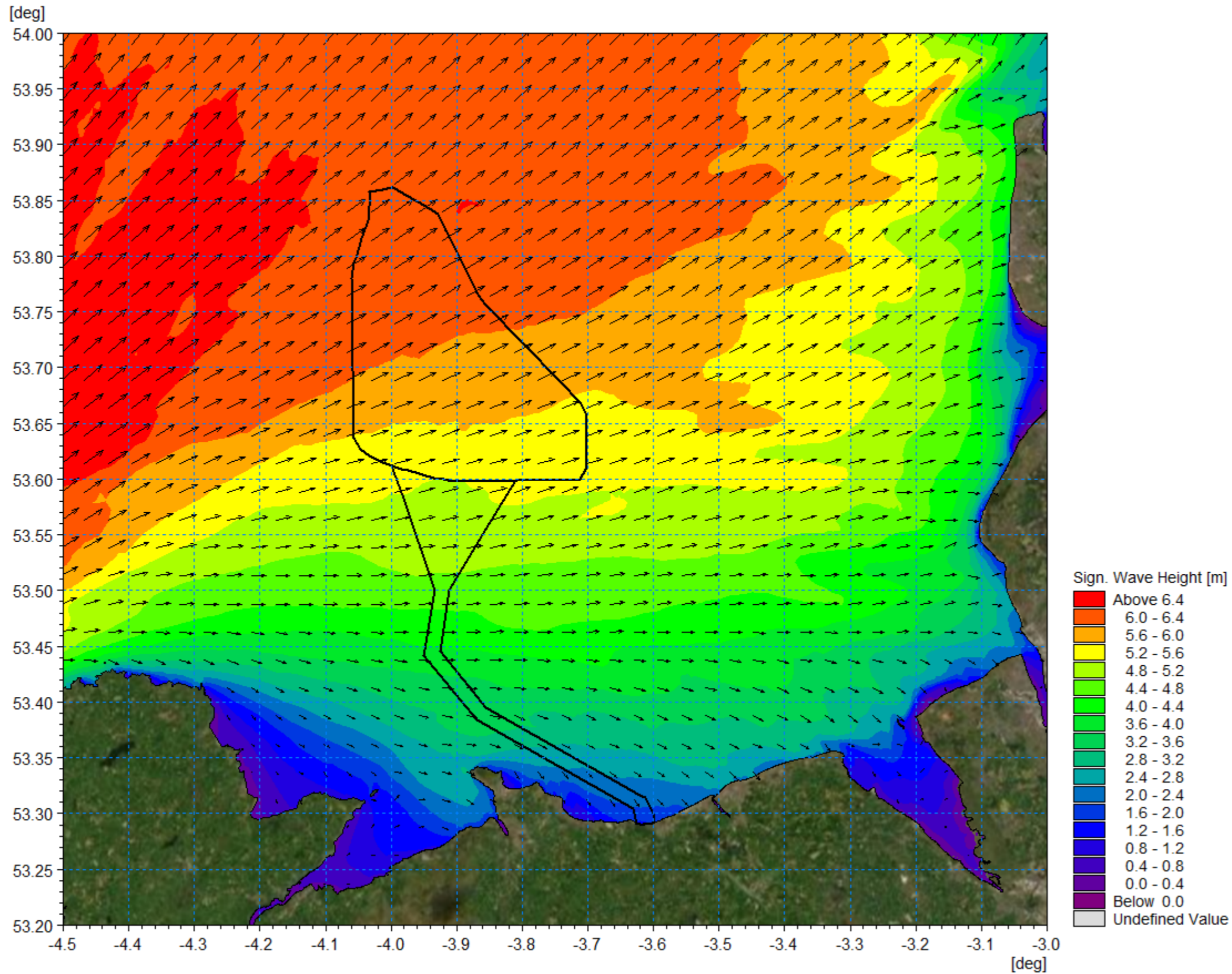


Figure 1.78: Post-construction wave climate 1in20 year storm 240° MHW.



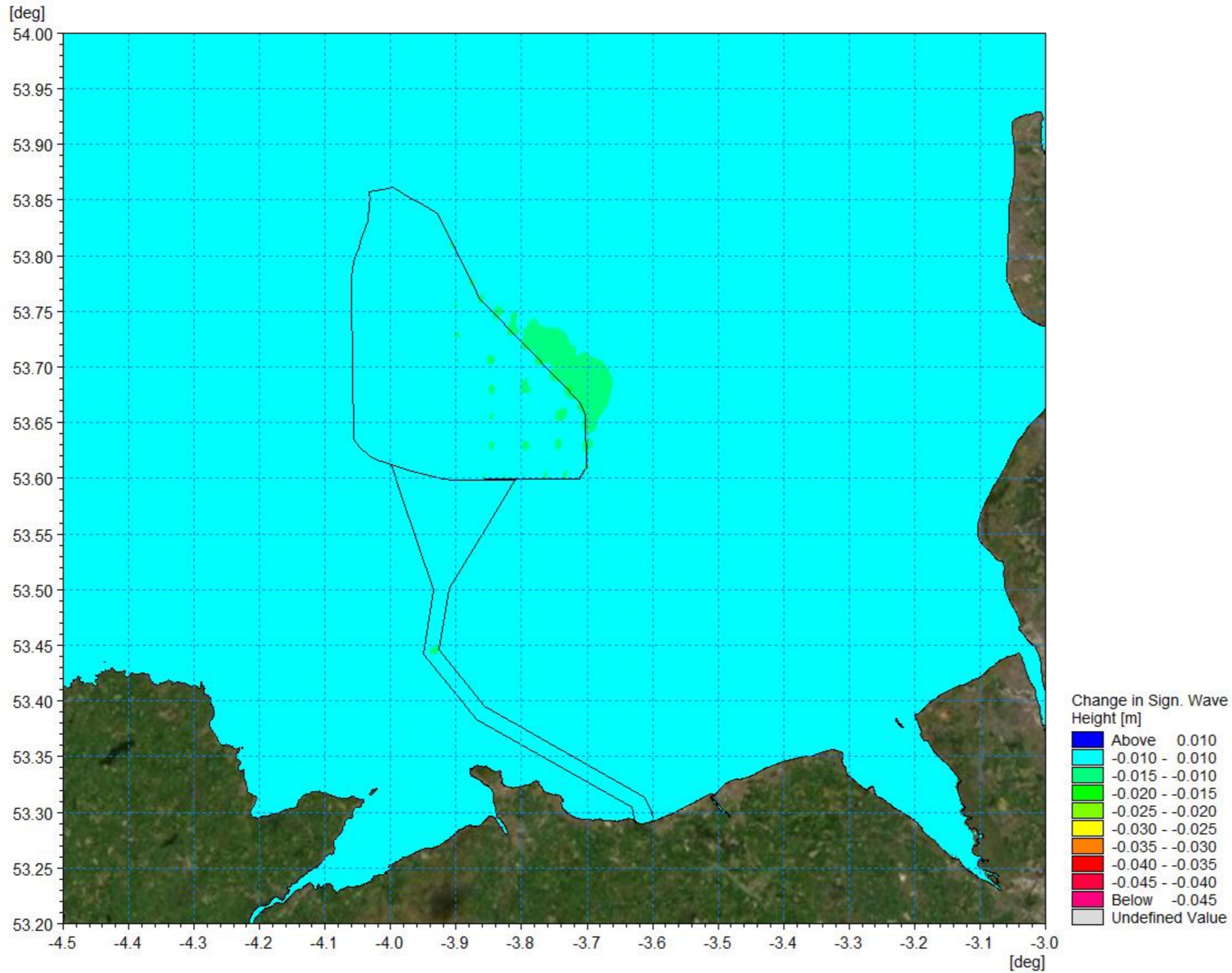


Figure 1.79: Change in wave climate 1in20 year storm 240° MHW (post-construction minus baseline).

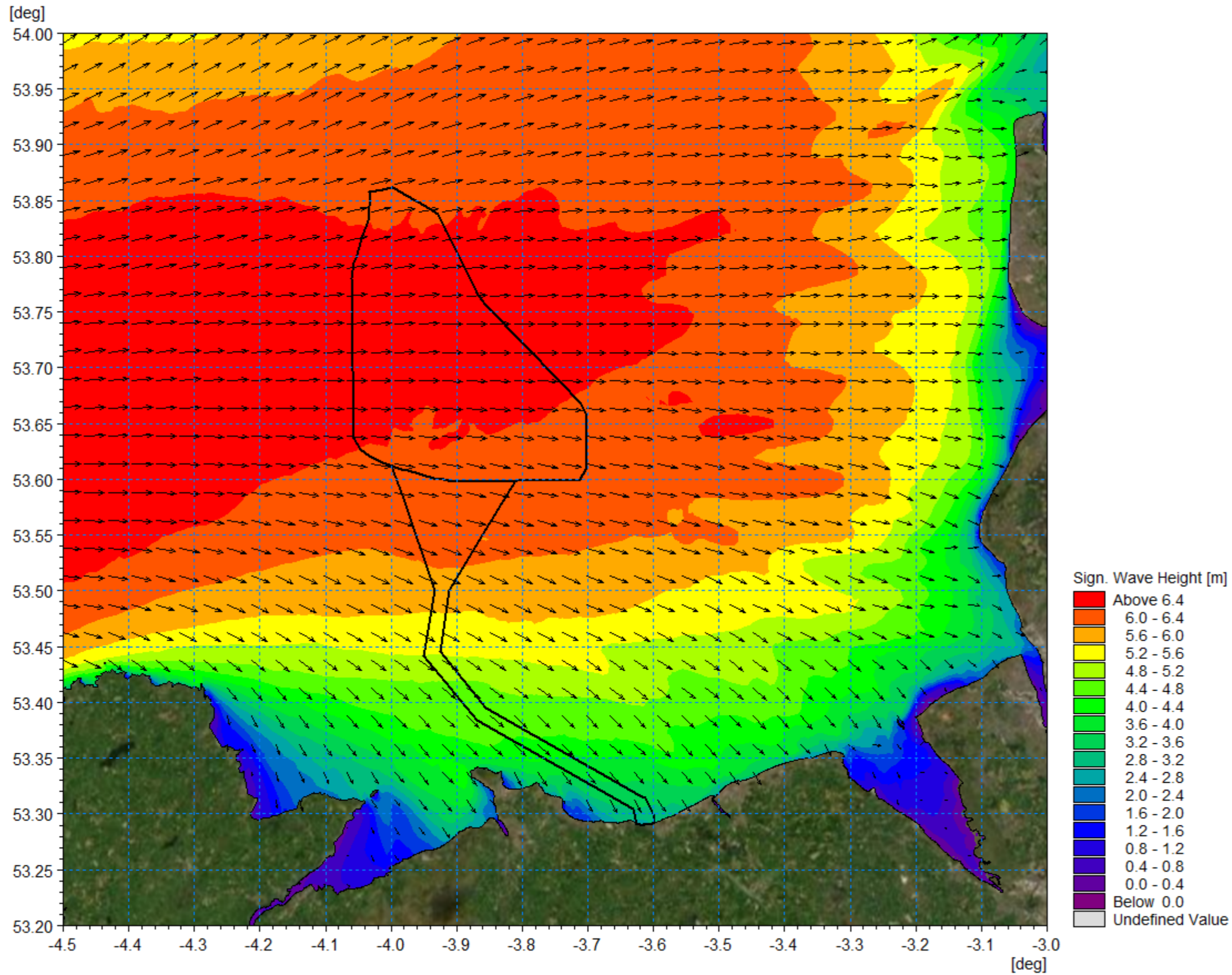


Figure 1.80: Post-construction wave climate 1in20 year storm 270° MHW.



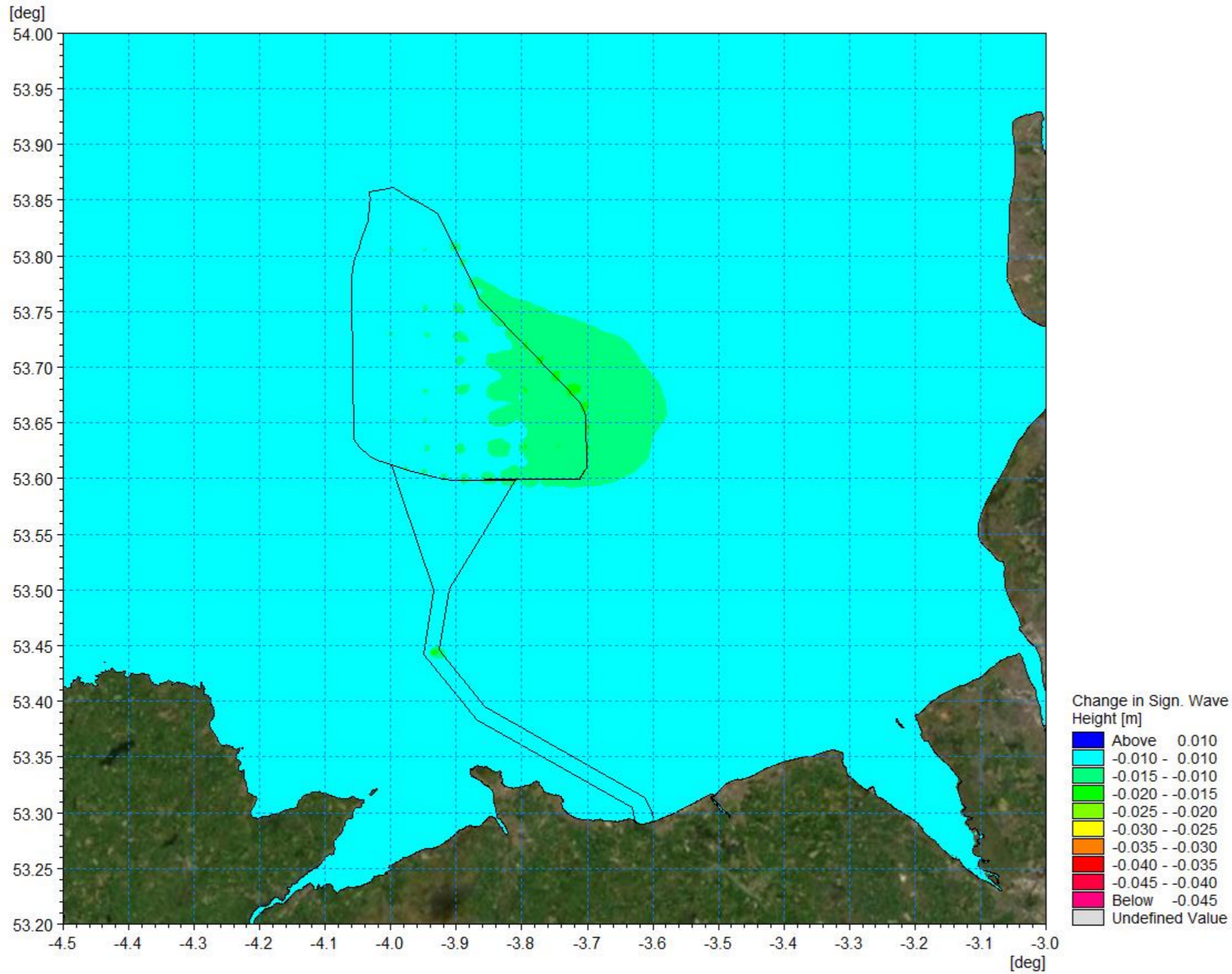


Figure 1.81: Change in wave climate 1in20 year storm 270° MHW (post-construction minus baseline).

### Littoral currents

- 1.7.2.8 The previous sections established the magnitude of the changes in tidal currents and wave conditions individually, however sediment transport regimes are driven by a combination of these factors. Although the modelling has demonstrated that the Mona Offshore Wind Project results in minor localised changes for each aspect, for the sake of completeness, the influence on littoral currents was examined.
- 1.7.2.9 The modelling was extended to include the post-construction scenario for the 1in1 year storm from 270°. The baseline littoral currents for mid ebb and mid flood were presented in Figure 1.54 and Figure 1.55 respectively. The corresponding post-construction littoral currents are shown in Figure 1.82 and Figure 1.85 for the ebb and flood tides.
- 1.7.2.10 As with the previous difference in current speed post construction, a log plotting scale was necessary to present the changes due to their localised nature. The changes for the flood tide are presented in Figure 1.83 a more detailed plot in Figure 1.84 whilst for the ebb tide Figure 1.86 and Figure 1.87 show the corresponding information.
- 1.7.2.11 During the flood tide the influence of the wave climate is in concert with the tidal current and during the ebb tide, the tidal flow is in opposition to the wave climate and the resultant littoral current is reduced in magnitude. The presence of the structures was seen to have a limited influence on the wave climate and there is little difference between changes in littoral current magnitude and the tidal flows alone due to the installation during the flood tide. The extent of the changes is larger for the ebb tide condition particularly at the south of the array area, although it should be noted that these are still <1% of baseline tidal flow. Overall, the magnitude of these changes remains limited to  $\pm 5\%$  of the baseline currents at 200m and reduces significantly with increased distance from each structure.



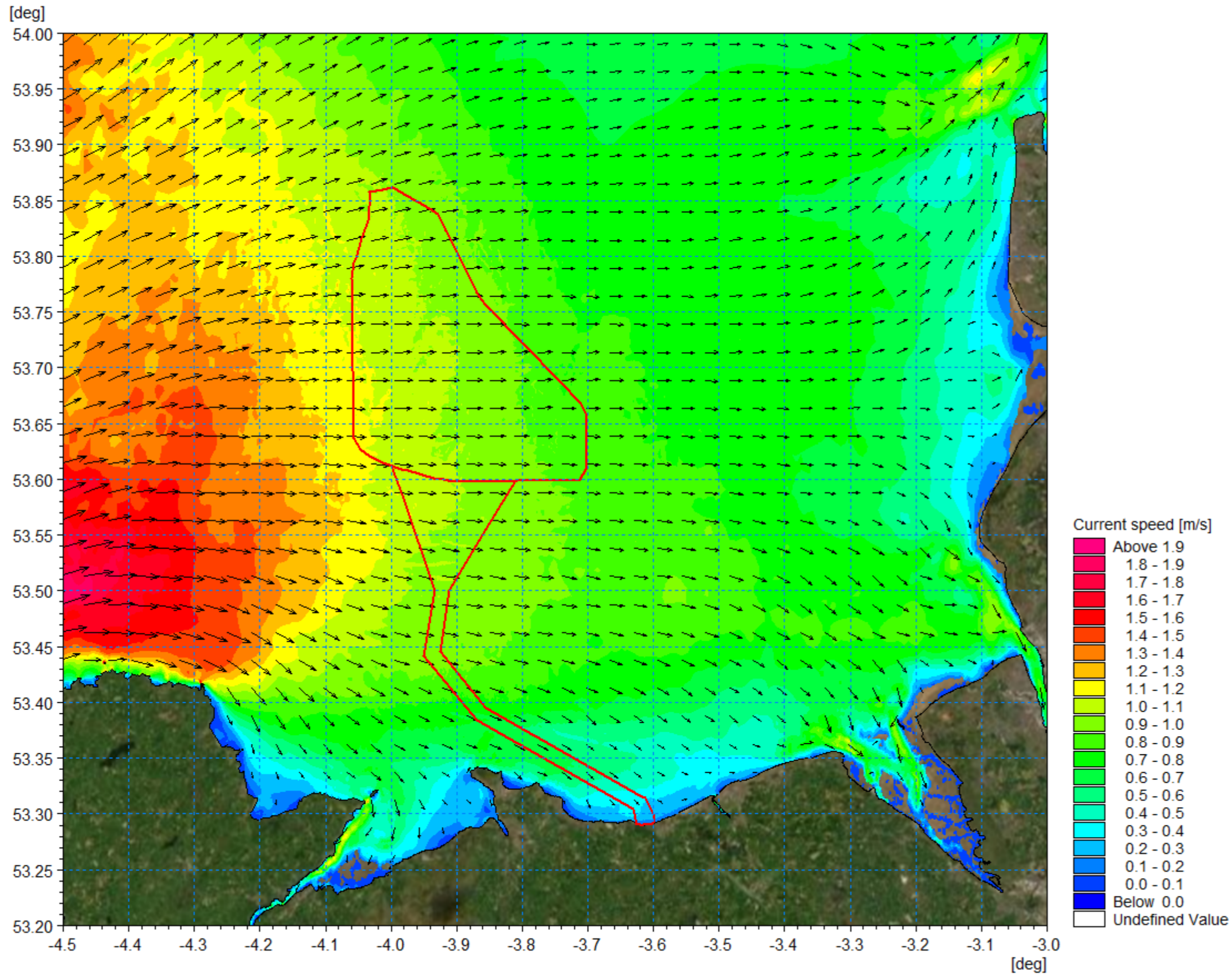


Figure 1.82: Post-construction littoral current 1in1 year storm from 270° - Flood Tide.

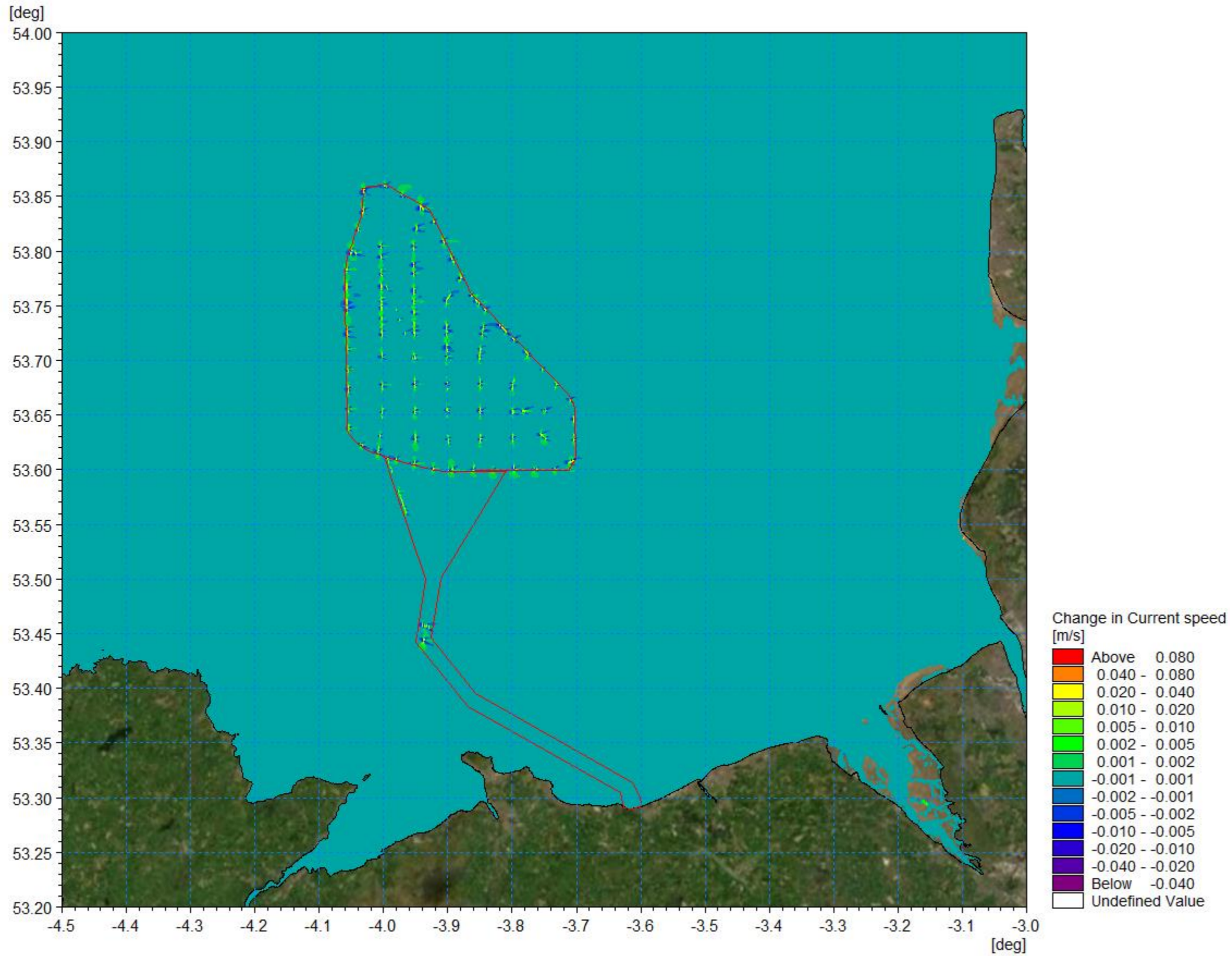


Figure 1.83: Change in littoral current 1in1 year storm from 270° - flood tide (post-construction minus baseline).



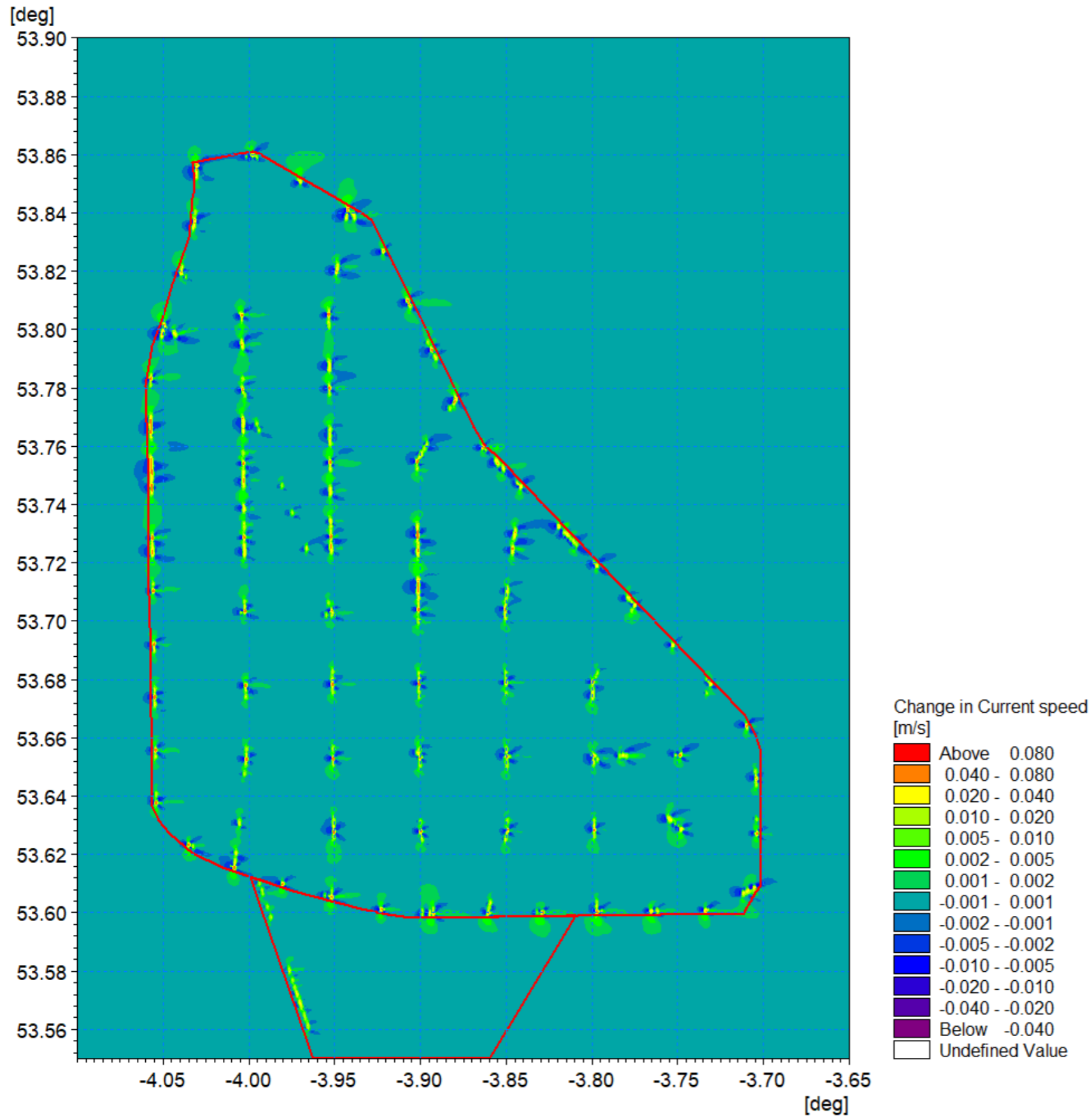


Figure 1.84: Change in littoral current 1in1 year storm from 270° - flood tide (post-construction minus baseline) detailed view.

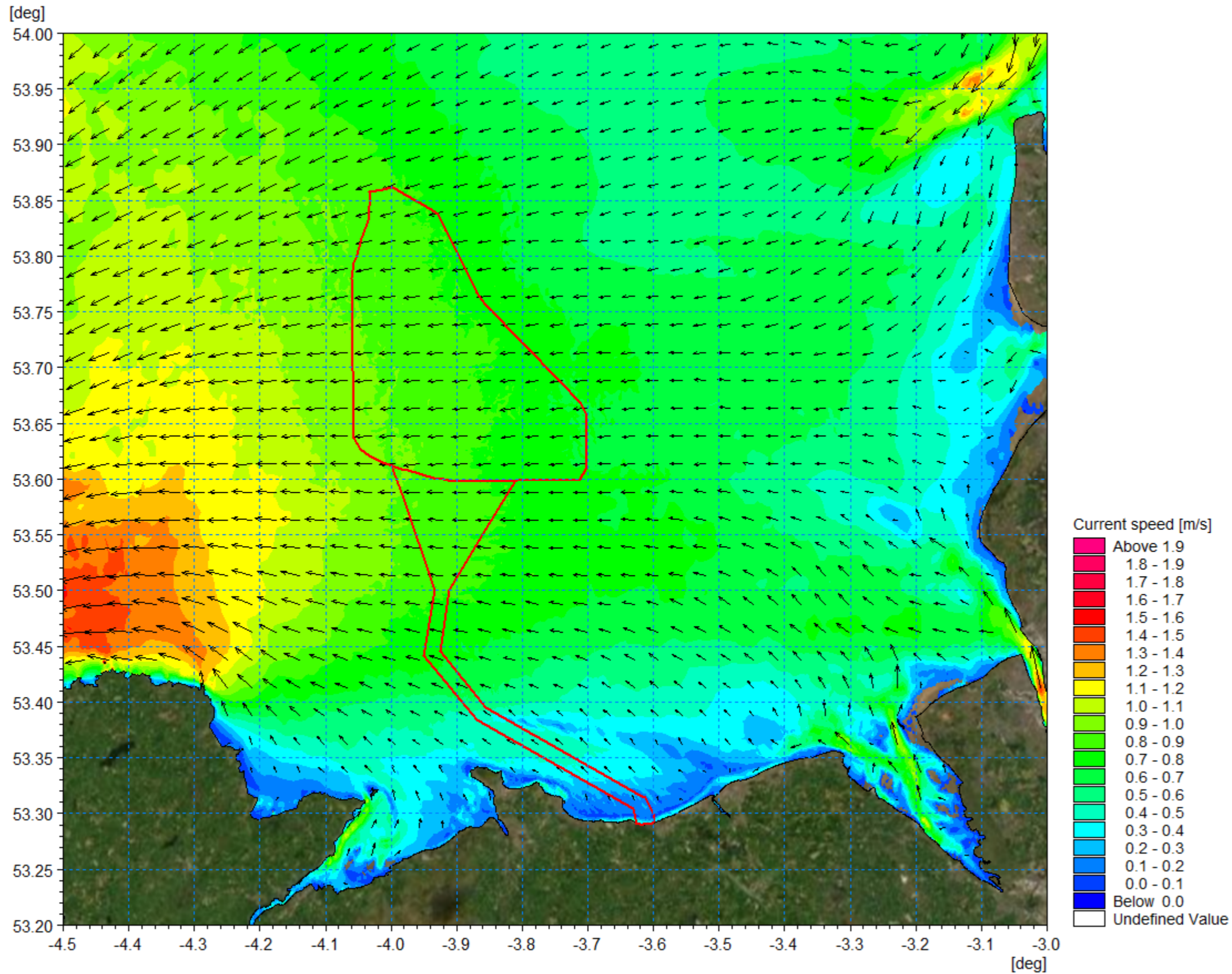


Figure 1.85: Post-construction littoral current 1in1 year storm from 270° - ebb tide.



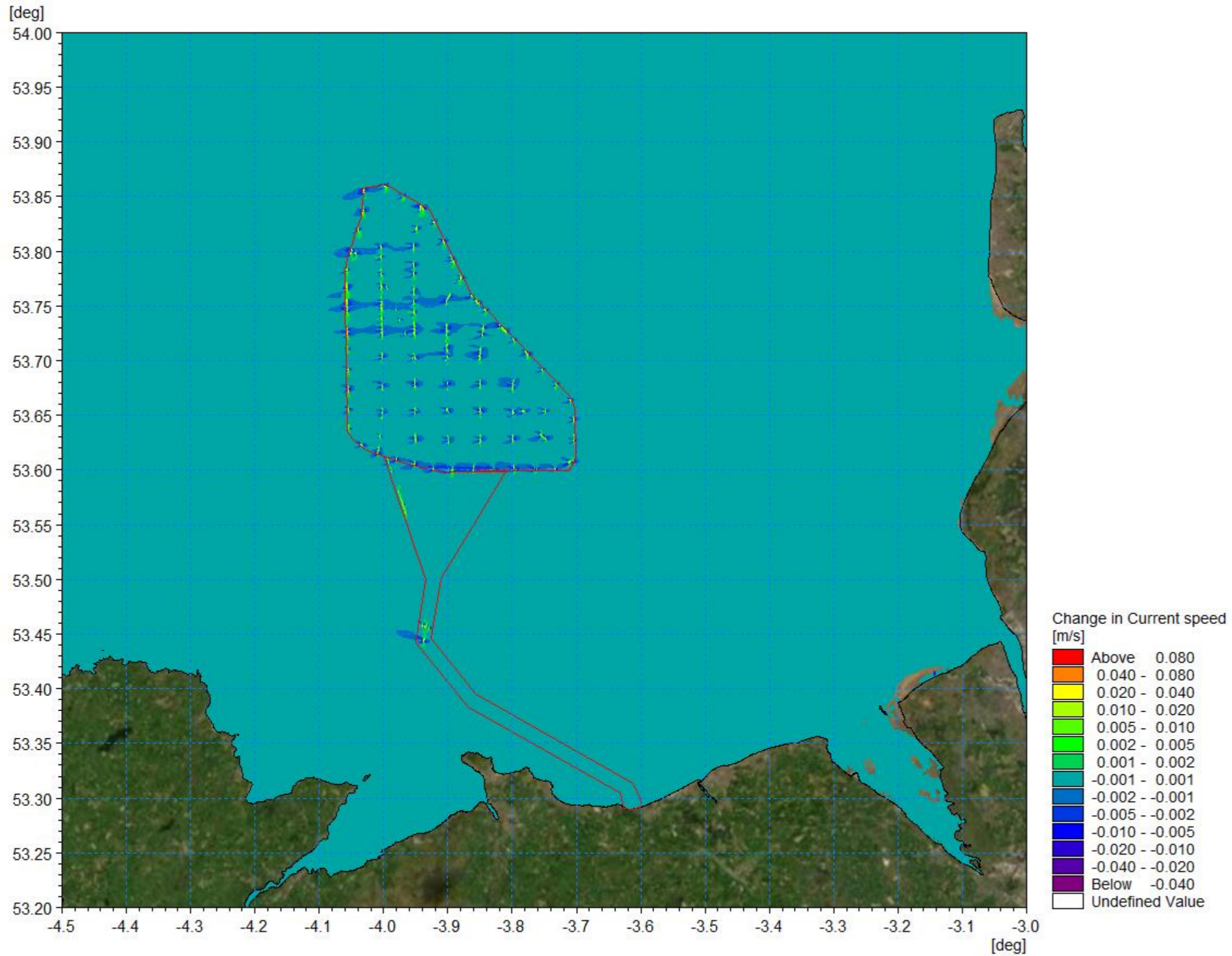


Figure 1.86: Change in littoral current 1in1 year storm from 270° - ebb tide (post-construction minus baseline).

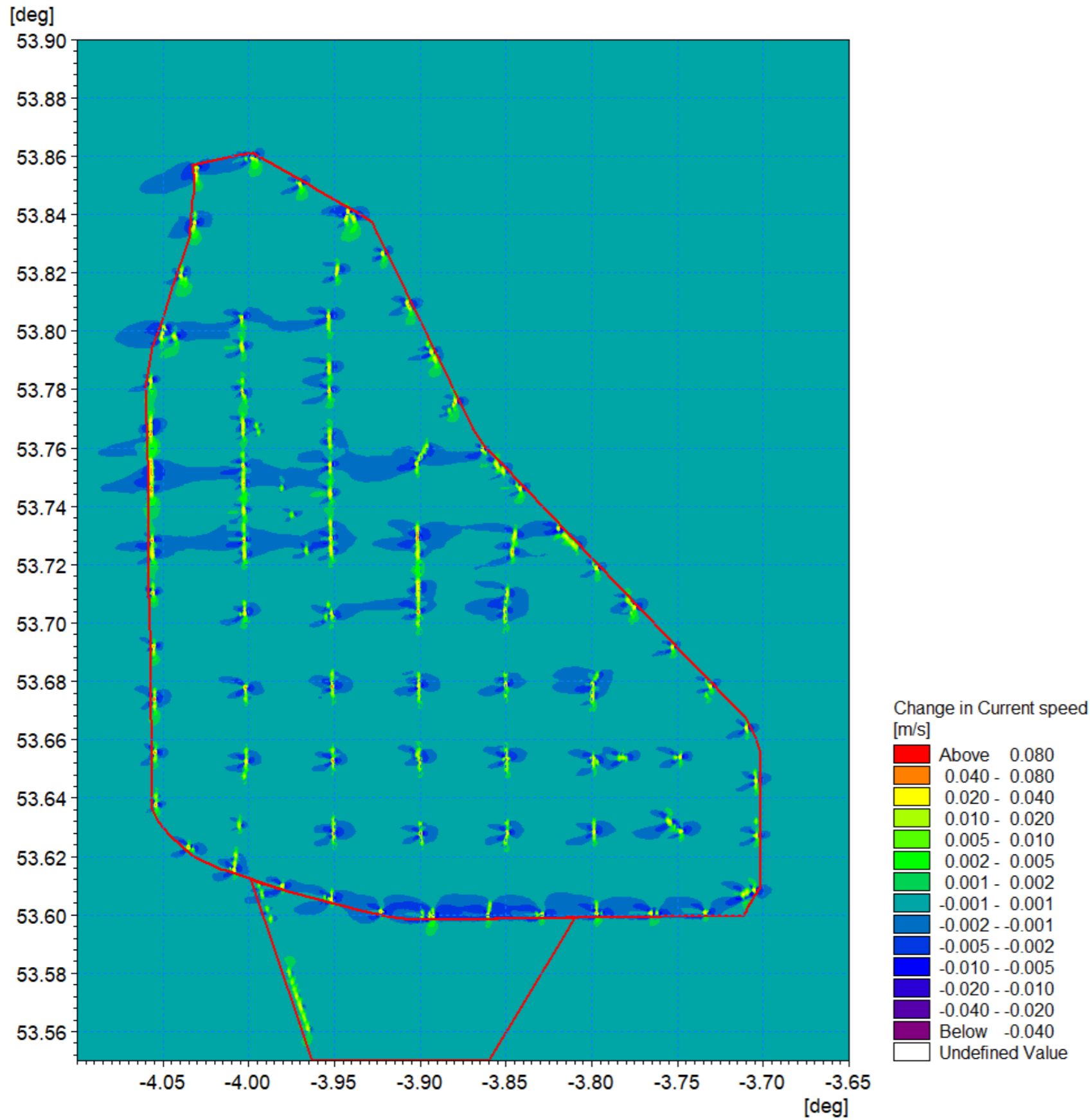


Figure 1.87: Change in littoral current 1in1 year storm from 270° - ebb tide (post-construction minus baseline) detailed view.



### 1.7.3 Post-construction sedimentology

#### Sediment transport

- 1.7.3.1 The numerical modelling methodology for sediment transport was described in section 1.6.6, which indicated how the baseline information was discretised to form the basis of the modelled scenarios. For the post-construction scenario, in addition to the Mona Offshore Wind Project structures being included in the tide and wave models, the bed material map was edited to represent the areas of scour protection where sediment supply is restricted. In each case an area of fixed bed was applied overlain with a thin layer of sand to initialise the model and avoid instabilities. The scour protection was defined as 56m diameter for each turbine structure leg and 49m diameter for each OSP leg. The models were then re-run for a spring tide under calm conditions.
- 1.7.3.2 There are a number of approaches for quantifying potential sediment transport, given that transport rates vary both across the area and due to tidal state and climate conditions. For this analysis, the residual current was calculated over the course of two tidal cycles (one day) with the structures in place and compared with that for the baseline (Figure 1.58) for the calm condition as this is effectively the driver for sediment transport. The post-construction residual current and changes are shown in Figure 1.88 and Figure 1.89 respectively. As with previous results a more detailed plot is presented in Figure 1.90.
- 1.7.3.3 The corresponding sediment transport was simulated over the course of one day where the equivalent baseline daily sediment transport rate was shown in Figure 1.59. The post-construction daily sediment transport rate and differences are shown in Figure 1.91 and Figure 1.92 respectively. It should be noted that both the sediment transport and difference plots use a log palette as there is a large range in sediment transport potential across the domain.
- 1.7.3.4 This analysis shows that although there are changes as a result of the installation of the Mona Offshore Wind Project structures and associated scour and cable protection, the extent and magnitude is limited. As anticipated, in areas of reduced residual current in the lee of structures the sediment transport rate is also reduced and vice versa. Within the context of this comparative study there is a maximum change in residual current and sediment transport of circa  $\pm 10\%$  which is largely sited within close proximity to the turbine foundation structures (less than 250m elongated in the direction of principle tidal currents). It is noted that areas of reduced residual current and sediment transport are often accompanied by a similar increase in close proximity. This indicates that the residual current and resulting sediment transport paths are adjusted to accommodate the structures rather than transport pathways being cut off.
- 1.7.3.5 This process was repeated for the 1in1 year storm. The baseline residual current (Figure 1.62) was compared with the equivalent post-construction residual current pattern as shown in Figure 1.93; with the difference in Figure 1.94 and in more detail in Figure 1.95. The pattern of changes is similar to the previous scenario but with a wider area of influence. It should however be noted that although the absolute values of these changes are increased from the purely tidal condition the underlying baseline residual currents are of greater magnitude under storm conditions and are proportionately smaller than those exhibited under calm conditions.

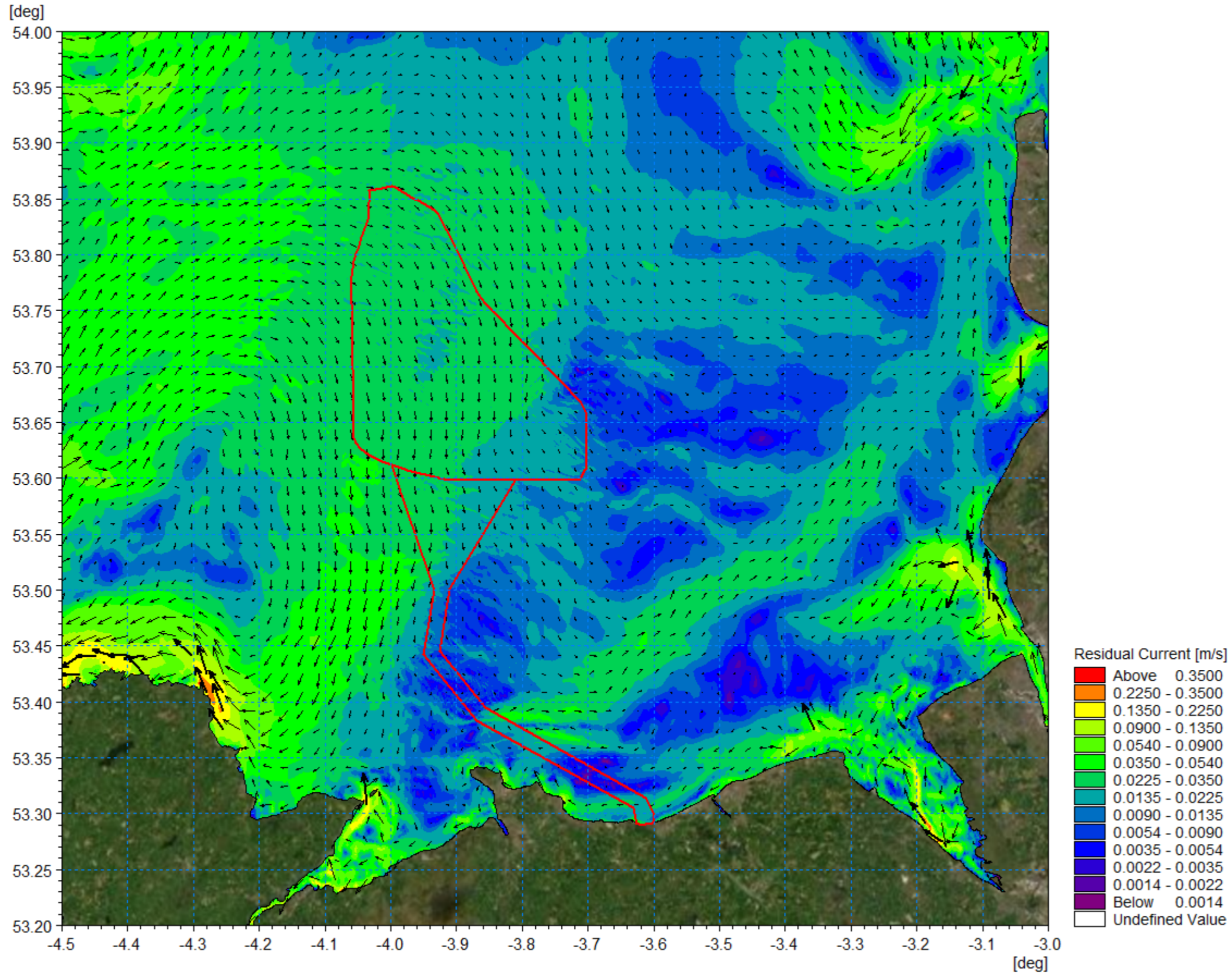


Figure 1.88: Post-construction residual current spring tide.



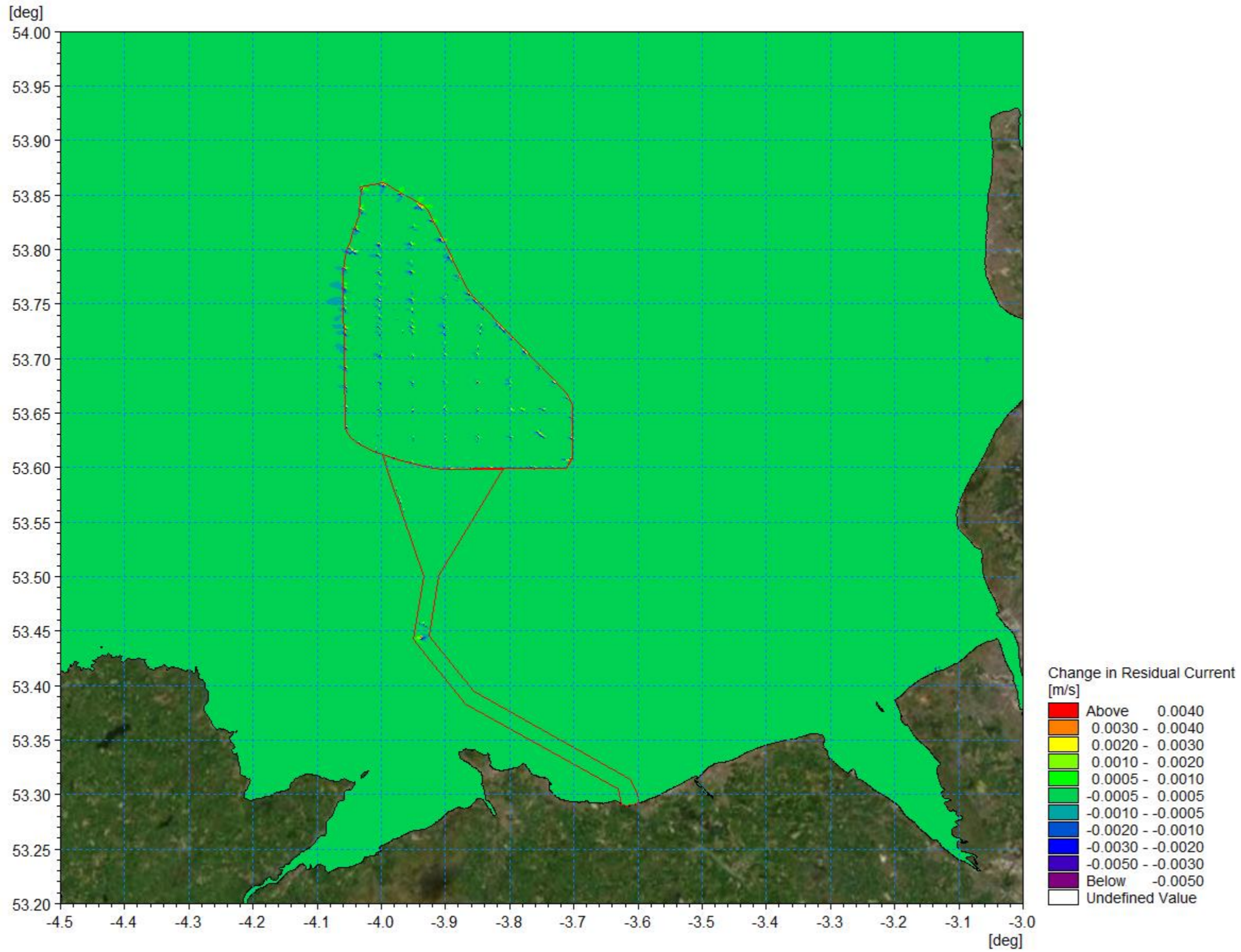


Figure 1.89: Change in residual current spring tide (post-construction minus baseline).

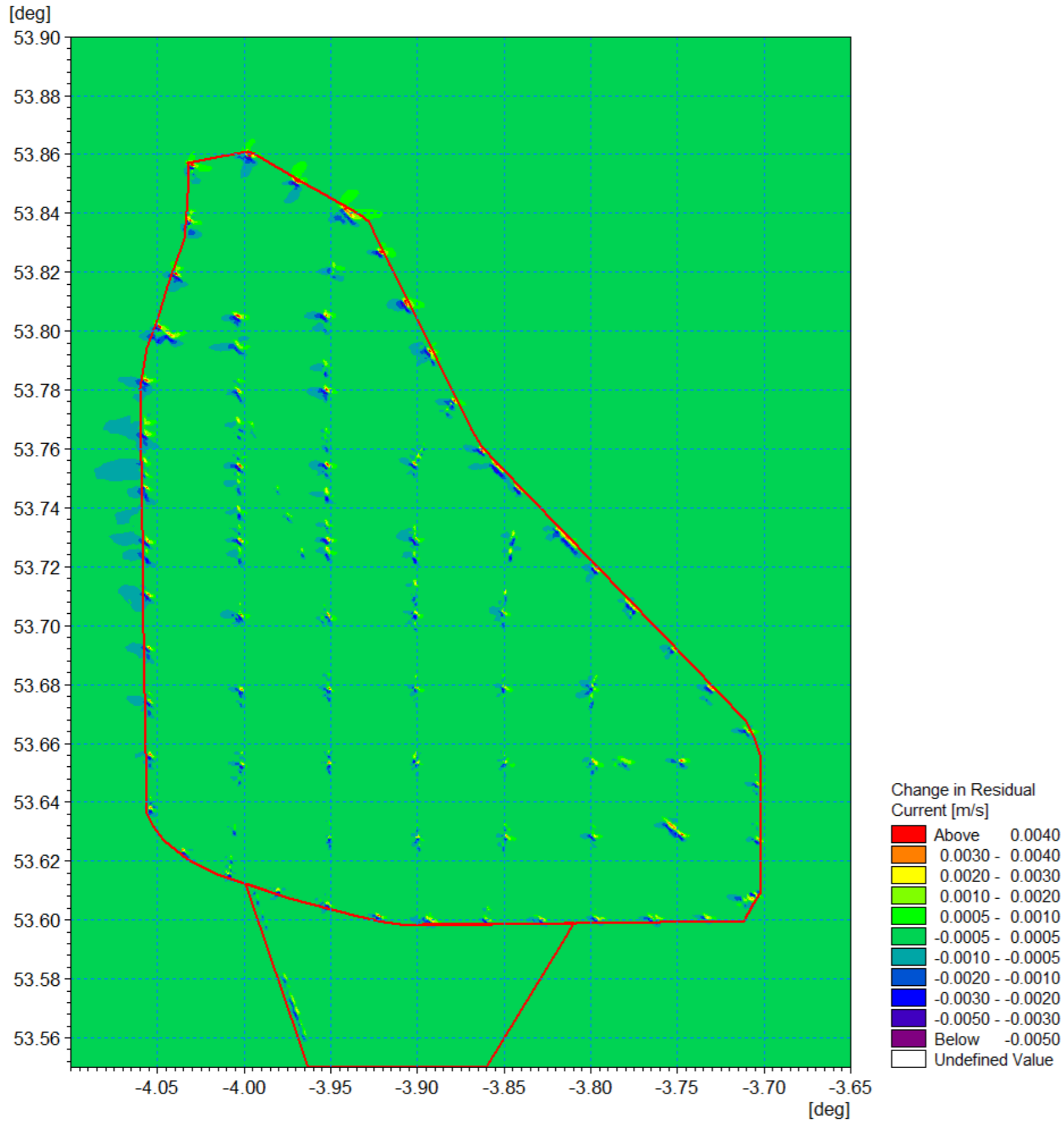


Figure 1.90: Change in residual current spring tide (post-construction minus baseline) Mona Offshore Wind Project detailed view.



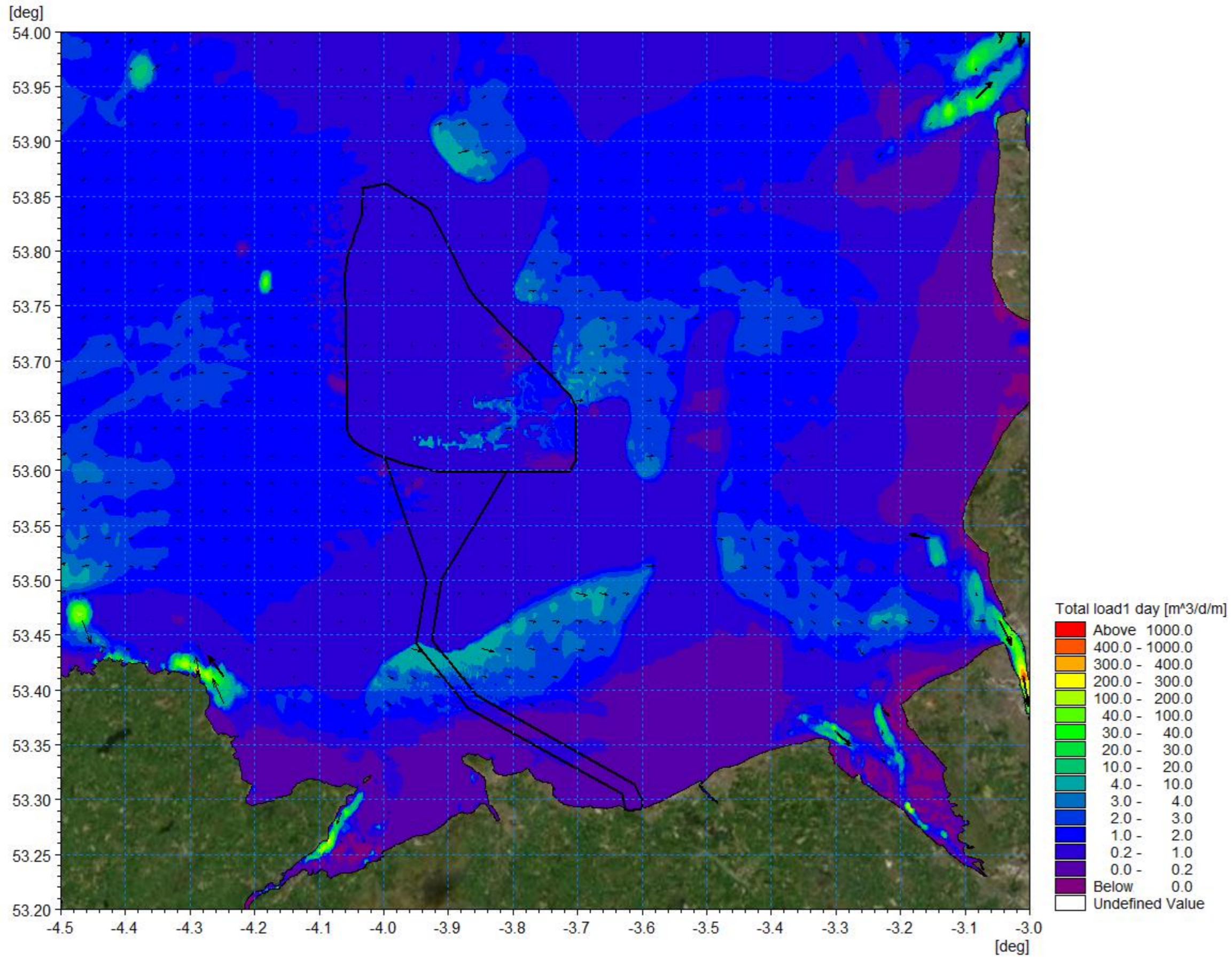


Figure 1.91: Post-construction potential sediment over the course of 1day (two tide cycles).



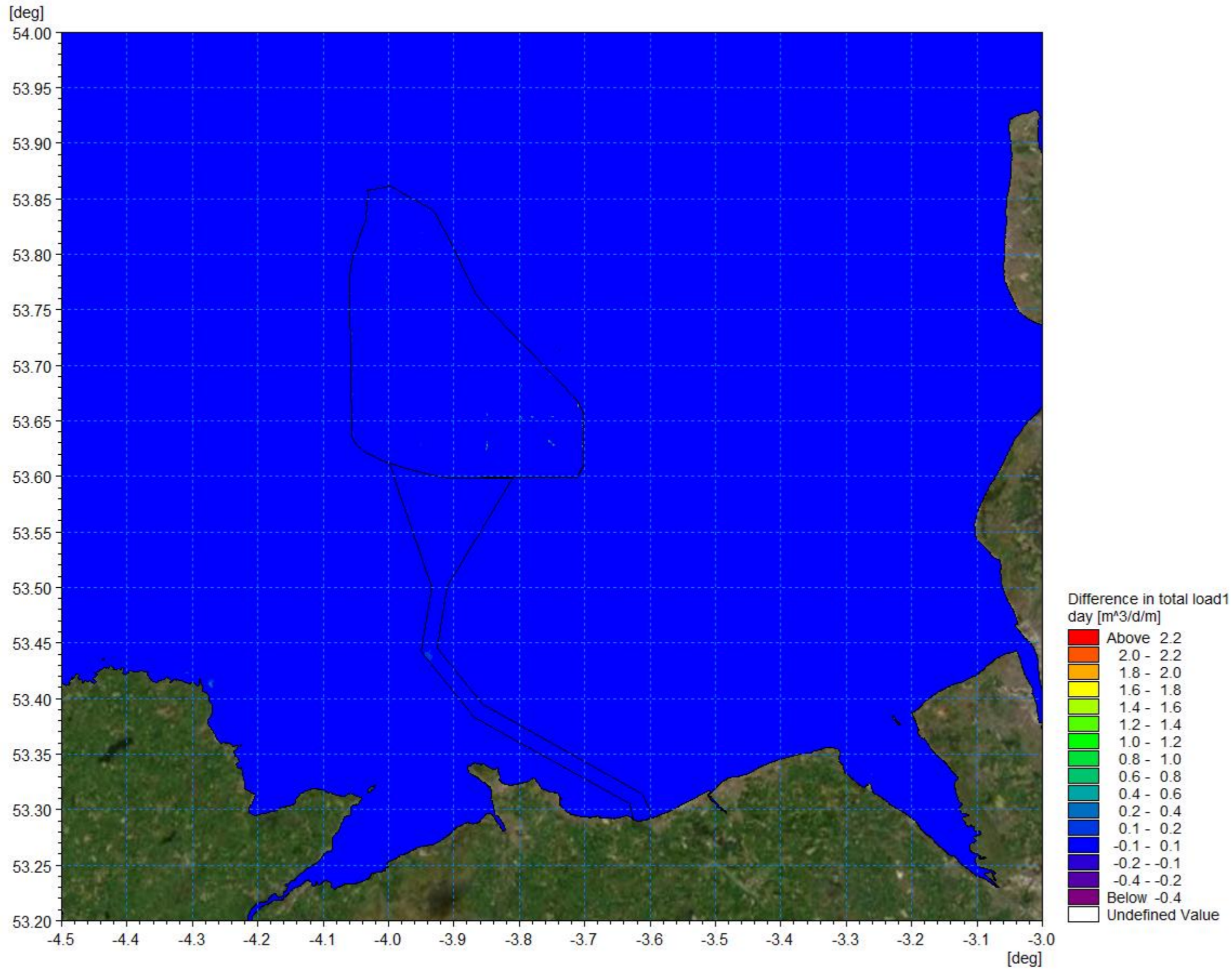


Figure 1.92: Difference in potential sediment transport over the course of 1day (post-construction minus baseline).



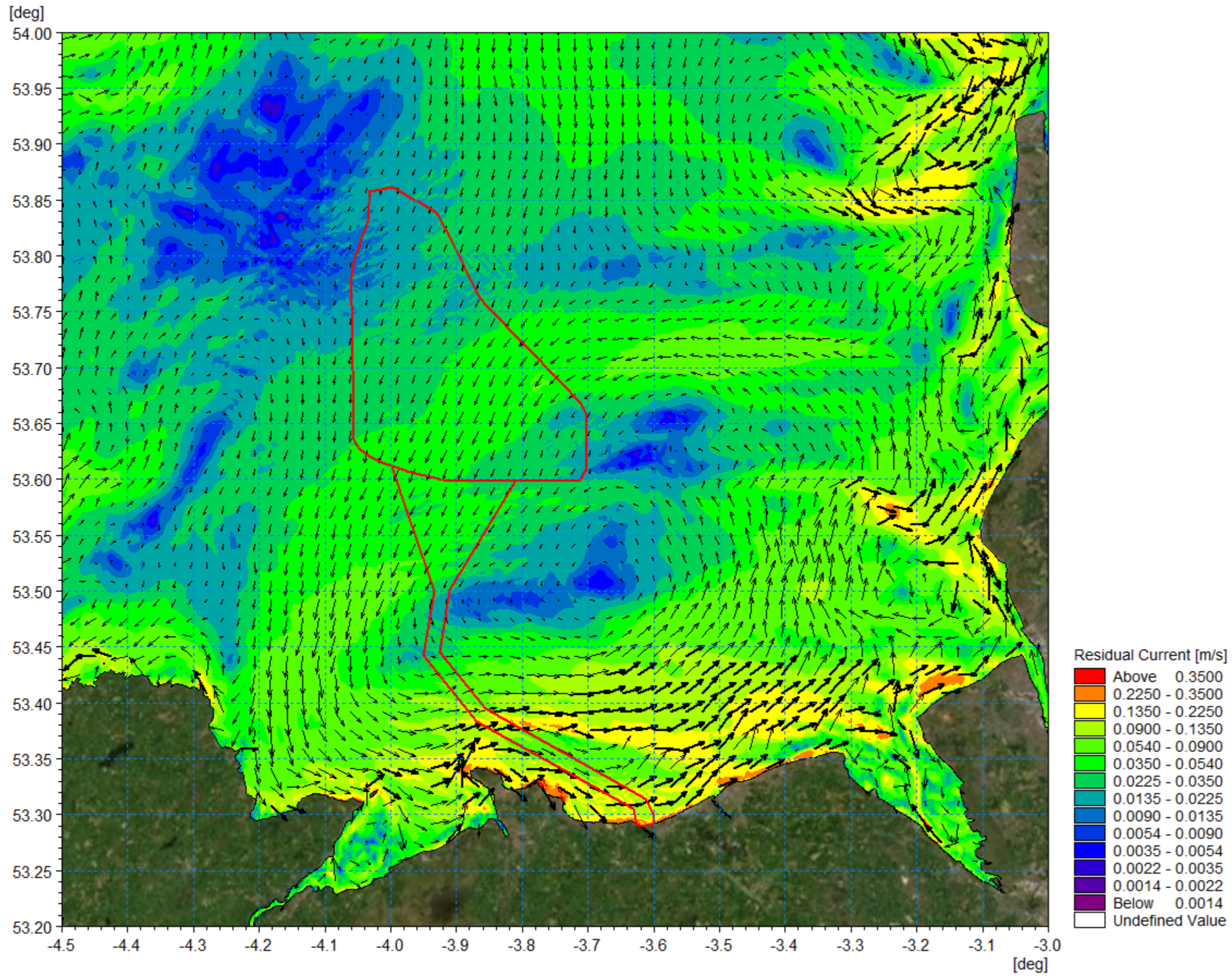


Figure 1.93: Post-construction residual current 1in1 year storm from 270° spring tide.



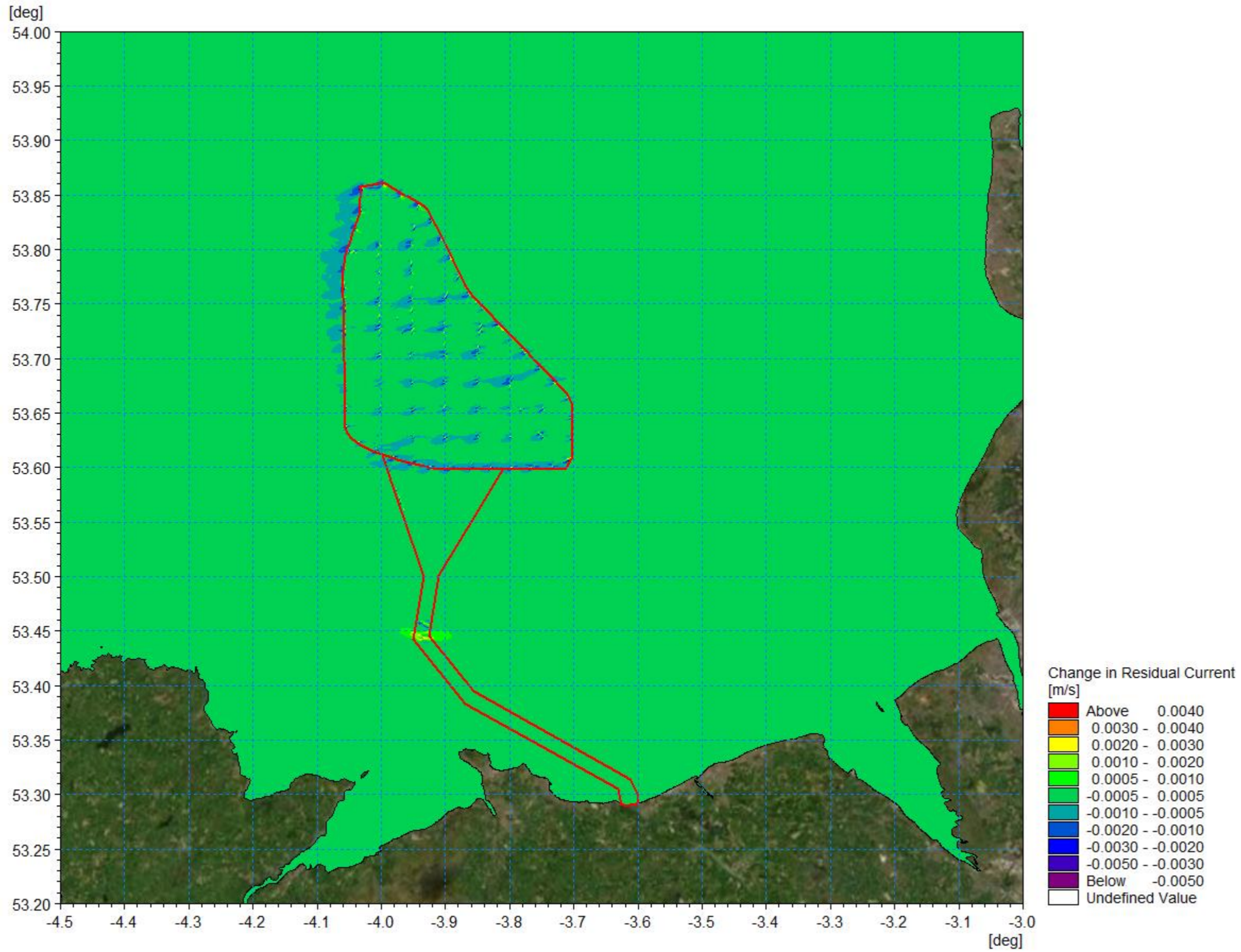


Figure 1.94: Change in residual current 1in1 year storm from 270° spring tide (post-construction minus baseline).



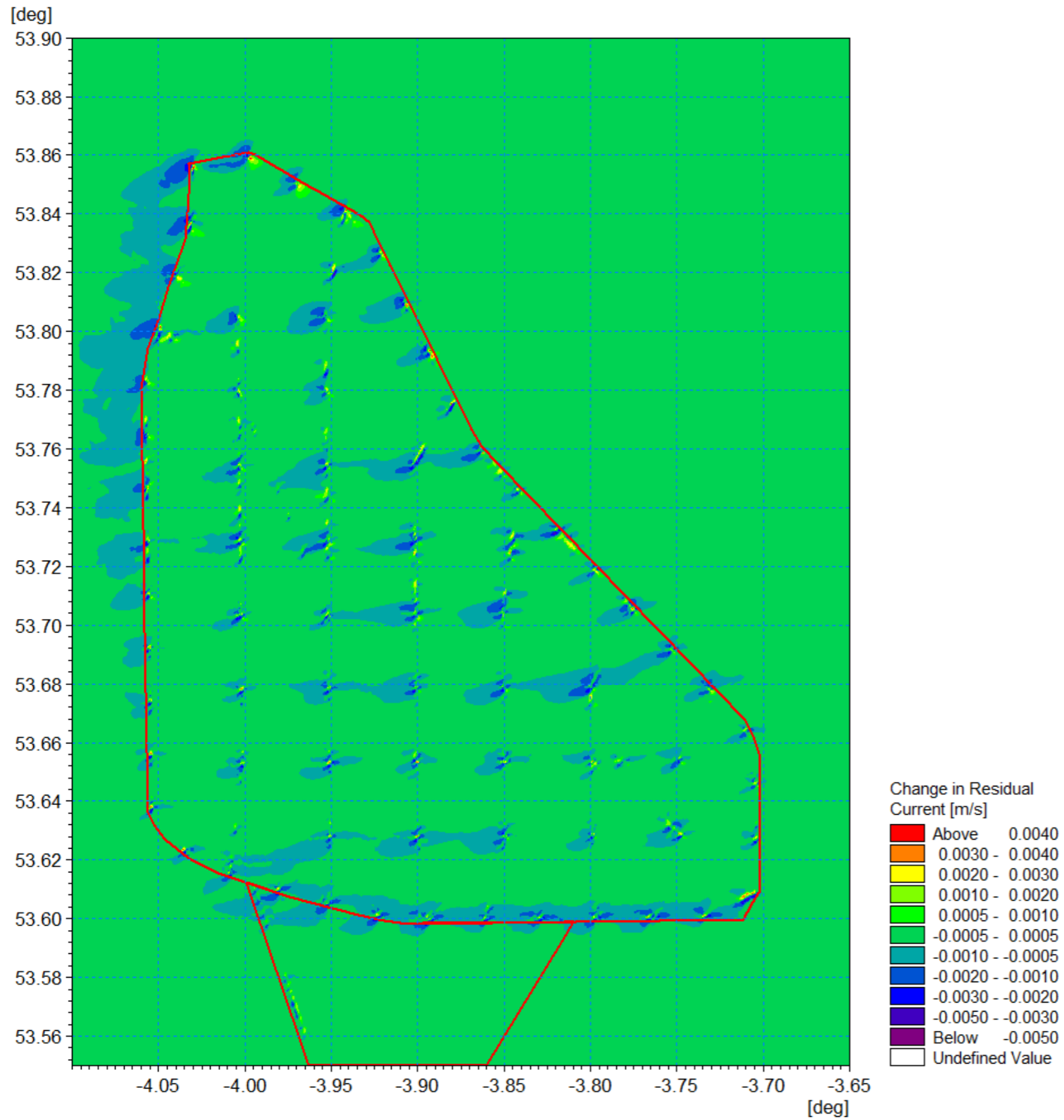


Figure 1.95: Change in residual current 1in1 year storm from 270° spring tide (post-construction minus baseline) detailed view.

## 1.8 Potential changes during construction

1.8.1.1 In addition to the changes in physical process resulting from the presence of the Mona Offshore Wind Project, the construction phase influences were quantified. The principal construction elements relate to the transport and fate of sediment brought into suspension due to seabed preparation, the installation of the foundation structures and the laying of inter-array/interconnector cables between the wind turbines/Offshore Substation Platforms and the Mona Offshore Cable Corridor to shore. An overview of the modelling techniques implemented is provide in Table 1.1.

1.8.1.2 As with the post-construction aspects, the approach was to examine the construction technique which represents the maximum design scenario in terms of coastal processes. In practice, these changes are therefore likely to be of lesser magnitude. In each scenario the modelling examined excess suspended sediment concentration (SSC) arising from the proposed activities (i.e. ambient SSC were not included). Baseline studies outlined in Section 1.6.7 indicate that turbidity levels vary greatly across the domain and throughout the year, being relatively low in deep water areas compared with active sediment transport mechanisms within the estuaries. Therefore, the excess SSC data presented would be applicable independent of the season in which the operations are undertaken.

1.8.1.3 The baseline residual currents and sediment transport modelling has corroborated the knowledge that the east Irish Sea is a sediment sink with active sediment transport processes. Sedimented material arising from the construction phase activities would therefore be amalgamated into the sediment transport regime. The numerical modelling provides depth averaged suspended sediment concentration values and do not therefore differentiate between bed load and water column suspended sediment.

1.8.1.4 During each phase of the assessment the transport of suspended sediment was modelled by undertaking simulations which released sediment at a rate and location appropriate to each type of construction. The sediment released was defined according to the characteristics derived from the BGS data at each specific location. Where a number of locations were encountered, such as a dredging path, then a representative grading was used. The sediment sample locations are presented in Figure 1.56.

### 1.8.2 Seabed preparation

1.8.2.1 Due to the nature of the seabed in the Mona Offshore Wind Project area and Mona Offshore Cable Corridor, the cable installation will require seabed preparation in the form of seabed features clearance. The Project Design Envelope (PDE) presented by the project description outlined in volume 1, chapter 3: Project description of the PEIR indicates that sand waves may be cleared for the offshore, inter-array and interconnector cabling along up to a 104m wide corridor. Clearance activities may extend along circa 70% of the offshore cable route with an average clearance depth of up to 5.1m and 50% of the inter-array cable route with an average clearance depth up to 5.1m.

1.8.2.2 The modelling undertaken to quantify the potential increases in suspended sediment concentration and sedimentation simulated the use of a suction hopper dredger to remove material from the crest of sandwaves and deposit material in the adjacent trough area. In practice plough dredging may be undertaken however this type of

operation would have less impact in terms of both suspended sediment concentrations and sedimentation footprint.

1.8.2.3 Two representative clearance operations were assessed, one relating to the offshore export cabling and a second for the inter-array cables, which has the same characteristics as clearance for the inter-connector cables. The geophysical survey data was used to identify areas of sandwaves where the operations are most likely to be required. Figure 1.96 indicates the sand areas by yellow shading and the clearance routes modelled are specified in blue for the inter-array and Mona Offshore Cable Corridor. In each case the clearance was undertaken in a southwest direction with a dredging rate of 10,000m<sup>3</sup>/h with a spill of 3%.

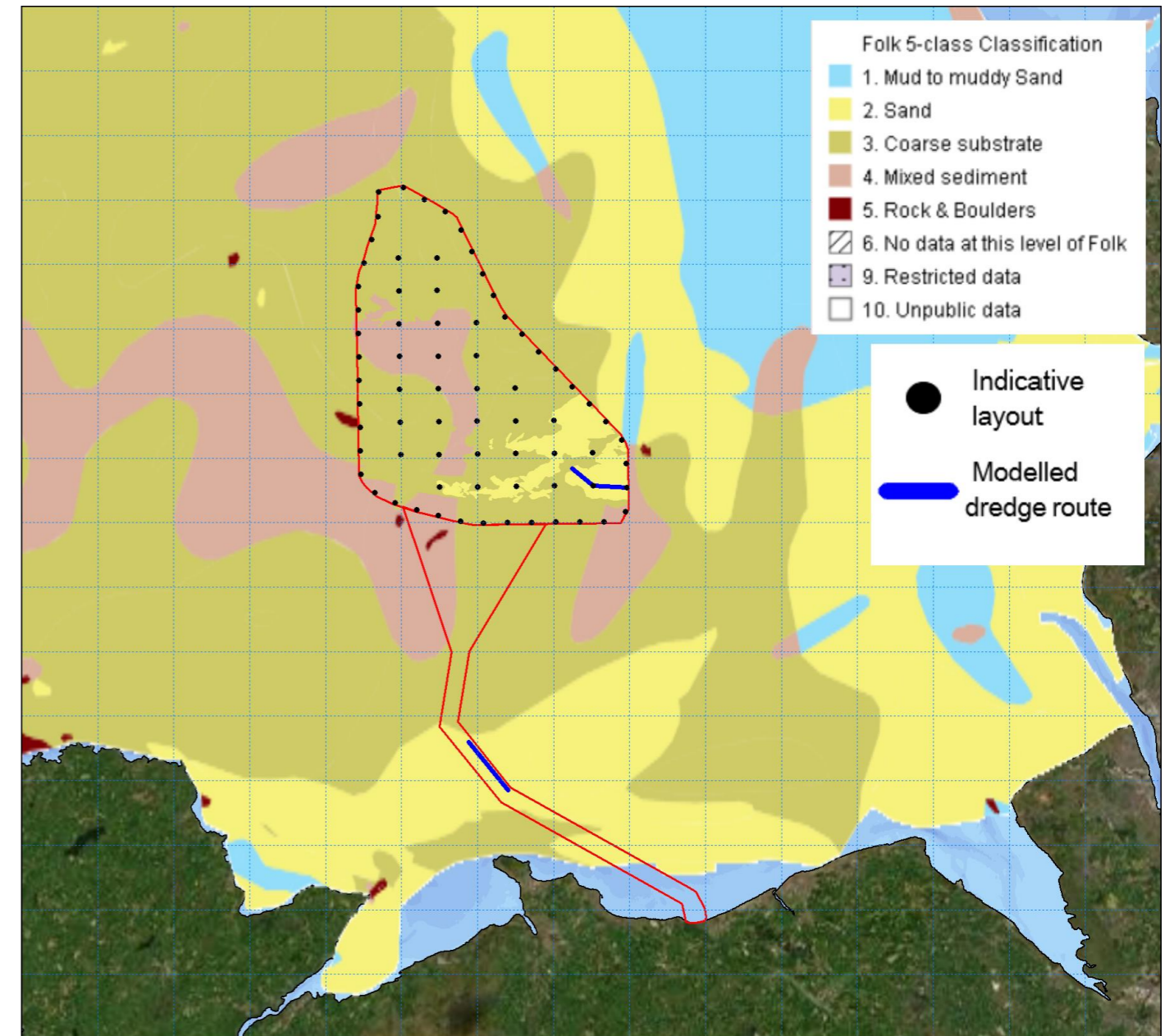


Figure 1.96: Sand wave clearance paths modelled.



### Offshore export cable sandwave clearance

- 1.8.2.4 The offshore export cable route was cleared at 100m/h along the 104m wide route for a period of four hours, in line with dredging rate and plant required to carry out the operation. The material was then deposited over a 45-minute period from the hopper with the modelled route of 5km taking two days to prepare. The redistributed material was classified using the properties identified from the sampling undertaken along the route simulated.
- Very coarse sand/gravel: 8%
  - Coarse sand: 23%
  - Medium sand: 48%
  - Fine sand: 10%
  - Very fine sand/mud: 11%.
- 1.8.2.5 The suspended sediment concentrations vary greatly during the course of the operation. During the dredging phase, when 3% of the material is spilled at the seabed, the sediment plumes exhibit much lower concentrations. These are typically <50mg/l along the clearance route as shown in Figure 1.98. During the dumping phase the plume is slightly larger (Figure 1.99) with concentrations reaching 1000mg/l at the release site. However, the most extensive increases are seen as the deposited material is redistributed on the successive tides, where sedimentation occurs on the slack tide reducing the SSC completely and resuspension and transport occurs when the tidal currents increase. Under these circumstance concentrations of 300 – 500mg/l are seen as illustrated in Figure 1.100 which shows SSC arising at peak current speed. The average suspended sediment concentration during the course of the operation is presented in Figure 1.101 with values <300mg/l with a plume envelope width of circa 20km which corresponds with the tidal excursion.
- 1.8.2.6 The average sedimentation depth is shown in Figure 1.102, with a detailed view shown in Figure 1.103 and illustrates how the deposited material is focussed within 100m of the site of release with a maximum depth 0.5 –1m whilst the finer sediment fractions are distributed in the vicinity at much smaller depths circa 5 – 10mm. The dispersion of the released material would continue on successive tides. The sedimentation one day following the cessation of the clearance operation is presented in Figure 1.104, with a detailed plot shown in Figure 1.105 and is consistent with this mechanism with the production of sandwaves visible.
- Constable Bank**
- 1.8.2.7 Overlapping with the Mona Offshore Cable Corridor is the sandbank known as Constable Bank. This sandbank meets the requirements for an annex 1 habitat under Annex 1 of the EC Habitats. Figure 1.97 shows the location of the Mona Offshore Cable Corridor with respect to the Constable Bank.



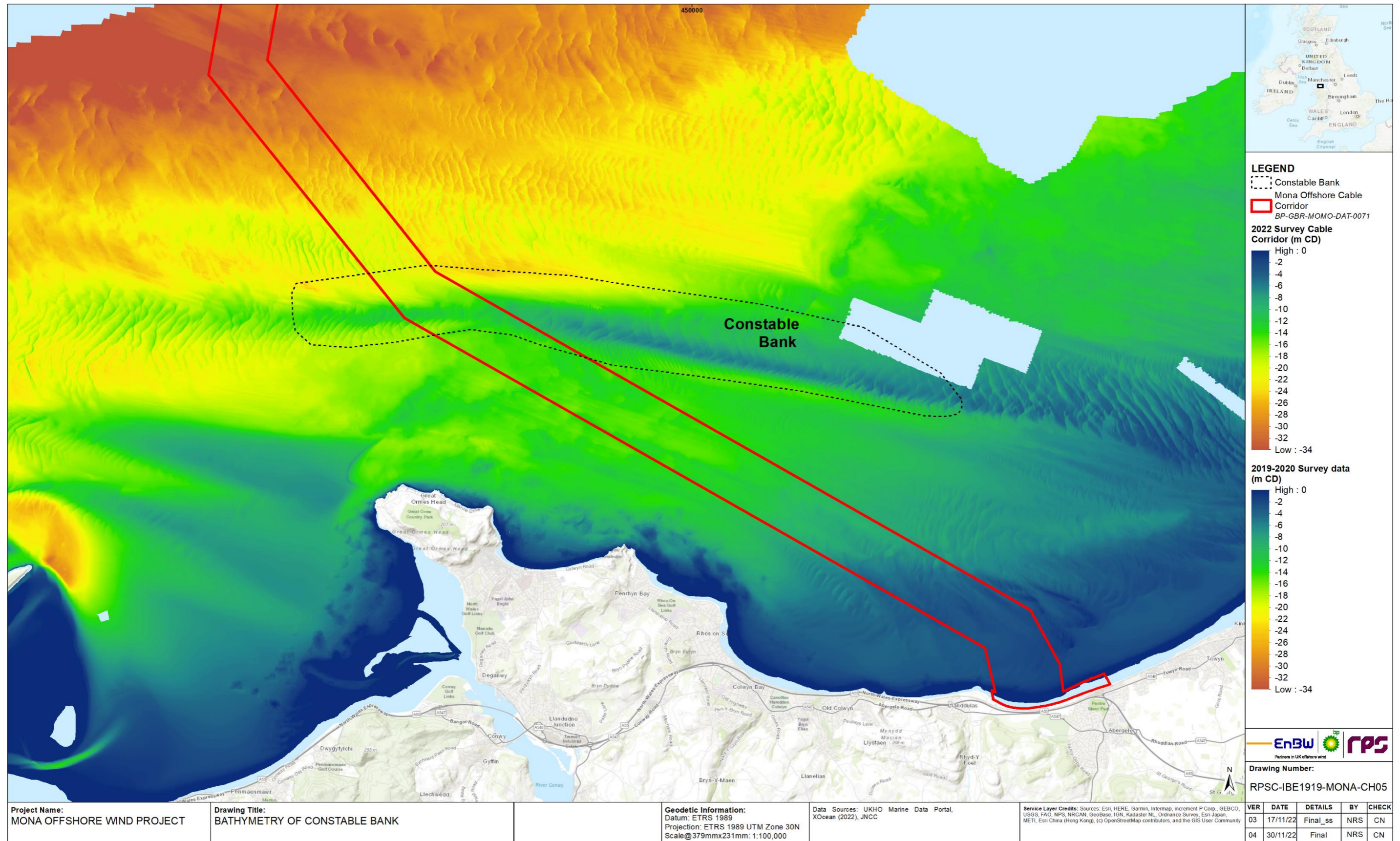


Figure 1.97: Location of Constable Bank in relation to the cable corridor.



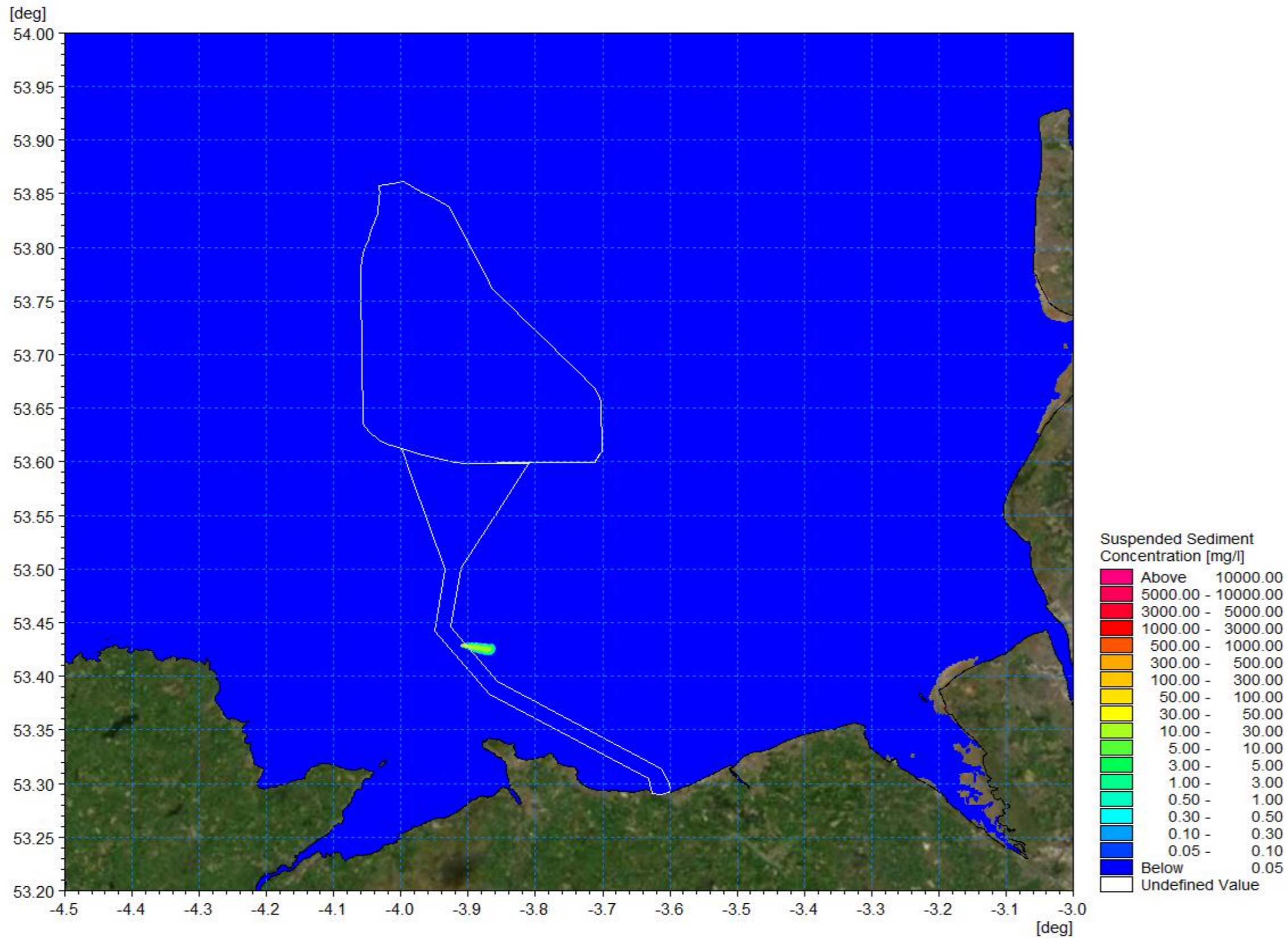


Figure 1.98: Suspended sediment concentration during dredging phase– offshore export cable path. <sup>1</sup>

<sup>1</sup> Modelled output does not include intertidal red line boundary vehicle access area.



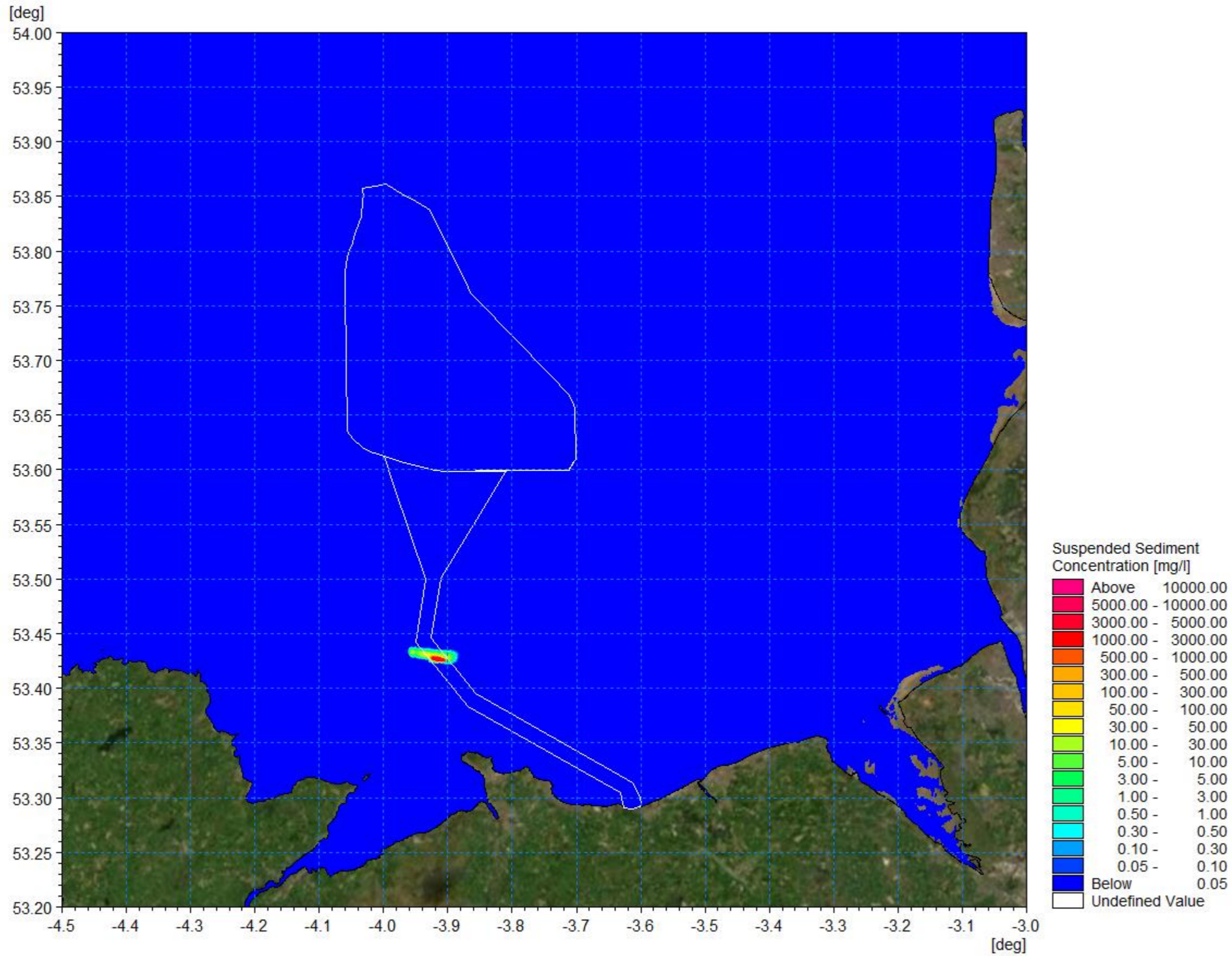


Figure 1.99: Suspended sediment concentration during dumping phase– offshore export cable path.



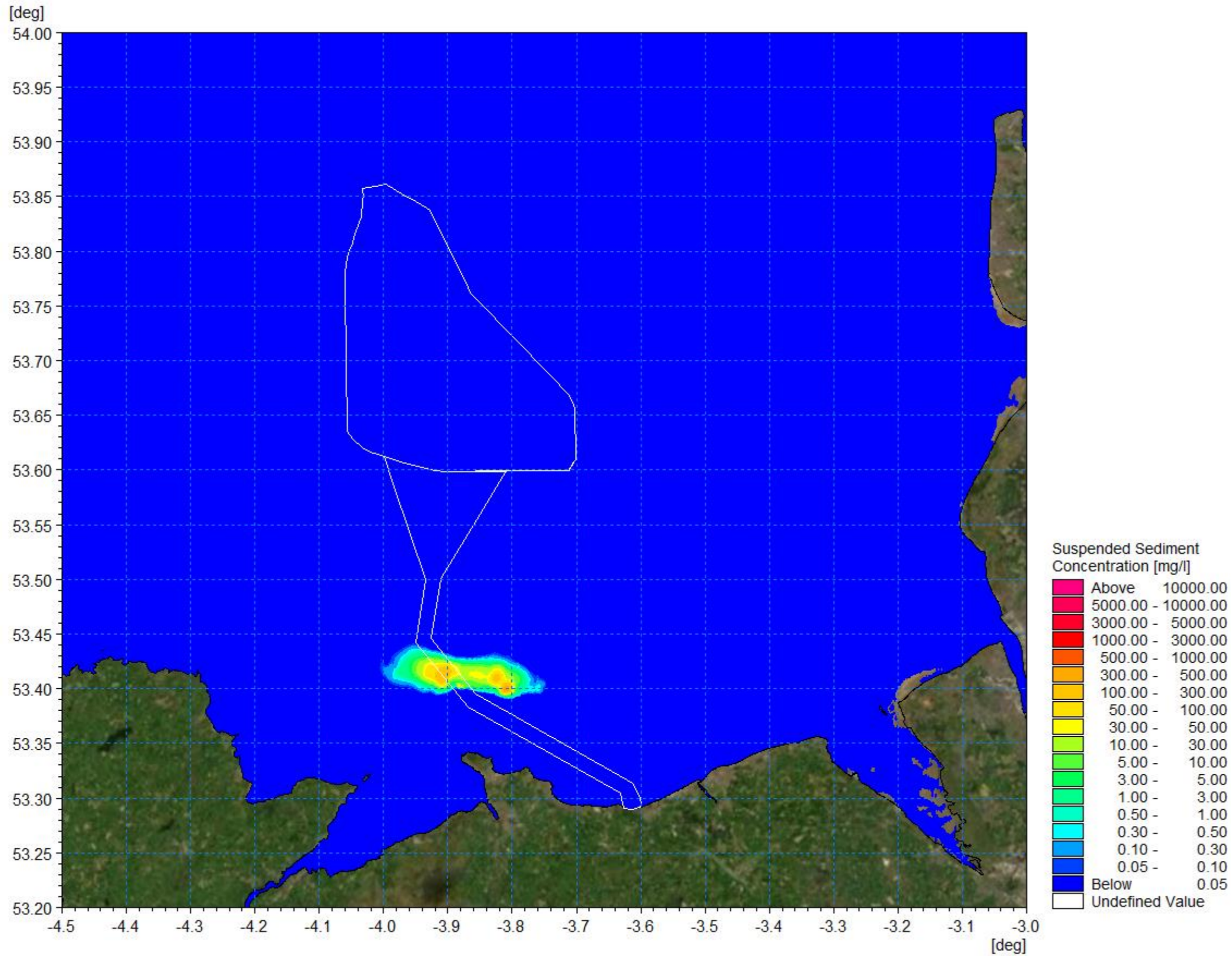


Figure 1.100: Suspended sediment concentration with sediment re-mobilisation – offshore export cable path.



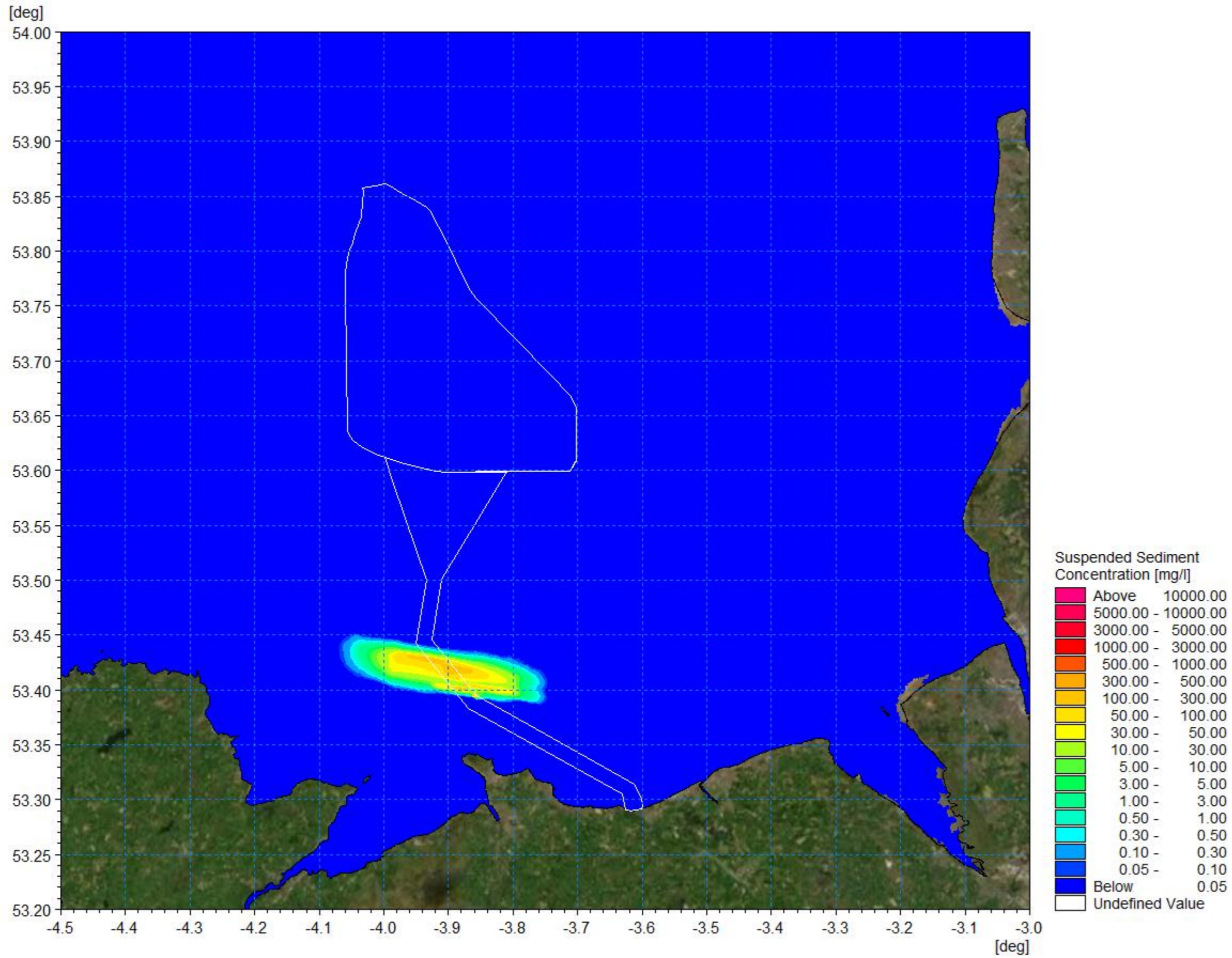


Figure 1.101: Average suspended sediment concentration during operation – offshore export cable path.



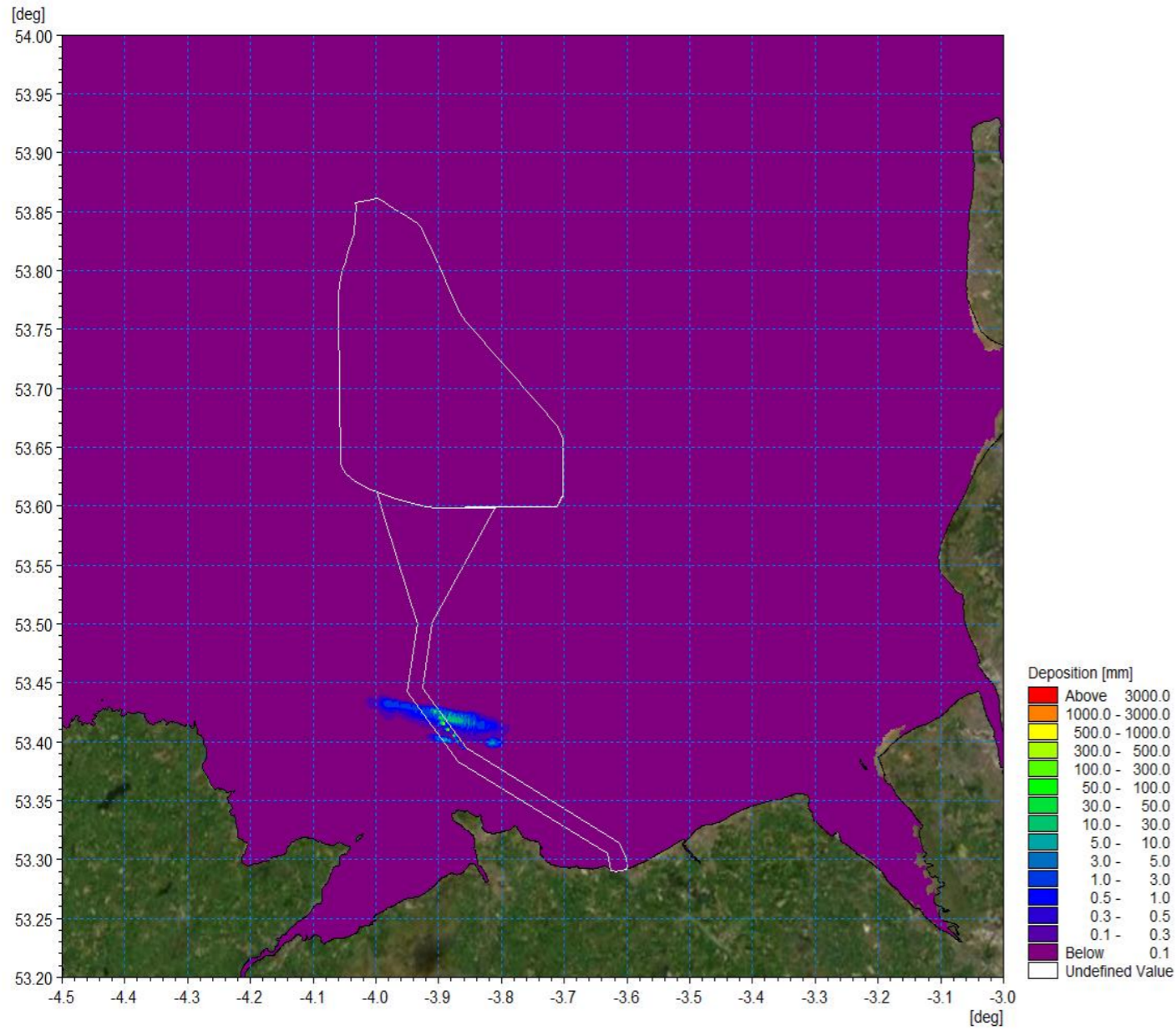


Figure 1.102: Average sedimentation during operation – offshore export cable path.

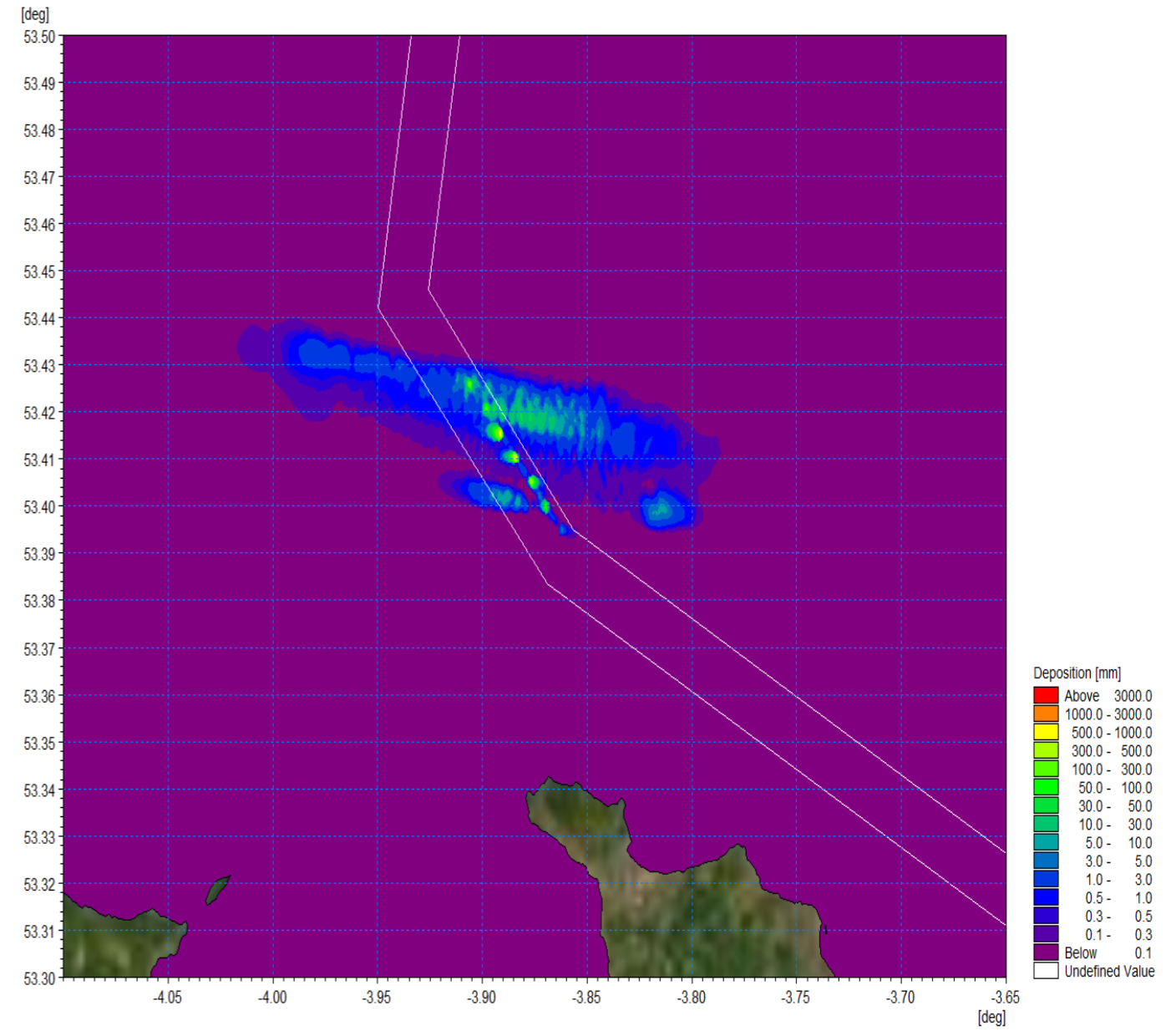


Figure 1.103: Average sedimentation during operation – offshore export cable path detailed view.

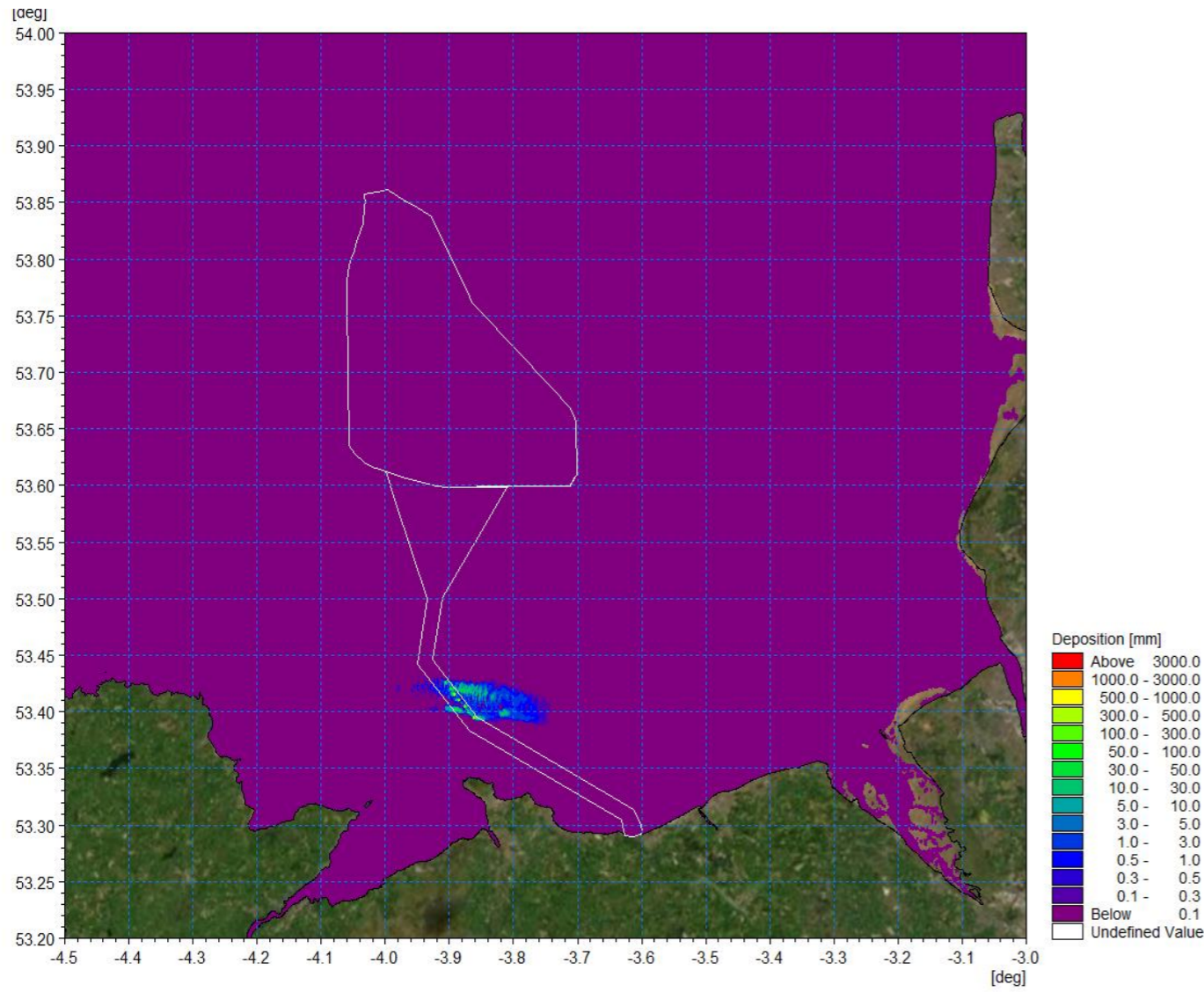


Figure 1.104: Sedimentation 1day following cessation of operation – offshore export cable path.

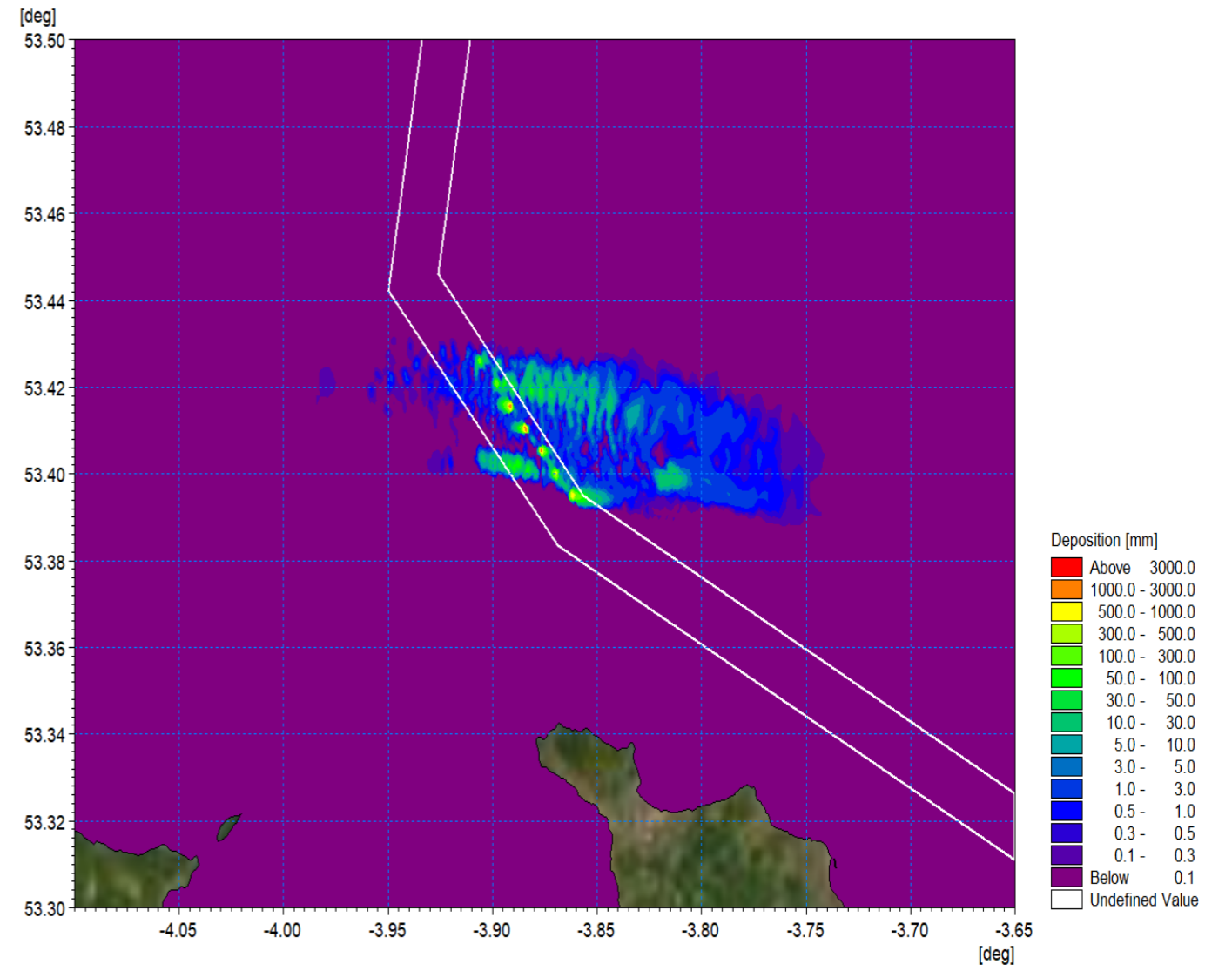


Figure 1.105: Sedimentation 1day following cessation of operation – offshore export cable path detailed view.



### Inter-array cable sandwave clearance

- 1.8.2.8 The inter-array cable route was cleared at 100m/h along the 104m wide route for a period of four hours, in line with the dredging rate and removal depth. The material was then deposited over a 45minute period from the hopper with the 5km modelled route taking two days to prepare. As previously, the redistributed material was classified using the properties identified from the sampling undertaken along the route simulated.
- Very coarse sand/gravel: 8%
  - Coarse sand: 23%
  - Medium sand: 48%
  - Fine sand: 10%
  - Very fine sand/mud: 11%.
- 1.8.2.9 The resulting suspended sediment concentrations showed similar characteristics to the offshore cable clearance. The dredging phase plumes were smaller than the dumping as 3% spill of the material is released along the route and again concentrations are <50mg/l as shown in Figure 1.106. Similarly, the release phase plume is slightly larger than the dredging plume with concentrations reaching 3000mg/l at the dump site, Figure 1.107. At this site the greatest area of increased suspended sediment concentration, extending a tidal excursion circa 20km from the site, is also associated with re-mobilisation of the deposited material on subsequent tides with concentrations of 500 – 1000mg/l whilst average levels <500mg/l as illustrated in Figure 1.108 and Figure 1.109 respectively.
- 1.8.2.10 The average sedimentation depth, shown in Figure 1.110 and in detail in Figure 1.111, is similar in form to that of the Mona Offshore Cable Corridor works. The sedimentation one day following the cessation of the clearance operation is presented in Figure 1.112 and Figure 1.113 and shows deposited material at the site of release with depth 1m whilst in the locality lower depths, typically <30mm, are present at circa 100m distance from the release with the formation of sandwaves being visible.

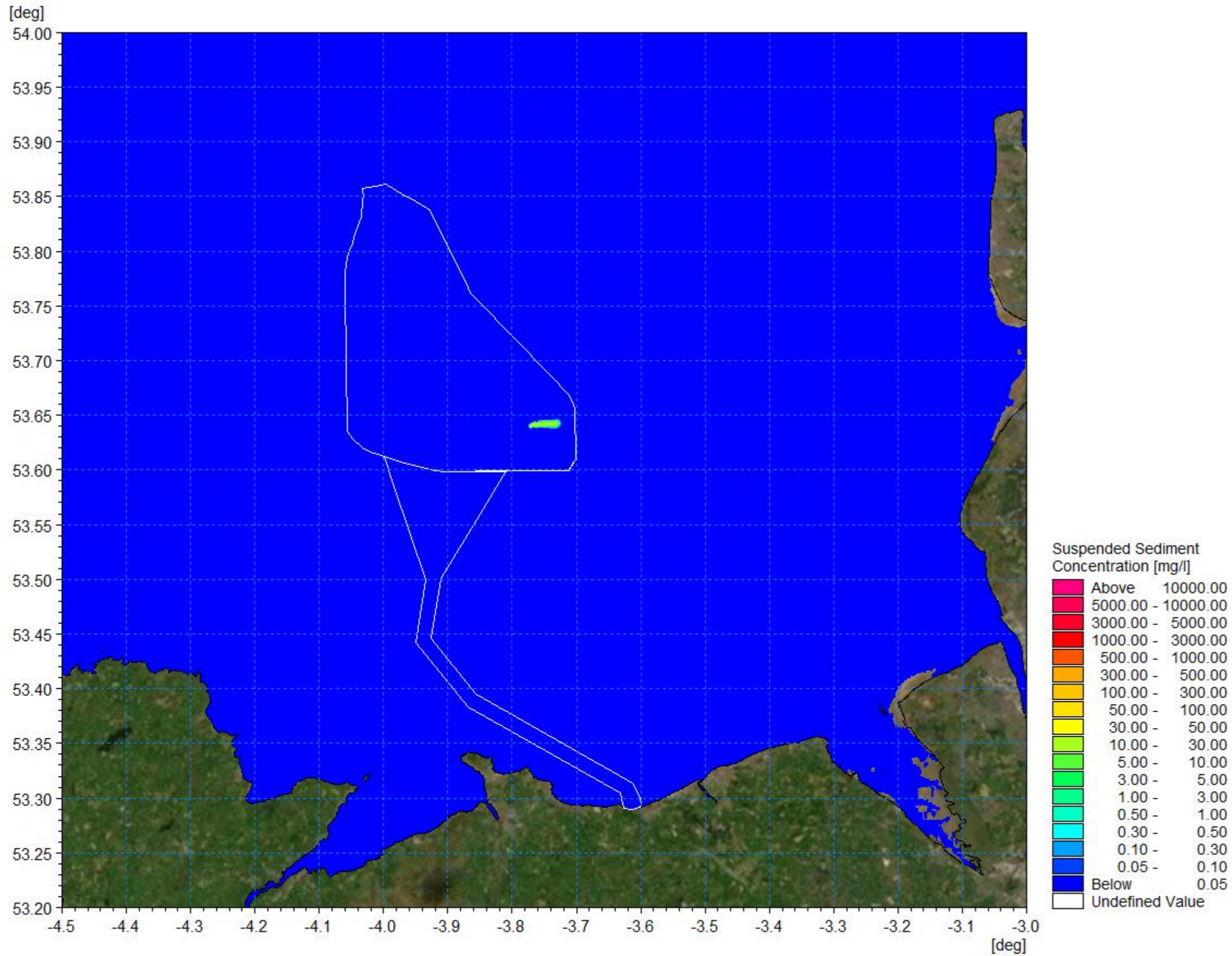


Figure 1.106: Suspended sediment concentration during dredging phase– inter-array cable path.



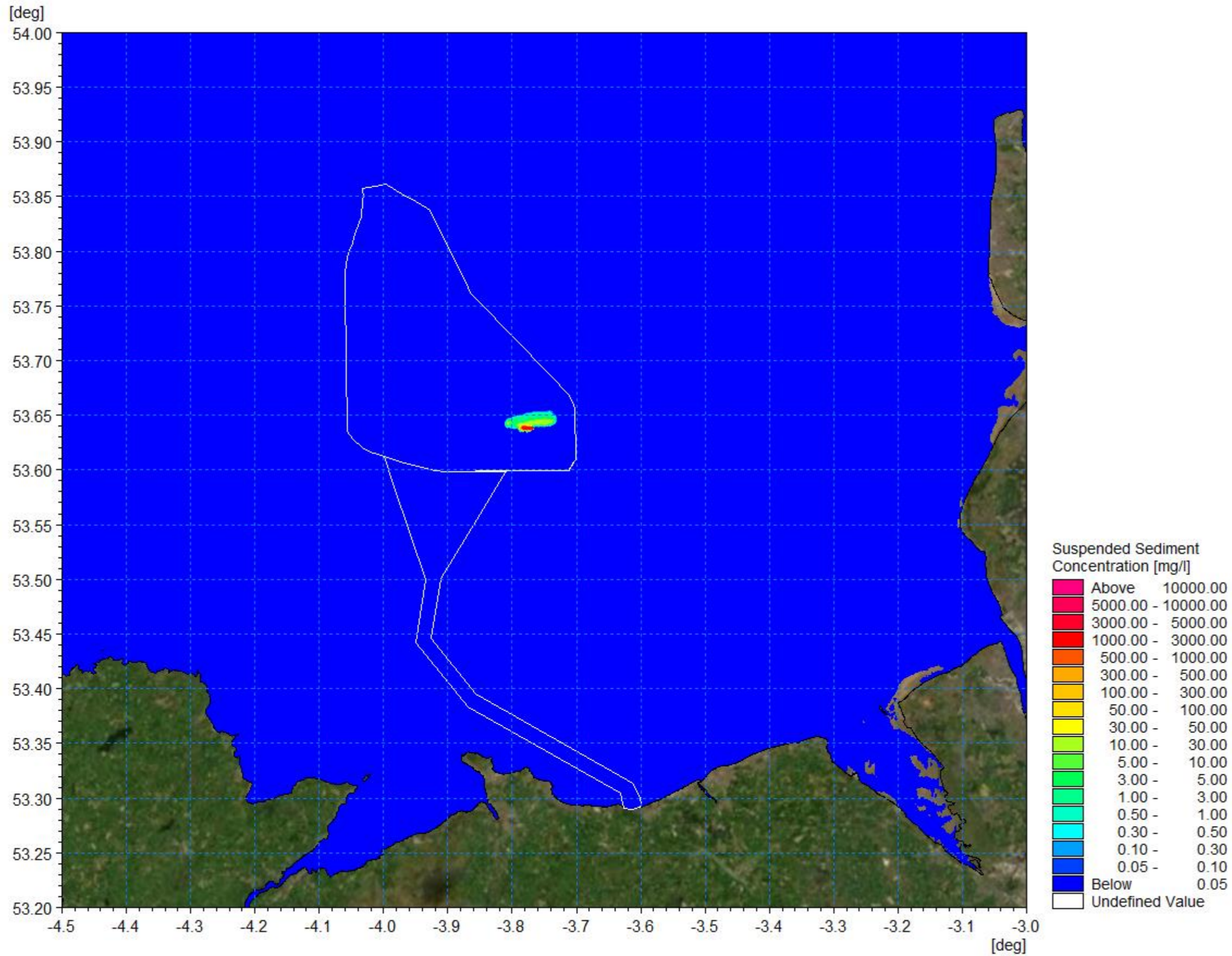


Figure 1.107: Suspended sediment concentration during dumping phase– inter-array cable path.



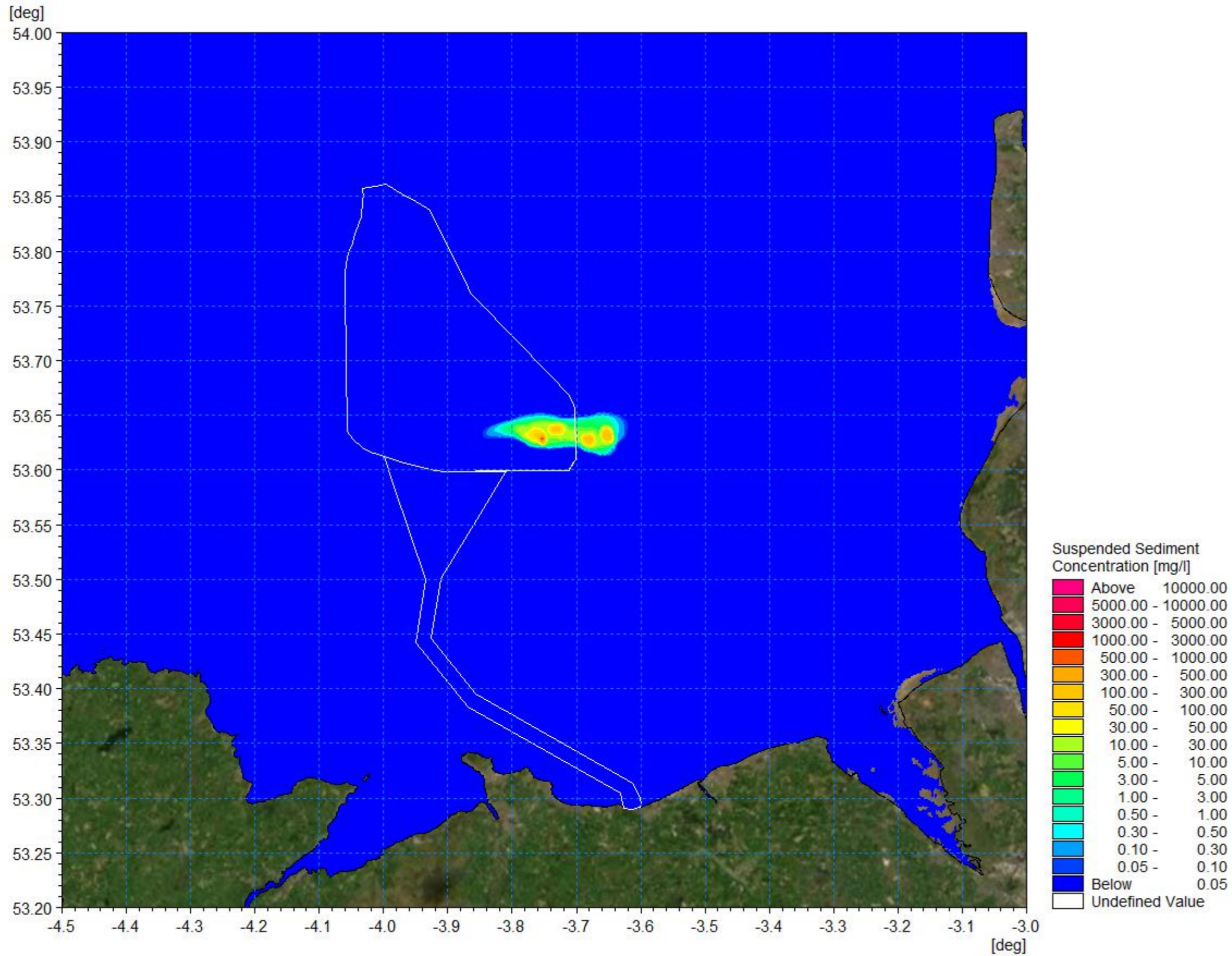


Figure 1.108: Suspended sediment concentration with sediment re-mobilisation – inter-array cable path.



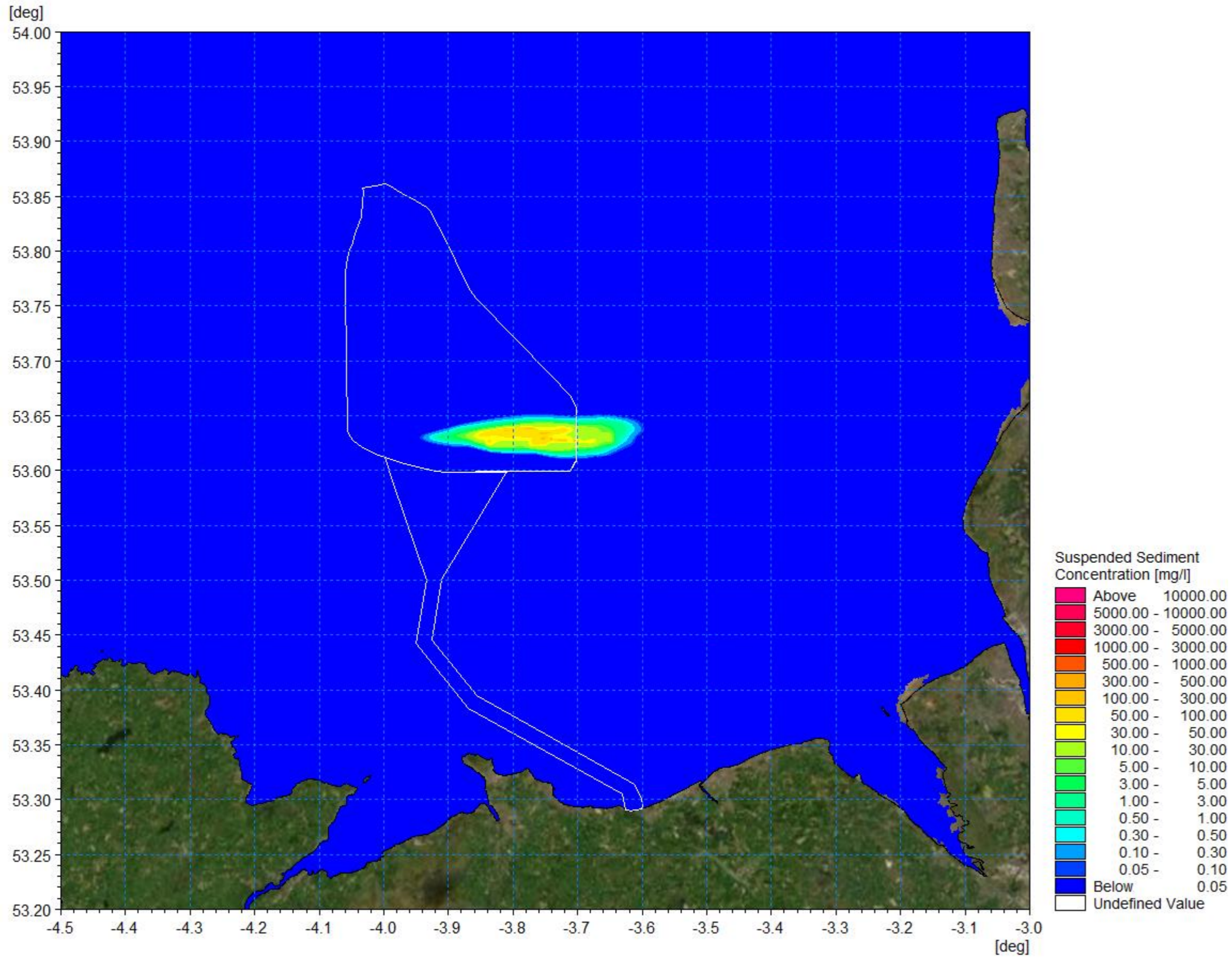


Figure 1.109: Average suspended sediment concentration during operation – inter-array cable path.



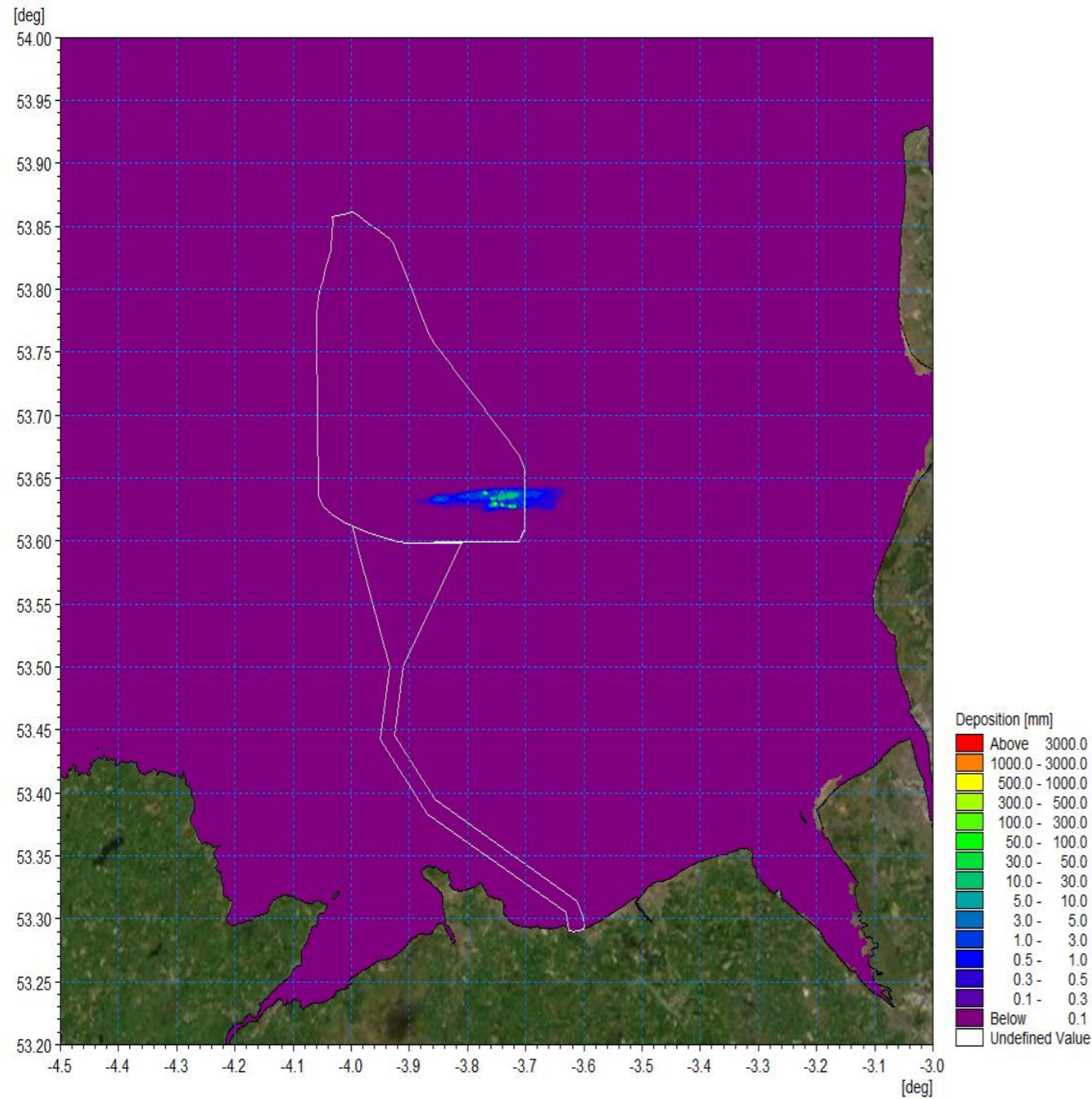


Figure 1.110: Average sedimentation during operation – inter-array cable path.

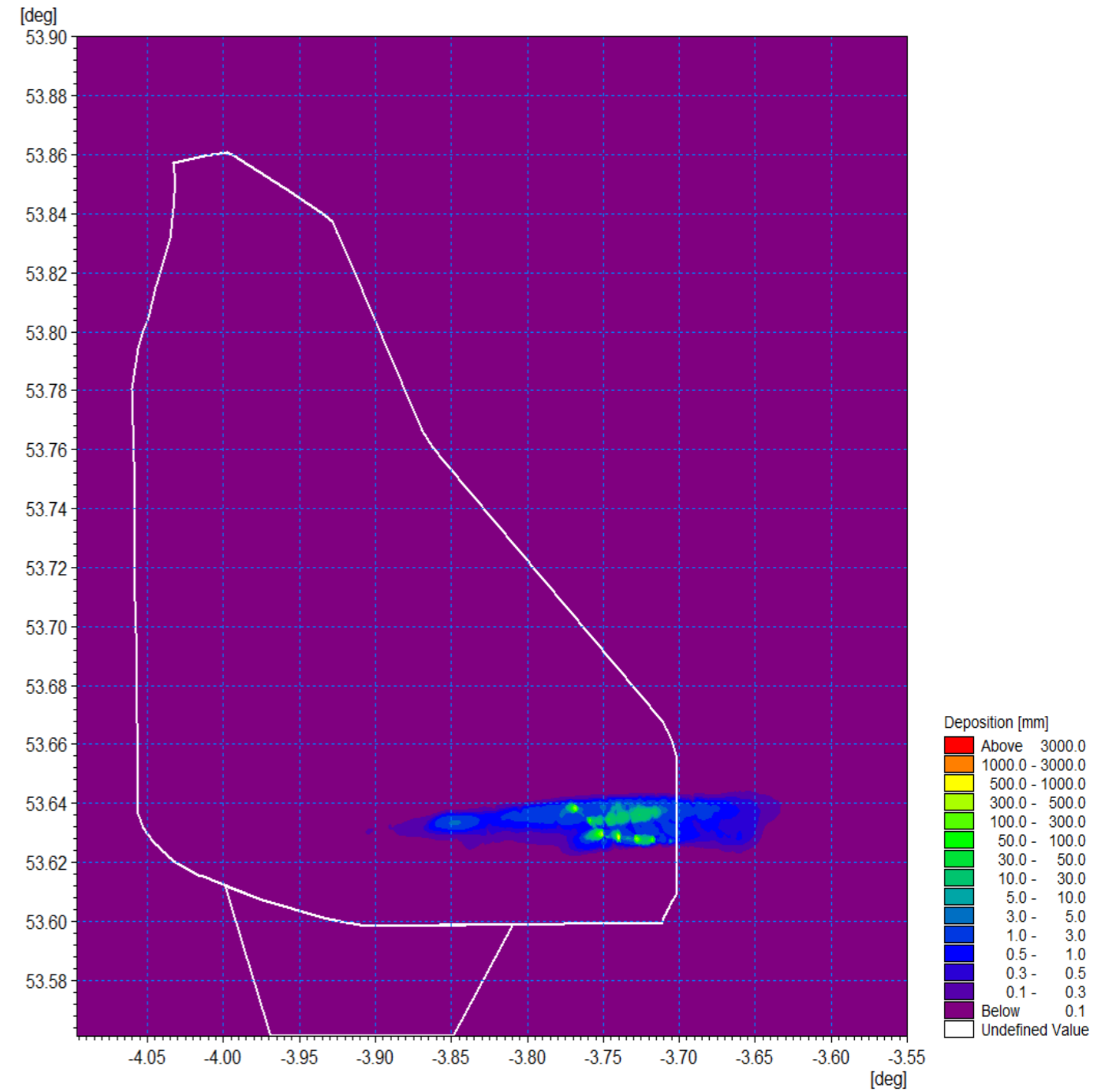


Figure 1.111: Average sedimentation during operation – inter-array cable path detailed view.



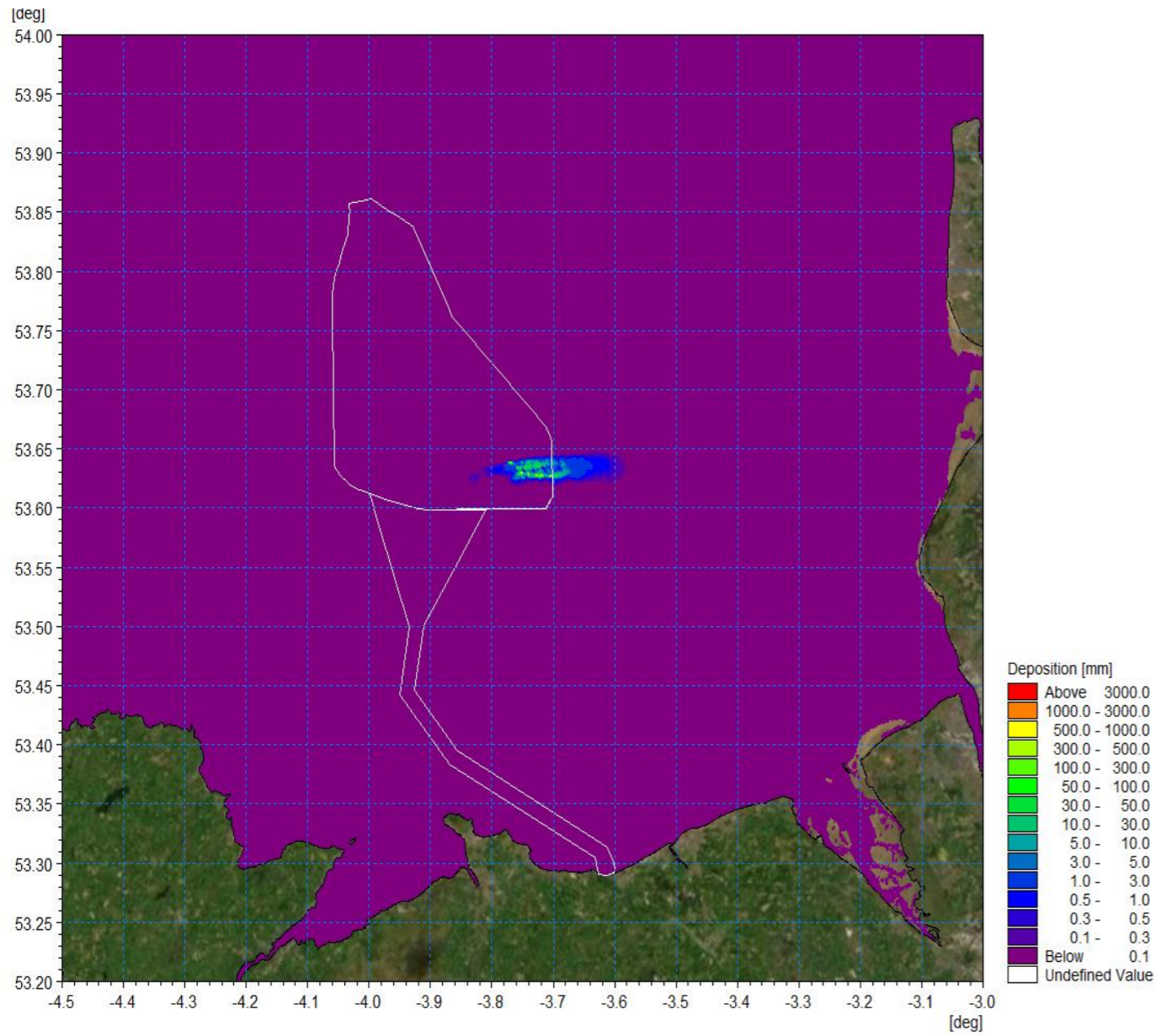


Figure 1.112: Sedimentation 1day following cessation of operation – inter-array cable path.

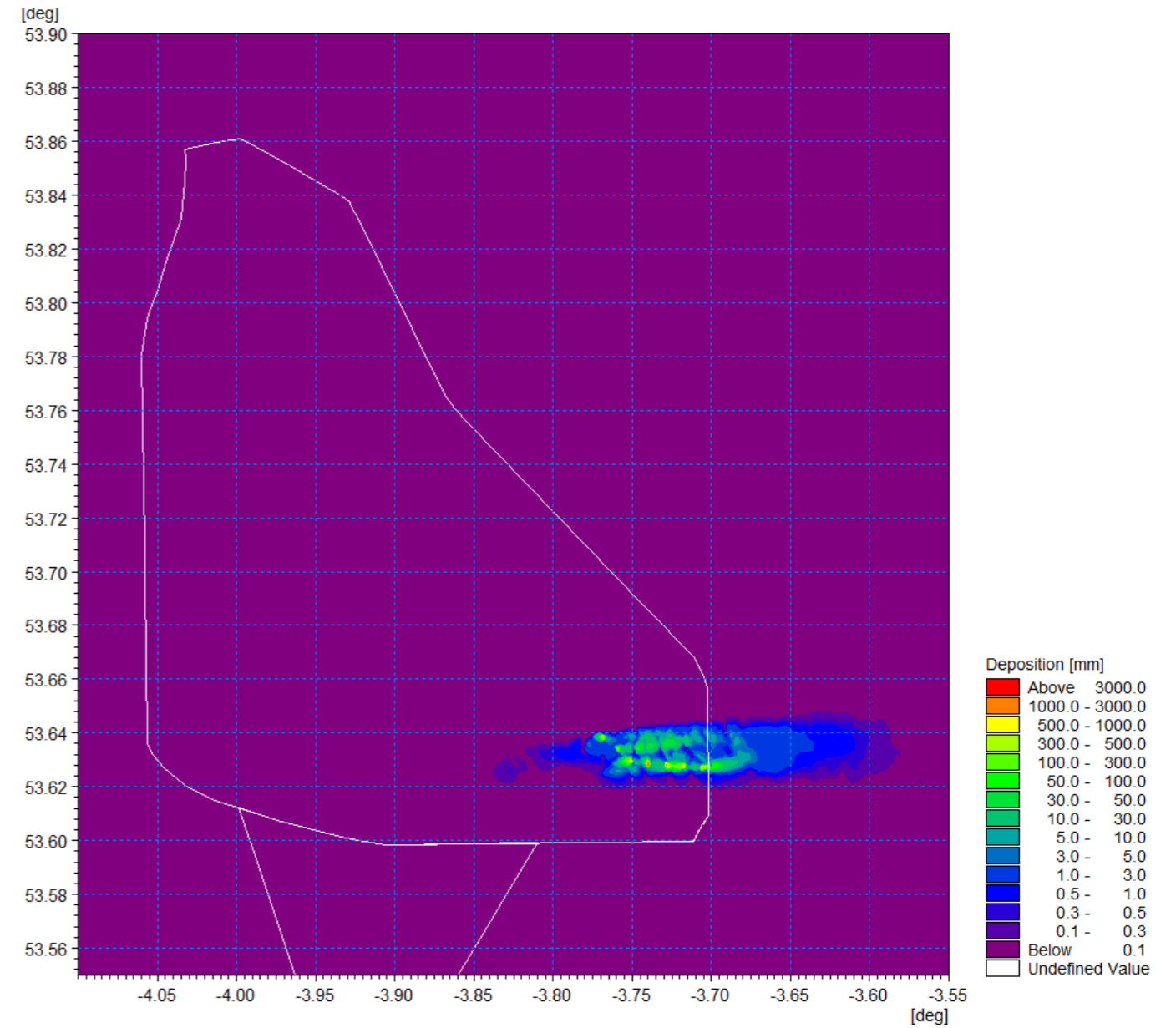


Figure 1.113: Sedimentation 1day following cessation of operation – inter-array cable path detail view.

### 1.8.3 Foundation installation

- 1.8.3.1 The project design envelope presented in volume 1, chapter 3: Project description of the PEIR includes a number of potential foundation types including piled and suction caissons foundations. The caissons were applied in the hydrographic assessments as they created the largest potential obstruction to tidal flow and sediment transport however the installation produces much less seabed disturbance than installation of piled foundations. Therefore, the piled structures were assessed in terms of potential increases in suspended sediment concentrations.
- 1.8.3.2 The largest potential release would be from augured (drilled) piles, where the material would be jetted and released to the water column as a plume. It is anticipated that all piles across the site may require drilling up to the full pile depth. The modelling assumed that at each site the material which is released has a similar composition to the sampled sediment. In reality, to require drilling (rather than driving) the sediments are generally less granular and augured material would be less easily brought into suspension therefore the modelled scenario provides a conservative assessment in terms of suspended sediment concentration.
- 1.8.3.3 A sample of four representative pile installation scenarios were simulated to cover the range of conditions in terms of water depth, tidal currents and sediment grading. It also took account of the proximity of piling where two concurrent events may take place. The modelling was undertaken using the MIKE MT module which allows the modelling of erosion, transport and deposition of cohesive and non-cohesive/granular sediments. This model is suited to sediment releases in the water column and allows sediment sources which may vary spatially and temporally. In this case, the cohesive functions were not utilised as the material released comprised sand. The sediment grading was defined for each location and assumed two concurrent drilling operations located at adjacent wind turbine or offshore platform locations to provide the largest augmented sediment plume concentration.
- 1.8.3.4 At each location it was assumed that the auguring was required to the 60m pile depth for an assumed 16m diameter pile with 0.9m casing as a worst-case scenario (i.e. 13,460m<sup>3</sup> per pile). The drilling rate was taken as 0.89m/h which was both prescribed in the project description presented in volume 1, chapter 3: Project description of the PEIR and also allowed the release to cover the full range of tidal conditions. The auguring was undertaken continuously over a 67hour period with material released throughout the water column.
- 1.8.3.5 For each location a set of results are presented. Firstly, the average suspended sediment plume during the course of the installation is shown. Due to the variation in suspended sediment levels, instantaneous plots of the sediment plumes are also presented during peak flood and ebb tides on two installation days. It should be noted that all the plots require the use of a log scale to cover this range of values whilst providing clarity and during slack water suspended sediment concentrations decrease significantly to values in the order of background levels.
- 1.8.3.6 The final set of plots relates to sedimentation. Due to the fine sandy nature of the material, it is clear that the sediment will be dispersed. It will be transported mid-tide, settle on slack water and be re-suspended and further dispersed on the resumption of tidal flow. For all simulations, sediment levels after the cessation of construction are presented. The piling activities do not remove any material from the immediate vicinity

of the site and the released material returns the native sediment back into the existing sediment transport regime.

#### Piling scenario A

- 1.8.3.7 The two piles locations were sited at the locations shown in Figure 1.114. The sediment release was modelled over successive neap tidal cycles and at the location coarser material is present with the following composition being implemented within the simulation.
- Very coarse sand/gravel: 20%
  - Coarse sand: 22%
  - Medium sand: 46%
  - Fine sand: 9%
  - Very fine sand/mud: 3%.
- 1.8.3.8 This location exhibits slightly coarser graded material than at other locations and current speeds are lower during neap tides therefore this presents a scenario with a reduced plume envelope and higher SCC for the range of potential operations. The average suspended sediment plot shown in Figure 1.115, illustrates the effect of the dominant flood tide with the plume envelope extending further to the east. Average concentrations are typically <10mg/l at the sites and reduce rapidly with distance from the two discharge locations. Where the plumes converge concentrations are <1mg/l.
- 1.8.3.9 Figure 1.116 and Figure 1.117 illustrate the instantaneous concentrations on the flood and ebb tide of the first day of the drilling whilst Figure 1.118 and Figure 1.119 correspond with the same information for the third day. Areas of increased suspended sediment are evident on the latter plots where material has been deposited on slack tide and subsequently re-suspended. Typically, the plume concentration is <10mg/l, and reduces with the distance from the site as the sediment is dispersed.
- 1.8.3.10 Figure 1.120 and Figure 1.121 show the average sedimentation, with the latter providing a more detailed view. It is evident that the greatest sedimentation depths occur at the drilling site itself with very localised values circa 300mm. This corresponds with the immediate settlement of coarser material fractions, the lower neap current speed and also for the portion of work undertaken on slack tide. Figure 1.122 and Figure 1.123 present sedimentation one day following cessation of the drilling operation. The coarser material is seen to remain at the drill site whilst the finer sand fraction migrates to the east on the residual current albeit with deposition depths <1mm due to the limited volume of material released.



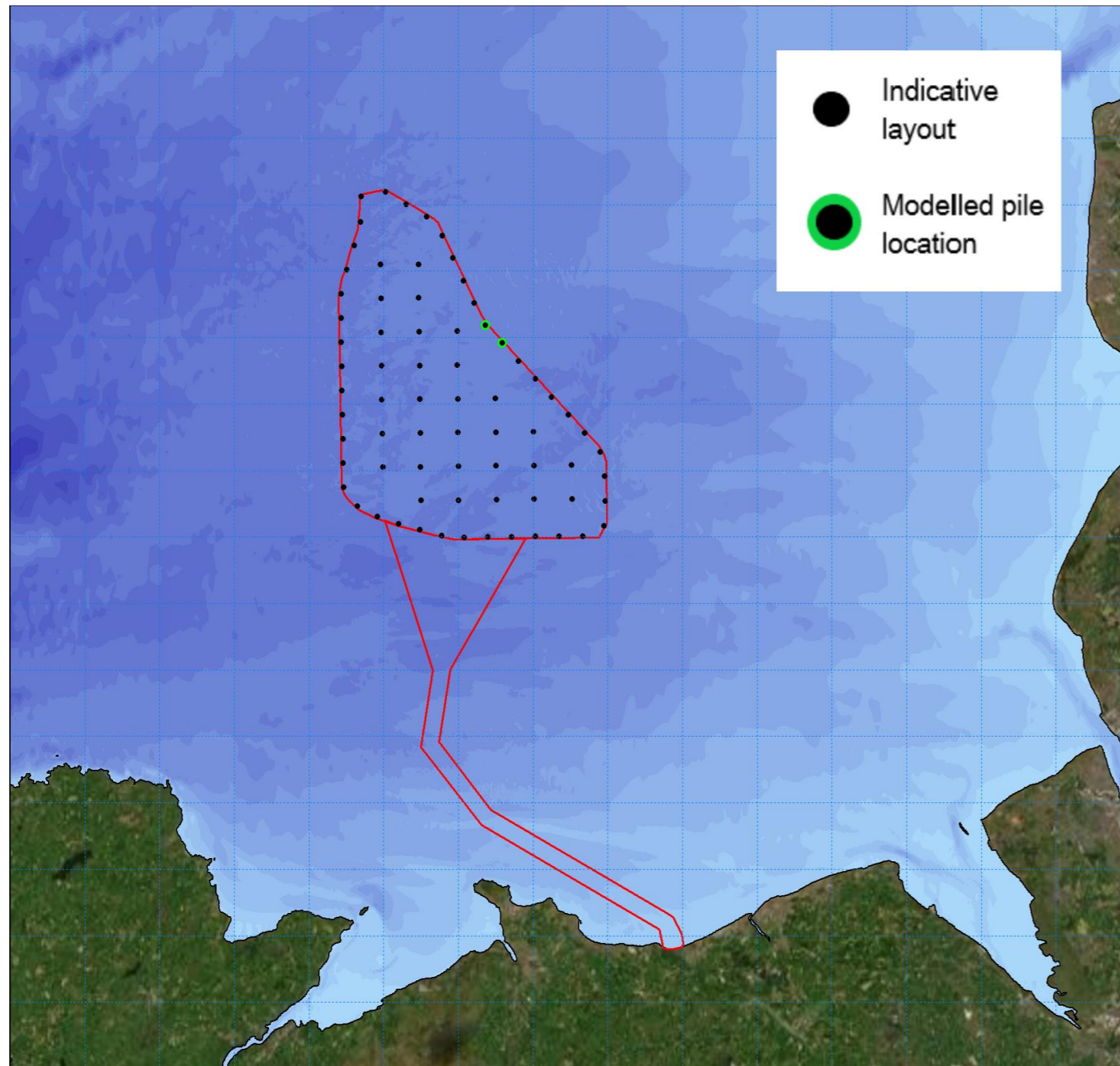


Figure 1.114: Location of modelled piled installation for piling - Scenario A.



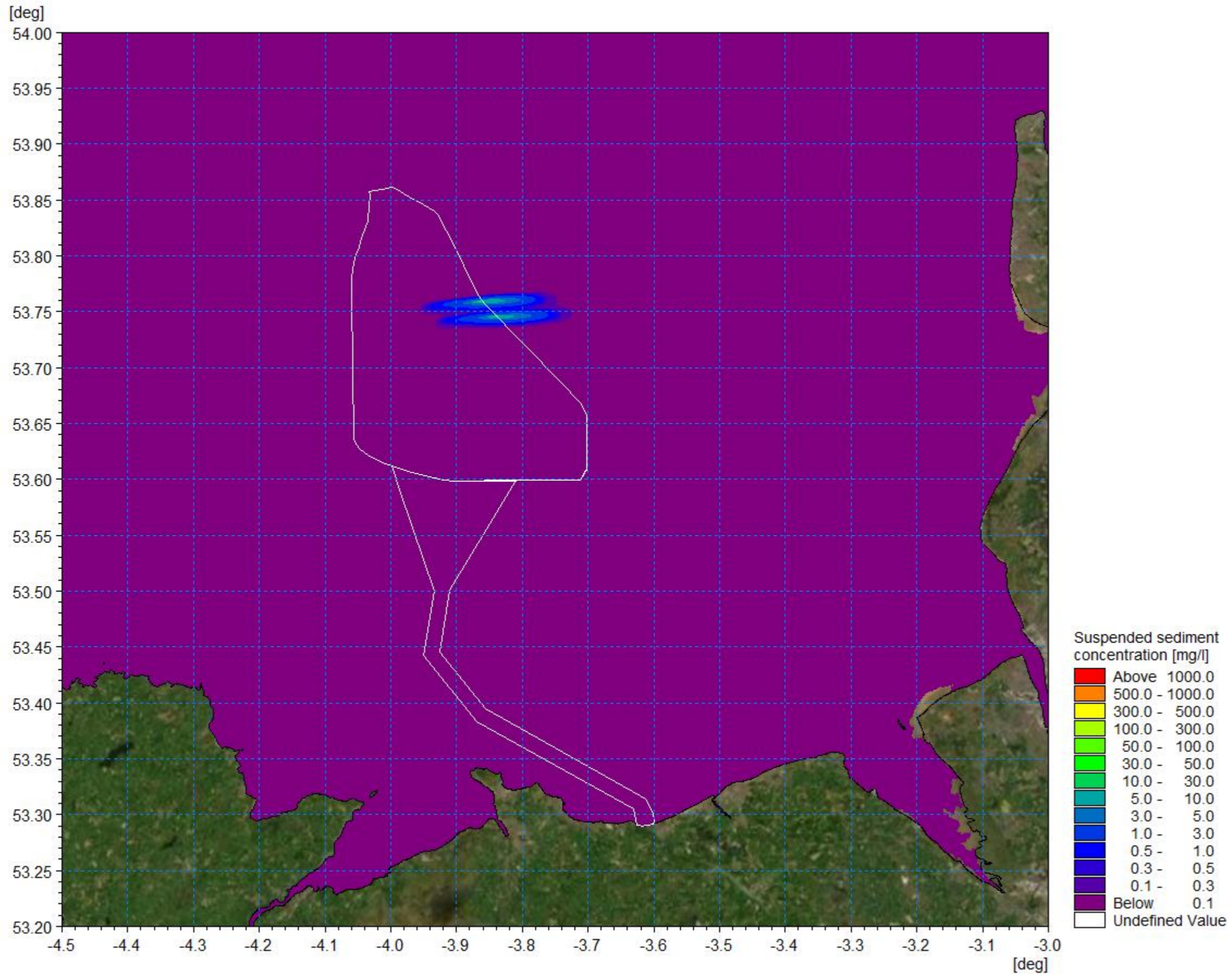


Figure 1.115: Average suspended sediment concentration – pile installation Scenario A.



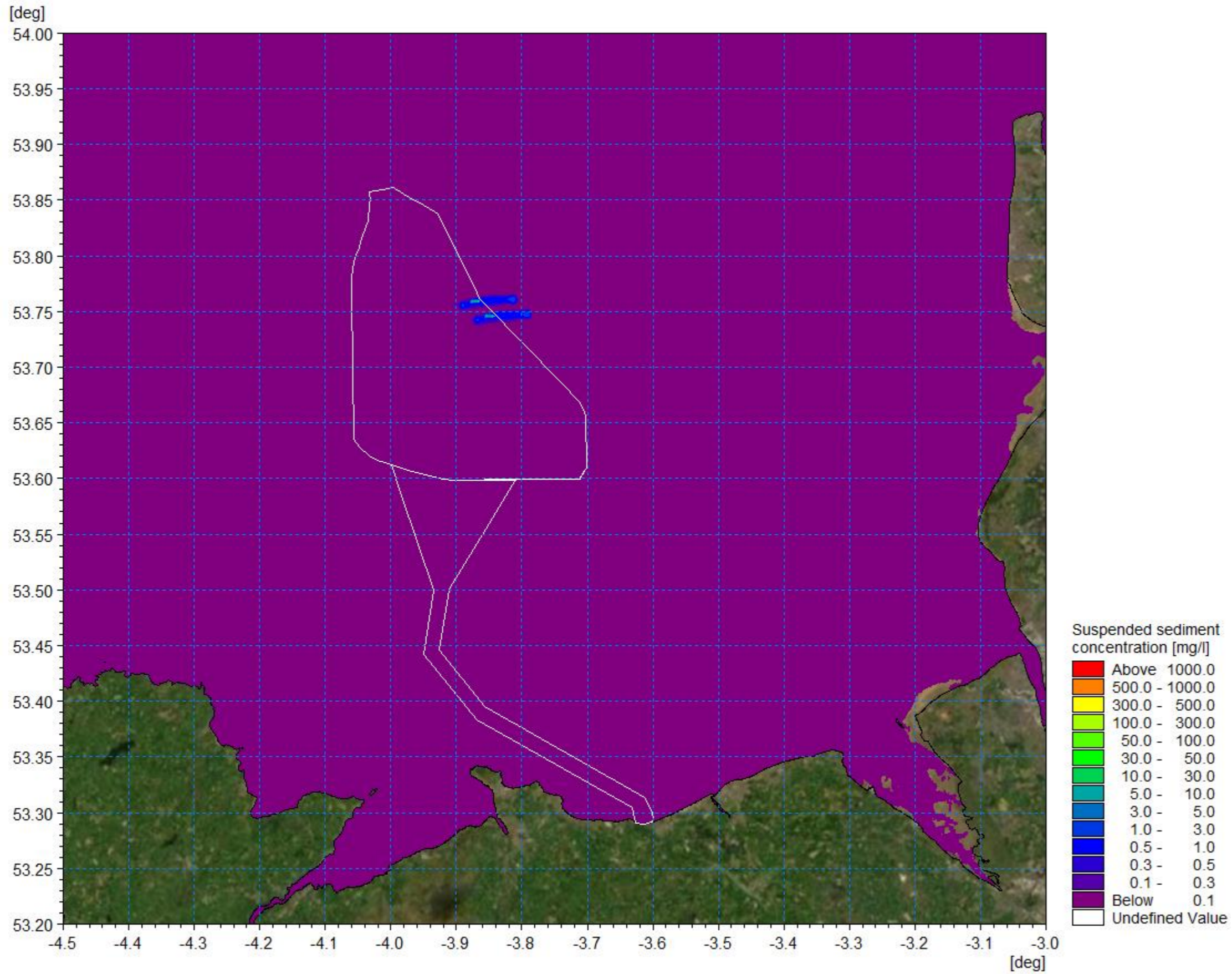


Figure 1.116: Suspended sediment concentration day 1 flood - pile installation Scenario A.



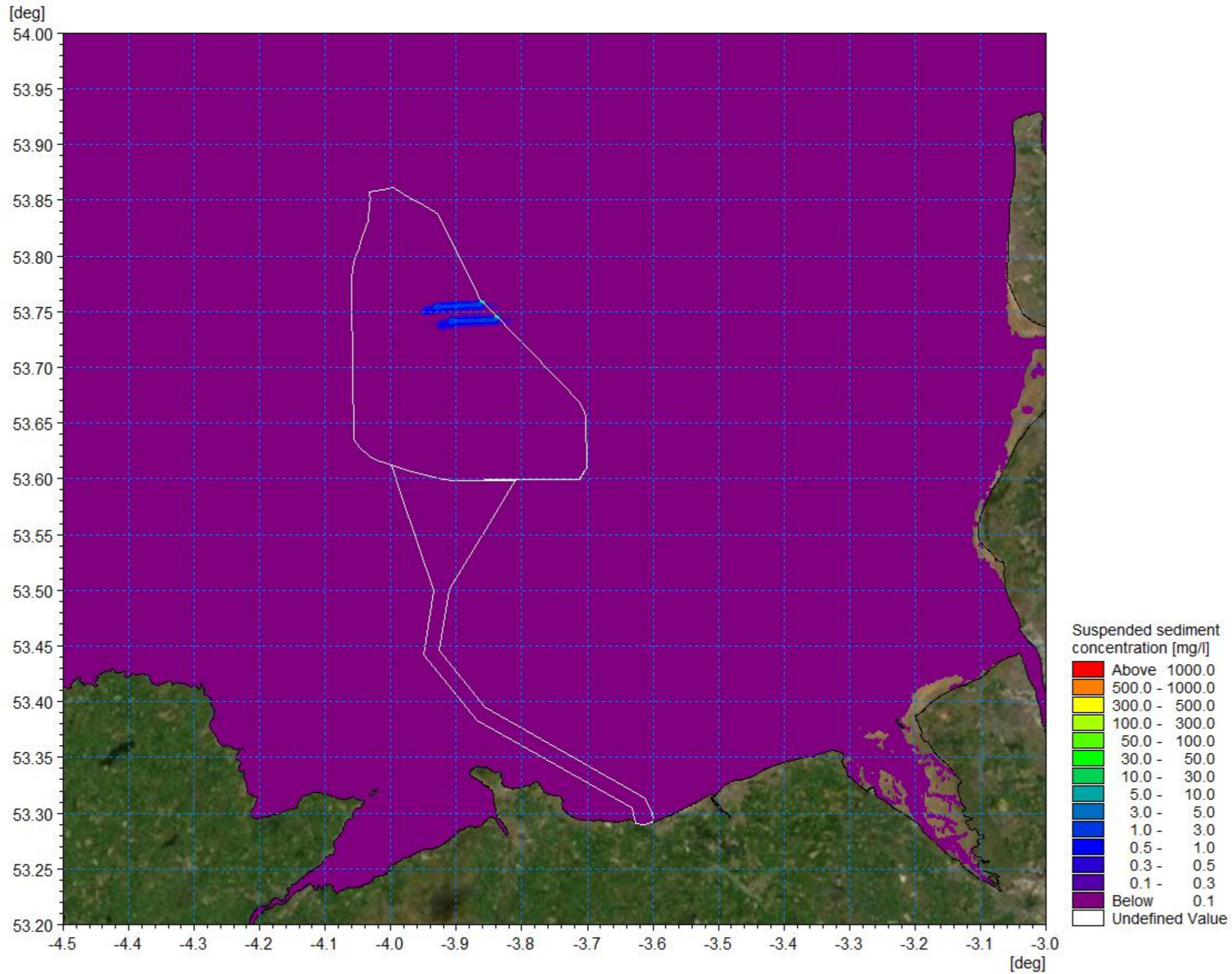


Figure 1.117: Suspended sediment concentration day 1 ebb - pile installation Scenario A.



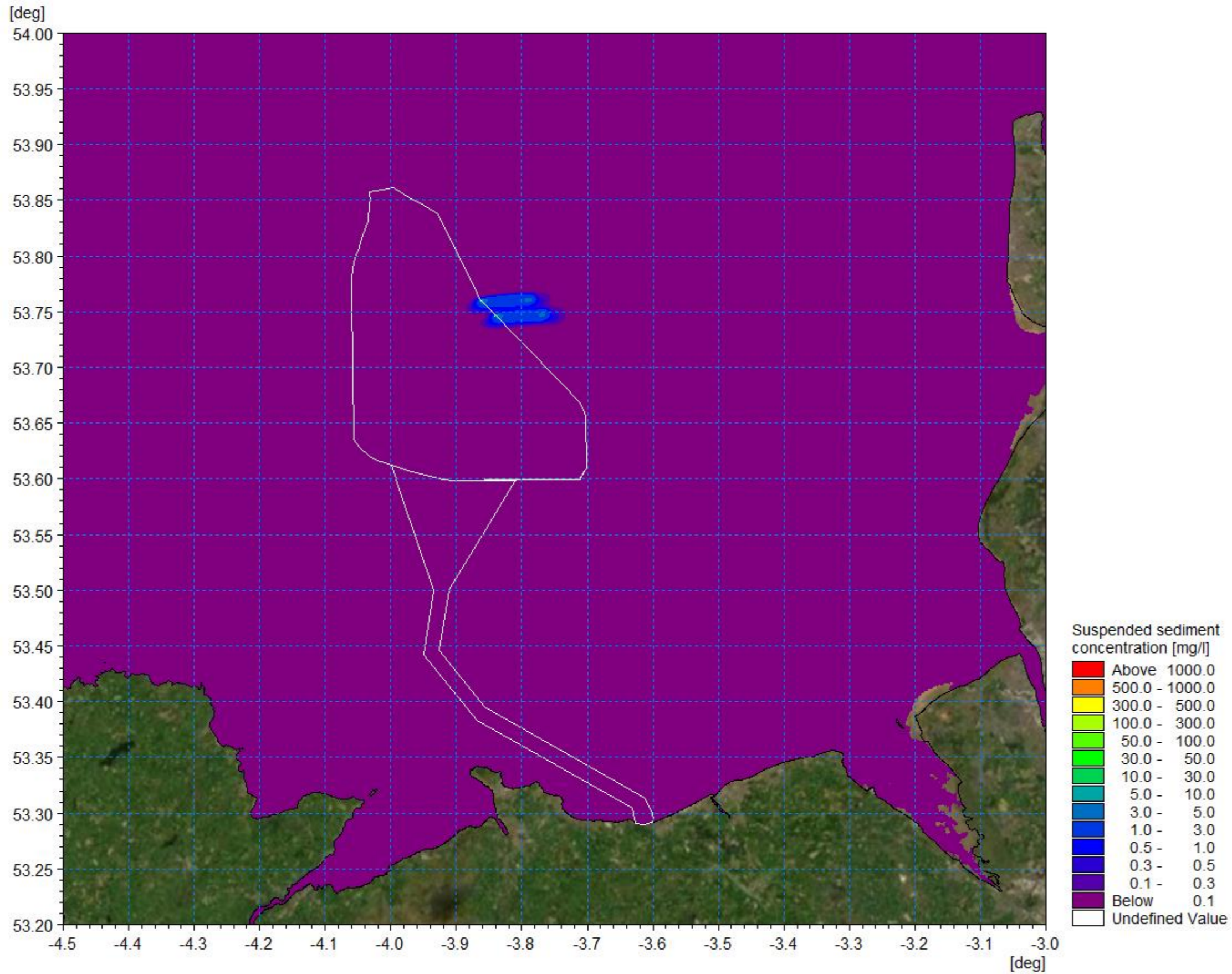


Figure 1.118: Suspended sediment concentration day 3 flood - pile installation Scenario A.



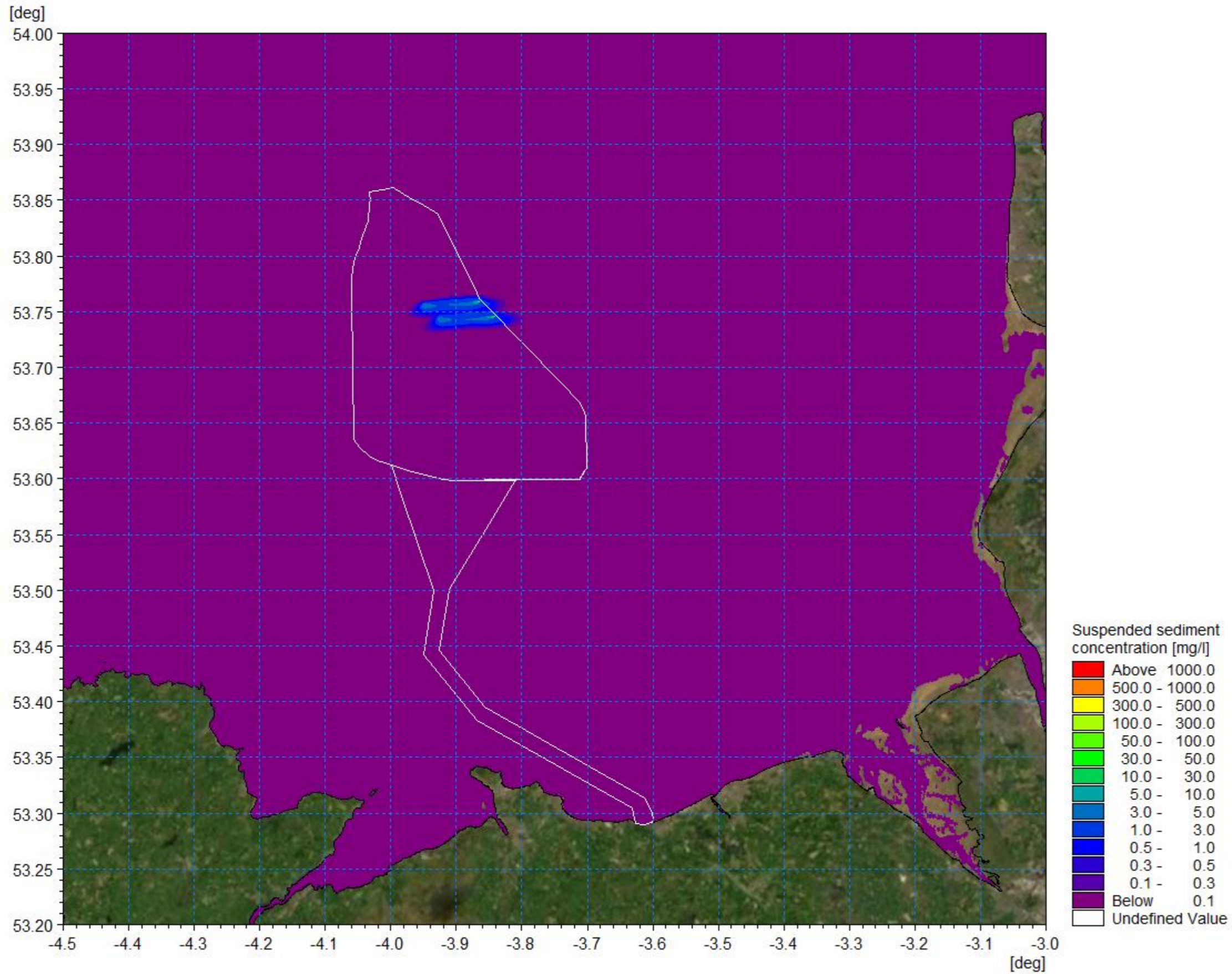


Figure 1.119: Suspended sediment concentration day 3 ebb- pile installation Scenario A.



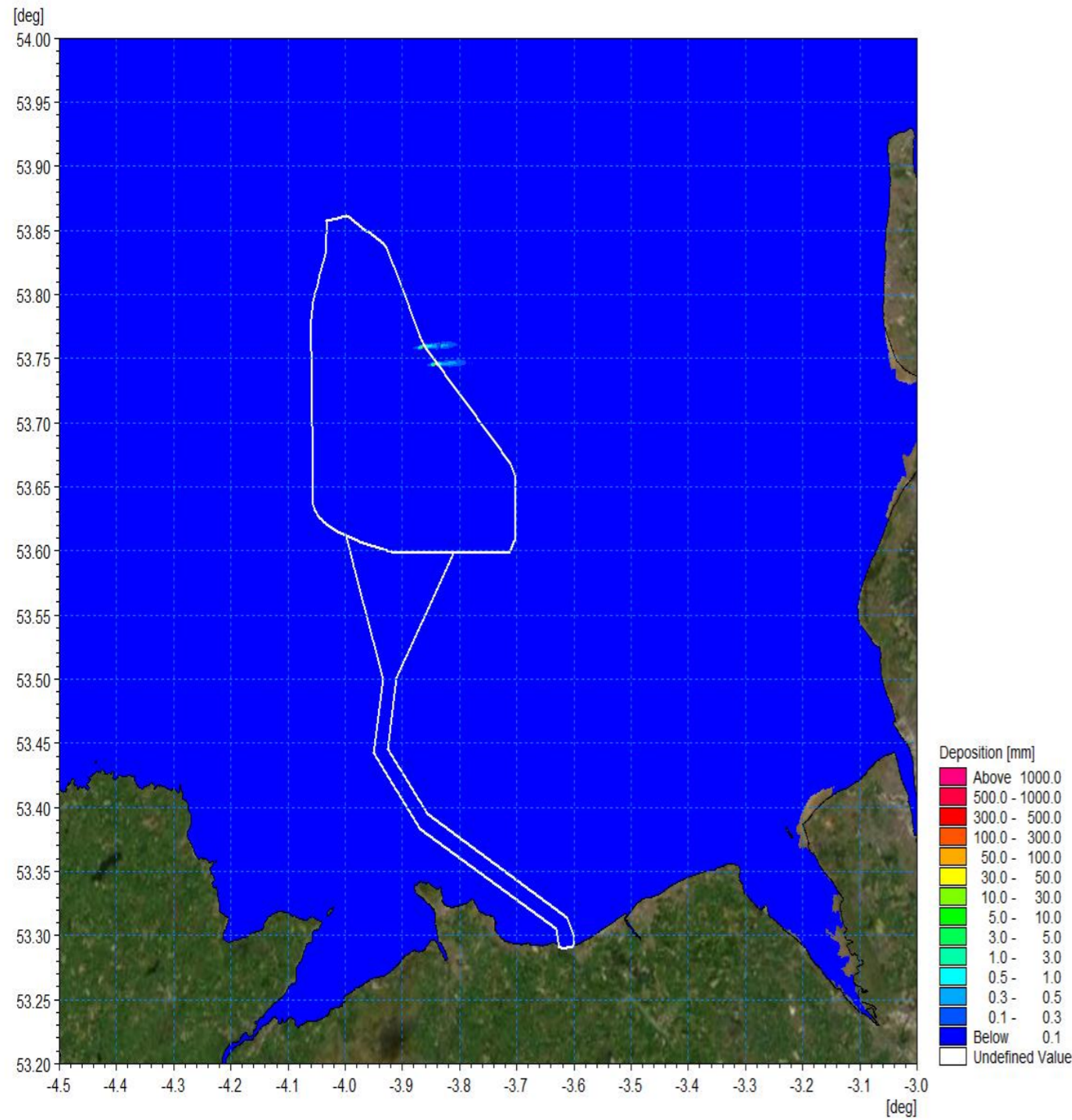


Figure 1.120: Average sedimentation during pile installation – Scenario A.

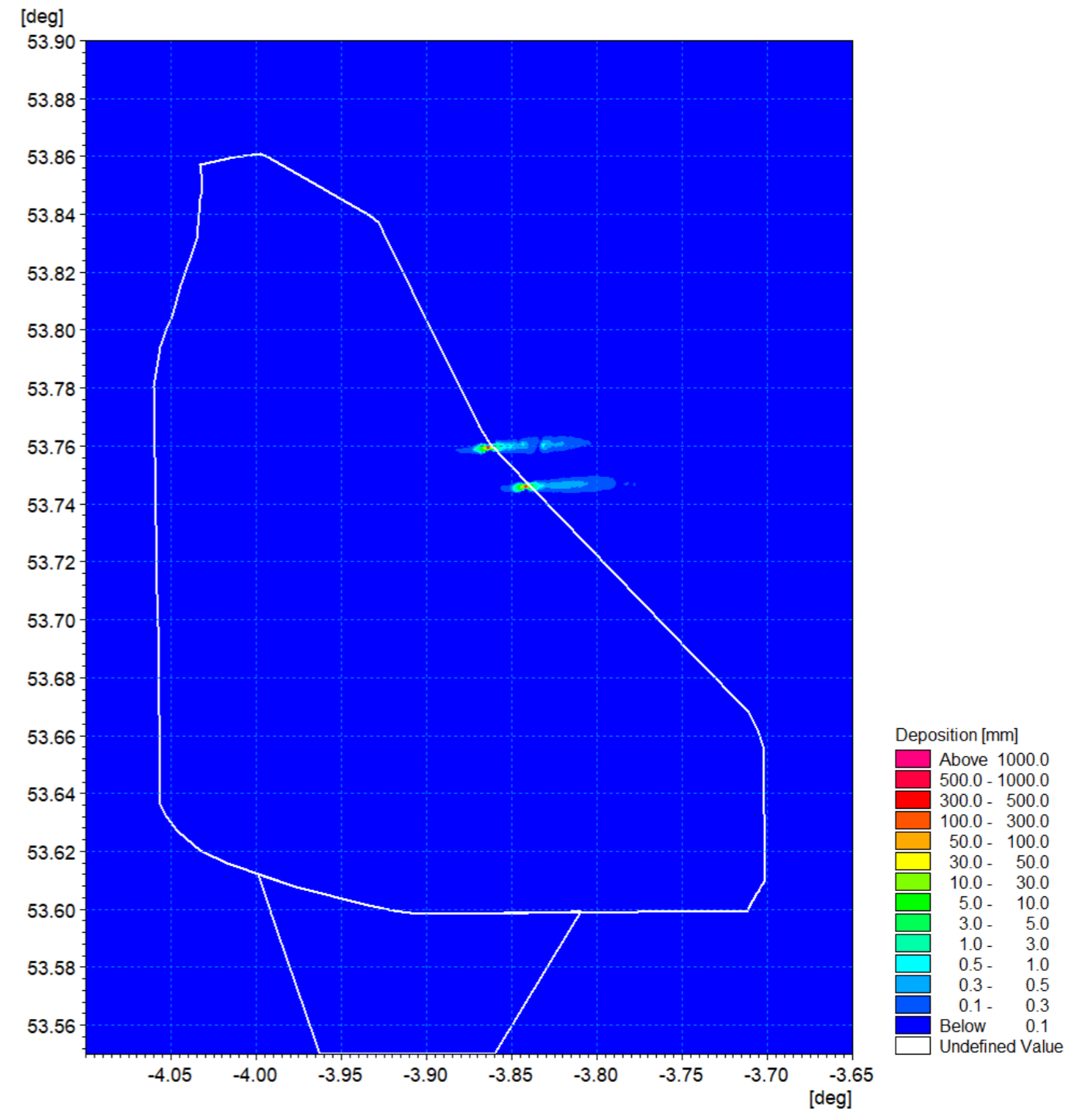


Figure 1.121: Average sedimentation during pile installation – Scenario A detail view.

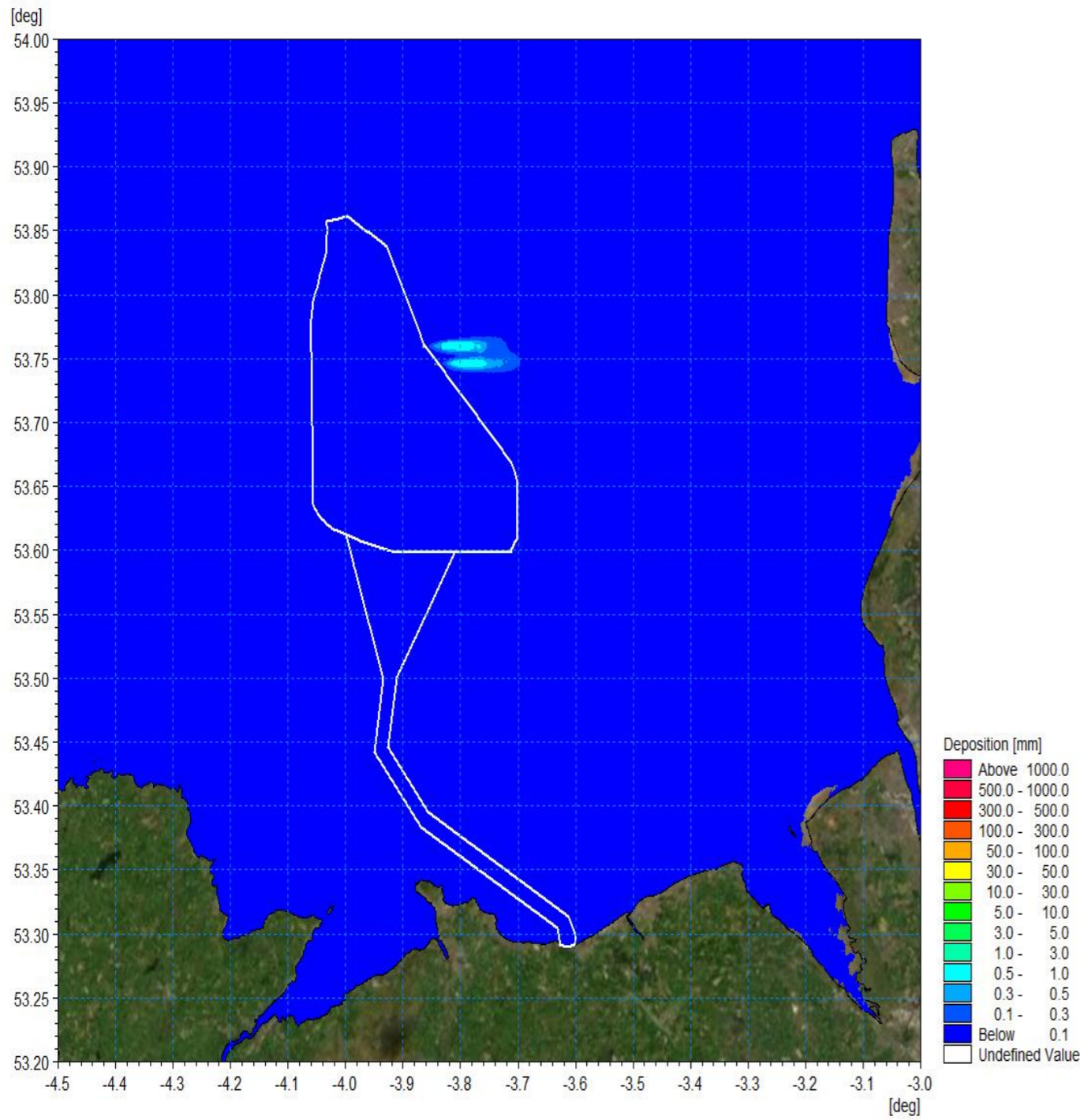


Figure 1.122: Sedimentation 1day following cessation of pile installation – Pile Scenario A.

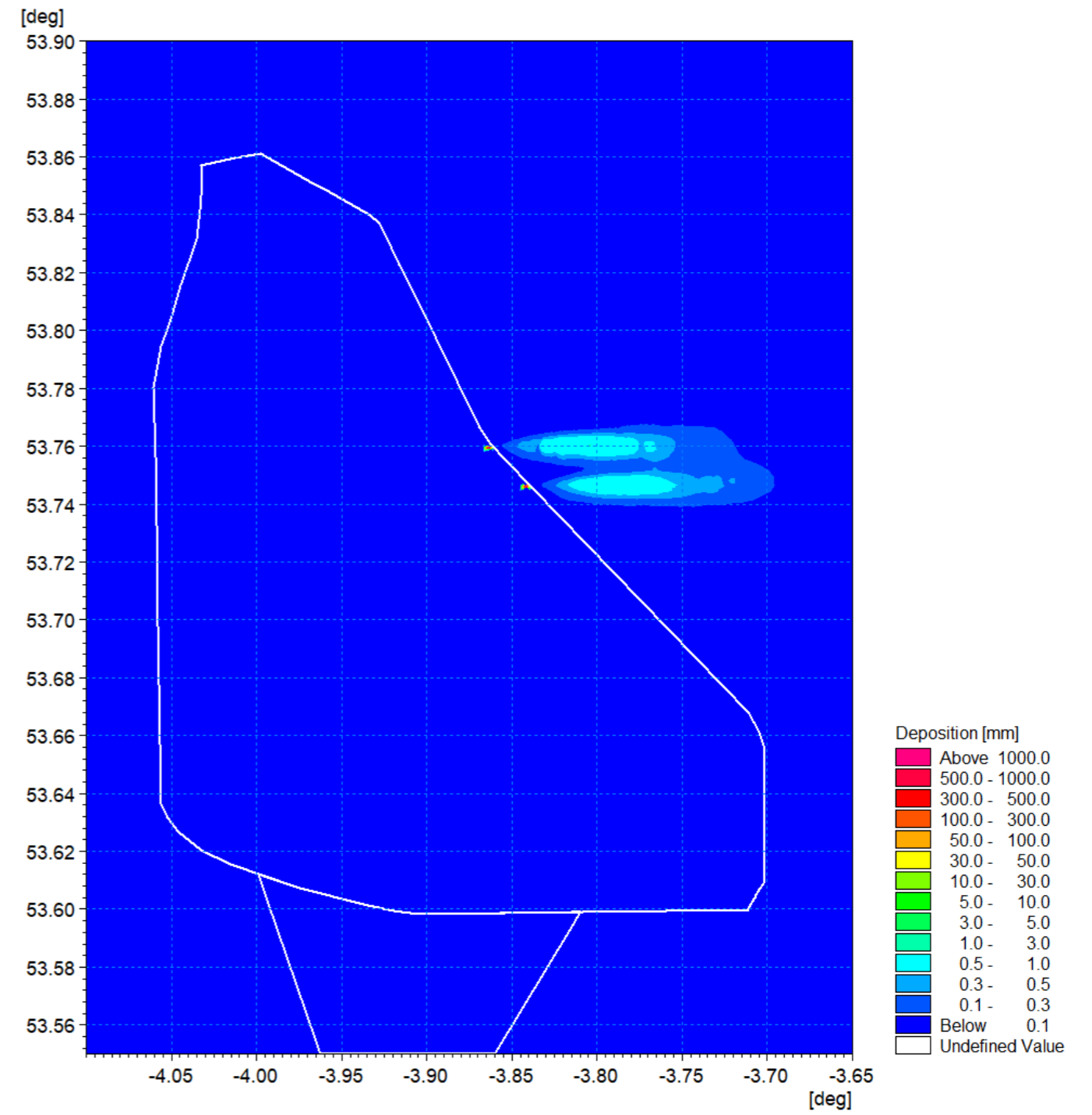


Figure 1.123: Sedimentation 1day following cessation of pile installation – Pile Scenario A detail view.



### Piling scenario B

- 1.8.3.11 The piling locations are sited to the east of the Mona array area as shown in Figure 1.124. The simulation was undertaken for successive spring tides and at this location finer sediment and sandwaves are present. The following composition was implemented within the modelling.
- Very coarse sand/gravel: 8%
  - Coarse sand: 23%
  - Medium sand: 48%
  - Fine sand: 10%
  - Very fine sand/mud: 11%.
- 1.8.3.12 The average suspended sediment plume envelope is shown in Figure 1.125. As anticipated the extent of the envelope is greater than that for the previous scenario as it was undertaken during spring tides when peak currents are typically double that of neap tides. It may be expected that the subsequent concentrations would be lower as the water depths are similar at the two locations however the stronger currents and finer material means that a greater proportion of the material is in suspension. The instantaneous figures for day one and three, ebb and flood tides are presented in Figure 1.126 to Figure 1.129, where peak concentrations are circa 50mg/l and average values are typically less than one fifth of this magnitude. At this location the transport cycle is also evident with material settling out on slack tides and becoming re-suspended with increasing current speeds.
- 1.8.3.13 The highly dispersive nature of spring tidal currents coupled with the finer material located at this site is evident in the sedimentation plots. The average sedimentation shown in Figure 1.130 and Figure 1.131 indicates this transport cycle with the material being dispersed to the east further following the end of the operation as illustrated in Figure 1.132 and Figure 1.133. The resulting sedimentation depths are typically <math><0.1\text{mm}</math> from the two drilling operations and demonstrates that this settlement would be imperceptible from the background sediment transport activity.

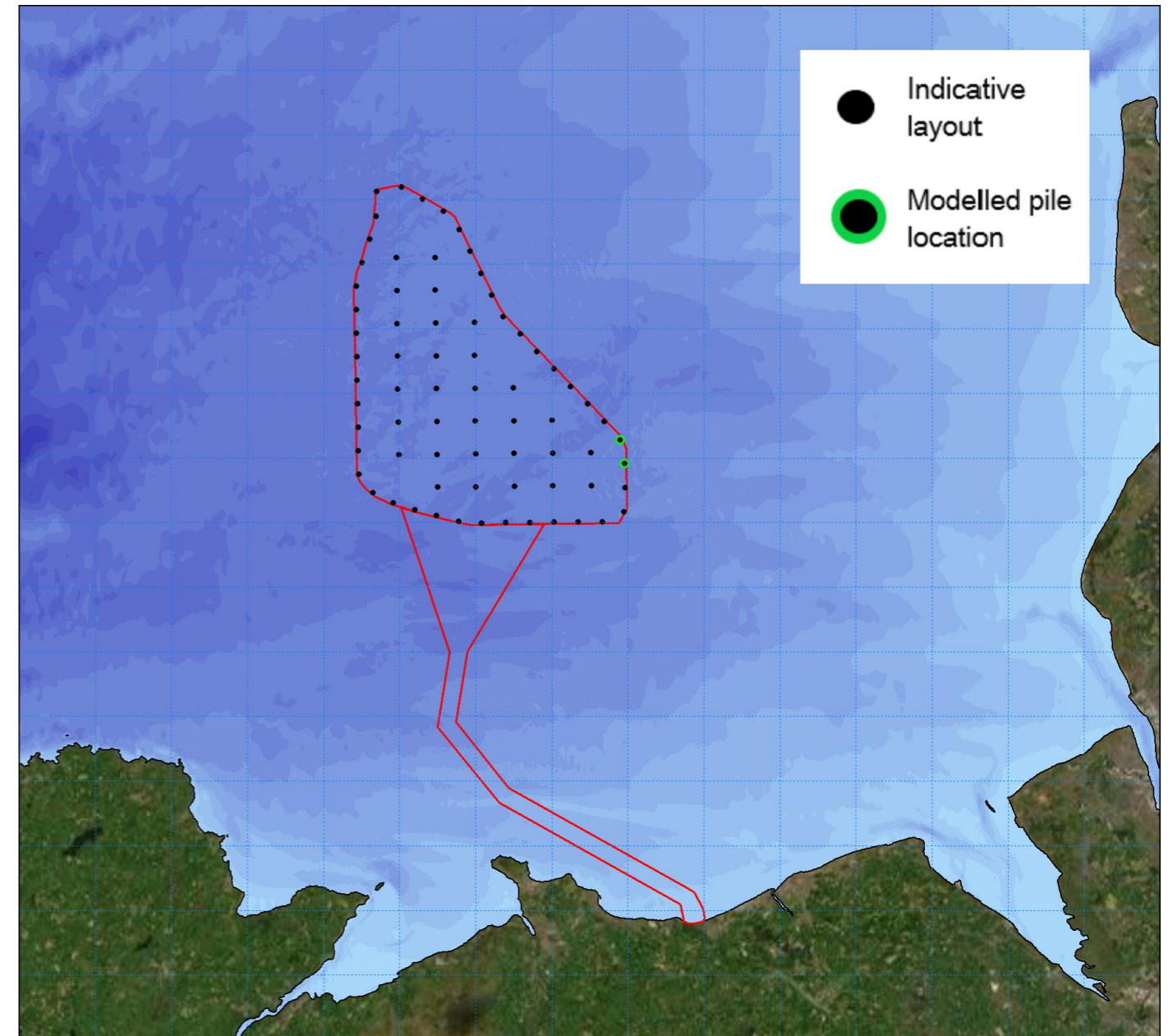


Figure 1.124: Location of modelled piled installation for piling Scenario B.



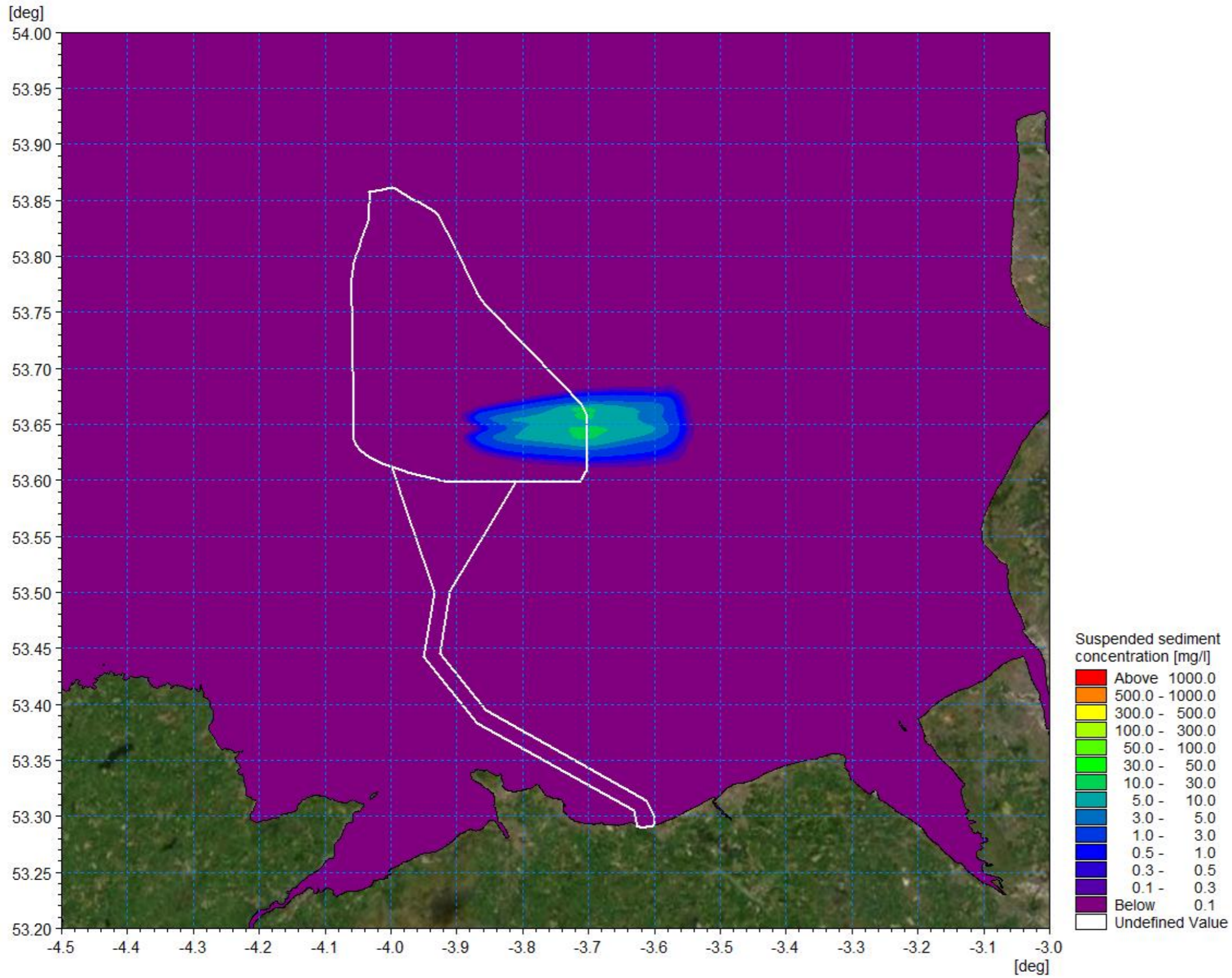


Figure 1.125: Average suspended sediment concentration – pile installation Scenario B.



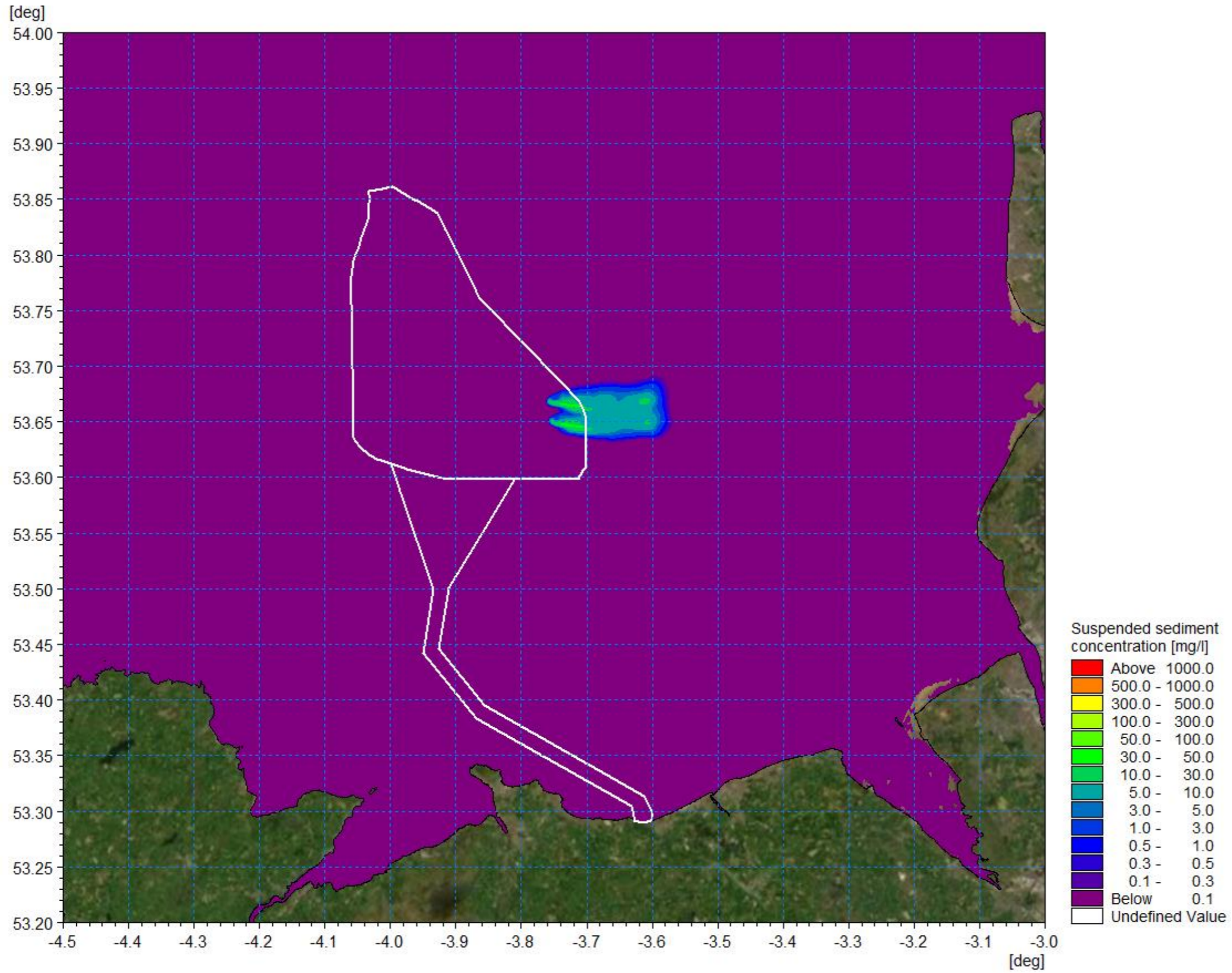


Figure 1.126: Suspended sediment concentration day 1 flood- pile installation Scenario B.



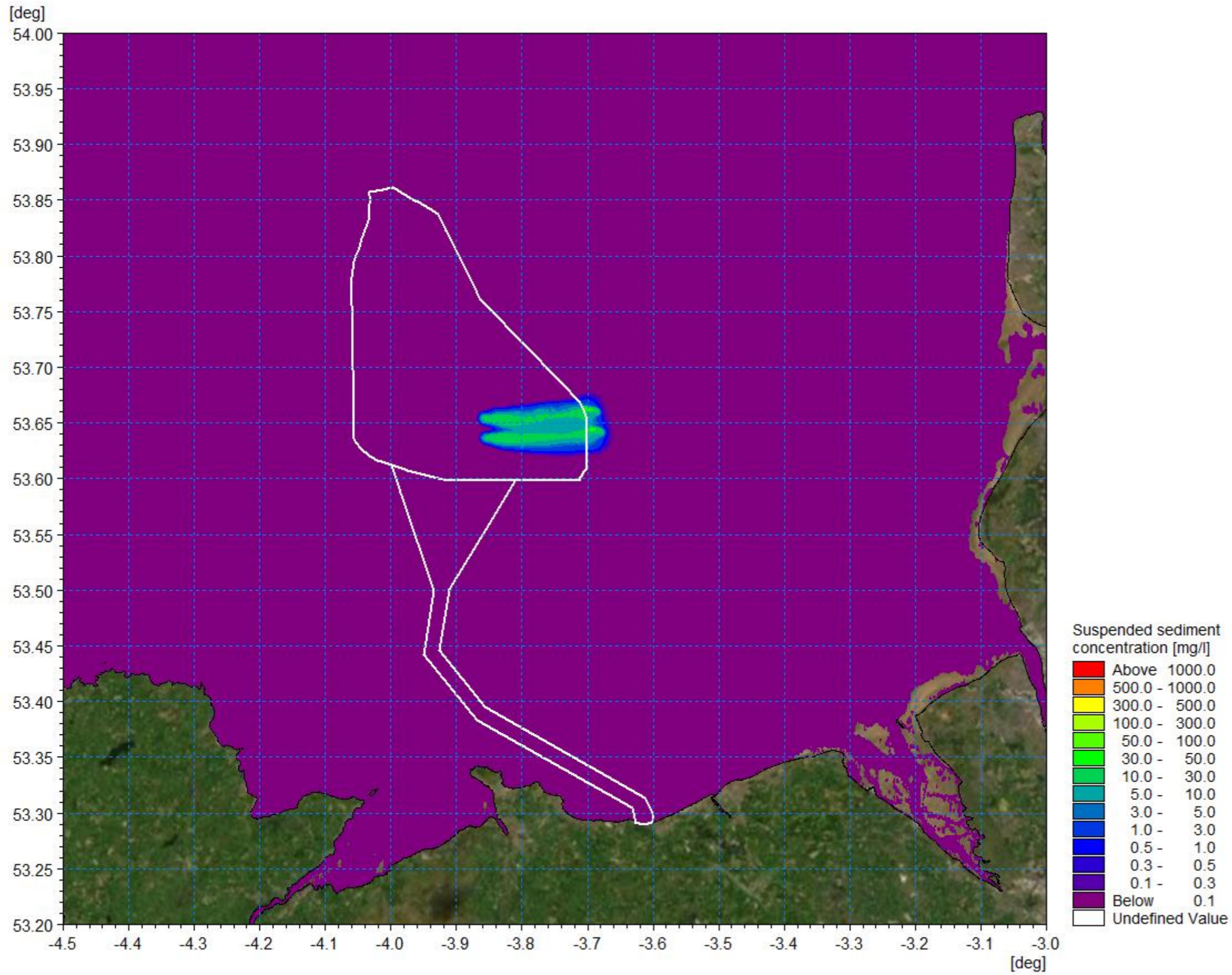


Figure 1.127: Suspended sediment concentration day 1 ebb- pile installation Scenario B.



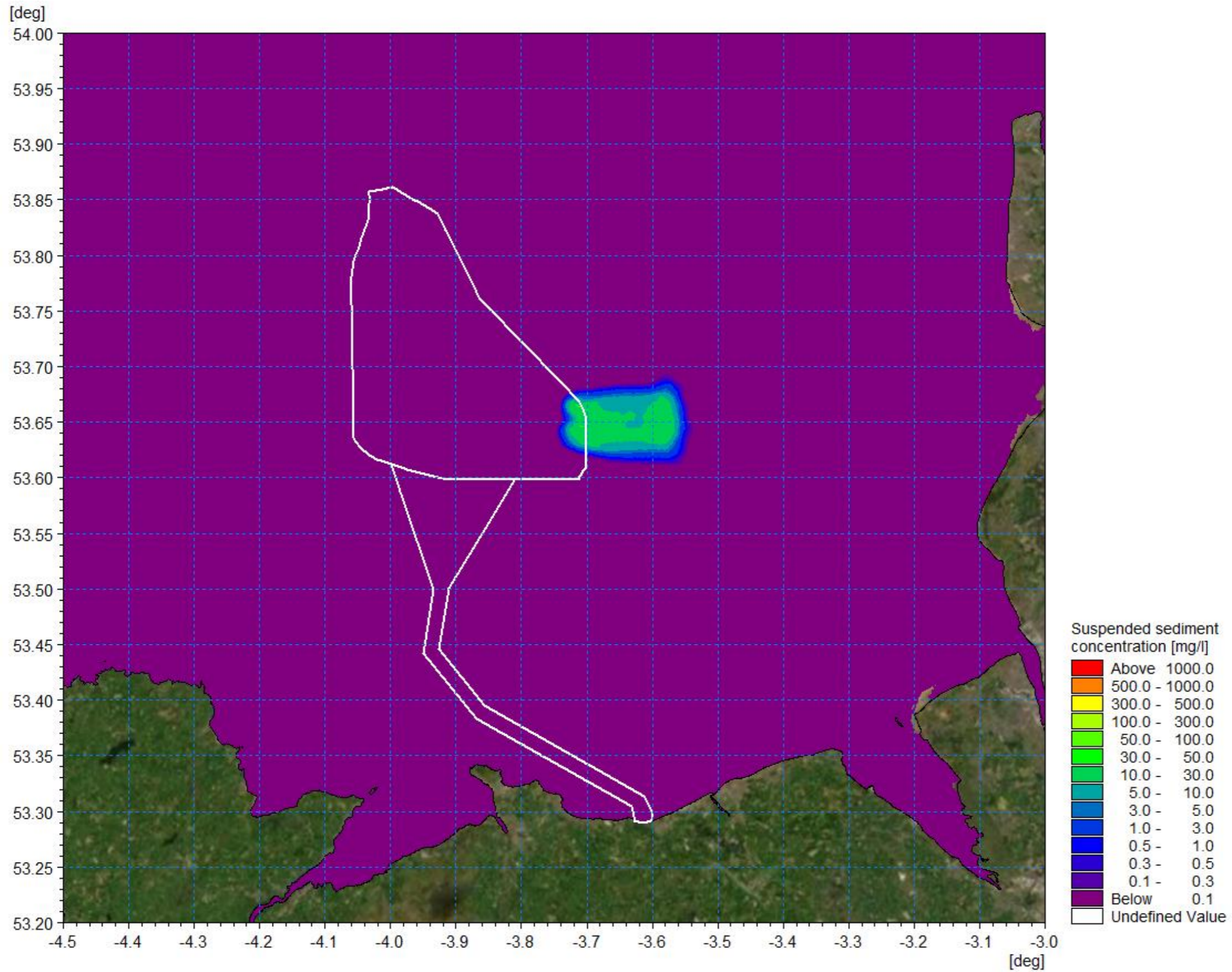


Figure 1.128: Suspended sediment concentration day 3 flood- pile installation Scenario B.



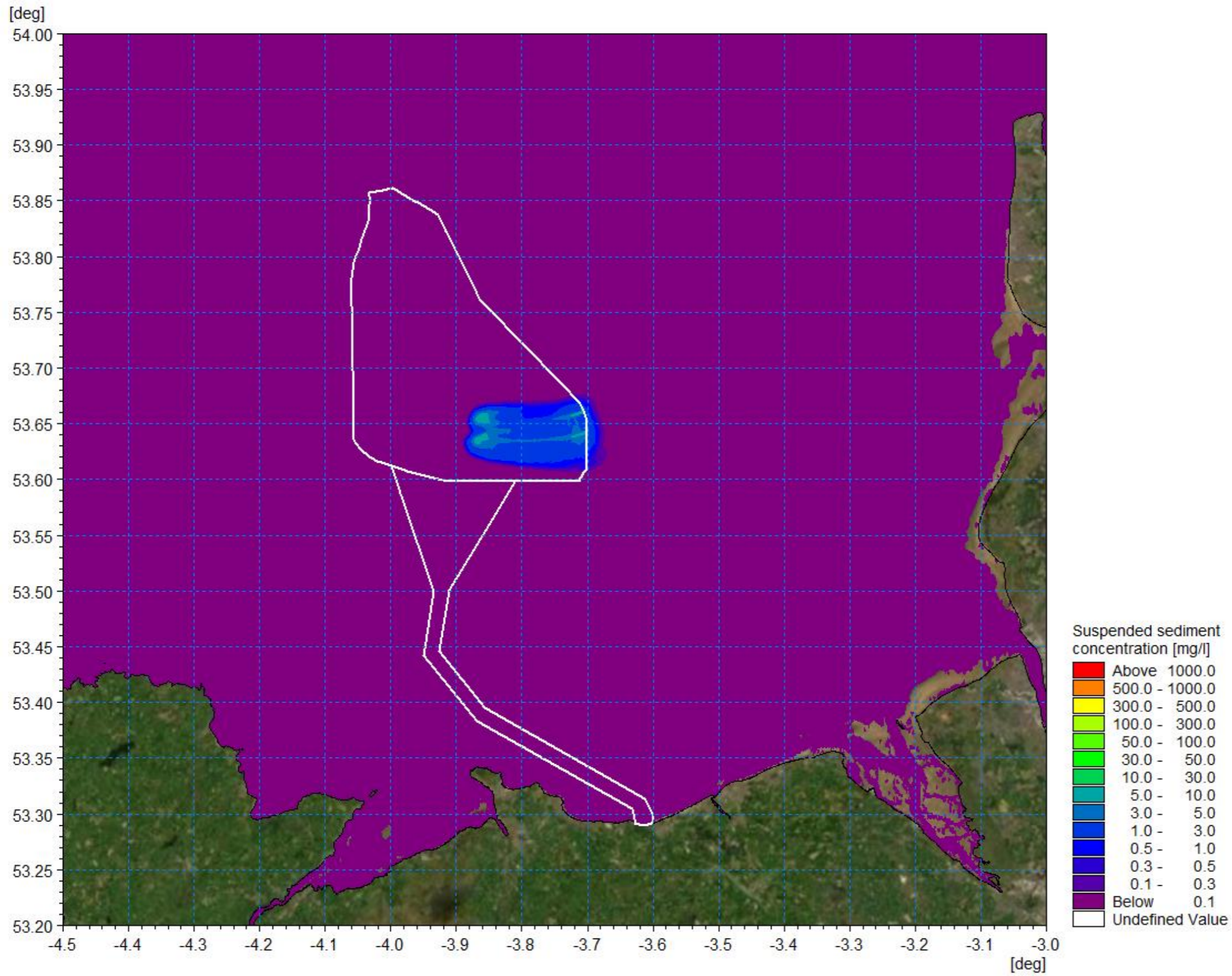


Figure 1.129: Suspended sediment concentration day 3 ebb- pile installation Scenario B.



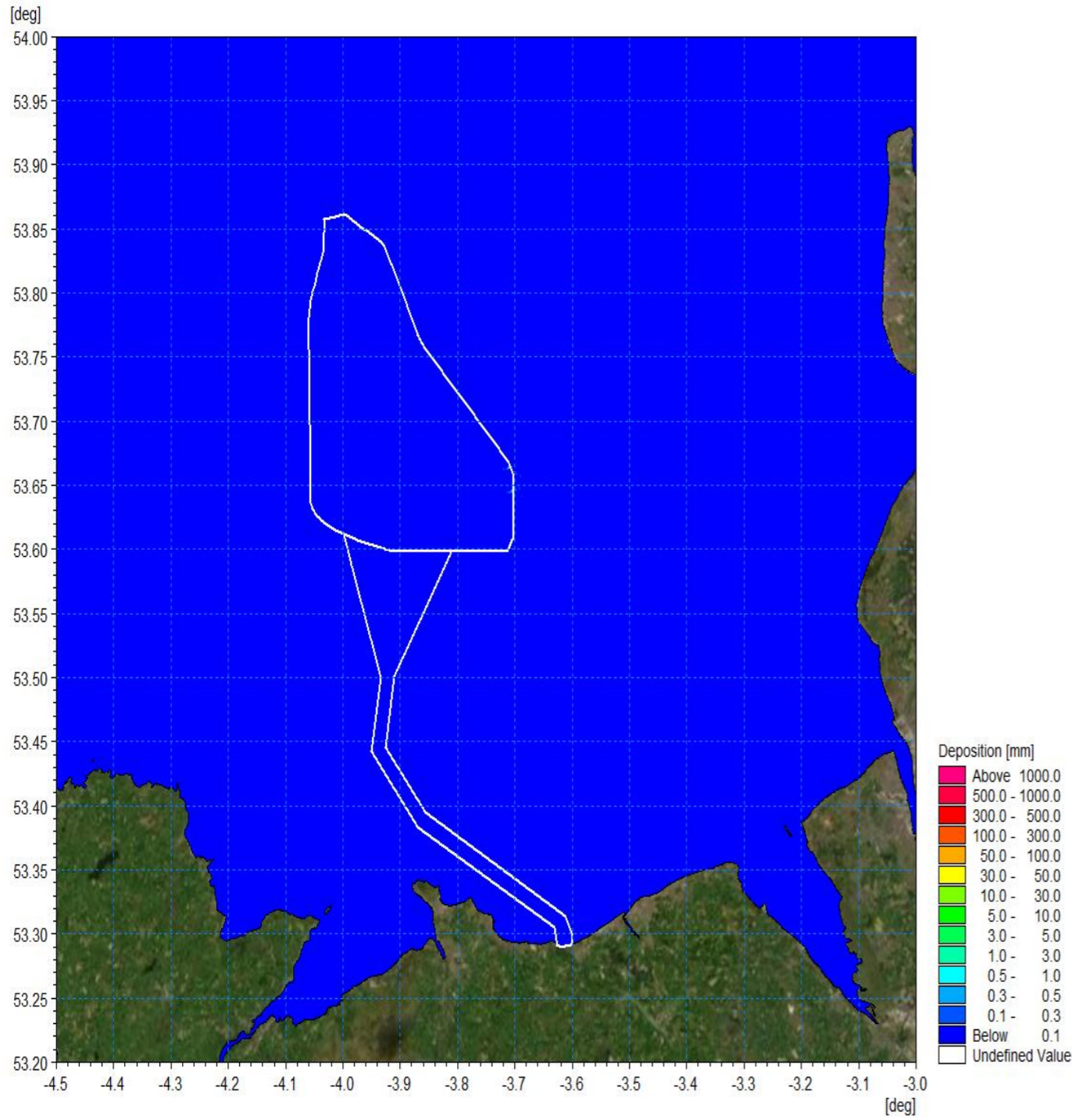


Figure 1.130: Average sedimentation during pile installation – Scenario B.

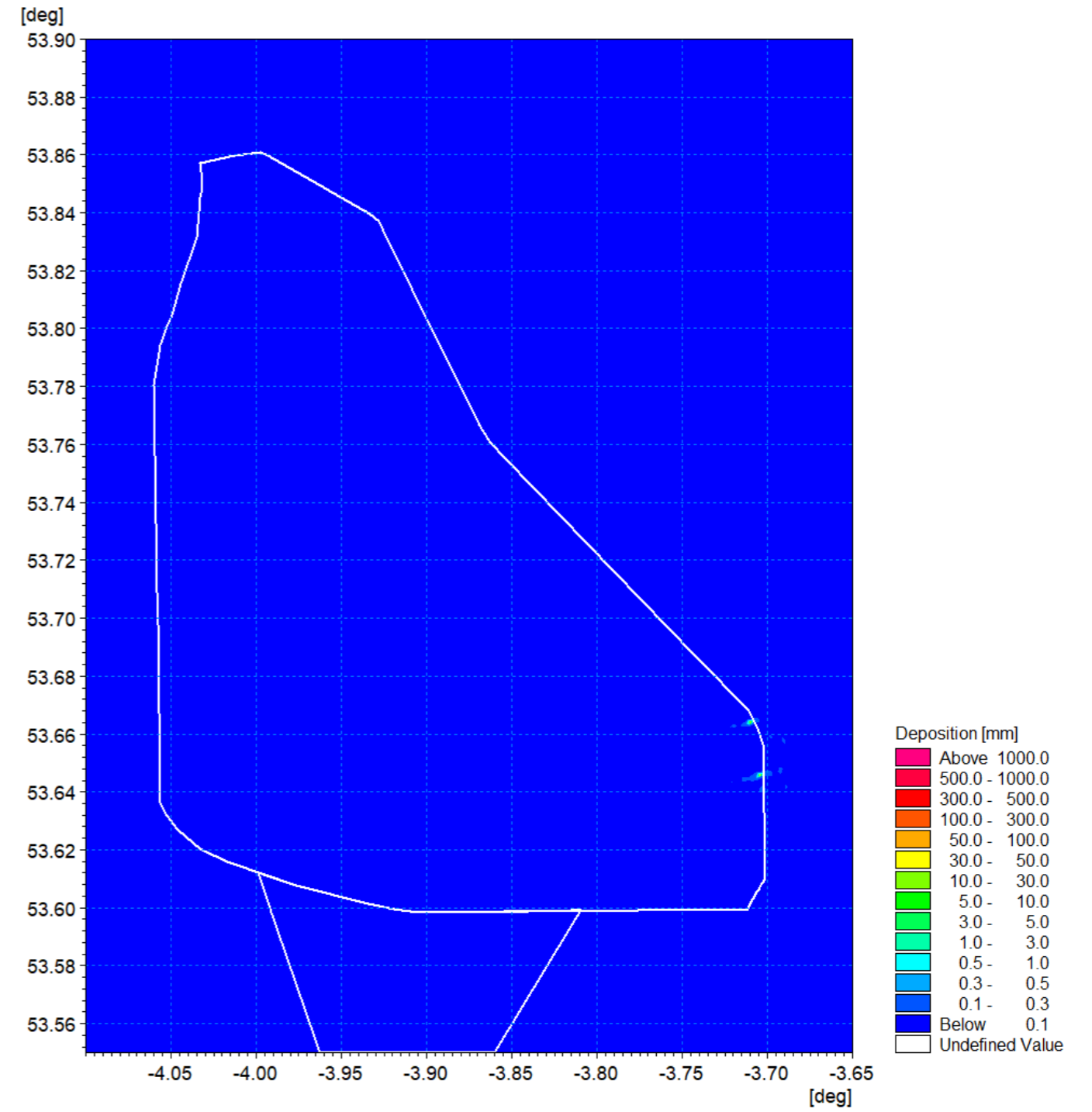


Figure 1.131: Average sedimentation during pile installation – Scenario B detail view.

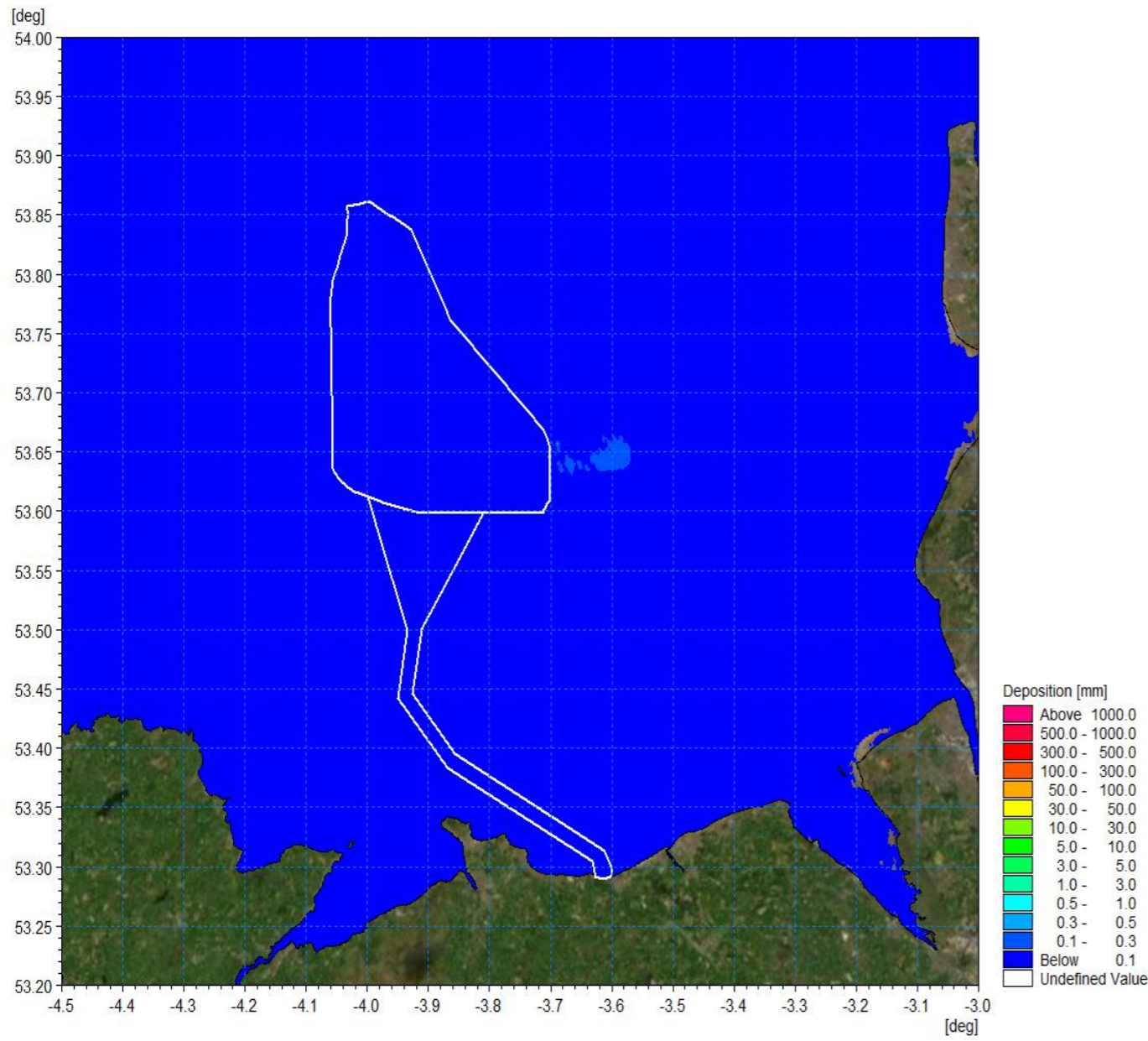


Figure 1.132: Sedimentation 1day following cessation of pile installation – Pile Scenario B.

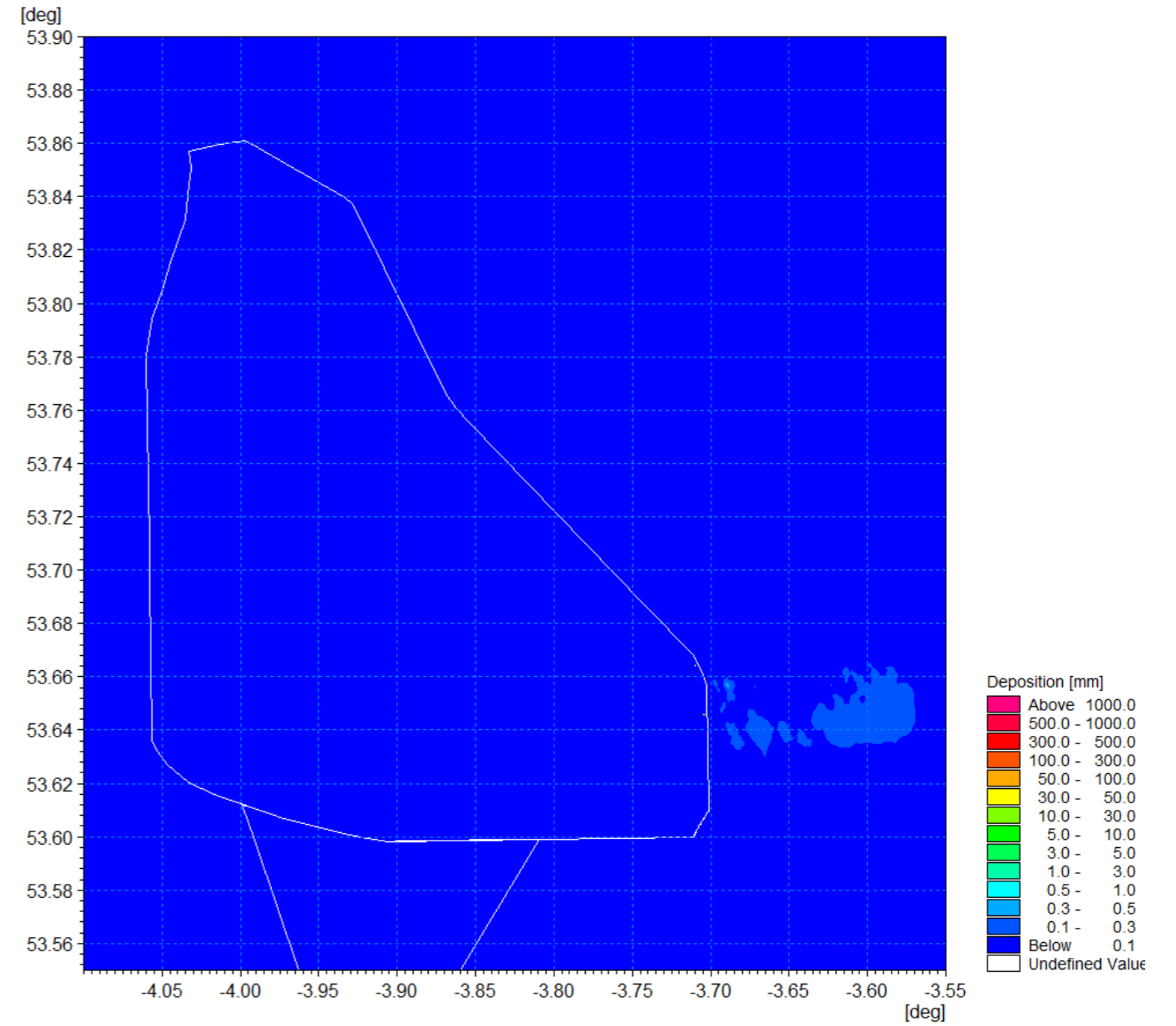


Figure 1.133: Sedimentation 1day following cessation of pile Installation – Pile Scenario B detail view.



### Piling scenario C

- 1.8.3.14 The piling locations are illustrated in Figure 1.134 and they are orientated normal to the tidal current to provide an augmented plume scenario under mean tidal currents. The sediment composition at this location comprised mixed sediments similar to those at scenario A as follows.
- Very coarse sand/gravel: 19%
  - Coarse sand: 22%
  - Medium sand: 46%
  - Fine sand: 9%
  - Very fine sand/mud: 4%.
- 1.8.3.15 The average plume envelope shown in Figure 1.135 has a similar extent to the circa 25km shown in the spring tide scenario B; this is accounted for by the average tidal range coupled with the orientation of the releases. Average concentrations of circa 50mg/l are evident where the plumes coalesce. This is similar to the unmerged values as the plumes are travelling in concert with the tide (and not towards one another) and at the point that the plume reaches the adjacent discharge it is highly dispersed.
- 1.8.3.16 The suspended sediments for peak flood and ebb tides on the first day are shown in Figure 1.136 and Figure 1.137 respectively. At the centre of the plume envelope peak values are circa 50mg/l. The plots for day three tides (Figure 1.138 and Figure 1.139) have been selected to illustrate the settlement and mobilisation patterns. With decreased current speed, sediment concentrations reduce as material settles and, as current speed increase through the tidal cycle, settled material is mobilised and concentration increase once again. Under these circumstances peak concentrations are <30mg/l and average values are typically one tenth of this value, with the peaks centred on areas of remobilised material.
- 1.8.3.17 The accumulated deposition from the two operations is evident in the sedimentation plots Figure 1.140 to Figure 1.143. As with scenario A, the coarser material is retained at the site of the operation with a similar maximum depth of 300mm. However, the material carried to the east on the residual current is circa twice the depth at 3mm. Once again, the formulation of sand ripples is evident. As noted previously, this is native material from the sediment cells and would be entrained into the baseline sediment transport patterns.

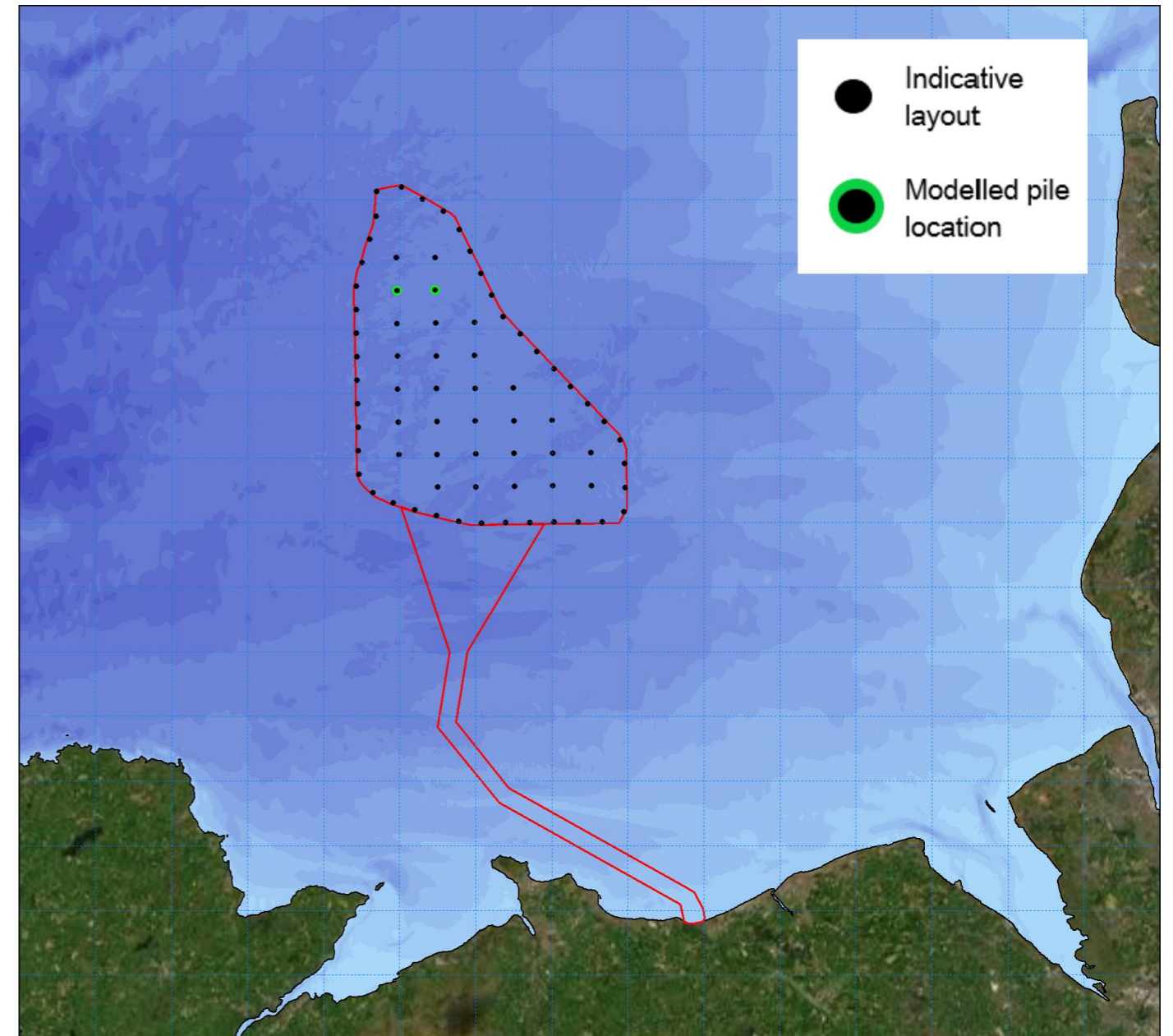


Figure 1.134: Location of modelled piled installation for Piling Scenario C.



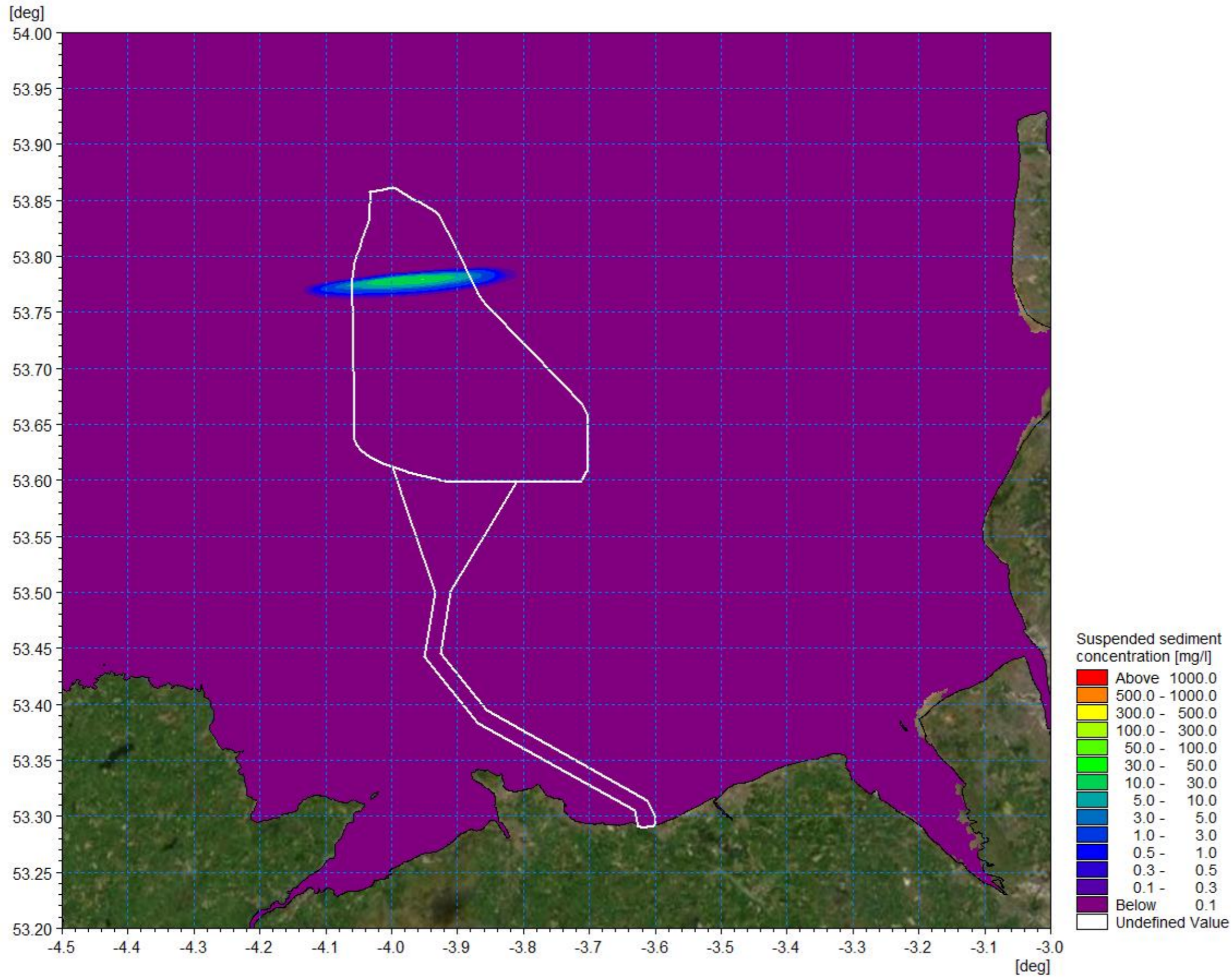


Figure 1.135: Average suspended sediment concentration – pile installation Scenario C.



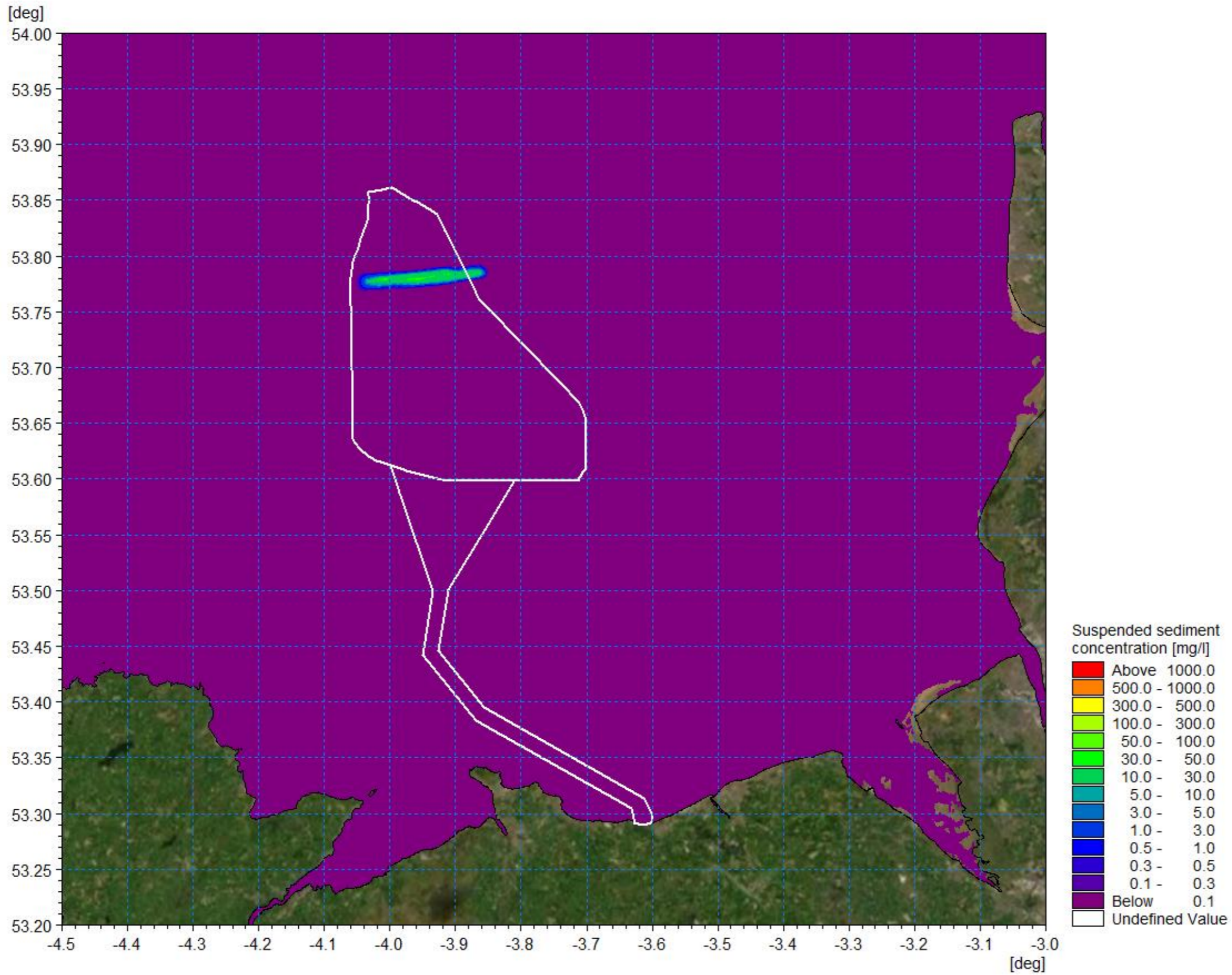


Figure 1.136: Suspended sediment concentration day 1 flood- Pile Installation Scenario C.



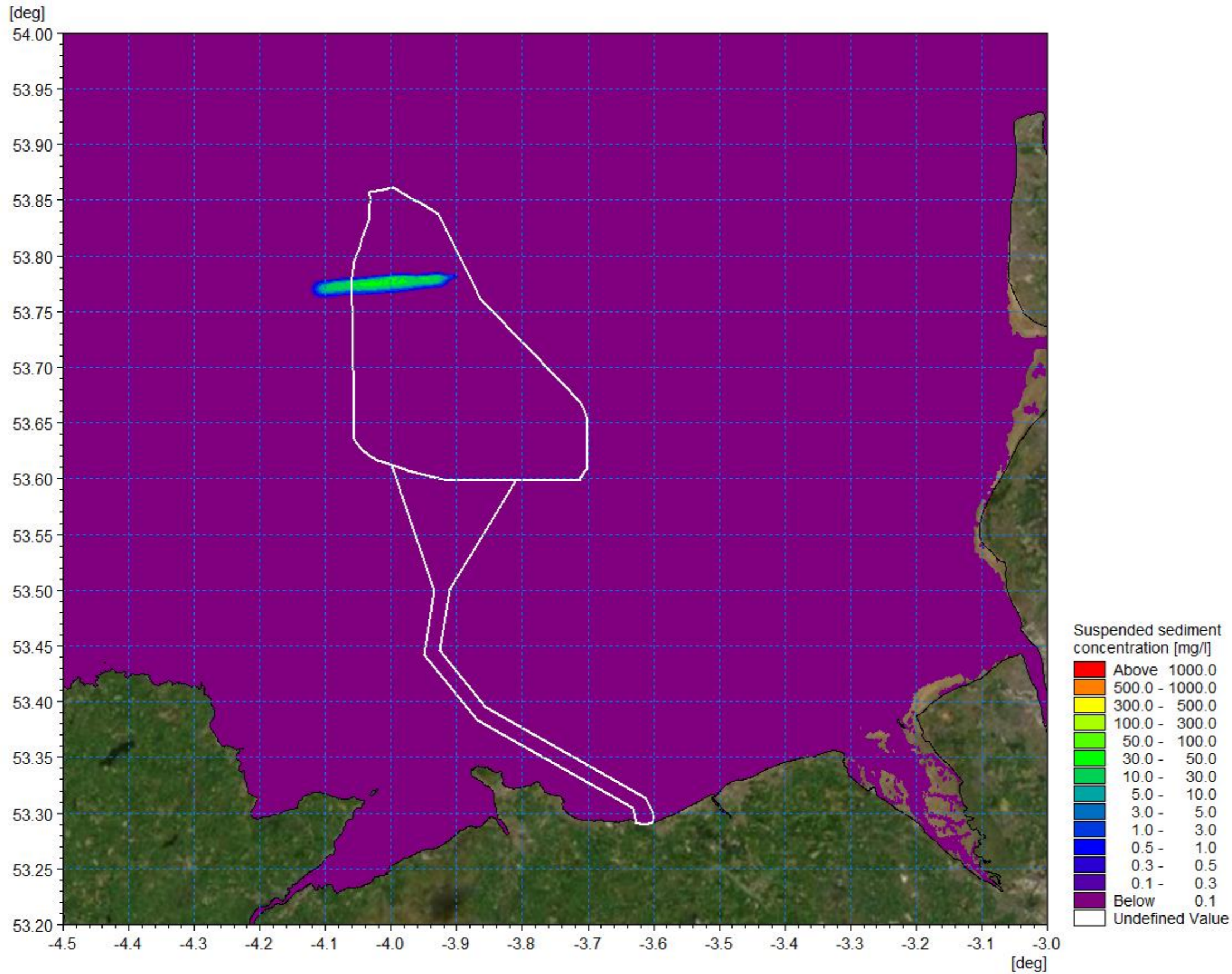


Figure 1.137: Suspended sediment concentration day 1 ebb- pile installation Scenario C.



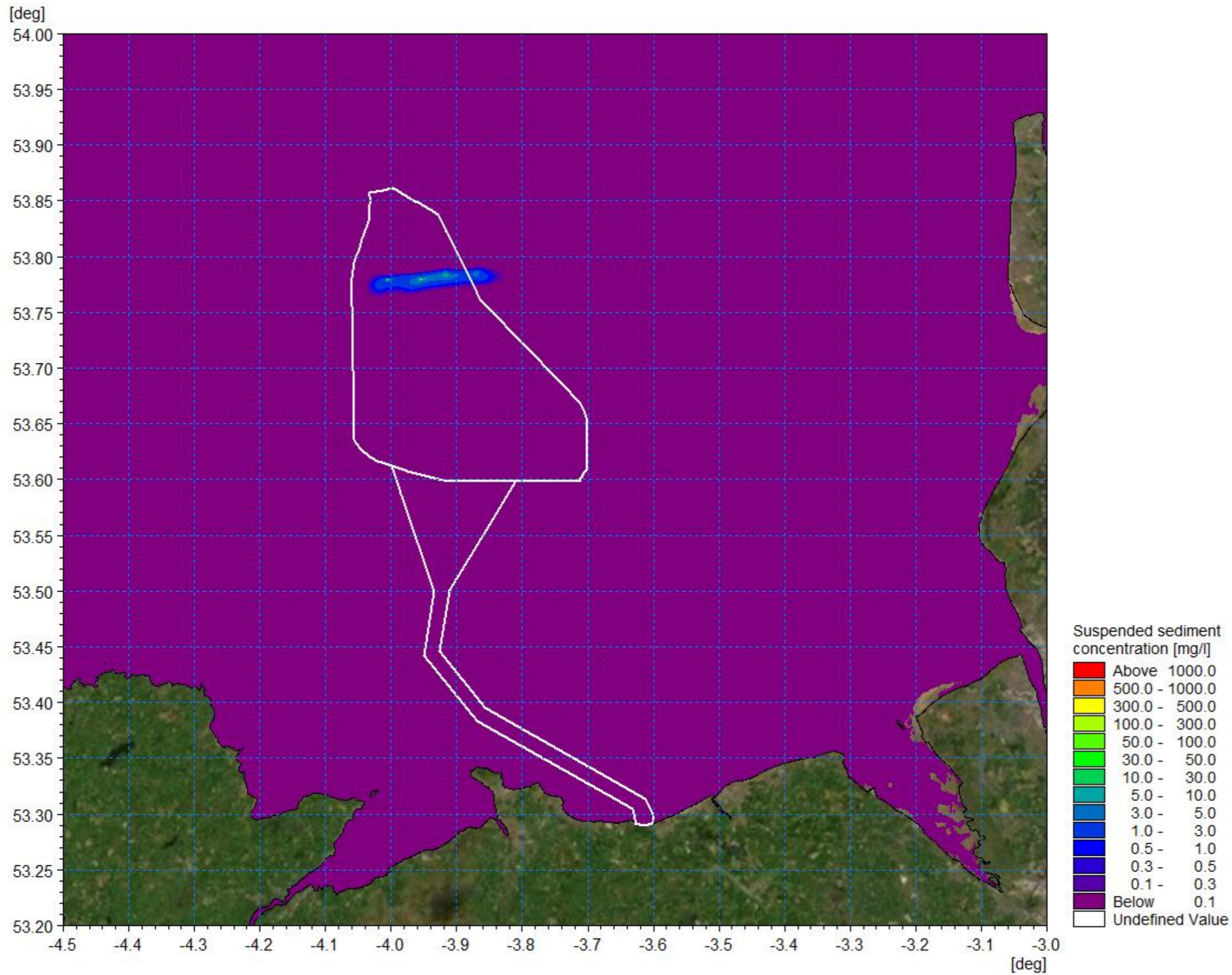


Figure 1.138: Suspended sediment concentration day 3 flood- pile installation Scenario C.



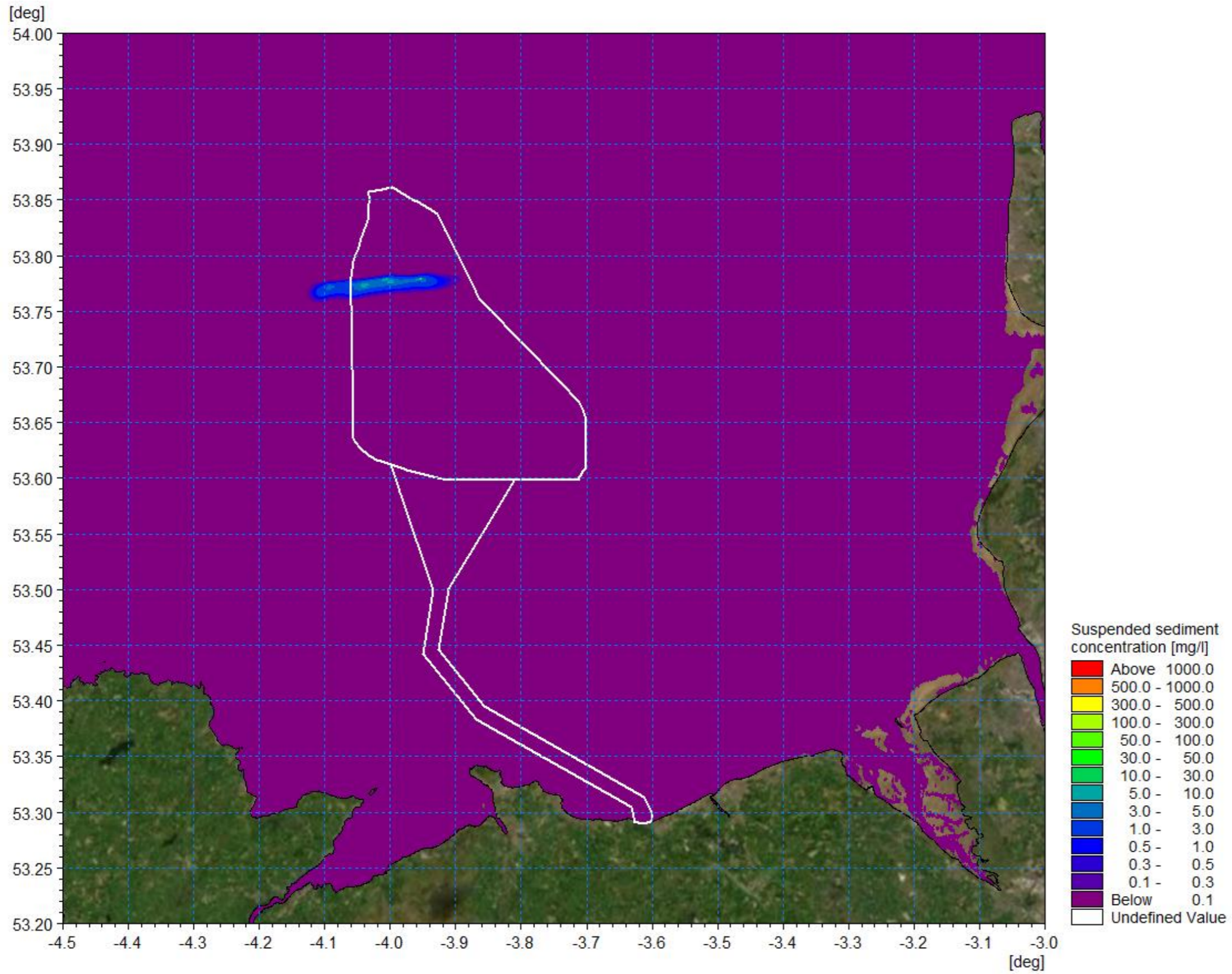


Figure 1.139: Suspended sediment concentration day 3 ebb- pile installation Scenario C.



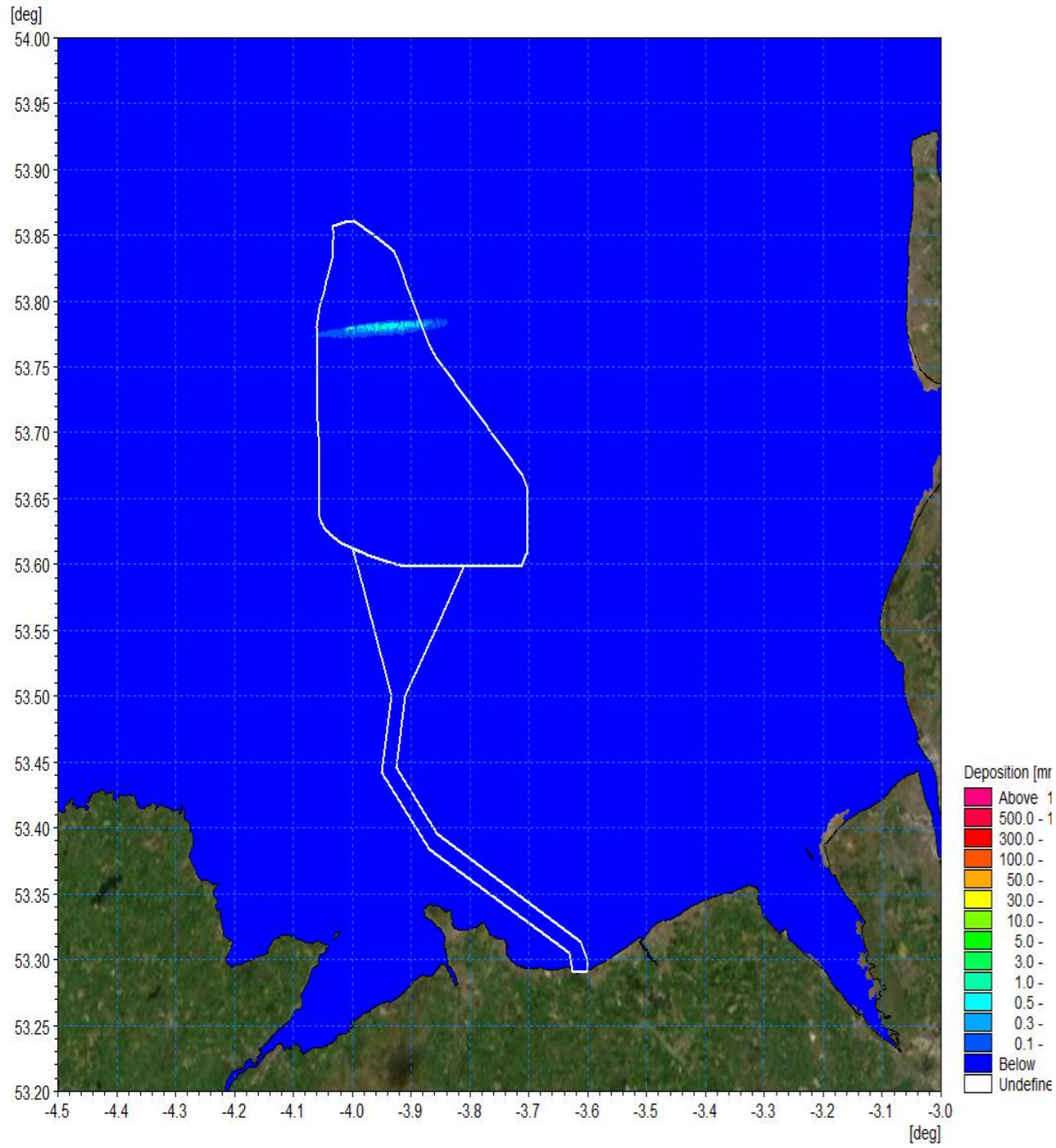


Figure 1.140: Average sedimentation during pile installation – Scenario C.

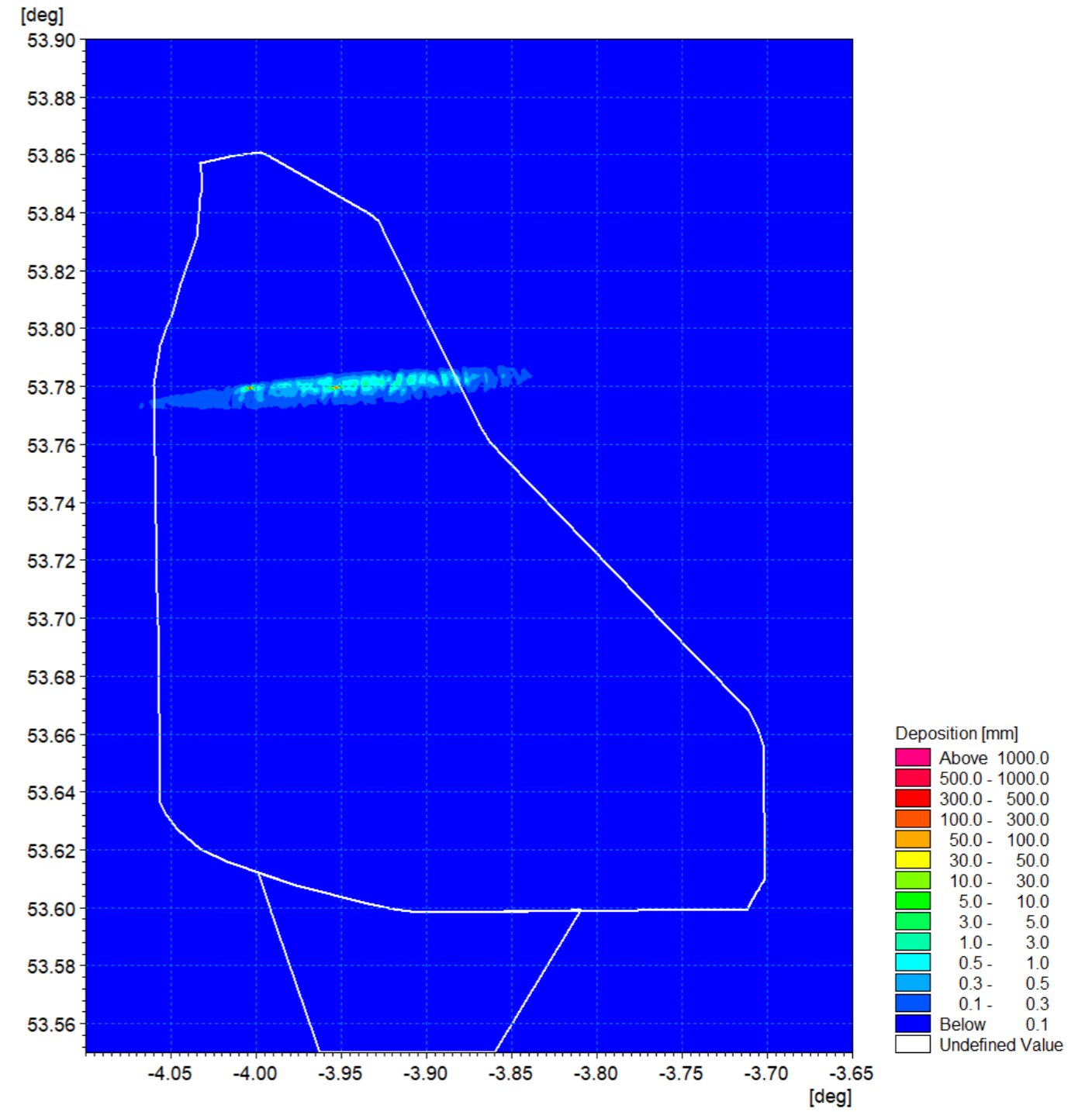


Figure 1.141: Average sedimentation during pile installation – Scenario C detail view.

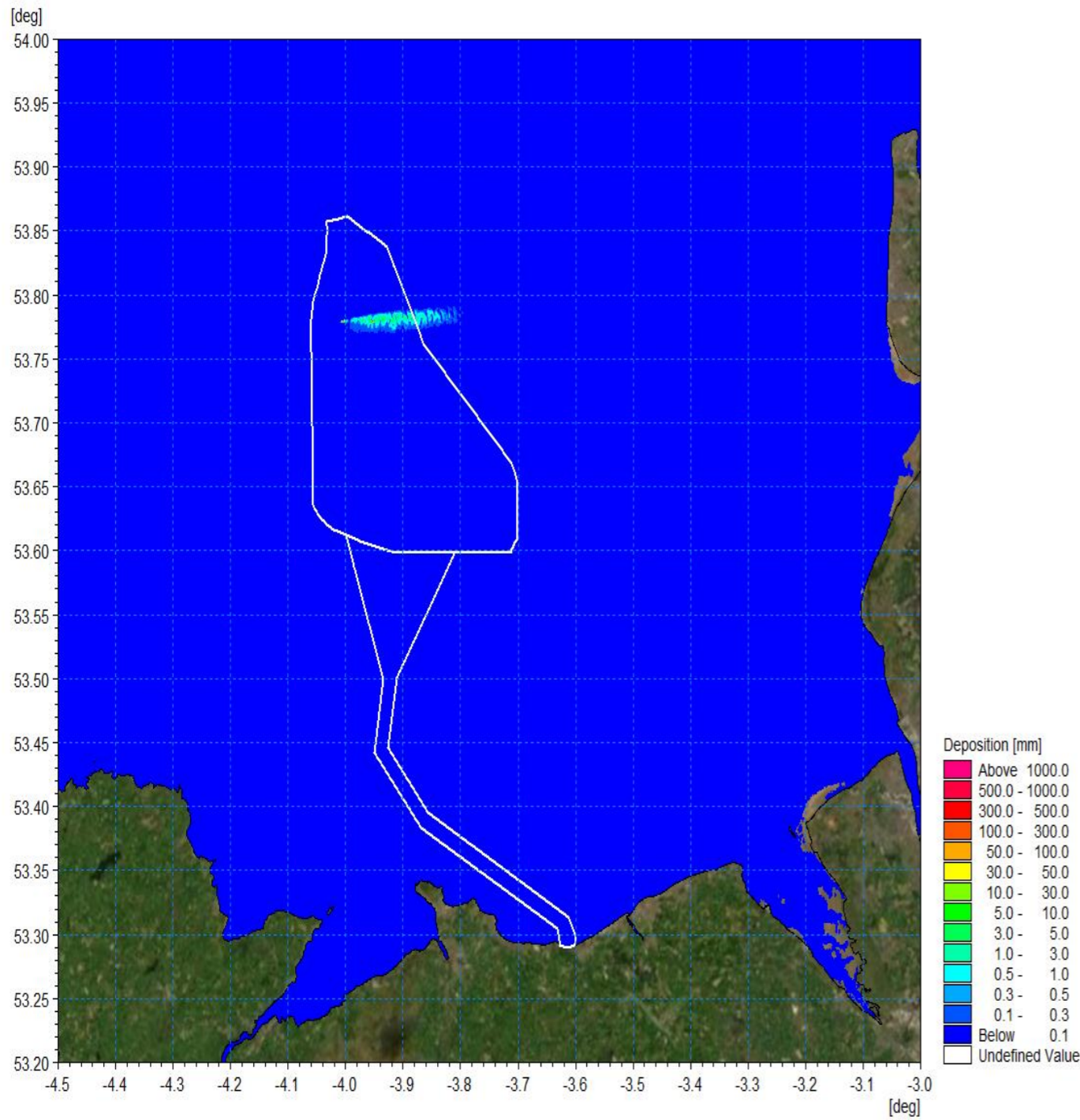


Figure 1.142: Sedimentation 1day following cessation of pile installation – Pile Scenario C.

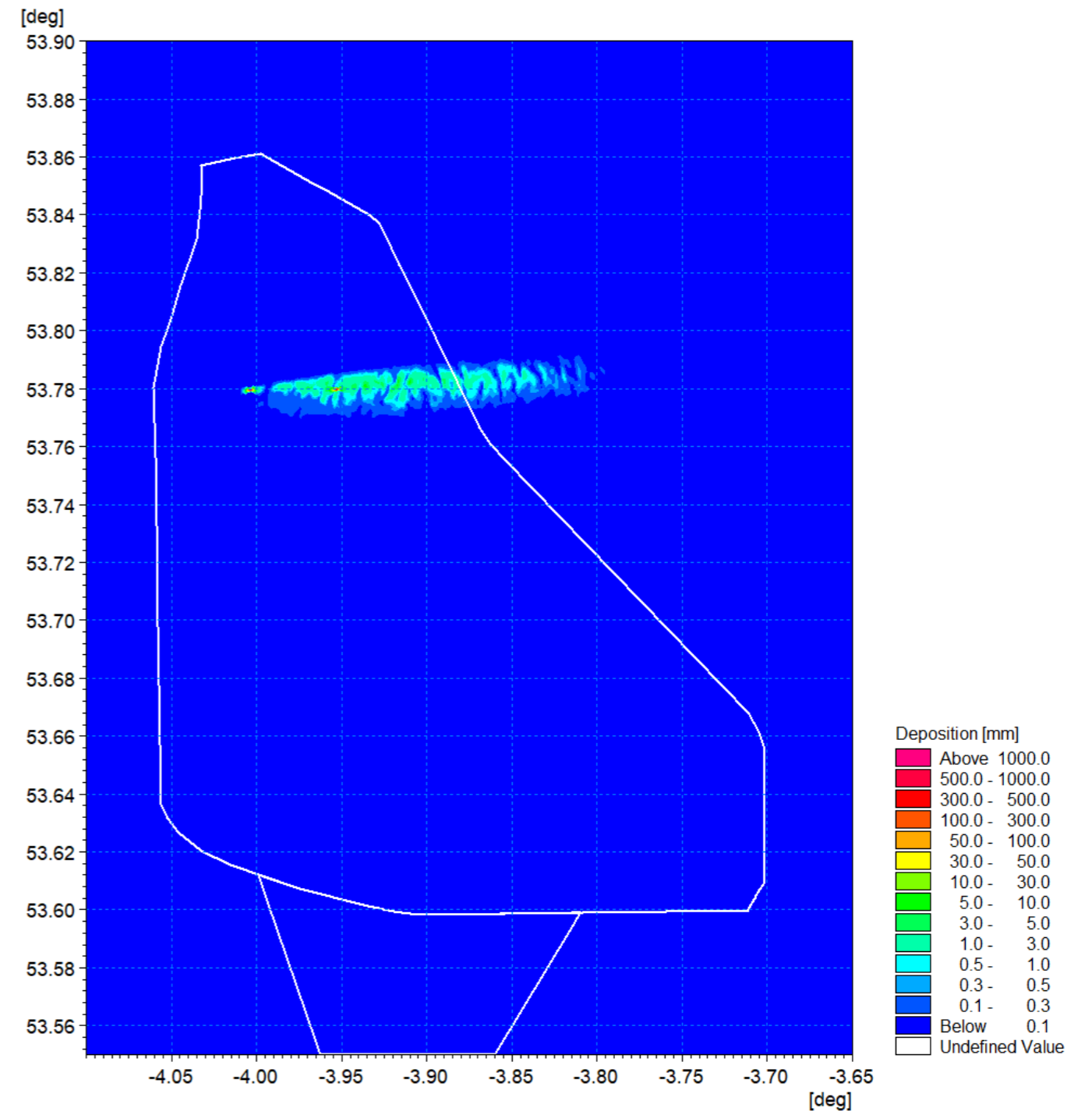


Figure 1.143: Sedimentation 1day following cessation of pile installation – Pile Scenario C detail view.



## 1.8.4 Cable installation

1.8.4.1 The third aspect of the construction phase is cable installation, including the inter-array cables, interconnector cables and export cables to shore. For the maximum design scenario in terms of release of sediment into the water column, cables were assumed to be trenched. A number of trenching techniques may be suited to the ground conditions; however it was assumed within the modelling that a trench of material of the maximum depth presented in the project description outlined in volume 1, chapter 3: Project description of the PEIR was mobilised into the lower water column as a result of the burial process, in line with the Business Enterprise and Regulatory Reform (BERR) guidelines (BERR, 2008). In reality the final installation technique may result in less sediment being mobilised and the maximum depth may not always be achieved with a corresponding reduction in the amount of material disturbed.

1.8.4.2 Similar to the pile installation, the model simulations used the sediment grading determined from BGS sediment sampling data. However, the modelling was undertaken using the MIKE particle tracking (PT) module. This module was implemented as it had the advantage that it could be used to describe the transport of material released in a specific part of the water column. In this way, the dispersion would not be over-estimated or the corresponding sedimentation under-estimated by the application of a current profile through the water column.

1.8.4.3 Trenching rates can vary widely depending on the bed material and equipment used; typically, rates are between 25m/h and 780m/h. For the simulation, a relatively high rate of 450m/h was used over an extensive sample route ensuring that material was released at all tidal states over a number of tides and ensuring initial concentrations were not underestimated.

### Inter-array/interconnector cables

1.8.4.4 Inter-array and interconnector cable installation will be undertaken along a number of paths which connect groups of turbines to a local hub (i.e. the Offshore Substation Platform OSP) or which connect two OSPs to each other. Each route would be undertaken as a separate operation and thus a single example has been selected to quantify the potential suspended sediment levels during the installation. Figure 1.144 shows an indicative turbine layout with the modelled inter-array cable route shown in green. This route was run from the north of the site, perpendicular to the tidal flow, then in line with tidal flows in an easterly direction. This ensured that the full extent of the site and tidal conditions were incorporated into the simulation.

1.8.4.5 The inter-array cabling was undertaken along the indicated route with a trench 3m wide at the bed and 3m in depth with a triangular cross-section in accordance with a trenching plough. Thus circa 220,500m<sup>3</sup> of material was mobilised during the 4day simulation along the 49km route. The sediment grading characteristics were derived from sediment sampling along the route and defined by the following sand fractions.

- Very coarse sand/gravel: 24%
- Coarse sand: 20%
- Medium sand: 35%
- Fine sand: 9%

- Very fine sand/mud: 12%.

1.8.4.6 The model results presented follow the same format as those for the piled foundation installation described in the previous section. Figure 1.145 shows the average suspended sediment concentration over the course of the trenching phase. It is clear that the sediment is dispersed on subsequent tides as the plume envelope illustrates the flood and ebb tidal excursions with peak values of 100-300mg/l.

1.8.4.7 Figure 1.146 to Figure 1.151 shows the suspended sediment patterns over the course of this operation, day two, three and four mid flood and ebb tides respectively. The volume of material mobilised is relatively large, and elevated tidal currents disperse the material giving rise to concentrations of up to 500mg/l. As was evident in the previous operations, the material settles during slack water and then is re-suspended to form a secondary plume which becomes amalgamated. This is further illustrated in Figure 1.152 and Figure 1.153 which show the average sedimentation and the sedimentation one day following cessation at slack water. The sedimentation is greatest at the location of the trenching and may be up to 30mm in depth where the coarser material has settled within close proximity, circa 100m. The depths reduce significantly with distance to <0.5mm which is indicated by the use of a log scale in all figures. Although the material is dispersed, it remains within the sediment cell and is therefore retained within the transport system.

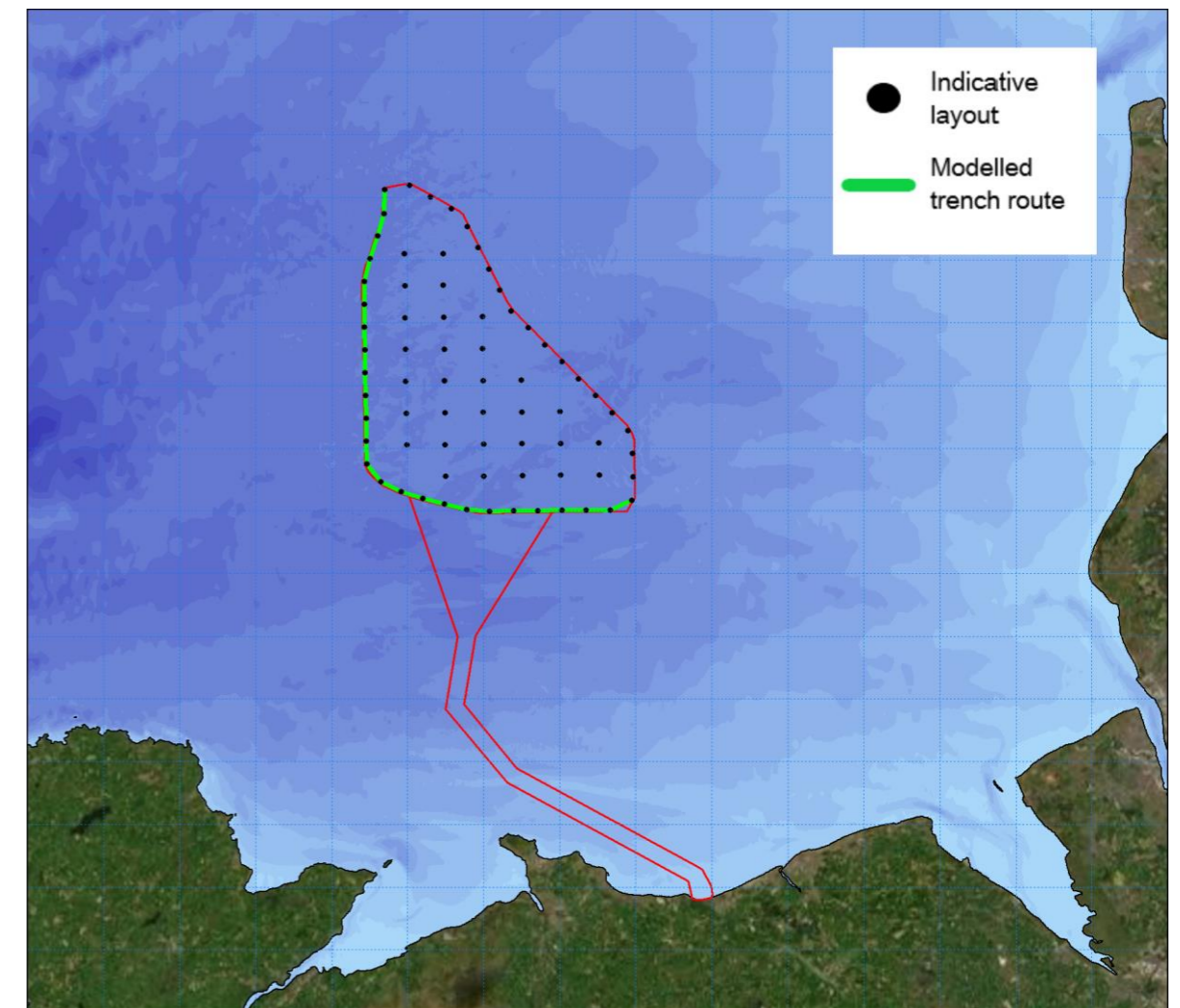


Figure 1.144: Modelled inter-array cable route.



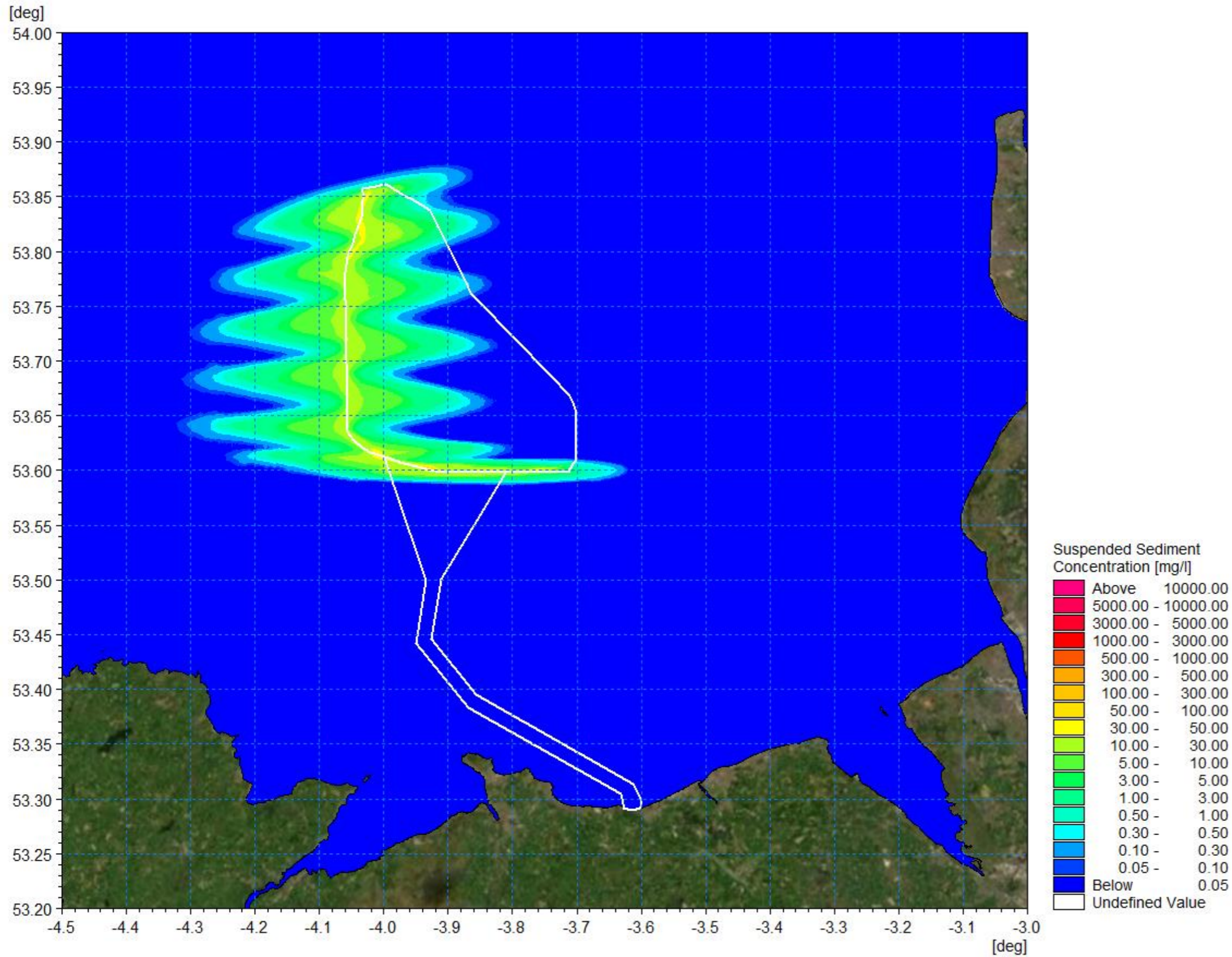


Figure 1.145: Average suspended sediment concentration during inter-array cable trenching.



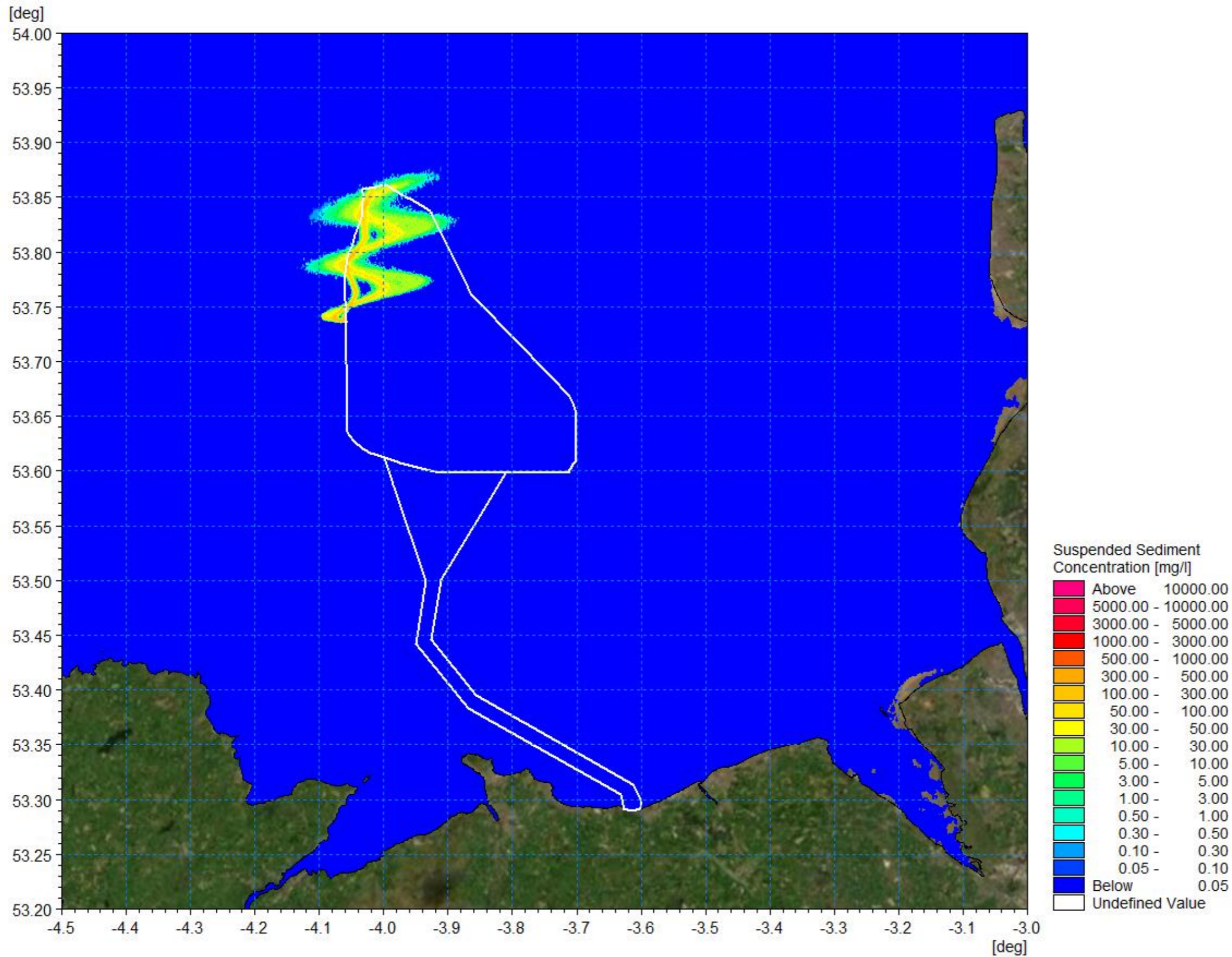


Figure 1.146: Suspended sediment concentration day 2 flood – inter-array cable installation.



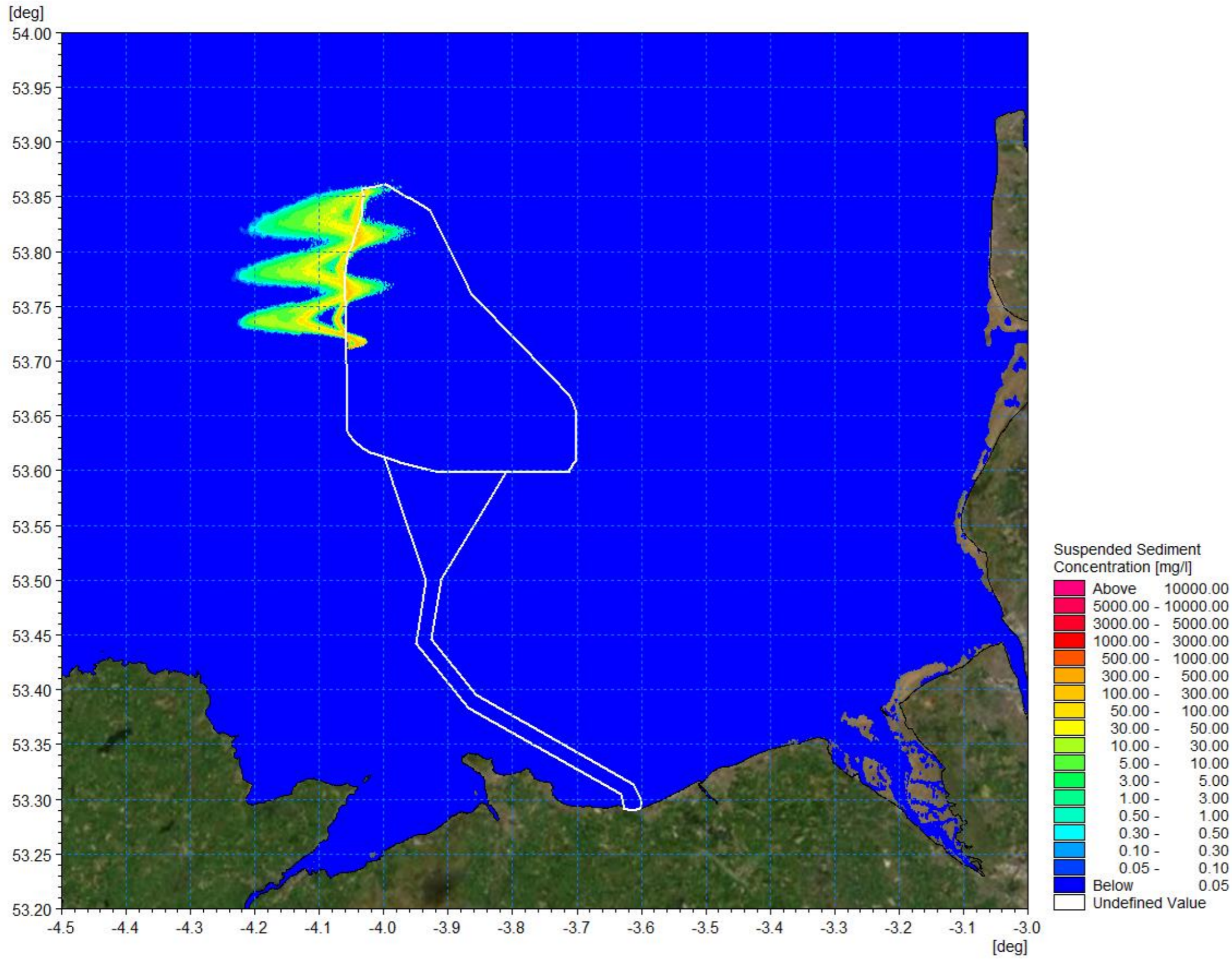


Figure 1.147: Suspended sediment concentration day 2 ebb – inter-array cable installation.



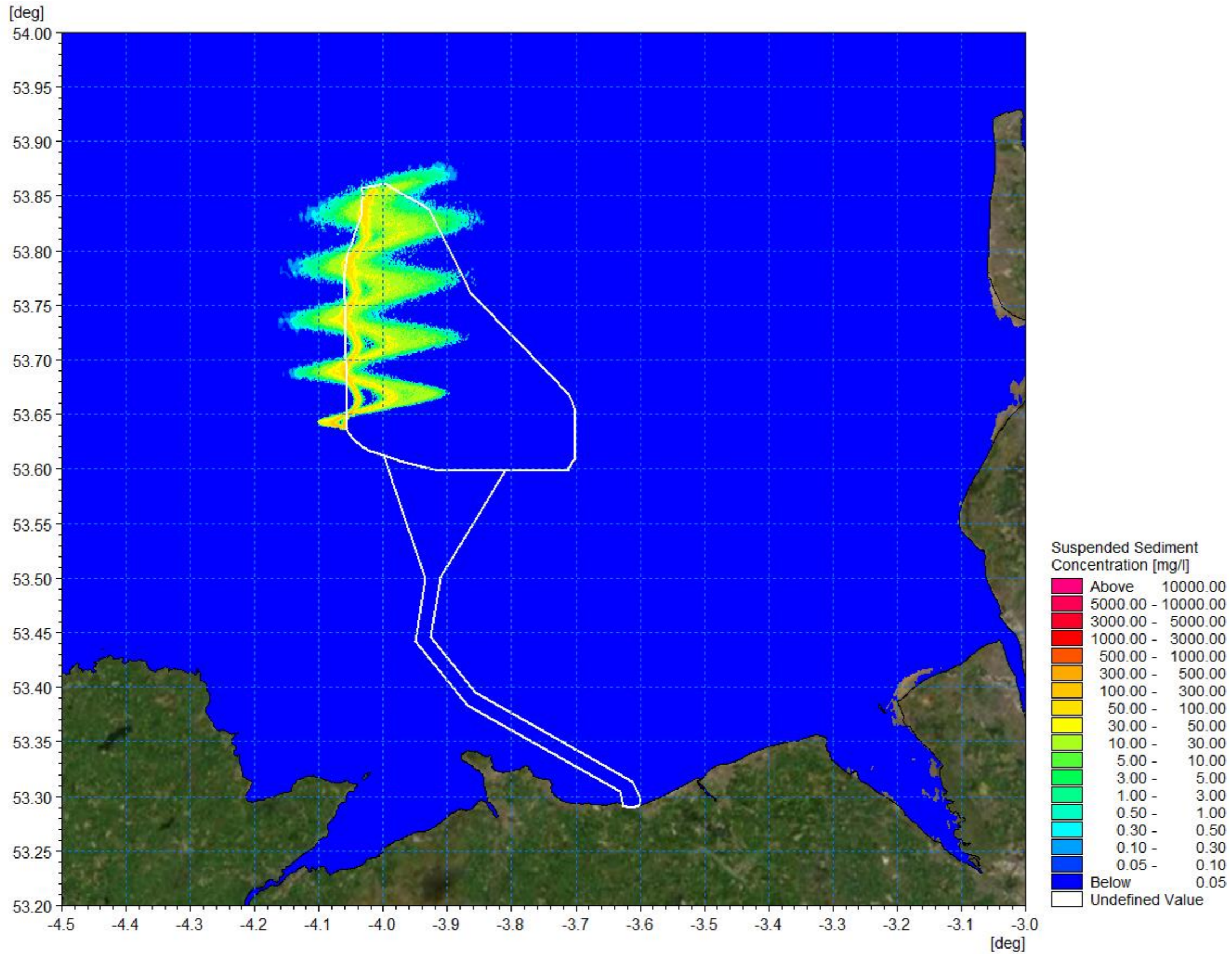


Figure 1.148: Suspended sediment concentration day 3 flood – inter-array cable installation.



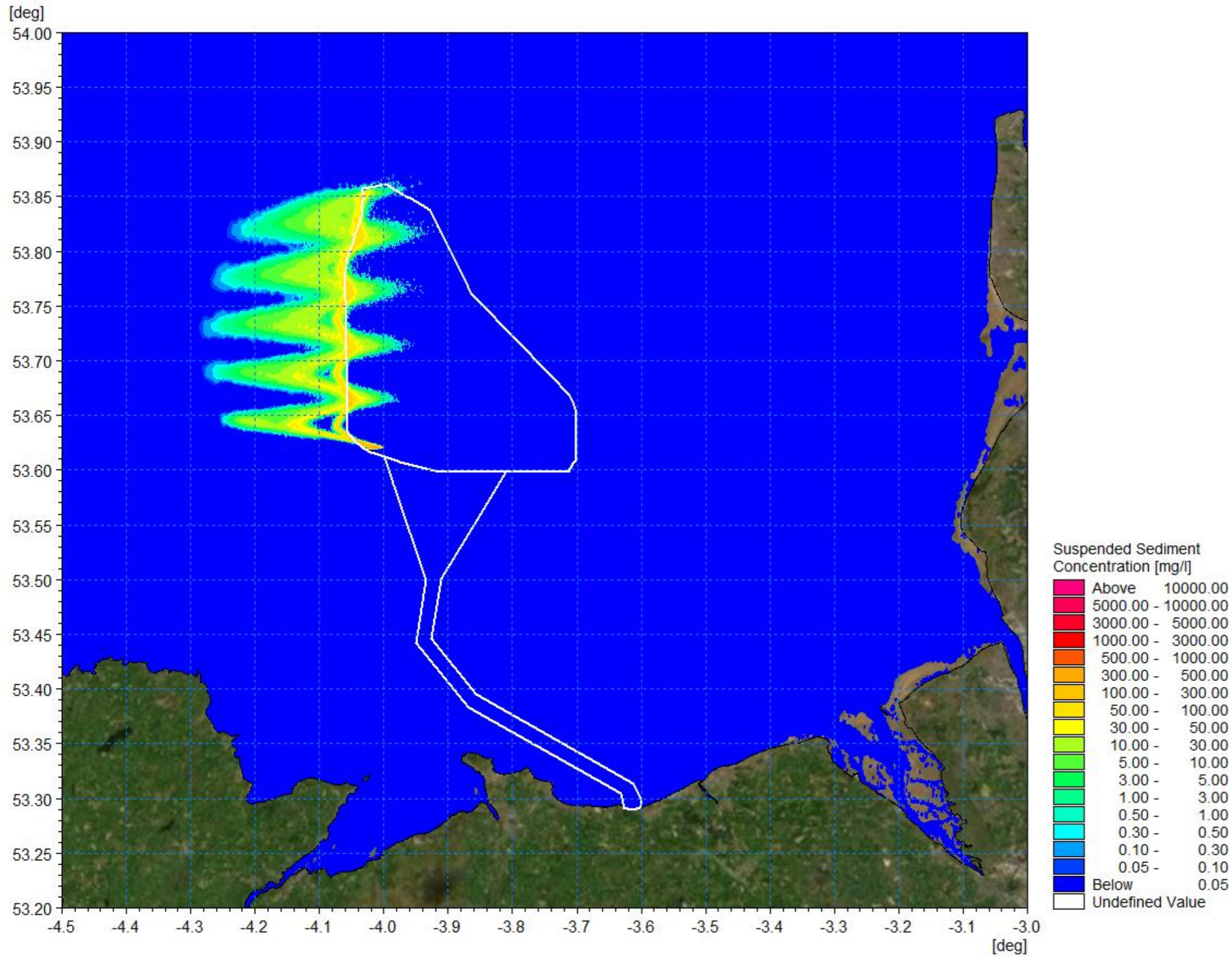


Figure 1.149: Suspended sediment concentration day 3 ebb – inter-array cable installation.



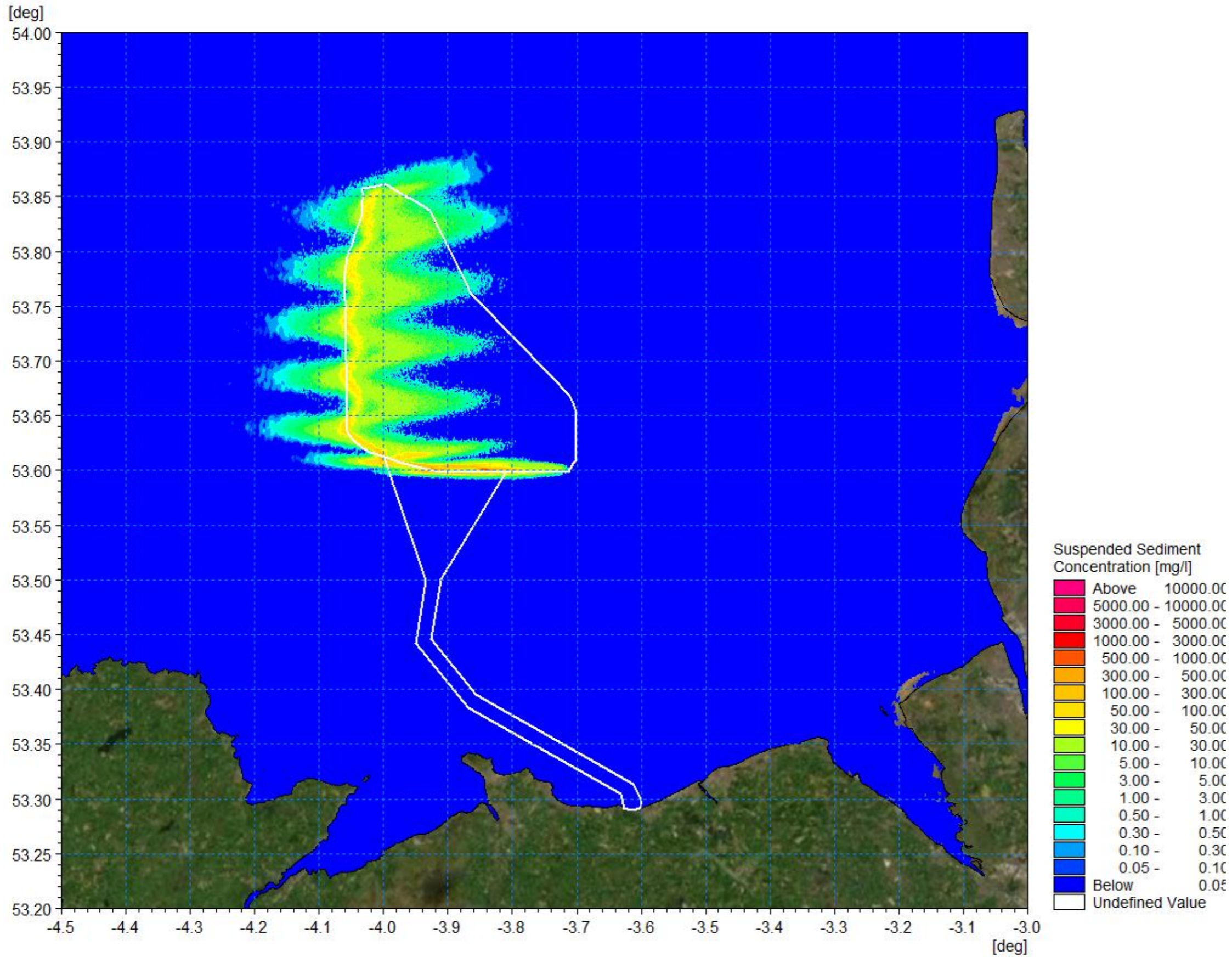


Figure 1.150: Suspended sediment concentration day 4 flood – inter-array cable installation.



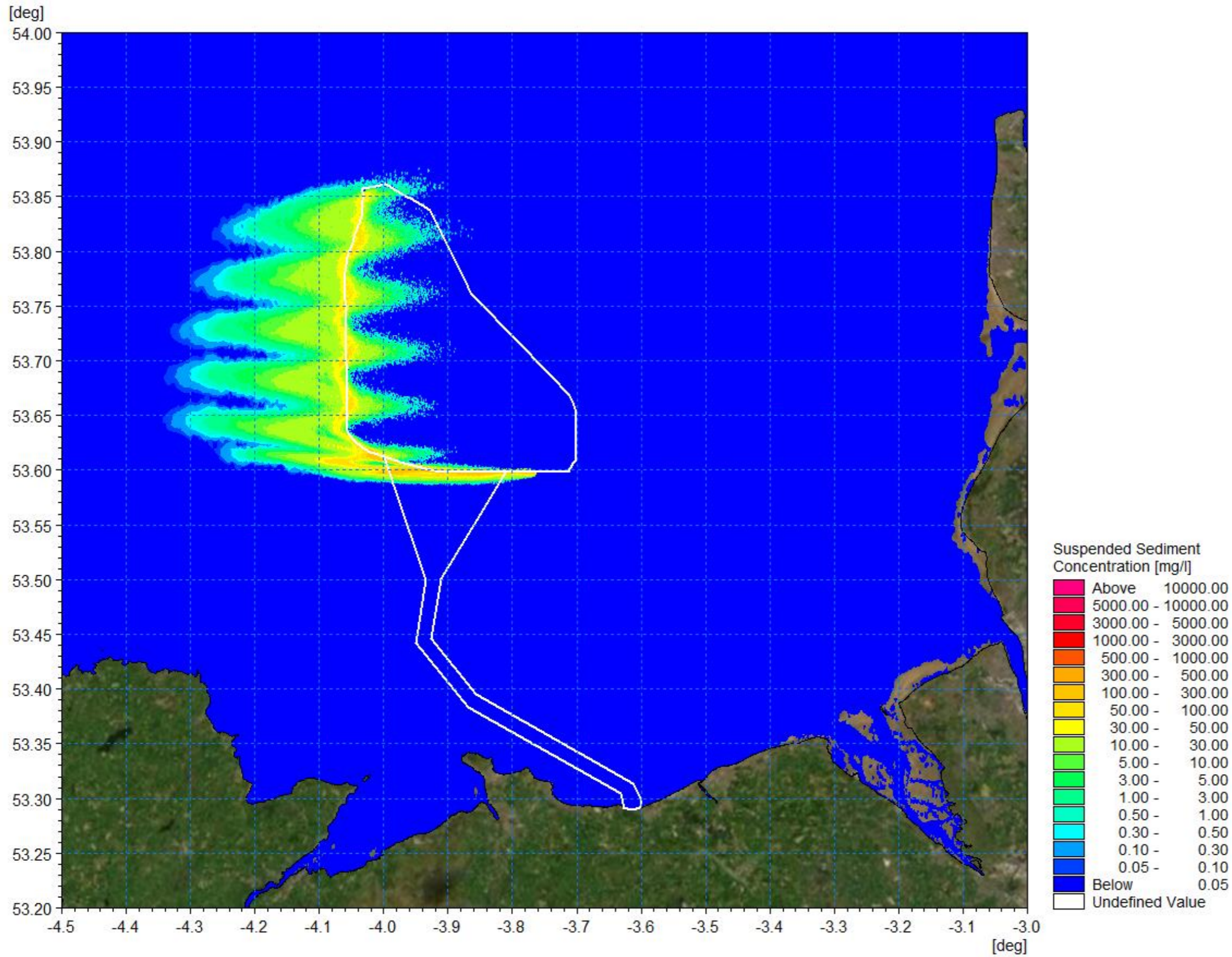


Figure 1.151: Suspended sediment concentration day 4 ebb – inter-array cable installation.



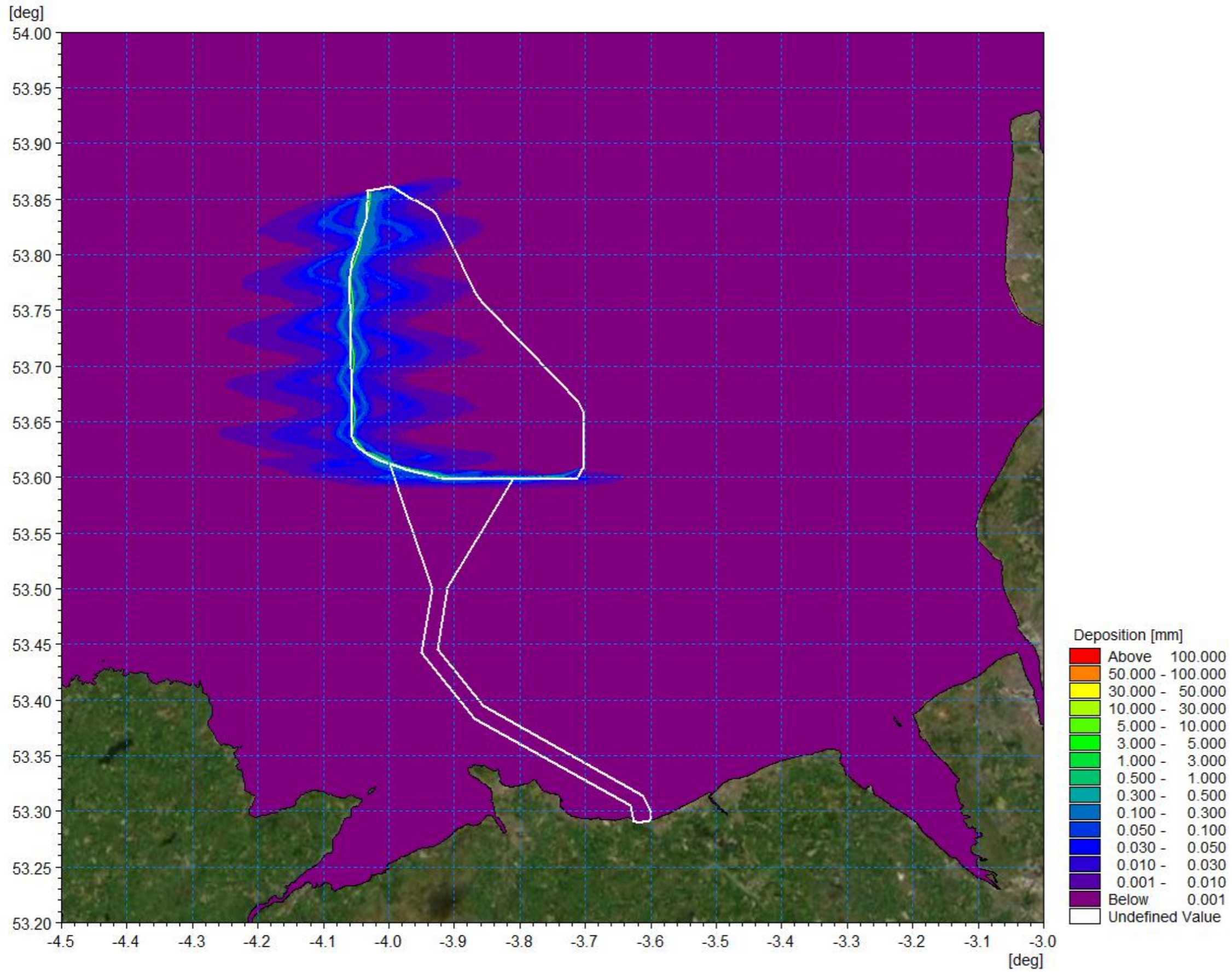


Figure 1.152: Average sedimentation during inter-array cable installation.



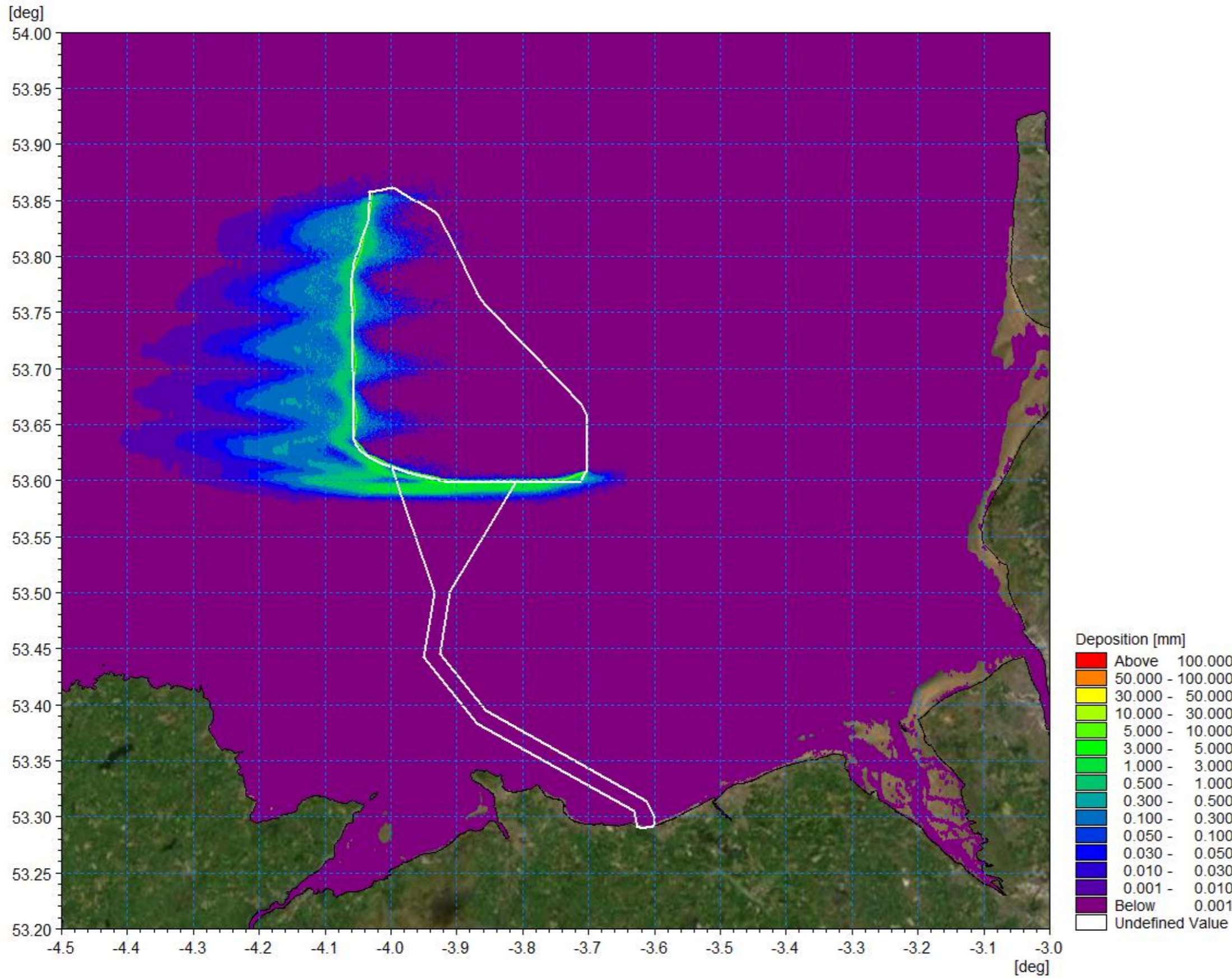


Figure 1.153: Sedimentation 1day following cessation of inter-array cable installation.



### Offshore export cables

- 1.8.4.8 The Mona Offshore Wind Project export cable route was examined using numerical modelling. The simulation assumed the same trenching rate as with the inter-array cables, (i.e. 450m/h), and that installation began from offshore and continued to the nearshore region of a trenchless landfall. Each trench was 3m at the surface extending to a depth of 3m, (i.e. the greatest burial depth proposed), with a triangular profile. The operation took approximately 4days to complete encompassing a range of tidal conditions and mobilised 206,550m<sup>3</sup> of material. The composition was determined from the sampling data and was of generally slightly more finely graded material than the inter-array route material.
- Very coarse sand/gravel: 20%
  - Coarse sand: 10%
  - Medium sand: 35%
  - Fine sand: 30%
  - Very fine sand/mud: 5%.
- 1.8.4.9 The trenching route modelled is illustrated by the green trace in Figure 1.154 and the average suspended sediment plume during the course of the operation is shown in Figure 1.155. The figure shows how the plume travels east and west on the tide as the release progresses along the route perpendicular to the tidal flow. This gives rise to average suspended sediment concentrations <50mg/l offshore rising to 300mg/l nearshore as the water depth decreases.
- 1.8.4.10 The instantaneous suspended sediment concentrations for mid flood and ebb tides are presented for day two, day three and day four in Figure 1.156 to Figure 1.161 respectively. They show increases where sediment is released at the cable location but also at the extent of each tidal cycle as material is re-suspended. The plume travels east and west on the tide as the release progresses along the route perpendicular to the tidal flow and sediment concentrations reduce to background levels on slack tides. Suspended sediment concentrations along the route range between 50 and 1000mg/l where the greatest levels are located at the source of the sediment release in the shallowest water.
- 1.8.4.11 Finally, Figure 1.162 shows the average sedimentation whilst Figure 1.163 illustrates sedimentation levels one day following cessation of the sediment release. Tidal patterns indicate that although the released material migrates both east and west by settling and being re-suspended on successive tides, the sedimentation level is small typically <0.5mm and the greatest levels of deposition occur along the trenching route as coarser material settles. Although the material is widely dispersed, sediment remains within the cell and would be drawn into the baseline transport regime with small increases in bed sediment levels. It is noted that due to the nature of the tidal flow mobilised sediment is carried offshore and does not accumulate along the coastline.

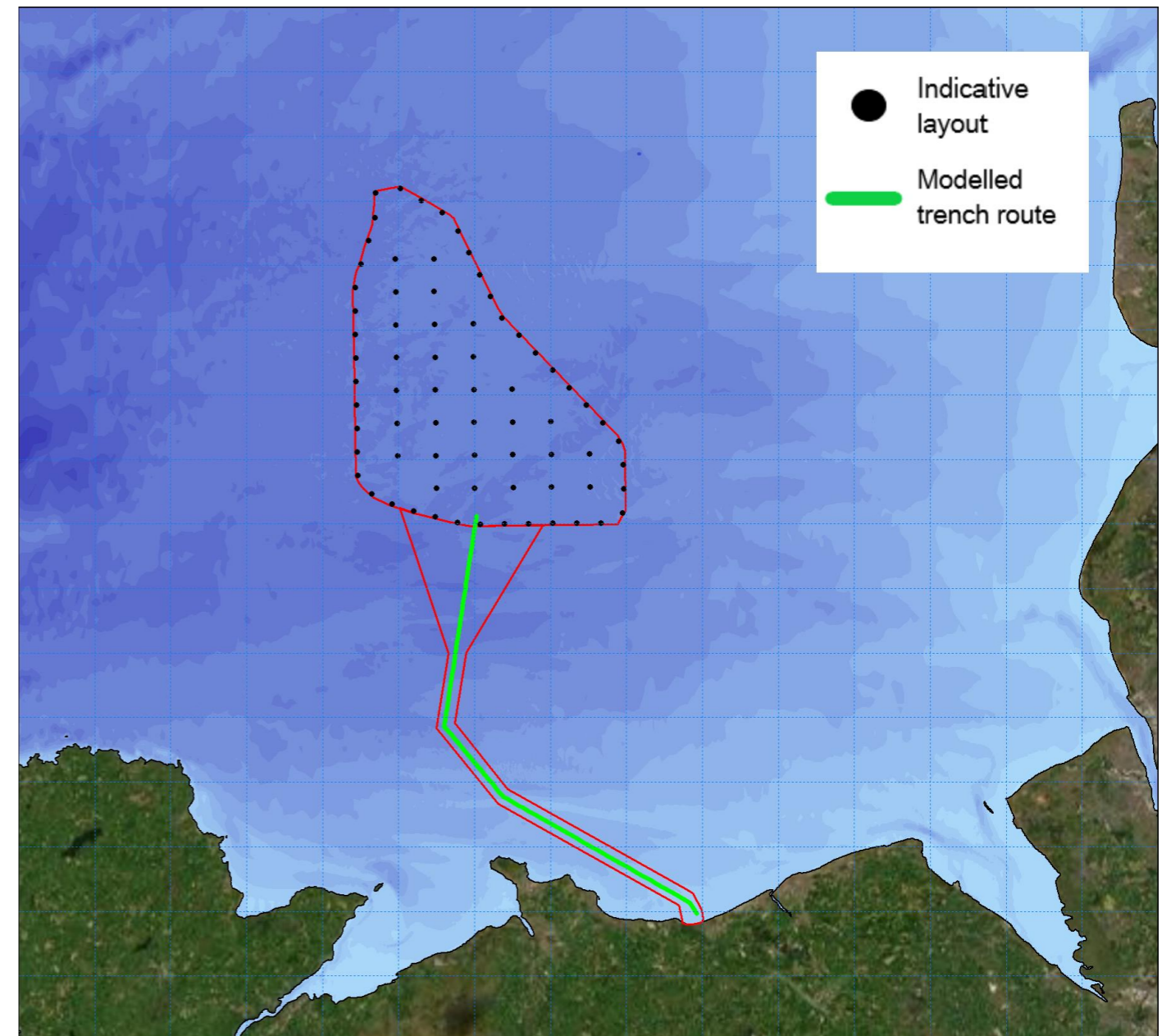


Figure 1.154: Modelled export cable route.



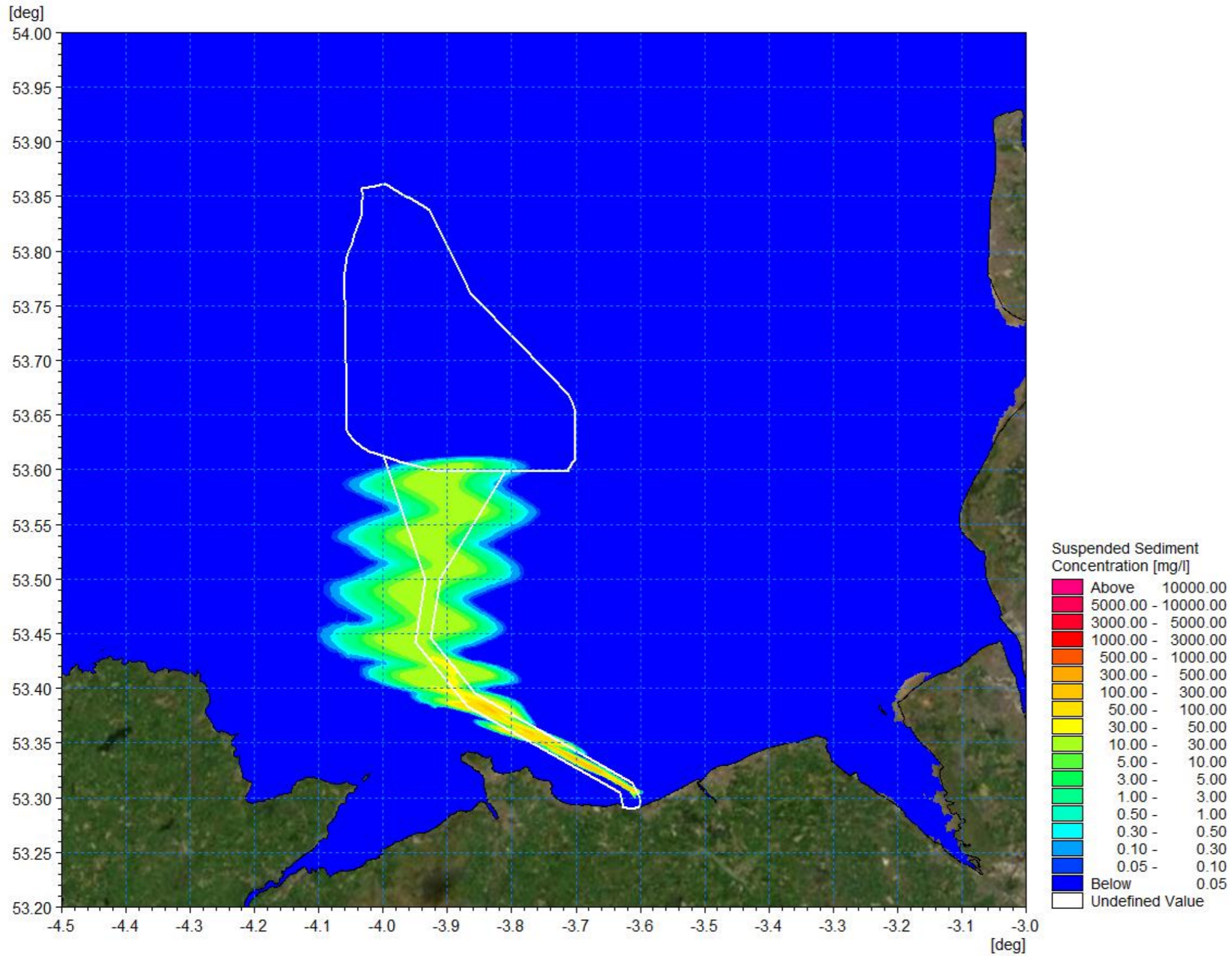


Figure 1.155: Average suspended sediment concentration during offshore export cable trenching.



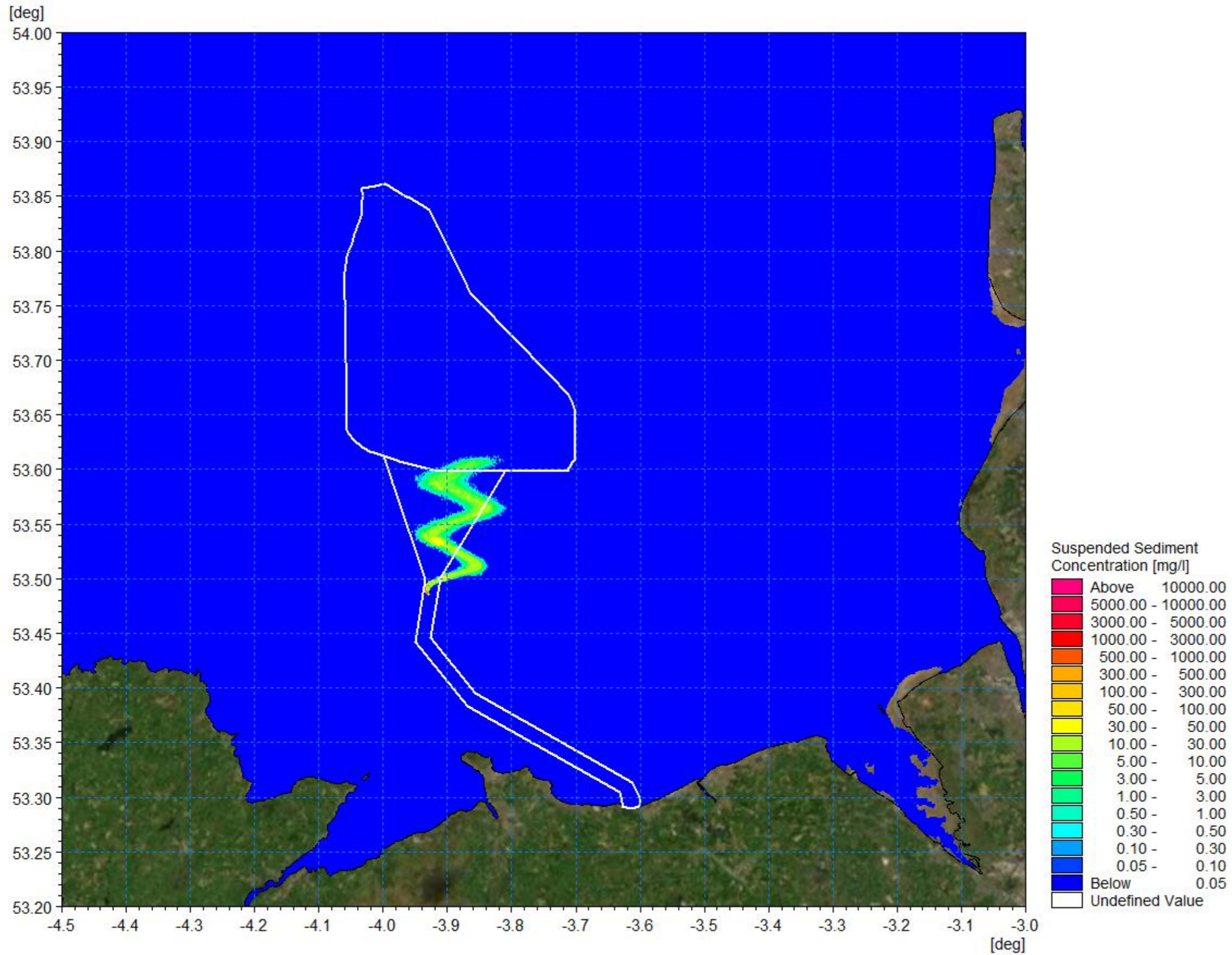


Figure 1.156: Suspended sediment concentration day 2 peak flood – offshore export cable installation.



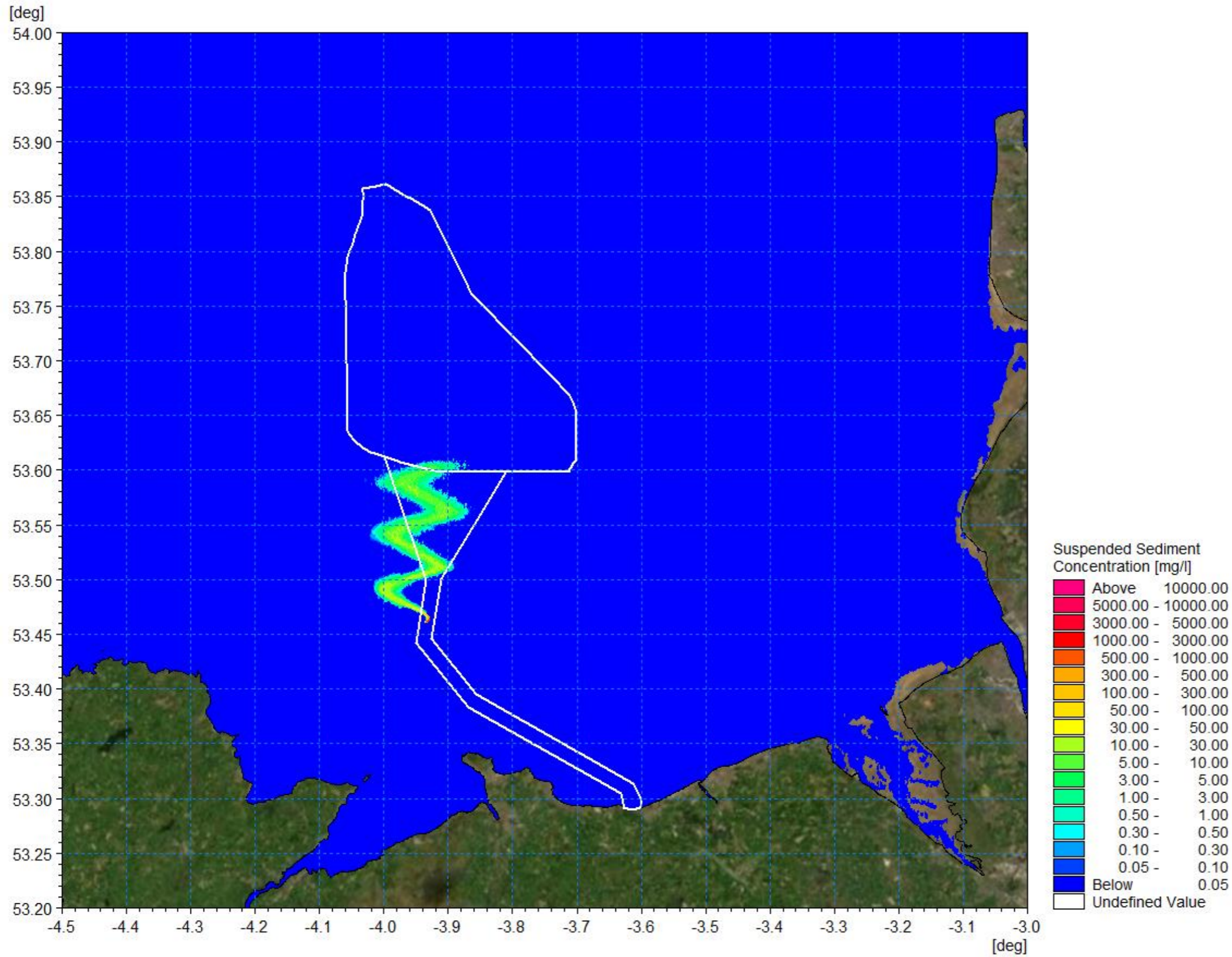


Figure 1.157: Suspended sediment concentration day 2 peak ebb – offshore export cable installation.



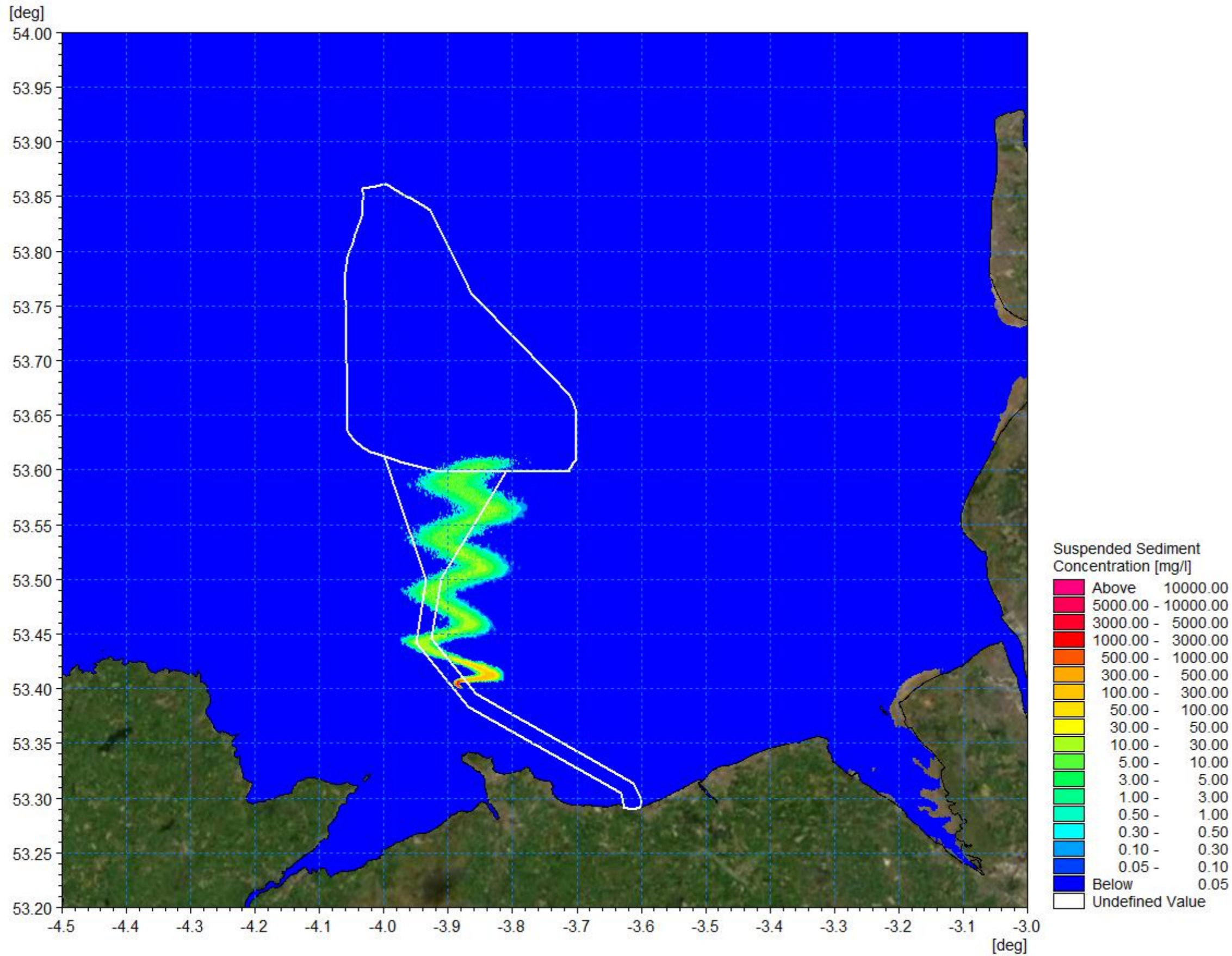


Figure 1.158: Suspended sediment concentration day 3 peak flood – offshore export cable installation.



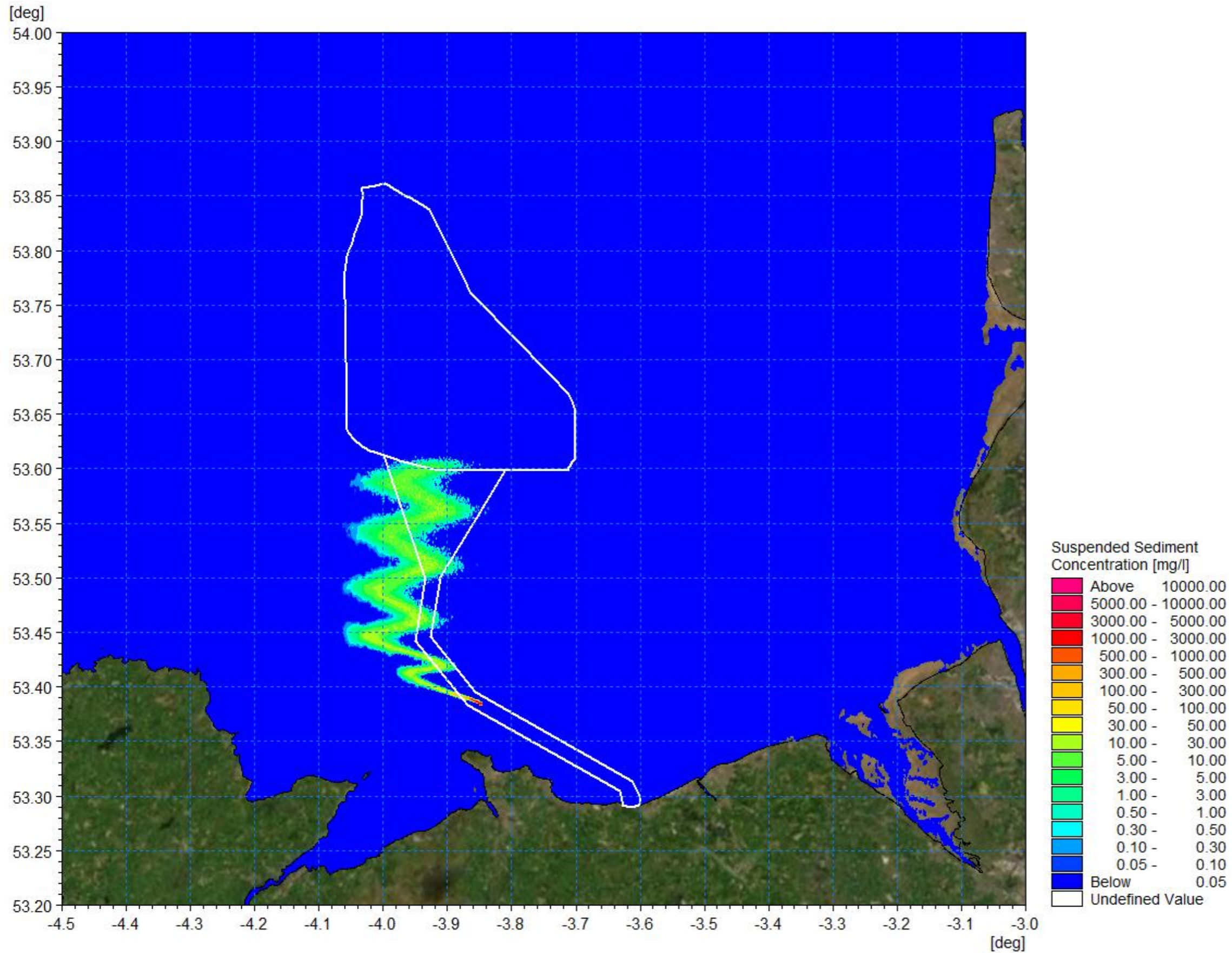


Figure 1.159: Suspended sediment concentration day 3 peak ebb – offshore export cable installation.



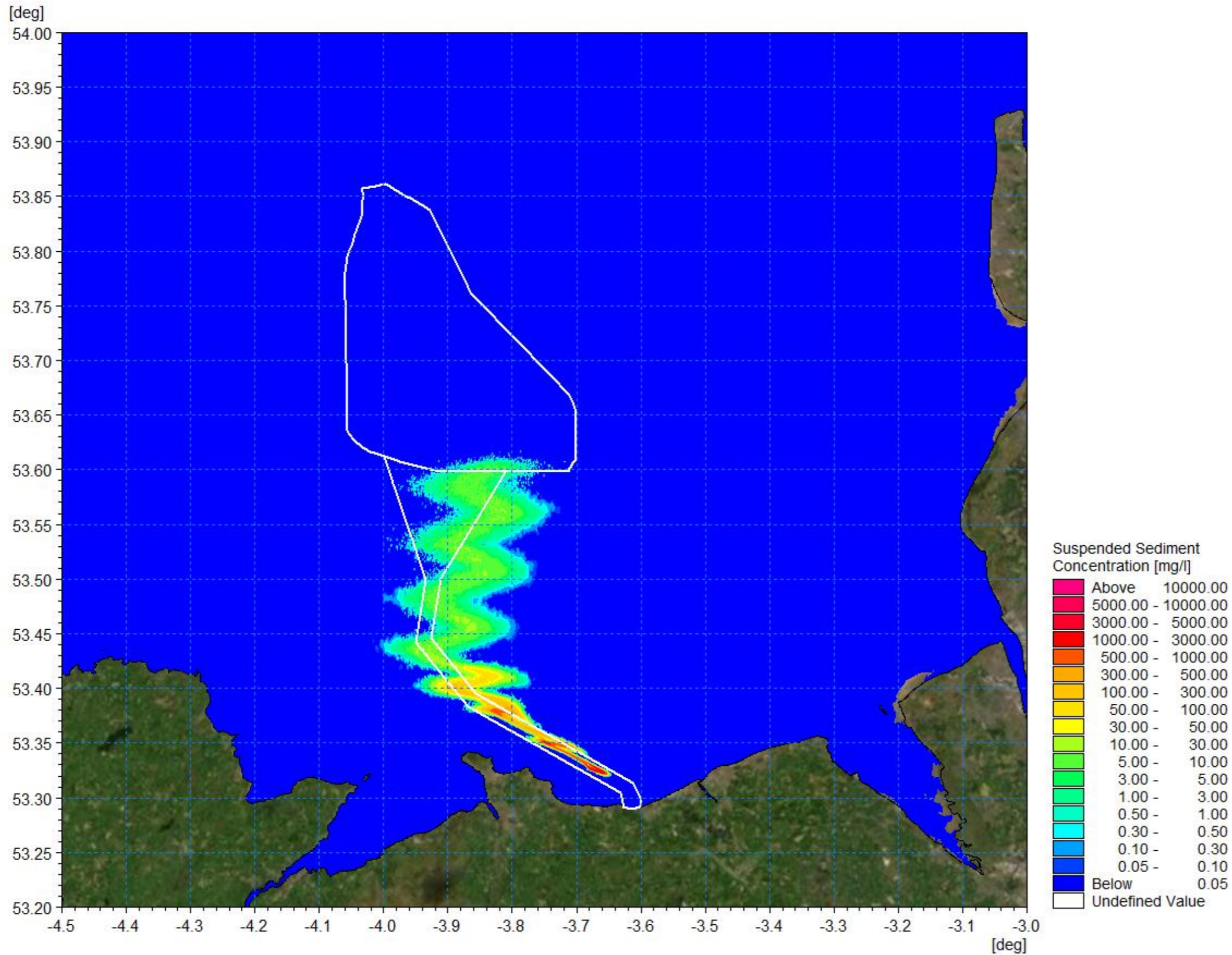


Figure 1.160: Suspended sediment concentration day 4 peak flood – offshore export cable installation.



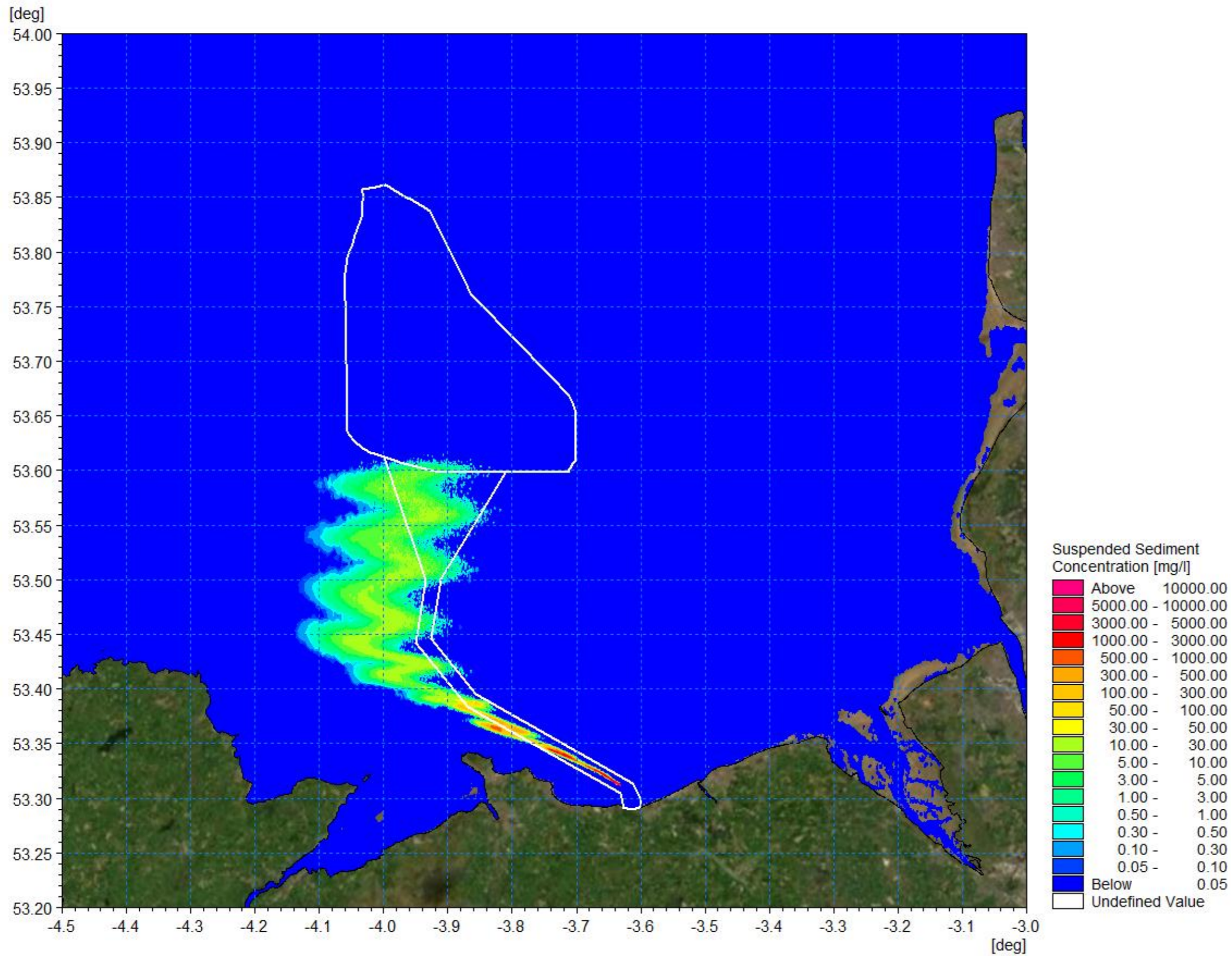


Figure 1.161: Suspended sediment concentration day 4 peak ebb – offshore export cable installation.



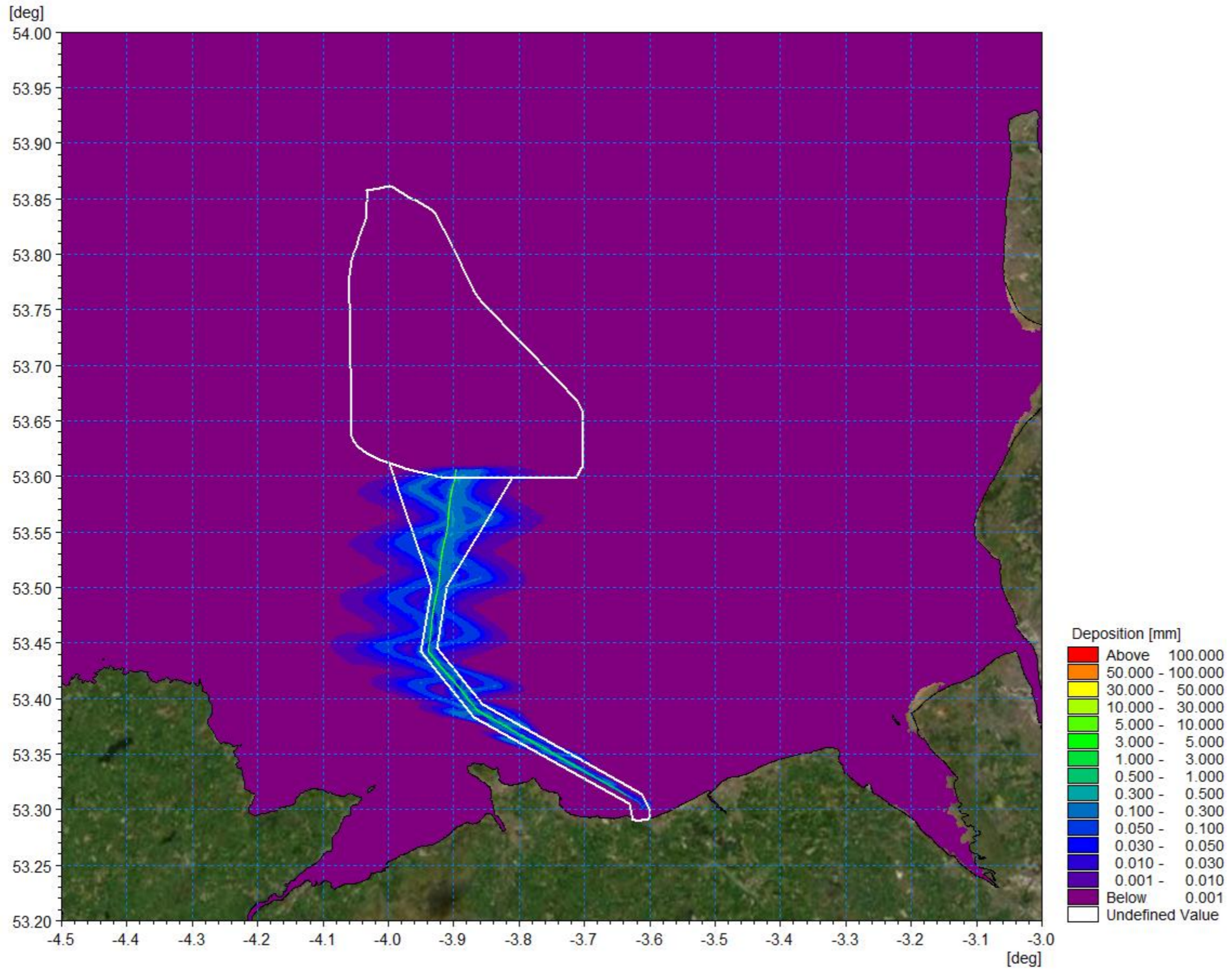


Figure 1.162: Average sedimentation during offshore export cable installation.



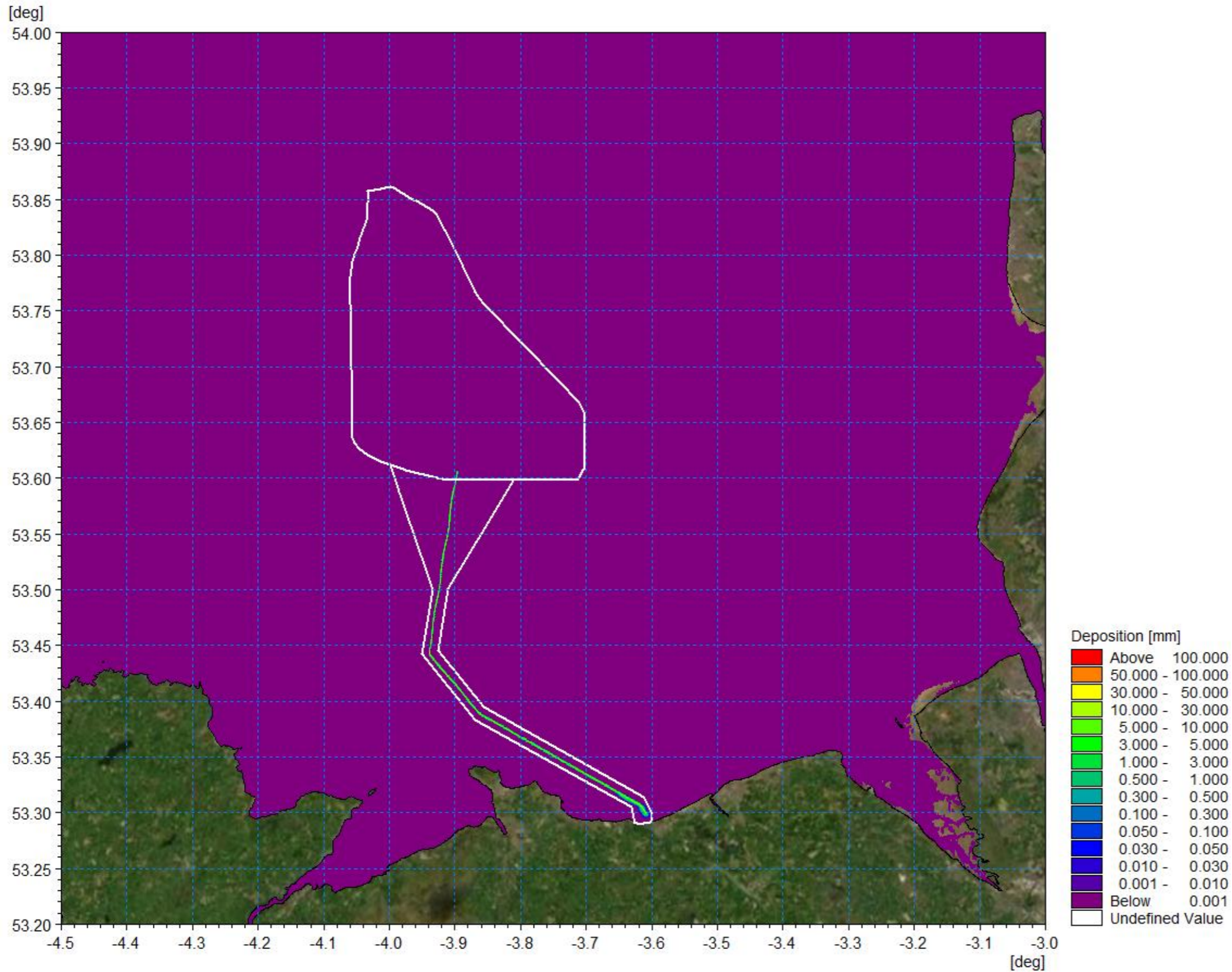


Figure 1.163: Sedimentation 1day following cessation of offshore export cable installation.



**Offshore export cables in the intertidal area**

1.8.4.12 The final scenario examined using numerical modelling related to trenching of offshore export cables in the intertidal area. The simulation assumed a lower trenching rate of 100m/h and was undertaken over an 8hour period. The installation began from offshore and continued 800m to the high water mark. The trench was 1m at the surface extending to a depth of 3m (i.e. the greatest burial depth proposed), mobilising 2,400m<sup>3</sup> of material. The composition was determined from the sampling data and comprised mainly fine sand.

- Very coarse sand/gravel: 0.5%
- Coarse sand: 0.5%
- Medium sand: 6%
- Fine sand: 55%
- Very fine sand/mud: 38%.

1.8.4.13 The trenching route modelled is illustrated by the green trace in Figure 1.164 and the average suspended sediment plume during the course of the operation is shown in Figure 1.165, with a detailed view in Figure 1.166. The figures show how the plume is strongly dependant on the prevailing tidal conditions at the time of sediment release. This gives rise to average suspended sediment concentrations 500 - 1000mg/l due to the limited water depth however the plume extent is restricted.

1.8.4.14 The instantaneous suspended sediment concentrations for mid flood and ebb tides are presented in Figure 1.167 and Figure 1.168 respectively. They show increases where sediment is released at the cable location but also at the extent of each tidal cycle as material is re-suspended. Suspended sediment concentrations are seen to exceed 1000mg/l where the greatest levels are located at the source of the sediment release in the shallowest water, however the plume excursion is circa 5km.

1.8.4.15 Finally, Figure 1.169 and Figure 1.170 show the average sedimentation whilst Figure 1.171 and Figure 1.172 illustrates sedimentation levels one day following cessation of the sediment release. Tidal patterns indicate that although the released material migrates both east and west by settling and being re-suspended on successive tides, some sediment is deposited on the shoreline with a maximum depth of around 10mm. It should however be noted that this is native material, originating from less than 1km from the shoreline and would therefore remain within the existing shoreline transport cell.

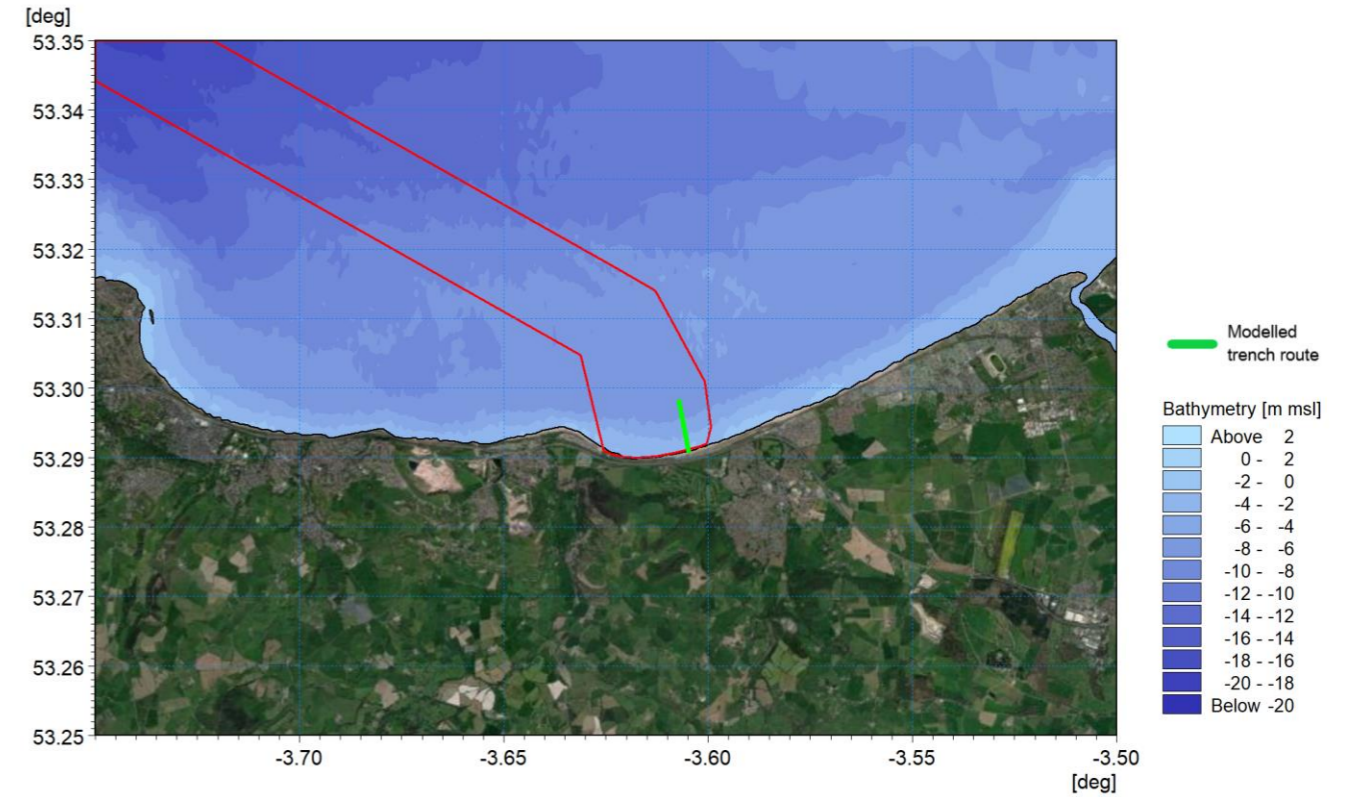


**Figure 1.164: Modelled offshore export cables in the intertidal area.**

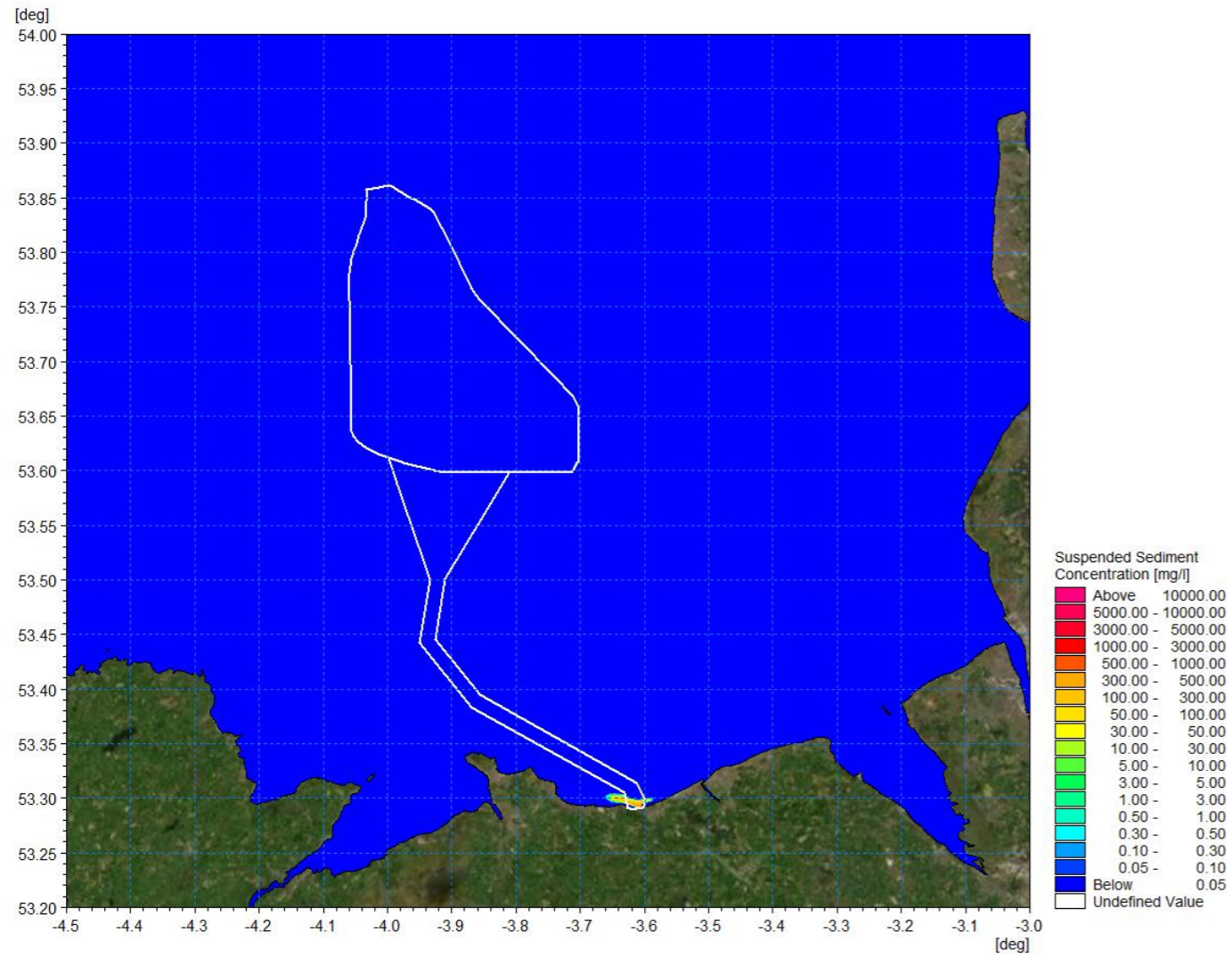


Figure 1.165: Average suspended sediment concentration during offshore export cables in the intertidal area trenching.

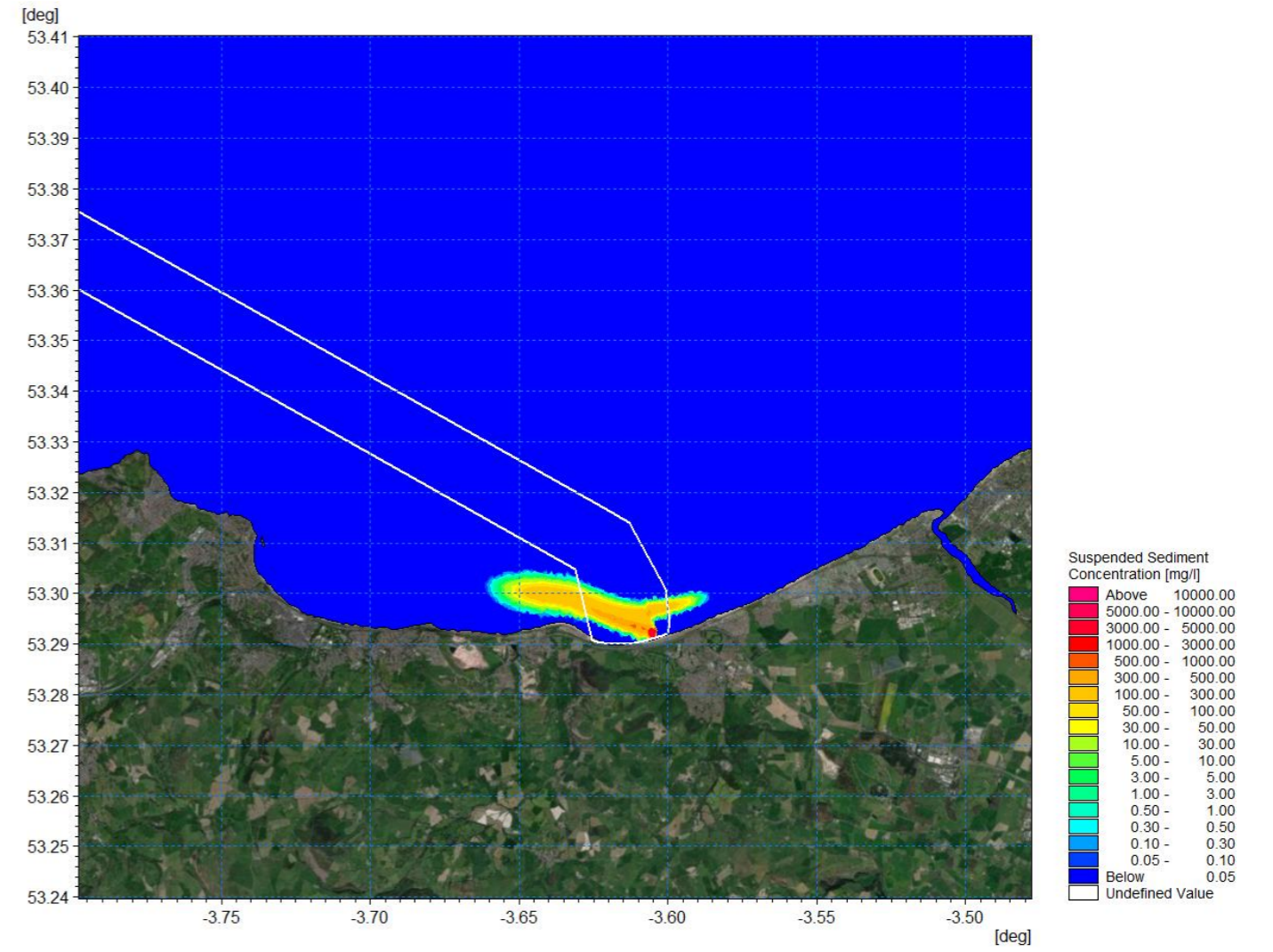


Figure 1.166: Average suspended sediment concentration during offshore export cables in the intertidal area trenching detailed view.



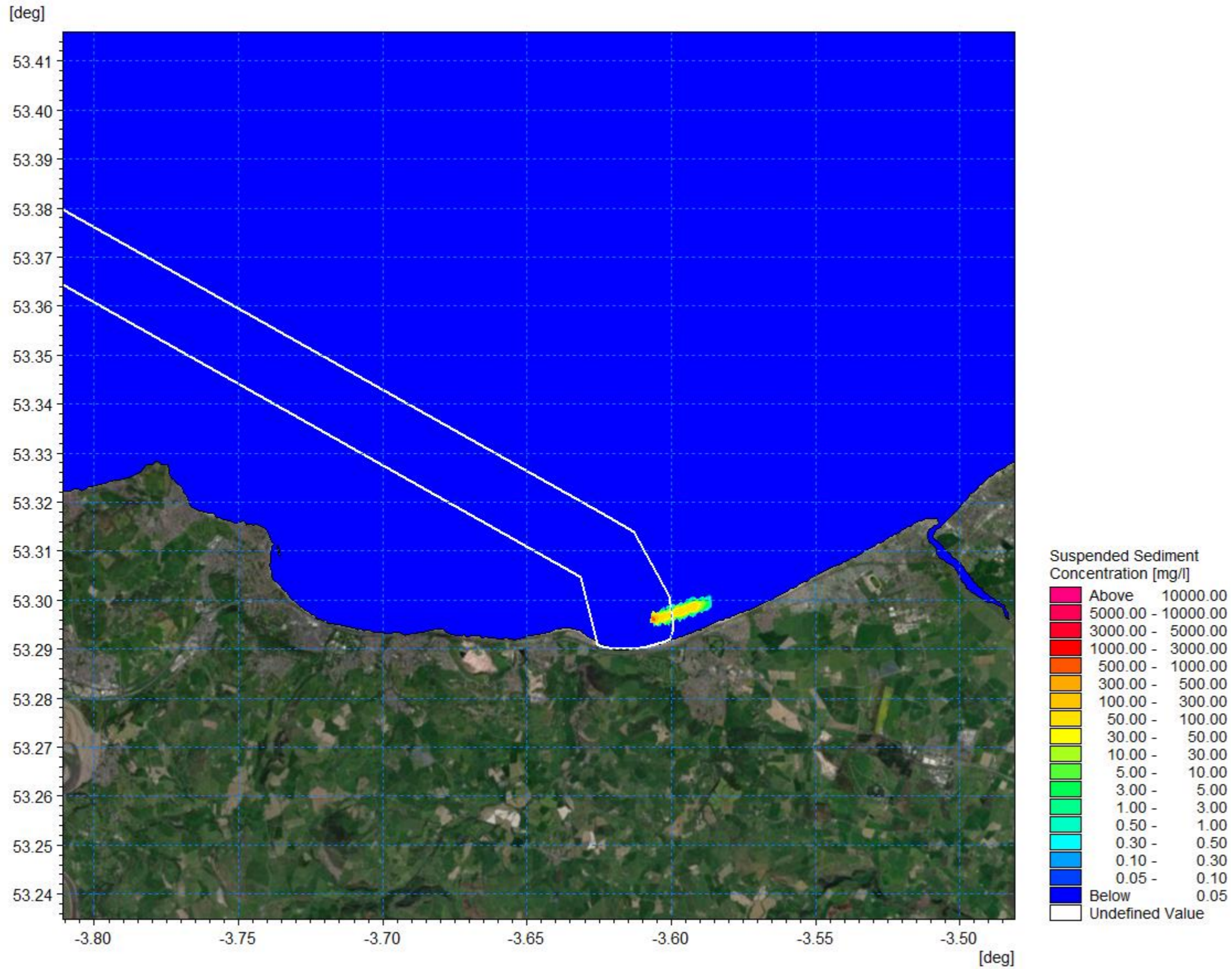


Figure 1.167: Suspended sediment concentration flood – offshore export cables in the intertidal area installation.



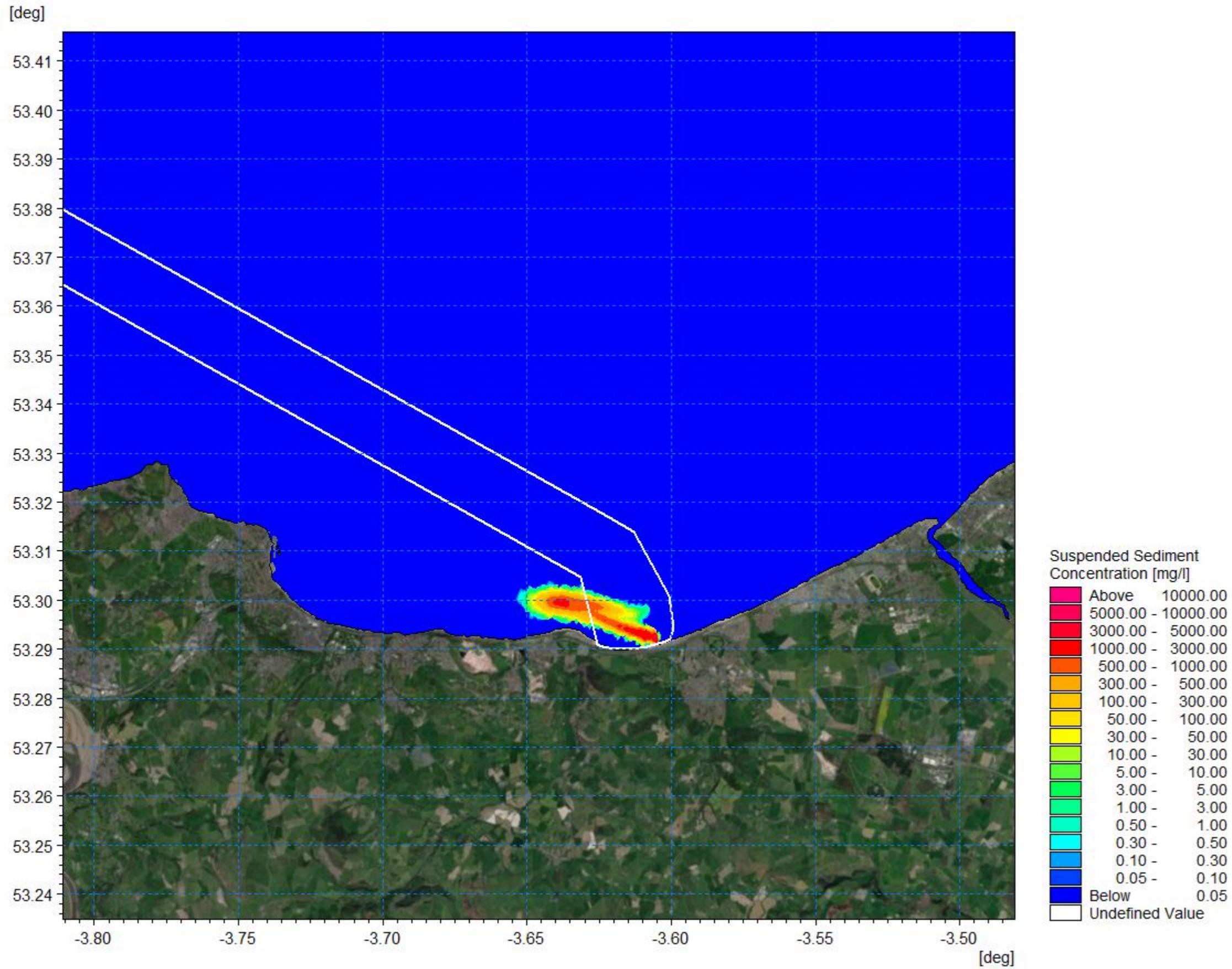


Figure 1.168: Suspended sediment concentration ebb – offshore export cables in the intertidal area installation.



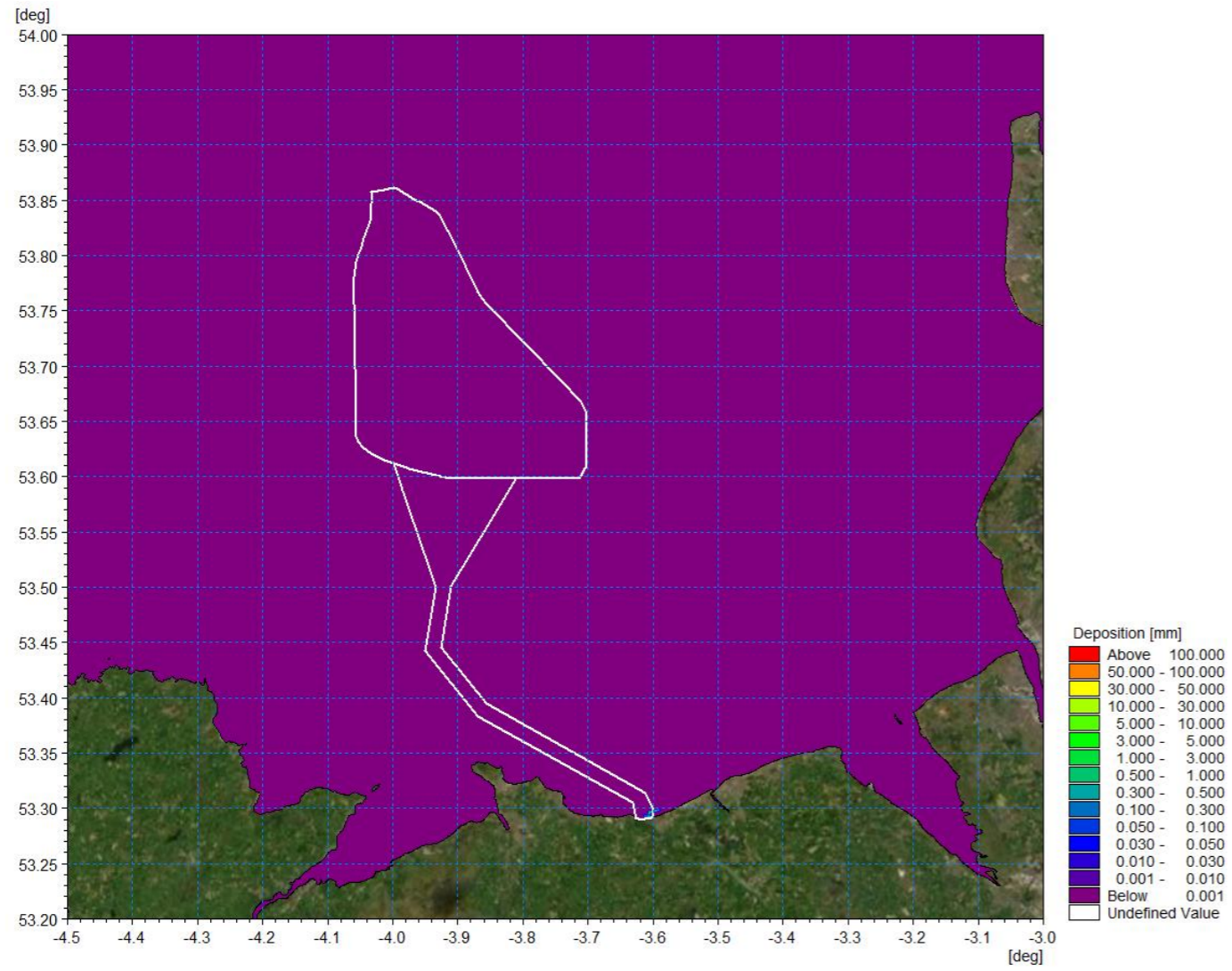


Figure 1.169: Average sedimentation during offshore export cables in the intertidal area installation.

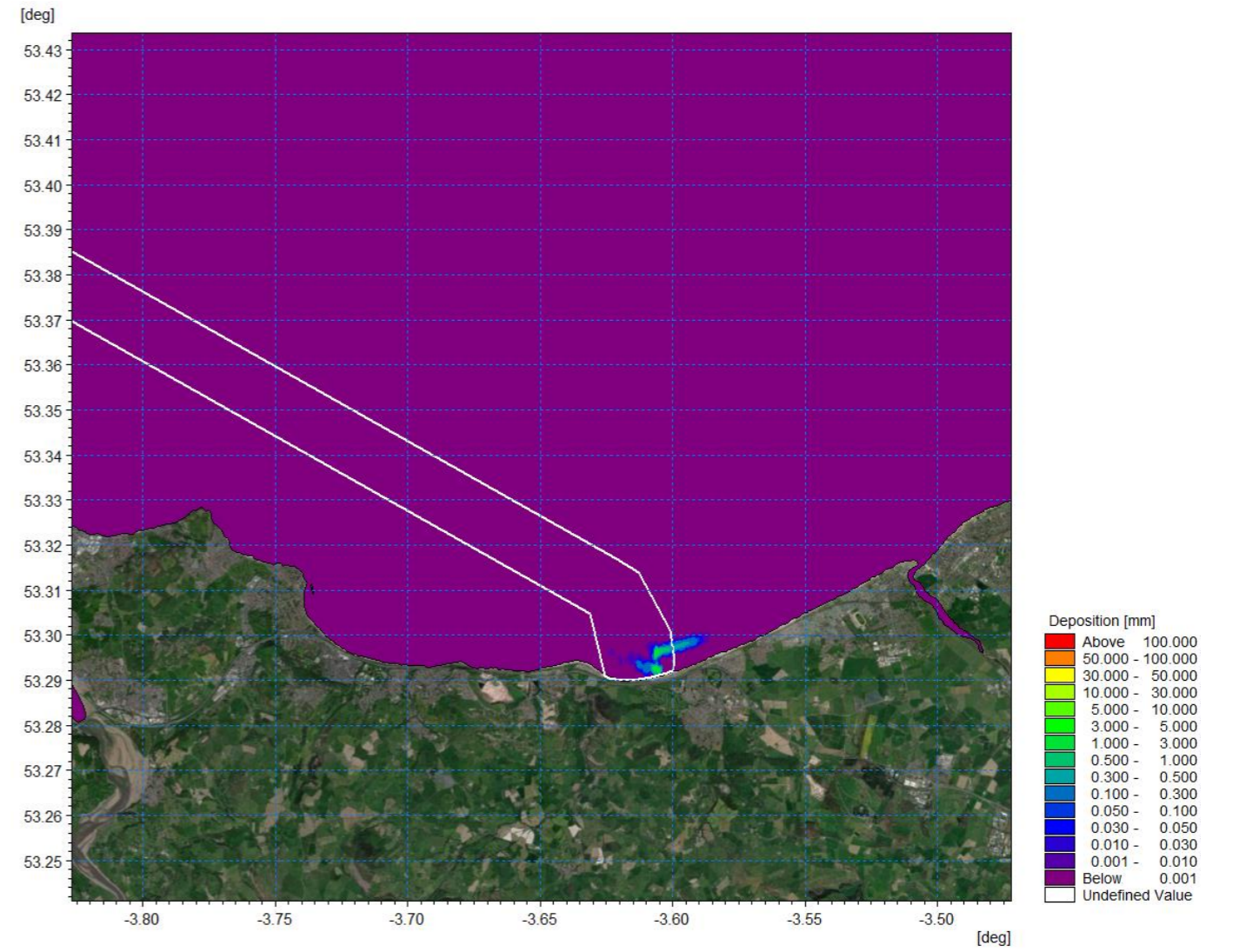


Figure 1.170: Average sedimentation during offshore export cables in the intertidal area installation detail view.



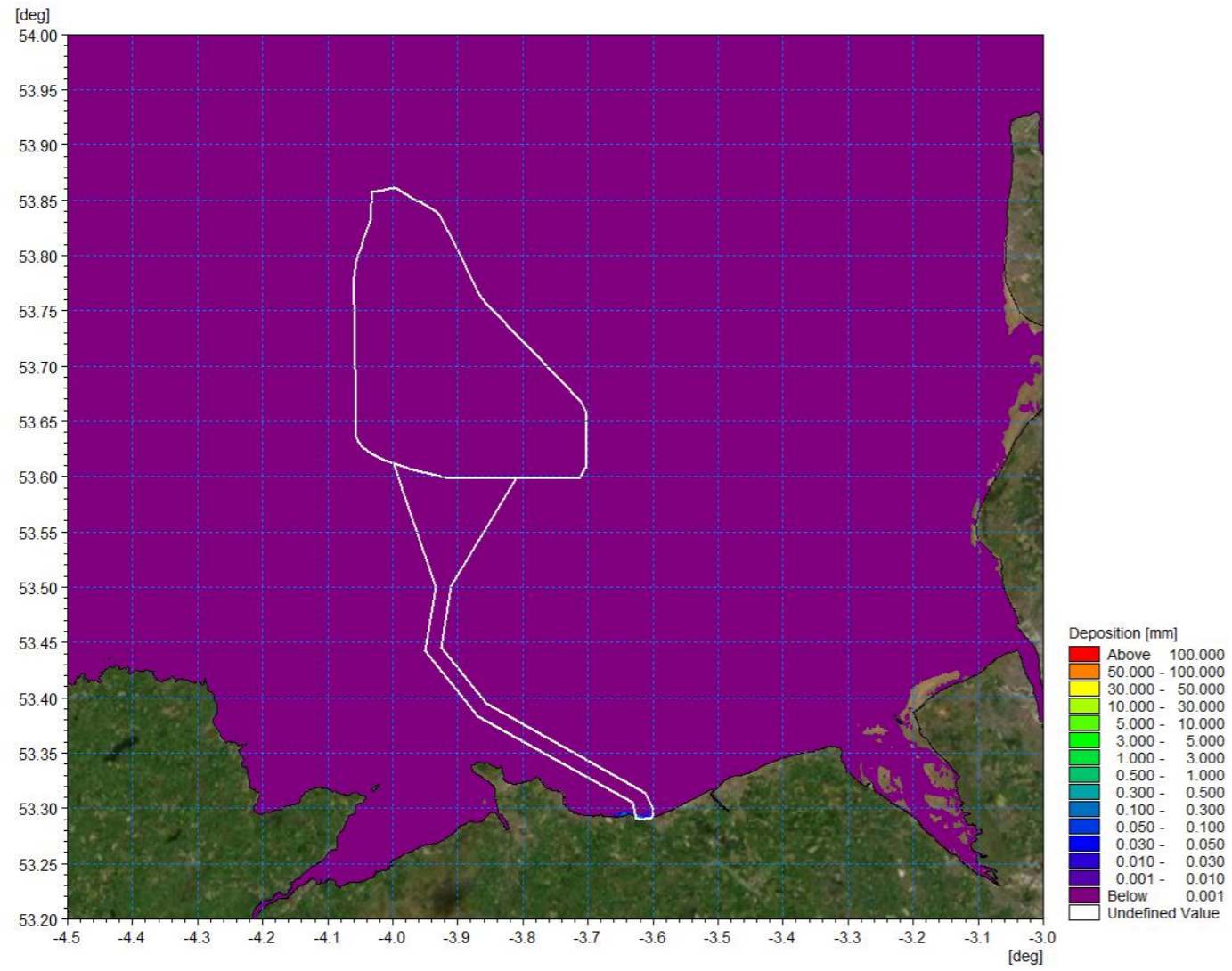


Figure 1.171: Sedimentation 1day following cessation of offshore export cables in the intertidal area installation.

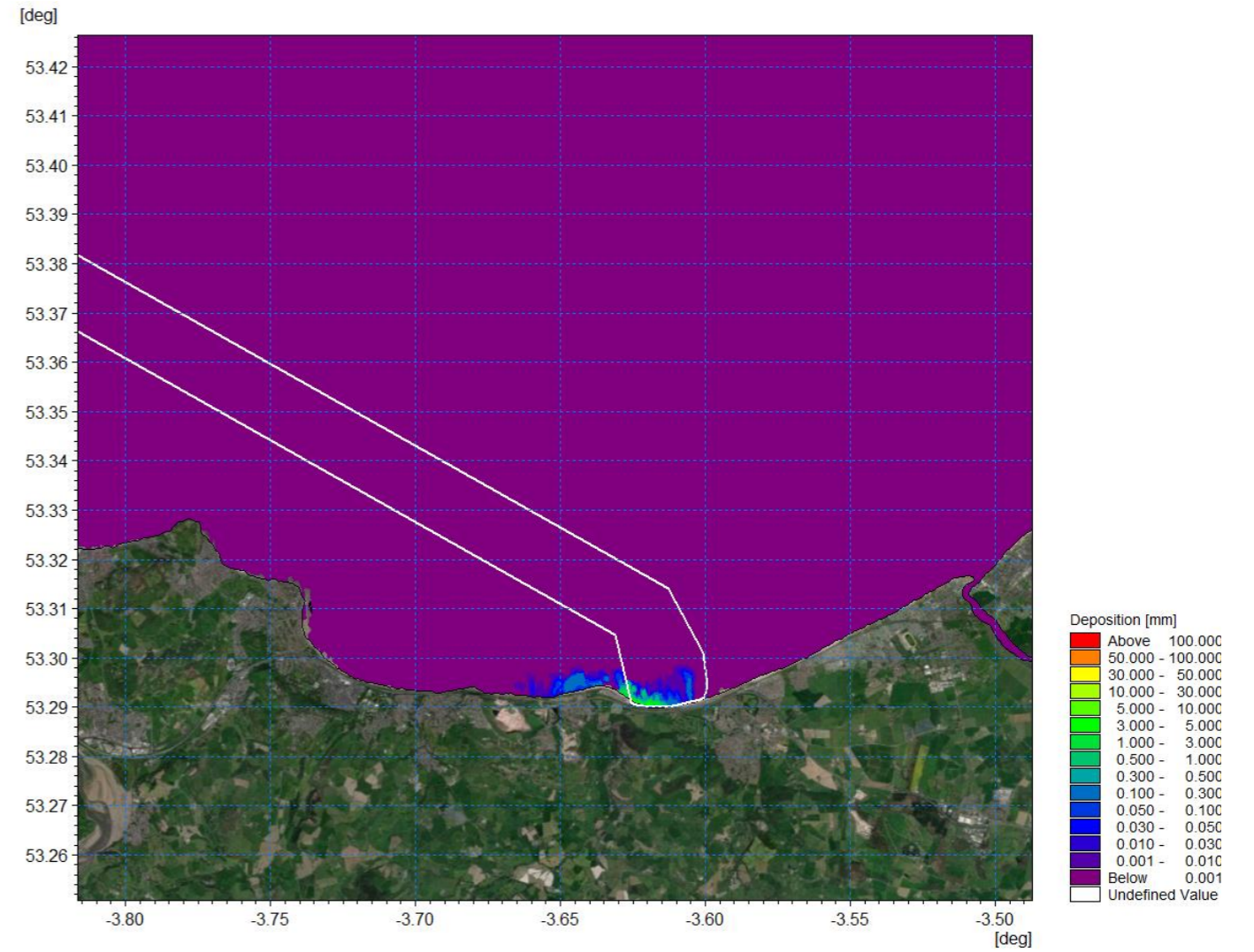


Figure 1.172: Sedimentation 1day following cessation of offshore export cables in the intertidal area installation detail view.



## 1.9 Summary

- 1.9.1.1 A numerical modelling study was undertaken to inform and qualify the potential impacts of the Mona Offshore Wind Project on physical processes. This report has outlined the baseline characteristics of the region in terms of physical processes. This includes tidal current, wave climate and sediment transport under both calm and storm conditions. Numerical modelling has been used to quantify the changes in physical processes due to the installation of the Mona Offshore Wind Project. The presence of the turbine foundations redirects both waves and tidal flow and although some changes in sediment transport were revealed, these were limited in magnitude and represented an adjustment in the transport path alignment.
- 1.9.1.2 The installation of the Mona Offshore Wind Project was seen to marginally reduce wave heights in the lee of the structures whilst a marginal increase was noted at the periphery, however during larger storm events these effects were less marked. Any significant changes in tidal currents and wave climate would not extend to the coastline and there would be no change in coastal processes in this area.
- 1.9.1.3 Finally, suspended sediment plumes for construction activities were quantified. In all cases, the material released was native to the bed sediments and, although there are periods of increased turbidity, the material was retained in the sediment cell and would be subsequently assimilated into the existing sediment transport regime.

## 1.10 References

ABPmer (2008) WebVision Atlas of UK Marine Renewable Energy Resources. Available: <https://www.renewables-atlas.info/explore-the-atlas/>. Accessed: June 2022.

ABPmer (2018) Data Explorer. Available: <https://www.seastates.net/explore-data/>. Accessed: June 2022.

BERR (2008). Review of Cabling Techniques and Environmental Effects applicable to the Offshore Windfarm Industry. Technical Report, Department for Business Enterprise and Regulatory Reform (BERR), in association with Defra, 164pp.

British Geological Survey (2022) Sediment sample data. Available: <https://www.bgs.ac.uk/information-hub/bgs-maps-portal/>. Accessed: May 2022.

British Oceanographic Data Centre (BODC) (2021). UK tide gauge network. Available at: [https://www.bodc.ac.uk/data/hosted\\_data\\_systems/sea\\_level/uk\\_tide\\_gauge\\_network/](https://www.bodc.ac.uk/data/hosted_data_systems/sea_level/uk_tide_gauge_network/). Accessed on: 24 June 2022.

Centre for Environment, Fisheries and Aquaculture Science (Cefas) (2016) Suspended Sediment Climatologies around the UK, CEFAS.

Centre for Environment, Fisheries and Aquaculture Science (Cefas) (2022). Wave data. Available at <https://wavenet.cefas.co.uk/map>. Accessed June 2022.

Department for Environment Food and Rural Affairs (2022). Bathymetry and SSSI information. Available at <https://environment.data.gov.uk/DefraDataDownload>. Accessed on: 15 June 2022.

European Centre for Medium-range Weather Forecast (ECMWF) (2022), Long term wind and wave datasets. <https://www.ecmwf.int/en/forecasts/datasets>.

EMODnet (2020) Bathymetry. Available: <https://www.emodnet-bathymetry.eu/>. Accessed May 2022.

EMODnet (2022b). EODnet Geology. Available at: <https://www.emodnet-geology.eu/>. Accessed on: 10 June 2022.

EMODnet (2022c). EODnet Geology. Available at: <https://www.emodnet-physics.eu/>. Accessed on: 28 June 2022.

EMU (2013) Irish Sea Zone, Hydrodynamic measurement campaign October 2010- October 2012. Report issued to Centrica Energy Renewable Investments.

Furgro (2022) Metocean Data Report, Morgan and Mona Offshore Wind Projects. Ref: 210674\_190291-MDR-01 02

Gardline Ltd (2022) Integrated Offshore Wind Farm Site Survey. Document number: 11602.

GEMS (2011) Metocean data collection, Ormonde wind farm project. Report prepared for: Offshore Design Engineering Ltd Document number: GSL10108-FIN-001-01.

Howarth M.J. (2005) Hydrography of the Irish Sea, SEA6 Technical Report, POL Internal document 174.

Integrated Mapping for the Sustainable Developments of Ireland's Marine Resource (INFOMAR) (2022), Seabed mapping data Geological Survey Ireland (GSI) and Marine Institute. Available at <http://www.infomar.ie/>. Accessed Feb 2022.

Marine Environmental Data Information Network (MEDIN) (2021). Bathymetry data. Available at: <https://data.admiralty.co.uk/portal/apps/sites/#/marine-data-portal>. Accessed on: March 2021.

Mellet, C, Long, D, Carter, G, Chiverell, R and Van Landeghem, K. (2015) Geology of the seabed and shallow subsurface: The Irish Sea. British Geological Survey Commissioned Report, CR/15/057 52pp.

National Network of Regional Coastal Monitoring Programmes (2022). Metocean data. Available at <https://coastalmonitoring.org/cco/>. Accessed June 2022.

National Oceanic and Atmospheric Administration (NOAA) (2022). Metocean data. Available at <https://www.dhigroup.com/data-portals/metocean-data-portal>. Accessed April 2022.

The Environment Agency National LiDAR Programme (2022). LiDAR data. Available at [Find open data - data.gov.uk](https://findopen.data.gov.uk). Accessed May 2022.

Whitehouse, R.J.S., Sutherland, J. and O'Brien, D. (2006) Seabed scour assessment for offshore windfarm. Proceedings Third International Conference on Scour and Erosion, November 1-3, CURNET, Gouda, The Netherland.

RPS (2018) Tide and Storm Surge Forecast (TSSF) model of Irish coastal waters.

UKHO (2022), Admiralty Tide Tables – Volume 1B.

XOCEAN Ltd (2022) 00275-BPX-UKX-WIND bp Elizabeth Project Processing Report.